EXPERIMENTAL INVESTIGATIONS OF BLUNT FORCE TRAUMA IN THE HUMAN SKELETON

By

Mariyam I. Isa

A DISSERTATION

Submitted to
Michigan State University
in partial fulfillment of the requirements
for the degree of

Anthropology—Doctor of Philosophy

2020

ABSTRACT

EXPERIMENTAL INVESTIGATIONS OF
BLUNT FORCE TRAUMA IN THE HUMAN SKELETON

By

Mariyam I. Isa

In forensic anthropology, skeletal trauma is a growing area of analysis that can contribute important evidence about the circumstances of an individual's death. In bioarchaeology, patterns of skeletal trauma are situated within a cultural context to explore human behaviors across time and space. Trauma analysis involves transforming observations of fracture patterns in the human skeleton into inferences about the circumstances involved in their production. This analysis is based on the foundational assumption that fracture behavior is the nonrandom result of interactions between extrinsic factors influencing the stresses placed on bone and intrinsic factors affecting bone's ability to withstand these stresses. Biomechanical principles provide the theoretical foundation for generating hypotheses about how various extrinsic and intrinsic factors affect the formation of fracture patterns, and about how these factors can be read from fracture patterns. However, research is necessary to test and refine these hypotheses and, on a more basic level, to document the relationships between "input" variables of interest and fracture "outputs."

One research approach involves the use of forensic and/or clinical case samples. Case-based approaches are important because they provide data from real scenarios and contexts that may be similar to those encountered in unknown cases. However, a limitation is that input variables are not directly measured or controlled and therefore cannot be precisely known. Therefore, case-based approaches offer incomplete means of hypothesis testing. Over the past decade, anthropologists have increasingly addressed this problem using prospective, experimental approaches. Experimental research provides the advantage of investigating fracture

patterns generated under known, replicable, laboratory-controlled conditions. While this type of research is believed to be most applicable to forensic cases when it is conducted on unembalmed postmortem human subjects (PMHS) within the perimortem interval, to date the majority of experimental studies have involved nonhuman models. Given micro- and macro-structural differences between species, it is yet unknown how results obtained in nonhuman bones scale to human bones. Experimental studies on PMHS are therefore warranted to test hypotheses and develop reference points for how fracture patterns form in response to various loading inputs.

The purpose of this dissertation is to document and evaluate basic relationships between several forensically relevant input variables and fracture behavior outputs through a series of blunt force impact experiments on human crania and femora. Part one of this dissertation investigates cranial fracture behavior in relation to the input variables of point of impact, number of impacts, impact surface, and kinetic energy. Part two investigates the relationship between impact direction and fracture behavior in the femur. The papers comprising this dissertation are united by three common goals: 1) to investigate fracture formation, including how and where fractures initiate and propagate relative to the impact site; 2) to document and compare fracture behavior in response to known input variables; and 3) to evaluate fracture features described in reference literature and gather evidence of their utility in reconstructing these input variables.

This research advances understanding of the interplay between impact variables and fracture behavior in cranial and postcranial blunt force skeletal trauma. Furthermore, this study contributes reference data associating known loading conditions with resultant fracture patterns in human material. This type of data is necessary to build interpretive and methodological theory in anthropological trauma analyses.

For my parents, thank you for everything. I love you.
I would also like to dedicate this dissertation to those who donated their bodies to science. Without the selfless generosity of these individuals and their families, this research would not have been possible.

ACKNOWLEDGMENTS

This dissertation would not have been possible without the support of my mentors, family, friends, and colleagues. As I reflect on the journey that brought me here, there are so many people for whom I feel intense gratitude. I would first like to thank my committee members, Drs. Fenton, Hefner, Wei, and Wrobel for freely and generously giving of their help, advice, and insight. I am a better scholar for the lessons they taught me and the discussions we had over the years. To my chair, Dr. Todd Fenton, thank you for taking a chance on me so many years ago. From the beginning you believed in me, treated me as a serious researcher, and gave me every opportunity to help me achieve my dream. These are gifts I hope to pay forward to my future students as I help them achieve their own dreams.

In addition to my committee, I am grateful to the others who mentored and helped me throughout my journey. Dr. Lynne Goldstein, thank you for giving me something to believe in when I needed it most. Your grace, intelligence, and fierce loyalty to your students inspire me. I will always cherish our Soup Spoon breakfasts. Dr. Stacey Camp, thank you for sharing your expertise and experience, for being unwaveringly open and honest about all things academic, and for being generous with your time and advice. Dr. Norm Sauer, thank you for helping to spark my interest in forensic anthropology and for tempering this passion with the wisdom that there is more to life than this field or this job. Cliff Beckett, engineering technician extraordinaire, thank you for your patience, your humor, and your ability to fix all things mechanical. Without your expertise, the experiments on which this dissertation were based would not have been possible. Joan Reid, our department's Graduate Secretary, thank you for your unparalleled commitment to students, for keeping us all on track, and for answering my many questions over the years.

I owe so much to my family, who have loved me, supported me, and cheered me on my entire life. To my mom and dad, Paula and Shahrin Isa, thank you for everything. Thank you for making me curious and persistent, for teaching me to stand up for myself, and for always listening with great interest as I ramble about the things that fascinate me most. Thank you for letting me find my own way, for always welcoming me home, and for never making me question whether you are proud of me. I am so lucky to have such amazing people as my parents. To my brother, Gabe, thank you for being my lifelong best friend. You are the coolest person I know and I am so proud of you. Finally, to my grandparents, Norma and George Johnston, thank you for your unwavering support and confidence in me. Grandpa, even though you are no longer here I have felt your presence every step of the way. I hope I am making you proud.

I am extremely grateful to Giacomo Fontana, who raised my spirits and encouraged me when I needed it most. Thank you for being the first to celebrate the smallest of my accomplishments, for holding space for me when I struggle, and for teaching me to take life less seriously. *Grazie mille*.

I would not have made it through this process without my friends. I have the best friends in the world; they inspire me every day. While I have many to thank, a few stand out. Dr. Amy Michael, I would not be the human or the anthropologist I am today without you. I am so grateful for your love, your loyalty, and your brilliant mind. Dr. Susan Kooiman, you are one of the strongest people I know. I am in constant awe of your ability to get things done and make it look easy. Thank you for coffee shop work dates, Crunchy's karaoke nights, and countless other adventures. Jack Biggs (and Kevin the border collie), thank you for brightening my life with laughs, plants, pastries, and puppy snuggles. Dr. Lisa Bright, thank you for being my go-to source for advice, obscure information, and the latest news. Your mind is a treasure trove and I

am lucky to have had glimpses inside. Emily Milton, I am thankful for the times we spent contemplating the mysteries of life, the universe, and anthropology. I will cherish our conversations – the intense and the intensely silly – forever. Autumn Painter and Jeff Painter, your friendship has meant so much to me. From the bottom of my heart, thank you for all the kind gestures that kept me afloat over the years. Betsy Woldeyohannes, you have a beautiful soul and a deeply compassionate heart. My life is better for having you in it. I aspire to see the world with as much depth and clarity as you do.

To my dear friends Gocha et al. (Dr. Tim Gocha, Kelsey Carpenter, Erica Christensen, Abbie Grande, Dr. Janet Finlayson, Justin Maiers, and Ryan Strand), thank you for keeping me laughing and for your intense friendship. You are some of the smartest and most raucous people I know. I know I can always count on you for inspiring conversations about life and science, for the worst jokes and best limericks, and for a reliably and undeniably good time.

My friends outside of anthropology have been instrumental in keeping me sane and grounded. Dr. Lauren Szczygiel, Dr. Ed Szczygiel, Dmitri Barvinok, Charlotte Grenier-Barvinok, Jon Roney, Andy White, and Carly Schneider, thank you for making me feel like a part of your family and for feeding me with your friendship as much as your food. Dr. Maeve Daly, Nick Kanillopoolos, Mallory Newsted, and Nora Wixom, thank you for your love and support throughout the many different seasons of our lives. It is an honor to know you and to have grown alongside you.

I am ever grateful to the members of the MSU Forensic Anthropology Laboratory for fostering an environment of mutual respect, support, and solidarity. I have learned so much from all of you. While I have worked with many wonderful people over the years, I give special thanks to Alex Goots and Elena Watson. Thank you for your grace and positivity in the face of

adversity, for your willingness to say yes to adventure, and for being the kindest human beings. *Spacca tutto*!

I also express my thanks to the MSU alumnae who taught me so much. Dr. Caitlin Vogelsberg and Dr. Jen Vollner, thank you for being my mama birds and taking me under your wing when I was taking my first steps in graduate school. Dr. Julie Fleischman, I admire your strength and thank you for inspiring me to forge my own path. Dr. Emily Streetman, thank you for teaching me everything from osteology to how to brew kombucha, and for being a true and loyal friend.

To the undergraduate students I had the distinct honor of teaching and mentoring, thank you for having faith in me and for allowing me to learn alongside you. I am eternally proud of you and cannot wait to see who you become. Special thanks to Lilli Antonelli, who assisted with the data collection on Chapter 5 of this dissertation.

Finally, this dissertation research would not have been possible without the generous support of the College of Social Science, the Department of Anthropology, and the National Science Foundation Graduate Research Fellowship Program. This funding afforded me the great privilege of being able to focus on my research and writing when it counted the most.

TABLE OF CONTENTS

LIST OF TABLES

LIST OF FIGURES

INTRODUCTION

"It is easy to reconstruct events from evidence of damage to the skeletal remains, but it is very difficult to do so correctly." (Maples 1986, 223)

Background

Trauma refers to the physical disruption of living tissue by outside forces (Christensen, Passalacqua, and Bartelink 2014). Skeletal trauma analysis involves the identification, description, documentation, and interpretation of traumatic alterations to bones and teeth (SWGANTH 2011).

In the context of forensic anthropology, trauma analysis can provide evidence regarding the circumstances of a death event or events related to disposal of the body (Symes et al. 2012). Forensic anthropologists are asked to evaluate skeletal trauma in cases in which soft tissue is decomposed or inadequate for autopsy, or when the trauma is particularly complex (Wedel, Galloway, and Zephro 2014). Anthropologists do not determine cause or manner of death, as these determinations are the legal responsibility of the medicolegal authority. However, anthropologists' assessments of trauma within a given case context can contribute to the interpretation of evidence and assist the medicolegal authority in determining cause and manner of death.

In the archaeological record, skeletal trauma presents biological evidence of humans' interactions with their physical and sociocultural environments. Whereas the ultimate goal of trauma analysis in a forensic context is to reconstruct specific events relevant to an individual case, the ultimate goal of bioarchaeologists is to place trauma within a sociocultural context (Walker 2001). Trauma analysis provides insight into such diverse issues as change in

subsistence strategies (Domett and Tayles 2006), reaction to resource stress (Torres-Rouff and Costa Junqueira 2006), funerary practice (Jones, Walsh-Haney, and Quinn 2015), construction of identity (Knudson and Torres-Rouff 2009), communication of power and symbolism (Pérez 2012; Tung and Knudson 2008) and consequences of structural inequality (Klaus 2012; de la Cova 2012). Violence is a particularly productive area of trauma research (Martin and Harrod 2015; Judd and Redfern 2012).

In studies of the more distant past, the identification and analysis of trauma can help address questions about hominin behavior and site formation processes. Patterns of perimortem fractures can provide evidence to suggest whether an assemblage more likely represents the result of intentional deposition or natural causes (L'Abbe et al. 2015). Additionally, comparisons of skeletal trauma patterns in modern humans and hominin ancestors have been used to suggest other behaviors in antiquity such as interpersonal violence (Zollikofer et al. 2002; Churchill et al. 2009; Wu et al. 2011), hunting (Camarós et al. 2016; Trinkaus and Buzhilova 2012), and modes of locomotion (Kappelman et al. 2016).

Regardless of the anthropological context or ultimate goals, the proximate goals of skeletal trauma analysis are similar. One is to assess trauma timing: whether the insult occurred antemortem, postmortem, or within the perimortem interval. These classifications are made based on the presence or absence of osteogenic response and the qualities of the skeletal tissue (Christensen, Passalacqua, and Bartelink 2014; SWGANTH 2011). For skeletal trauma, the perimortem interval includes alterations that do not exhibit signs of osteogenic response (i.e., healing or infection) and that were incurred while the bone was in a biomechanically fresh state, generally around the time of death. Perimortem trauma is of particular forensic interest because of its potential relevance to the death event or events surrounding the disposition of the body.

Another goal of trauma analysis is to assess the mechanism that caused the trauma. Anthropologists have traditionally used categories such as sharp force, blunt force, and gunshot or high-velocity projectile to describe skeletal trauma (SWGANTH 2011; Symes et al. 2012). However, these categories are not discrete, as trauma occurs along a biomechanical continuum governed by a series of mechanical and anatomical variables (Kroman 2007; Kroman and Symes 2013). Two variables of importance are the loading rate and the surface area over which the load is applied. The primary difference between high velocity projectile trauma and the other traditional categories is the loading rate. High velocity projectile trauma is associated with objects moving at a very high (fast) rate and impacting a small surface area. In contrast, sharp and blunt force trauma involve lower (slower) rates of loading. In sharp force trauma, the load is applied over a small, often narrow surface, whereas in blunt force trauma it is applied over a broader surface area. This dissertation focuses on blunt force trauma, the range of trauma associated with a relatively low-velocity impact between a body and a blunt surface (SWGANTH 2011).

Assessments of timing and mechanism represent the primary objectives of trauma analysis (Berryman, Lanfear, and Shirley 2012; Wedel, Galloway, and Zephro 2014; SWGANTH 2011). However, anthropologists may make additional interpretations based on fracture patterns. In a forensic context, courts often expect more precise interpretations beyond timing and mechanism (Berryman, Lanfear, and Shirley 2012). These include interpretations about the direction or location, minimum number, and sequence of impact, general characteristics of the injuring object, tool, or surface, and/or the type or amount of force required to produce a particular pattern of trauma (Berryman, Lanfear, and Shirley 2012; Christensen, Passalacqua, and Bartelink 2014; Symes et al. 2012). These types of higher resolution

interpretations are also important for strengthening foundations for biocultural interpretations of fractures in antiquity (Lovell and Grauer 2019). A lack of baseline data and standardized methodological approaches for making these higher-resolution interpretations represents a current gap in trauma analysis.

Many theoretical and methodological advances in skeletal trauma analysis can be traced to the latter decades of the twentieth century. Trauma analysis became a mainstream component of forensic anthropology casework during the "Professionalization" era (1970s-1990s) of the subfield (Sledzik et al. 2007). In this era, collaborations between anthropologists and local medical examiner offices helped to highlight anthropologists' potential contributions to death investigations (Passalacqua and Fenton 2012). Anthropologists' ability to distinguish skeletal trauma from other bone tissue changes and their knowledge of bone biology, structure, and repair processes provided valuable information that helped inform determinations of cause and manner of death. Early publications on skeletal trauma included primarily case studies (Kerley 1976, 1978; Angel and Caldwell 1984; Sauer 1984; Frayer and Bridgens 1985; Maples 1986; Maples et al. 1989). In the 1980s and 1990s, forensic anthropologists began to undertake systematic approaches to trauma research (Passalacqua and Fenton 2012). Pioneers in this effort included Hugh Berryman, Steve Symes, O.C. Smith, and colleagues collaborating at the same medical examiner's office in Memphis, Tennessee (Smith et al. 1991; Berryman et al. 1991; Symes et al. 1991; Smith, Berryman, and Lahren 1987). Seminal publications including those by Berryman and Symes (Berryman and Symes 1998) and Alison Galloway (Galloway 1999) helped to formalize a framework for conducting trauma analysis, including grounding the interpretation of fracture patterns within the theoretical context of biomechanics.

These theoretical and methodological advances coincided with concern over the validity of scientific evidence presented in court. *Frye v. United States* (Frye v. United States 1923) established general acceptance within the relevant field as the standard for admissibility of evidence. However, the 1993 decision in *Daubert v. Merrell Dow Pharmaceuticals, Inc.* (Daubert v. Merrill Dow Pharmaceuticals, Inc. 1993) established a new standard for the admissibility of expert testimony, requiring that the reasoning or methodology underlying the testimony must be scientifically valid. This has led the field of forensic anthropology to consider and attempt to formalize the theoretical and methodological bases for the discipline and its various analyses (Boyd and Boyd 2011). Following the work of Schiffer (Schiffer 1988) describing high-level, middle-range, and low-level theory in archaeology, Boyd and Boyd propose three dynamic and interacting forms of theory in forensic anthropology: foundational, interpretive, and methodological (Boyd and Boyd 2011, 2018). Berryman et al. (Berryman, Berryman, and Saul 2018) apply this structure to the theoretical framework for trauma analysis. Trauma analysis begins with the fundamental assumption that fracture behavior is nonrandom, subject to the laws of physics, and therefore predictable to a certain degree (Berryman, Berryman, and Saul 2018). Biomechanical principles provide the overarching foundational theory for understanding the specific phenomena of fracture patterns. Meanwhile, casework and research inform interpretive theories, the means by which analysts transform observations of fracture patterns into inferential statements about the specific events that caused them. Finally, systems of classifying and describing fracture patterns and features reflect methodological theories, which in turn may influence how interpretations are made (Boyd and Boyd 2011; Berryman, Berryman, and Saul 2018). This theoretical framework underpins the approach taken in this dissertation.

Foundational Theory

The foundational theory informing trauma analysis is based on principles of biomechanics (Berryman et al. 2018). These principles can be used to explain fracture behavior as the nonrandom product of "extrinsic" factors influencing how force is applied to a bone and "intrinsic" factors related to how the bone resists the stresses produced by these applied forces.

The term "biomechanics" is fairly recent, even if the study it describes is not. Herbert Hatze provided one of the first formal definitions in 1974, describing biomechanics as "the study of the structure and function of biological systems by the means of the methods of mechanics" (Hatze 1974). It is a practical theory used to explain biological and mechanical behaviors of the tissues comprising living beings in response to applied forces (Kieser, Taylor, and Carr 2012). Biomechanics has applications in many fields including medicine, dentistry, botany, zoology, and recently, forensic sciences. The emerging field of forensic biomechanics applies methods of mechanics and knowledge of the structure and function of biological systems at various scales to explain forensically relevant biological phenomena including skeletal and soft tissue trauma and blood spatter patterns (Kieser, Taylor, and Carr 2012).

Different biomechanical problems draw on different areas of applied mechanics. Principles of statics have been used to analyze forces in joints and muscles, principles of dynamics to analyze motion and gait, principles of solid mechanics to investigate biological systems under various load conditions, and principles of fluid mechanics to investigate the flow of blood or air through various body systems (Özkaya and Leger 2012). However, biological tissues and systems are more complex than the manmade materials and systems traditionally analyzed using mechanical methods (Fung 1993; Kieser 2013; Roesler 1987). Depending on the question addressed, the object of biomechanical interest may be considered at multiple levels of

organization including the material, tissue, organ, and organism levels (Fung 1993; Roesler 1987). Unlike manmade materials, there are also challenges inherent in measuring and sampling biological materials and developing life-like testing conditions. Therefore, Fung (Fung 1993) describes the basic approach of biomechanics as an iterative process of hypothesis generation and testing that may include various steps of mathematical modeling, analysis, and experimental measurements.

Basic principles

This section reviews some of the basic principles of biomechanics relevant to trauma analysis and discussed throughout the course of this dissertation.

A force can be described as a push or pull acting on a body (Hall 2012). Newton's three laws of motion describe the relationship between the forces acting on a body and the motion of a body in response to these forces. Newton's first law describes force qualitatively: an object at rest or moving with a constant velocity will remain in that state until an external force is applied (Kieser 2013). Newton's second law describes force quantitatively (Kieser 2013). One way of stating this is in terms of acceleration, or the rate of change of velocity: a force (F) applied to a body of mass (m) will cause an acceleration (a) of the body proportional to the force and inversely proportional to the mass: $F=ma$. Another way of stating Newton's second law is in terms of momentum. Objects in motion have a momentum (p) equal to the mass multiplied by the velocity (v): $p=mv$. Force is equal to the change in momentum (Δp) over time (t): $F= \Delta p/t$. The product of force and time is the impulse (J): $J=Ft$. These two equations give rise to the impulse momentum theorem. A force acting on a body for a specific amount of time results in a change in momentum of that body: $J = Ft = \Delta p$. The important takeaway is that the motion of a body depends on the magnitude and the duration of the applied force (Hall 2012). Finally,

Newton's third law asserts that there are no isolated single forces. When one object exerts a force on another object, the second object exerts a force of equal magnitude and opposite direction on the first (Özkaya and Leger 2012). While forces may be equal in magnitude, they may have different effects due to differences in the properties of these objects (Kieser 2013).

The force or combination of forces applied to a structure is called the load (Frankel and Nordin 2012). Load is sometimes denoted *P*. In the human body, forces are applied during standing, sitting, and other weight-bearing activities, through the action of muscles, and when the body strikes or is struck by an object (Frankel and Nordin 2012). Loading causes acceleration and/or deformation of a structure. Acceleration produces displacement, or movement relative to the original position. Deformation involves a change in shape or size relative to the original configuration. The extent of deformation depends on various intrinsic factors (for example, the material properties, size, and shape of the object) and the direction, duration, and magnitude of the applied load (Özkaya and Leger 2012).

Forces can be applied in various directions, resulting in various types of loading. Tensile loading (tension) refers to the application of equal and opposite forces outward from a structure's surface. This causes the structure to lengthen in the direction of the load. Compressive loading (compression) refers to the application of equal and opposite forces toward a structure's surface. This causes the structure to shrink in the direction of the load. Shear loading refers to forces applied parallel to a structure's surface. This causes internal, angular deformation. Bending refers to the application of force such that a structure bends about an axis. Meanwhile, torsion refers to the application of force such that a structure twists about an axis. All of these types of loading occur in bone, although most often bones are subjected to combinations of loading (Nordin and Frankel 2012).

Stress (σ) is the intensity of a load (P) per unit area (A) that develops on a surface within a structure in response to an externally applied load (Özkaya and Leger 2012). This relationship can be expressed: $\sigma = P/A$. Strain (ε) is a measure of the deformation that develops within a structure in response to externally applied loads (Özkaya and Leger 2012). Strain is a unitless measure calculated as the change in dimension (Δl) divided by the original dimension (l). This relationship can be expressed: $\varepsilon = \Delta l/l$.

Different types of loading produce different types of stresses and strains: tensile, compressive, and shear loads produce tensile, compressive, and shear stresses and strains, respectively. Even in more complex loading, stresses and strains can be simplified into these categories (Frankel and Nordin 2012). For example, bending produces tensile stresses and strains on the convex side of the neutral axis and compressive stresses and strains on the concave side. Compressive and tensile stresses act normal (perpendicular) to the loading surface, and are therefore referred to as normal stresses (denoted σ). In contrast, shear stresses act tangentially to the loading surface and are denoted τ (Özkaya and Leger 2012).

Biological tissues are often described according to their structural and/or material properties (Pal 2014). Structural properties characterize intact tissues and are dependent on the size and shape of the tissue. These properties are typically described according to relationships between load and deformation. In contrast, material properties characterize the material that makes up a tissue and are largely independent of geometry. These properties are described according to relationships between stress and strain (Pal 2014).

A structure or material may have different properties depending on the direction of loading applied. In order to determine structural properties, load-deformation tests are conducted in which the structure is loaded in the manner of interest and deformation of the structure is

measured and plotted as a function of the applied load (Martin et al. 2015). Up until a certain point, application of loading will produce nonpermanent, or elastic deformation. This part of the load-deformation curve usually shows a linear relationship. With increased loading, structures deform permanently (plastic deformation) and do not recover their original shape after the load is removed. The point at which the structure begins to plastically deform is the yield point. The highest load a structure can sustain before failure is the ultimate load. Finally, the point at which fracture occurs is the failure point. In cortical bone, the ultimate load and failure point usually coincide (Martin et al. 2015).

Several important properties can be determined by examination of the load-deformation curve (Frankel and Nordin 2012). The load the structure can sustain before failure is the strength; this can be taken as the yield point or the failure point. The stiffness of the structure is the load required to deform a structure a given amount; this can be calculated as the slope of the linear (constant) portion of the load-deformation curve. Finally, the energy the structure can store before failure is calculated as the area under the load-deformation curve up until the point of failure (Frankel and Nordin 2012). Energy is a quantitative property that is transferred to an object to perform work (Hall 2012). Work (W) is the product of force and distance (d): $W=Fd$.

A load-deformation curve can be converted into a stress-strain curve by applying appropriate formulas to convert load to stress and deformation to strain (Martin et al. 2015). This process can be used to determine material properties. Often, materials testing is carried out using coupons (specimens of standardized dimensions). Stress-strain curves are typically similar in shape to load-deformation curves, and similar properties can be determined from this curve. Material strength refers to the maximum stress a material can sustain before deformation or failure. Material stiffness is the amount of stress required to produce a certain amount of strain.

In simple solid materials, stress and strain are linearly proportional. For normal (compressive and tensile) loading, this relationship can be expressed as $E=\sigma/\varepsilon$, where E is a constant (Young's modulus). Stiffer materials such as glass have higher moduli whereas more ductile materials such as rubber have lower moduli. Finally, toughness refers to the amount of energy a material can absorb before failure and is calculated as the area under the stress-strain curve up until the point of failure (Martin et al. 2015).

Structure and properties of bones

Intrinsic factors related to the structural and material properties of bone influence how bone behaves in response to applied loads. Some properties of relevance include anisotropy and viscoelasticity. Bone is anisotropic, meaning it exhibits different mechanical properties depending on the direction of the applied force. Additionally, bone is viscoelastic, meaning its mechanical behavior is time dependent and varies depending on the rate of loading. The modulus of elasticity (Wright and Hayes 1976), ultimate strength (Carter and Hayes 1977) and fracture toughness (Kulin, Jiang, and Vecchio 2011) have all been shown to vary with the loading rate.

Bone structure is also important in understanding its mechanical responses. Bone is heterogenous and has a hierarchical structure. Currey (Currey 2012) describes four scales for examining bone structure: nanoscale (referring to the organic and inorganic building blocks of bone), microscale (referring to histological structures), mesoscale (referring to differences between cortical and trabecular bone tissue) and whole bone scale. The structure and properties at each of these levels may influence the mechanical behavior of whole bones.

At the nanoscale, bone is a composite material composed of tightly packed collagen fibrils, mineral crystals, and water (Ruppel, Miller, and Burr 2008; Currey 2012; Fratzl et al. 2004). Collagen fibrils (primarily Type I collagen) are thought to be oriented differently within

and throughout bone to enhance mechanical properties at specific sites (Ruppel, Miller, and Burr 2008). Mineral crystals (predominately carbonated hydroxyapatite) have been shown to have a plate-like organization, packed parallel to one another in the gaps between collagen fibrils (Fratzl et al. 2004; Eppell et al. 2001). Generally, these organic and inorganic components of bone are understood to affect material strength. Collagen contributes primarily to toughness, or the capacity of bone to absorb energy prior to fracture (Viguet-Carrin, Garnero, and Delmas 2005). Collagen denaturation significantly decreases the toughness of bone but has little effect on its stiffness (Wang et al. 2006). Meanwhile, mineral content affects the stiffness of bone (Viguet-Carrin, Garnero, and Delmas 2005). As mineral content increases, stiffness increases while toughness decreases (Currey 2012). Mineral has a higher elastic modulus than collagen, therefore more mineral produces less strain for a particular load. However, more mineralization might inhibit collagen from deforming. This may in turn prevent the formation of microcracks and leave bone more susceptible to catastrophic failure (Currey 2012). Various authors have suggested the formation of microcracks is an important toughening mechanism in bone (Nalla, Ager, and Ritchie 2005; Koester, Ager, and Ritchie 2008; Cheong et al. 2017).

At the microstructural level, there are several histological types of bone. Woven bone is found in fetal bone and in adult bone in the early stages of fracture repair. Produced quickly as osteoblasts lay down osteoid, it is composed of randomly arranged collagen fibers. Woven bone is mechanically weak (Currey 2012). It is eventually replaced by lamellar bone, which is highly organized, with parallel collagen fibers primarily organized into concentric sheets (lamellae). As bone remodels, osteoclasts resorb old bone and osteoblasts fill these channels with new bone, forming Haversian systems. Haversian systems, also known as secondary osteons, are composed of lamellar bone organized around a central (Haversian) canal containing blood vessels. They are

newer than surrounding interstitial bone, and therefore are less mineralized (Currey 2012). As such, increases in the proportion of secondary Haversian tissue are associated with significant decreases in ultimate strength, modulus of elasticity, and energy absorbing capacity (Wright and Hayes 1976). The presence of osteons also affects the path of failure (Behiri and Bonfield 1980). The cement lines that separate Haversian systems from surrounding interstitial bone represent a stress discontinuity that directs crack formation (Currey 2012). Cracks tend to travel between osteons, parallel to the long axis of the bone (Behiri and Bonfield 1989). Koester et al. (Koester, Ager, and Ritchie 2008) found that microcracks formed at cement lines and travelled longitudinally regardless of loading orientation.

At the mesoscale, bone is composed of two types of tissue: cortical (compact) bone and trabecular (cancellous) bone. Cortical bone is composed of lamellar bone and comprises the smooth, hard outer cortex of the skeletal elements. Trabecular bone comprises the inner layer of these elements, and is found at the ends of long bones, within flat bones like those of the cranium, and within vertebral bodies. Trabecular bone has a spongy appearance, consisting of a lattice of bony rods and plates that provide a framework for bone marrow (Oftadeh et al. 2015). The relative amount of cortical bone to trabecular bone varies among and within individual bones, according to functional requirements (Carter and Spengler 1978). The classification of bone as cortical or trabecular is somewhat arbitrary and primarily based on porosity (Currey 2012). The porosity of cortical bone ranges from 5 to 30%, while trabecular bone porosity ranges from 30 to 90% (Carter and Spengler 1978). Research has shown that the mechanical properties of cortical and cancellous bone are different and cannot be extrapolated from one another (Rice, Cowin, and Bowman 1988). It can be difficult to measure properties of trabeculae due to their small size and because it is an extremely heterogenous material whose properties depend on the

anatomical site being tested (Ciarelli et al. 1991; Oftadeh et al. 2015; Currey 2012). However, apparent density (the product of bone volume fraction and bone tissue density) strongly influences the elastic modulus and strength of trabecular bone (Rice, Cowin, and Bowman 1988; Ciarelli et al. 1991). Because trabecular bone is less dense and less mineralized than cortical bone, it is more flexible (exhibits lower stiffness) and weaker (exhibits lower mechanical strength) than cortical bone (Rice, Cowin, and Bowman 1988; Ciarelli et al. 1991; Rho, Ashman, and Turner 1993). Importantly, cortical bone exhibits greater mechanical strength in compression compared to tension (Reilly and Burstein 1975) and is therefore expected to fail in tension before compression.

Whole bone geometry is also important to consider. The structure and function of the cranial vault, for example, differs from the structure and function of the femur. The primary function of the cranial vault is to protect the brain. It is a three-layered structure composed of an inner endosteal table and an outer periosteal table sandwiching a diploe layer. The inner and outer tables are composed of relatively rigid cortical bone, while the diploe layer is structurally soft and is composed of trabecular bone and blood vessels (Yoganandan and Pintar 2004; Gurdjian 1975). The outer table, which is externally oriented and bears muscular loads, is generally thicker, denser, and stiffer than the inner table (Boruah et al. 2015; Peterson and Dechow 2002; Gurdjian 1975). In contrast, the inner table, which experiences stresses primarily from intracerebral pressures transmitted through the dura, is thinner, less dense, and more compliant (Peterson and Dechow 2002).

In contrast, the primary functions of the femur involve support and facilitation of muscle attachment and movement. Femoral structure largely reflects the loading to which the bone is exposed: compression and bending. Standing, walking, and other activities tend to impart axial

compression. Due to the anterior curvature of the femoral shaft, this produces a net bending moment acting on the diaphysis. The proximal and distal articular surfaces are composed of trabecular bone covered by a thin cortex. The trabeculae here are thought to direct large loads away from the joint and into the cortical bone (Currey 2012). The roughly tubular diaphysis is composed of dense cortical bone that is relatively strong when loaded axially compared to transversely (Reilly and Burstein 1975). The tubular structure of the diaphysis also serves to increase resistance to bending (Frankel and Nordin 2012). Compared to the alternative of a solid cylinder, a tubular configuration increases the distance of the bone's mass from the neutral axis. This increases the moment of inertia, which in turn increases the bending strength and stiffness (Frankel and Nordin 2012).

Finally, various factors on the level of the individual including sex, age, pathological conditions, health status, or drug use may affect bone structure on any of these levels, which may in turn affect bone behavior.

Interpretive Theory

Biomechanical principles provide the foundational theory for trauma analysis. Meanwhile, casework and research help to establish interpretive theories: the means by which analysts transform observations of fracture patterns into inferential statements about their cause. Research is particularly important in this regard: it provides a means of hypothesis testing, as well as a "database" for recognizing and interpreting patterns of trauma in individual forensic cases (Boyd and Boyd 2018).

Berryman et al. (Berryman, Berryman, and Saul 2018) propose the "fracture assessment triad" as a framework for hypothesis building in trauma analysis and research. They divide the information necessary to interpret skeletal trauma into three categories: extrinsic factors, intrinsic

factors, and fracture behavior. Extrinsic factors include those such as the direction and magnitude of the force, the velocity of the impact, the mass, and the area over which force was applied. Intrinsic factors include those related to the various scales of bone structure, anatomical features such as sutures, foramina, and processes, and individual influences such as age and pathology. Finally, fracture behavior includes observable features such as the angle, location, and shape of fracture (Berryman, Berryman, and Saul 2018). Given two items in the triad, the third can be logically inferred using deductive reasoning. Inferences about extrinsic factors are often the target in trauma analysis, as these are related to the cause of the trauma. While the fracture assessment triad presents a framework for hypothesis building, research is necessary to inform, test, refine, and retest these hypotheses.

Casework is one means by which anthropologists establish interpretive theory in trauma analysis. The interpretation of fractures as part of trauma analysis is itself an act of hypothesis formation. For example, an analyst may observe fracture patterns exhibiting plastic deformation and, based on knowledge of the viscoelastic properties of bone, form a hypothesis that the fracture was caused by the application of a low-velocity impact. Publication of case studies has been important in advancing understanding of skeletal trauma. Inductive case studies are "theory in their own right" (Boyd and Boyd 2011; Dobres and Robb 2005) and can suggest new ways to evaluate and interpret data. As an example, Fenton et al. (Fenton, DeJong, and Haut 2003) present a case study template for a collaborative anthropology, pathology, and biomechanics approach in assessing whether a particular set of circumstances (a punch to the head) could have caused a particular observed pattern of cranial fractures. The template this case study provided can and has subsequently been applied to assess other forensic cases.

Case studies also represent an important form of trauma research. Examination of larger samples of forensic or clinical cases can provide evidence in support or rejection of a hypothesis and help to refine or form new hypotheses. Hart (Hart 2005) investigated the hypothesis that cranial concentric fractures caused by blunt force and gunshot trauma can be differentiated on the basis of beveling direction. This hypothesis was informed through expectations based on biomechanical principles and supported in a study carried out on a sample of forensic cases (n=120). Case studies can also be used to explore patterns of trauma produced in different injury scenarios. Guyomarc'h et al. (Guyomarc'h et al. 2010) investigated the hypothesis that cranial trauma produced in fatal falls could be differentiated from homicidal blunt force blows in a sample of forensic cases (n=113). They find support for previously proposed criteria (e.g. lateralization of injuries and fracture length) and refine the original hypothesis by suggesting new criteria (e.g. cranial fracture type and the presence of postcranial trauma).

Advantages of case studies are that they include real injury scenarios and forensic populations, and are therefore relevant to the contexts encountered in future, unknown cases. However, a disadvantage of this retrospective approach is that extrinsic variables of interest – for example, the magnitude and direction of force or the velocity of the impact – are not controlled, cannot be directly measured, and may remain unknown in the absence of detailed witness accounts. Therefore, retrospective, case-based approaches offer incomplete means of hypothesis testing how and why particular fractures form in response to particular independent variables.

Recently, anthropologists have addressed this problem using prospective, experimental approaches. Experimental research provides the advantage of investigating fracture patterns generated under known, replicable, laboratory-controlled conditions. Impact testing provides an

important means of relating known input parameters to resultant fracture behavior including mechanical response, fracture formation, and fracture patterns.

The most successful of these studies have applied theory and methodology from biomechanics research. The subfield of injury biomechanics in particular shares common interests with anthropological trauma analysis. Aims of injury biomechanics include identifying and explaining injury mechanisms, quantifying the mechanical response of the body and its components to impact, determining tolerance to impact, and evaluating safety and prevention methods (King 2015). The automotive industry has supported a variety of research aimed at the derivation of injury tolerance criteria in order to develop safety standards and design and evaluate the biofidelity of anthropomorphic test dummies (Bass and Yoganandan 2015; Yoganandan and Pintar 2004). While there is a clear overlap between anthropology and biomechanics, the two fields study fractures in very different contexts. Typically, biomechanics-driven research focuses on determining the point at which fracture occurs and does not provide detailed information about fracture patterns. Additionally, much of this research has taken place in the context of car crashes. In contrast, anthropologists are most interested in *how* bones fracture in a variety of contexts (Berryman, Berryman, and Saul 2018).

One issue in experimental trauma studies is the selection of appropriate models. Various models have been explored including animal, synthetic, and human material. To date, most experimental studies of fracture patterns have involved nonhuman models (e.g., Powell et al. 2012, 2013; Vaughan et al. 2016; Wheatley 2008; Reber and Simmons 2015; Cohen et al. 2016). Nonhuman bone is often used as a proxy for human bone (Zephro, Galloway, and Wedel 2014). Porcine bone is commonly used because it is thought to approximate various properties of human bone (Pearce et al. 2007; Aerssens et al. 1998). The use of animal models is advantageous in that

specimens are relatively easy and relatively inexpensive to acquire, allowing for data collection on large samples. However, due to structural and compositional differences between nonhuman and human bones, it is often unclear how the results of such experiments scale to human subjects. Additionally, species is an important factor to consider, as studies have shown differences in structural and material properties between human bone and various types of mammalian bone (Aerssens et al. 1998; Wang, Mabrey, and Agrawal 1998).

Some researchers have investigated the use of synthetic material such as polyurethane. Examples include the work of Khalil et al. (Khalil, Raymond, and Miller 2015) on synthetic tibia and Smith et al. (Smith et al. 2015) and Ruchonnet et al. (Ruchonnet et al. 2019) on synthetic crania. An advantage of synthetic bones is that they are uniform, theoretically reducing the influences of intrinsic variation on fracture patterns. Another advantage is that they are relatively easy to acquire, and do not present ethical issues or logistical obstacles. This is especially important in countries where current legislation limits or prohibits research on human remains. However, a disadvantage is that synthetic materials do not exhibit the same micro- or macrostructure as bone. Synthetic crania, for example, consist of simple spheres and lack relevant features such as cranial sutures. Additionally, while bone has a heterogenous microstructure, the microstructure of polyurethane is much more uniform. Smith et al. (Smith et al. 2015) report that while gross features of fracture generated in synthetic crania were similar to those observed in bone, finer details differed.

Experiments on human material in a fresh-frozen state are thought to provide the best analogies to bone behavior in living human subjects (Kroman and Symes 2013; Yoganandan and Pintar 2004). However, this type of material is often difficult and expensive to obtain. As such, relatively few anthropology-driven experimental studies of skeletal trauma have involved human

material. Notable exceptions include the work of Kroman (Kroman 2007) on various segments of the body, Kroman and colleagues (Kroman, Kress, and Porta 2011) on the human cranium, Daegling et al. (Daegling et al. 2008) on human ribs, and the ongoing work of Agnew, Harden, and colleagues (Harden et al. 2019; Agnew et al. 2020) on rib fracture. Kroman's dissertation (Kroman 2007) presents an important example of the contribution of experimental trauma research to the development of interpretive theory. This research helped spur a shift toward understanding trauma along a biomechanical continuum rather than within discrete categories of injuries, and refined hypotheses regarding the importance of the extrinsic variables of force, surface area, and acceleration. However, there is still much work to be done to explore how these variables and others affect fracture formation in various regions of the skeleton.

Methodological Theory

In trauma analysis, methodological theories include the reasons that inform the use of certain protocols or systems of collecting and analyzing data from fracture patterns. Methodology guides how observations are made and which data are collected, and therefore plays an important role in determining the interpretations that can be made. Best practice documents such as the one produced by the Scientific Working Group for Forensic Anthropology (SWGANTH 2011) present some procedures for describing, documenting, and interpreting skeletal trauma. However, these guidelines are limited to classifying trauma timing and mechanism and outlining unacceptable practices. They do not provide guidelines for identifying evidence of and making interpretations about higher resolution issues such as the direction, location, or minimum number of blunt force impacts.

The identification and selection of fracture features for use in these higher resolution interpretations present an area in need of critical investigation. L'Abbé et al. (L'Abbé et al. 2019)

highlight the problem of nomenclature based on comparative morphology. Historically, trauma analyses have been undertaken in close proximity to a medical context. Forensic anthropologists deliver reports to the medicolegal authority on a case, often a medically trained forensic pathologist. Therefore, the type, scale, and nomenclature anthropologists use to describe – and ultimately interpret – fractures have traditionally mirrored those used to describe clinical injuries. This can present problems, as clinical injuries are often studied two-dimensionally using radiological images, whereas trauma analysis is conducted in three dimensions on whole bones (L'Abbé et al. 2019). The use of categories such as "butterfly fractures" to describe fracture morphology may actually inhibit correct interpretation of their cause. Various circumstances – including blunt force and gunshot impacts – can produce similar gross fracture patterns. Instead, L'Abbé et al. (L'Abbé et al. 2019) and others (e.g., Symes et al. 2012; Berryman, Berryman, and Saul 2018; Kroman and Symes 2013) encourage analysts to identify features of bone failure in tension, shear, and compression. These units of analysis can be used to interpret stresses across a structure and reconstruct how and where a bone failed. However, other units of analysis have also been proposed including fracture angle (Reber and Simmons 2015), "incomplete" fracture patterns (Fenton et al. 2012) and recently, fractography (Christensen et al. 2018).

Methodological issues are also relevant to why experimental research undertaken in injury biomechanics may be of limited use for anthropological trauma analyses. Namely, there is a mismatch between the scale and units of analysis applied to describe injuries in these studies and those used to interpret skeletal trauma in anthropology cases. Experimental injury biomechanics research has focused largely on the presence/absence and severity of fracture. Many studies use the Abbreviated Injury Scale (AIS), an anatomical coding system developed by the Association for the Advancement of Automotive Medicine to classify and describe injuries

by type, location, and severity (Gennarelli and Wodzin 2006). However, this framework includes injuries to soft tissue as well as bone and provides little information on fracture morphology. When fracture patterns are described, they are often focused on gross morphology (Kress et al. 1995; Porta et al. 1999; Frick 2003; Martens et al. 1986).

Based on the issues outlined here, there is a need for research aimed at documenting how and where fractures form with respect to input variables of interest, and evaluating the utility of various fracture features for reconstructing these variables. Given the various systems available, it would also be useful to compare various units of analysis within the same sample.

Anthropological Applications of Trauma Research and Analysis

Trauma research has applications in modern, forensic cases as well as in the archaeological record. Skeletal trauma is of anthropological interest in that it represents direct evidence of human behaviors and interactions. Reconstruction of these behaviors has been described as a two stage process (Walker 2001). The first stage is identifying the proximate cause of – in other words, the mechanical and biological processes responsible for – the trauma. This involves making assessments about the mechanism of injury, the type and direction of loading, the locations and minimum number of impacts, the intensity of an impact, and characteristics of the impact surface. The second stage is identifying the ultimate cause. This involves reconstructing the physical and sociocultural context of the trauma and hypothesizing possible behaviors and intentions (Walker 2001). This dissertation addresses issues related to the resolution of proximate cause. Accurate assessments of proximate cause are necessary to ground consequential interpretations of ultimate cause.

In forensic cases, assessment of the proximate cause of skeletal fractures along with information about the scene and material context allows practitioners to evaluate hypotheses for

the ultimate cause. One way of conceptualizing ultimate cause is the manner of death, the medicolegal classification of a death as natural, accident, suicide, homicide, or undetermined. This designation directs how a case is investigated and potentially prosecuted. Information about the proximate cause of trauma can help inform the medicolegal authority's determination of manner of death. Multiple, high-energy cranial impacts involving a small, focal surface (proximate cause) may suggest the action of an assailant (i.e., a homicide) rather than the result of self-inflicted injuries (i.e., a suicide). If a decedent presents with extensive lower limb fractures, reconstruction of loading direction may help differentiate vertical deceleration injuries consistent with a jump or a fall from horizontal deceleration injuries consistent with a pedestrian-vehicle collision (Rockhold and Hermann 1999; Crowder and Adams 2014; Tersigni-Tarrant 2015). This information in concert with the physical context of the remains – e.g., recovery location and material evidence – would provide additional data to support one hypothesis over another. Proximate cause can also be evaluated against witness statements in order to shed light on the ultimate cause. In pediatric cases, inconsistencies between the pattern and severity of injuries and the caregiver's explanation raise suspicion of child abuse (Christian and Committee on Child Abuse and Neglect 2015).

In nonmodern contexts, the ultimate cause of skeletal trauma is open to broader interpretation. With the potential exceptions of historically documented cases, interpretations cannot be verified against witness accounts or through crime scene investigation as in forensic cases. The timing, pattern, and extent of trauma and the archaeological and taphonomic contexts are used to determine the most probable range of proximate causes. Subsequent reconstruction of the ultimate cause requires careful sociocultural and historical contextualization and consideration of several plausible alternate hypotheses. Broadly, hypotheses for the ultimate

cause of trauma include a non-human agent, a self-inflicted incident, an accident inflicted by another person, or an intentional act inflicted by another person (Trinkaus and Buzhilova 2012). Within this last category, a possible interpretation is violence.

Definitions of violence tend to focus on intentional physical force involving direct, person-on-person activities, however violence can take other forms (Martin and Harrod 2015). Martin and Osterholtz define violence as a "diverse set of bioculturally embedded processes that employ power and force to harm others through physical violence and death, and through non-lethal tactics involving intimidation, pain, domination, fear, and subordination (often through symbolism), or through structural violence and the restriction of access to necessary resources" (Martin and Osterholtz 2016, 472). Unlike other social science disciplines, which tend to view violence as abnormal and aberrant behavior, anthropology views violence as a culturally mediated form of complex social behavior (Martin and Harrod 2015, 118). Anthropologists are therefore well positioned to study violence in its various forms and culturally and historically contingent meanings. Inter-group violence includes warfare, raiding, feuding, ambushes, captive taking and slavery, and other activities. Intra-group violence occurs between family members, intimates, acquaintances, or strangers in the same cultural group (Martin and Harrod 2015). Research on intra-group violence includes studies of gendered violence (Stone 2012) and violence against children (Gaither 2012). Other areas of emerging scholarship include structural violence (Klaus 2012; de la Cova 2012) and the symbolic role of violence in ritual performance (Pérez 2012; Jones, Walsh-Haney, and Quinn 2015).

The interpretation of trauma in the archaeological record typically takes a differential diagnosis approach used in paleopathology (Judd and Redfern 2012; Lovell and Grauer 2019). Fracture patterns are considered, the points for and against several alternative diagnoses are

evaluated, and a conclusion is proposed. These differential diagnoses often draw heavily on clinical literature, with modern data used as a baseline from which to extrapolate ancient behaviors (Judd and Redfern 2012; Lovell and Grauer 2019). Clinical data can be useful for establishing patterns of known accidental versus intentional injuries, but present limitations. Changes in technologies used in warfare, transportation, and other aspects of daily life make it difficult to extrapolate the causes of trauma in the archaeological record from modern causes (Judd and Redfern 2012). Furthermore, clinical studies tend to use eponyms and/or prioritize location and two-dimensional morphology to describe fracture patterns. This can inhibit interpretation by obfuscating biomechanical processes (L'Abbé et al. 2019; Caldwell, Shorten, and Morrell 2019). Consider parry fractures, transverse fractures of the distal ulna without involvement of the radius (Judd 2008). These can form when an individual uses a forearm to deflect a blow from an attack. As such, distal ulna fractures are often interpreted as defensive injuries and used to infer violence (Judd 2008; Spencer 2012). However, these fractures can also originate from a fall or other accident. Therefore, the presence of a transverse distal ulna fracture is not in itself diagnostic (Judd 2008).

Along with clinical data, a biomechanical approach can help clarify the proximate cause of trauma and aid with differential diagnoses of ultimate cause. Continuing with the parry fracture example, information about mechanical variables such as the direction of loading could help weigh alternative diagnoses. Similarly, interpretations about other variables such as the implement, number, and severity of impacts have been used as evidence in support of a differential diagnosis of violence. The presence of fractures attributable to weapons is often cited as evidence of interpersonal violence (Kanz and Grossschmidt 2006; Jordana et al. 2009; Murphy et al. 2010; Nagaoka 2012; Spencer 2012). Recent studies have used experimental

approaches to investigate fracture patterns produced with historical and ancient weapons (e.g., Gordón and Bosio 2012; Downing and Fibiger 2017; Dyer and Fibiger 2017; Forsom and Smith 2017). These studies demonstrate the benefit of experimental data for evaluating ancient trauma. Beyond weapon wounds, extensive fragmentation has been interpreted as evidence of multiple cranial blows, and in turn, evidence of violence (Spencer 2012). Similarly, the severity of fracture has been used to suggest "extreme force" and support an interpretation of violence (Robbins Schug et al. 2012, 140). These interpretations could be strengthened with baseline data connecting fracture patterns with known mechanical variables.

Summary and Objectives

In recent decades, trauma analysis has become a routine part of forensic anthropology casework. While timing and mechanism of fracture form the basic components of trauma analysis, anthropologists are often required to make higher resolution interpretations about factors such as the point or direction of impact, the minimum number and sequence of impacts, the energy involved, and characteristics of potential tools or objects used. However, forensic anthropologists currently operate without standard guidelines or methods to assist in reconstructing these details. This is an area of weakness considering recent calls for validation of basic premises and techniques in the forensic sciences (NAS 2009). Bioarchaeological and paleoanthropological studies also apply forensic methods of trauma analysis to make broader interpretations about complex social behaviors, human-environment interactions, and site formation processes. Experimental research aimed at documenting fracture formation and critically evaluating methodological strategies is needed to improve, inform, and provide new tools for determining the biomechanical causes of skeletal trauma.

This dissertation investigates the relationship between various independent extrinsic variables and fracture behavior in a series of blunt force impact experiments. Applying the multi-level theoretical framework proposed by Berryman and colleagues, biomechanics serves as the high-level theory that is used to explain and hypothesize relationships between input variables and fracture behavior. Impact experiments are used to test hypotheses regarding these relationships, thereby contributing to the formation of interpretive theory connecting fracture patterns to their causes. Finally, this research addresses current methodological theories in trauma analysis, documenting fracture features according to various units of analysis.

In order to maximize applicability to living subjects, the current experiments use crania and femora obtained from unembalmed postmortem human subjects (PMHS) in the perimortem interval. Biomechanical methods of experimentation are used to produce fractures and monitor mechanical responses. Three primary goals form the general approach of this project: 1) to investigate fracture behavior including mechanical response, fracture initiation and propagation, and various features of the resultant fracture patterns; 2) to document these results in relation to independent variables including point, direction, and number of impacts, impact surface area, and input energy; and 3) to evaluate fracture features described in reference literature and gather evidence of their utility in reconstructing these variables.

Part one (Papers 1-3) investigates questions related to cranial fracture produced in blunt force lateral head impacts. Independent variables explored in this section include the location and number of impacts, the shape of the impact surface, and the kinetic energy of the impact. Paper 1 investigates how and where cranial fractures form relative to the point of impact, as well as how impact surface shape influences this process. Paper 2 addresses the issues of identifying and sequencing impact sites in cases involving multiple impacts. Specifically, the effects of impact

surface shape and impact number on the type and location of cranial fractures are explored. Finally, Paper 3 explores the effects of impact surface shape and kinetic energy. These papers use skeletal material, photographs, diagrams, force-time-displacement impact data, and high-speed video generated in 48 cranial impact experiments on 24 heads. Experiments were conducted from 2016 to 2018 as part of a National Institute of Justice grant (Award No. 2015-DN-BX-K013) titled "Building a Science of Adult Cranial Fracture."

Part two (Papers 4 and 5) investigates the effects of impact direction on femur fractures produced in bending. Various units of analysis are explored including complete fractures, incomplete fractures, fracture surface morphology, and fractography. Paper 4 investigates 3-point bending with axial compression, an impact configuration designed to simulate an impact to a standing individual. Meanwhile, Paper 5 investigates more complex fracture patterns produced in concentrated 4-point bending. These studies use skeletal materials, photographs, diagrams, mechanical data, and high-speed video generated in 22 bending experiments.

REFERENCES

REFERENCES

Aerssens, J., S. Boonen, G. Lowet, and J. Dequeker. 1998. "Interpsecies Differences in Bone Composition, Density, and Quality: Potential Implications for in Vivo Bone Research." *Endocrinology* 139 (2): 663–70.

Agnew, A.M., A.L. Harden, S. Akshara, J.H. Bolte IV, and Y. Kang. 2020. "Rib Fractures: An Experimental Approach to Identifying Intrinsic Sources of Variability." In *Proceedings of the 72nd American Academy of Forensic Sciences Annual Scientific Meeting*, 165. Anaheim, CA: American Academy of Forensic Sciences.

Angel, J.L., and P.C. Caldwell. 1984. "Death by Strangulation: A Forensic Anthropological Case from Wilmington, Delaware." In *Human Identification: Case Studies in Forensic Anthropology*, edited by T.A. Rathbun and J.E. Buikstra, 168–75. Springfield, IL: Charles C. Thomas.

Bass, C.R., and N. Yoganandan. 2015. "Skull and Facial Bone Injury Biomechanics." In *Accidental Injury: Biomechanics and Prevention*, edited by N. Yoganandan, A.M. Nahum, and J.W. Melvin, 203–20. New York: Springer-Verlag.

Behiri, J.C., and W. Bonfield. 1980. "Crack Velocity Dependence of Longitudinal Fracture in Bone." *Journal of Materials Science* 15: 1841–49.

Behiri, J.C., and W. Bonfield. 1989. "Orientation Dependence of the Fracture Mechanics of Cortical Bone." *Journal of Biomechanics* 22 (8): 863–72.

Berryman, H.E., J.F. Berryman, and T.B. Saul. 2018. "Bone Trauma Analysis in a Forensic Setting: Theoretical Basis and a Practical Approach for Evaluation." In *Forensic Anthropology: Theoretical Framework and Scientific Basis*, edited by C.C. Boyd and D.C. Boyd, 213–34. Chichester, West Sussex, UK: John Wiley & Sons Ltd.

Berryman, H.E., A.K. Lanfear, and N.R. Shirley. 2012. "The Biomechanics of Gunshot Trauma to Bone: Research Considerations within the Present Judicial Climate." In *A Companion to Forensic Anthropology*, edited by D.C. Dirkmaat, 390–99. Chichester, West Sussex, UK: Blackwell Publishing, Ltd.

Berryman, H.E., and S.A. Symes. 1998. "Recognizing Gunshot and Blunt Cranial Trauma Through Fracture Interpretation." In *Forensic Osteology: Advances in the Identification of Human Remains*, edited by Kathleen J. Reichs, 2nd ed., 333–52. Springfield, IL: Charles C. Thomas.

Berryman, H.E., S.A. Symes, O.C. Smith, and S.J. Moore. 1991. "Bone Fracture II: Gross Examination of Fractures." In *Proceedings of the 43rd Annual Meeting of the American Academy of Forensic Sciences*. Anaheim, CA.

Boruah, S., G.R. Paskoff, B.S. Shender, D.L. Subit, R.S. Salzar, and J.R. Crandall. 2015. "Variation of Bone Layer Thicknesses and Trabecular Volume Fraction in the Adult Male Human Calvarium." *Bone* 77: 120–34.

Boyd, C.C., and D.C. Boyd. 2011. "Theory and the Scientific Basis for Forensic Anthropology." *Journal of Forensic Sciences* 56 (6): 1407–15.

Boyd, C.C., and D.C. Boyd. 2018. "The Theoretical and Scientific Foundations of Forensic Anthropology." In *Forensic Anthropology: Theoretical Framework and Scientific Basis2*, edited by C.C. Boyd and D.C. Boyd, 1–18. Chichester, West Sussex, UK: John Wiley & Sons, Inc.

Caldwell, R.A., P.L. Shorten, and N.T. Morrell. 2019. "Common Upper Extremity Fracture Eponyms: A Look Into What They Really Mean." *Journal of Hand Surgery* 44 (4): 331–34.

Camarós, E., M. Cueto, C. Lorenzo, V. Villaverde, and F. Rivals. 2016. "Large Carnivore Attacks on Hominins during the Pleistocene: A Forensic Approach with a Neanderthal Example." *Archaeological and Anthropological Sciences* 8 (3): 635–46.

Carter, D.R., and W.C. Hayes. 1977. "The Compressive Behavior of Bone as a Two-Phase Porous Structure." *Journal of Bone and Joint Surgery* 59 (7): 954–62.

Carter, D.R., and D.M. Spengler. 1978. "Mechanical Properties and Composition of Cortical Bone." *Clinical Orthopaedics and Related Research* 135: 192–217.

Cheong, V.S., A. Karunaratne, A.A. Amis, and A.M.J. Bull. 2017. "Strain Rate Dependency of Fractures of Immature Bone." *Journal of the Mechanical Behavior of Biomedical Materials2* 66: 68–76.

Christensen, A.M., J.T. Hefner, M. Smith, J. Webb, M. Bottrell, and T.W. Fenton. 2018. "Forensic Fractography of Bone." *Forensic Anthropology* 1 (1): 32–51.

Christensen, A.M., N.V. Passalacqua, and E.J. Bartelink. 2014. "Analysis of Skeletal Trauma." In *Forensic Anthropology: Current Methods and Practice*, edited by A.M. Christensen, N.V. Passalacqua, and E.J. Bartelink, 344–71. Oxford: Elsevier Inc.

Christian, C.W., and Committee on Child Abuse and Neglect. 2015. "The Evaluation of Suspected Child Physical Abuse." *Pediatrics* 135 (5): e1337–54.

Churchill, S.E., R.G. Franciscus, H.A. McKean-Peraza, J.A. Daniel, and B.R. Warren. 2009. "Shanidar 3 Neandertal Rib Puncture Wound and Paleolithic Weaponry." *Journal of Human Evolution* 57 (2): 163–78.

Ciarelli, M.J., S.A. Goldstein, J.L. Kuh, D.D. Cody, and M.B. Brown. 1991. "Evaluation of Orthogonal Mechanical Properties and Density of Human Trabecular Bone from the Major Metaphyseal Regions with Materials Testing and Computed Tomography." *Journal of*

Orthopaedic Research 9: 674–82.

Cohen, H., C. Kugel, H. May, B. Medlej, D. Stein, V. Slon, I. Hershkovitz, and T. Brosh. 2016. "The Impact Velocity and Bone Fracture Pattern: Forensic Perspective." *Forensic Science International* 266: 54–62.

Crowder, C.M., and B.J. Adams. 2014. "Interpreting Blunt Force Trauma: A Case Report." In *Broken Bones: Anthropological Analysis of Blunt Force Trauma*, edited by V.L. Wedel and A. Galloway, 2nd ed., 314–26. Springfield, IL: Charles C. Thomas.

Currey, J.D. 2012. "The Structure and Mechanics of Bone." *Journal of Materials Science* 47: 41–54.

Daegling, D.J., M.W. Warren, J.L. Holtzman, and C.J. Self. 2008. "Structural Analysis of Human Rib Fracture and Implications for Forensic Interpretations." *Journal of Forensic Sciences* 53 (6): 1301–7.

Daubert v. Merrill Dow Pharmaceuticals, Inc. 1993, 509 U.S.57.

de la Cova, C. 2012. "Patterns of Trauma and Violence in 19th-Century-Born African American and Euro-American Females." *International Journal of Paleopathology* 2: 61–68.

Dobres, M.A., and J.E. Robb. 2005. "'Doing' Agency: Introductory Remarks on Methodology." *Journal of Archaeological Method and Theory* 12 (3): 159–66.

Domett, K.M., and N. Tayles. 2006. "Adult Fracture Patterns in Prehistoric Thailand: A Biocultural Interpretation." *International Journal of Osteoarchaeology* 16 (3): 185–99.

Downing, M., and L. Fibiger. 2017. "An Experimental Investigation of Sharp Force Skeletal Trauma with Replica Bronze Age Weapons." *Journal of Archaeological Science: Reports* 11: 546–54.

Dyer, M., and L. Fibiger. 2017. "Understanding Blunt Force Trauma and Violence in Neolithic Europe: The First Experiments Using a Skin-Skull-Brain Model and the Thames Beater." *Antiquity* 91 (360): 1515–28.

Eppell, S.J., W. Tong, J.L. Katz, L. Kuhn, and M.J. Glimcher. 2001. "Shape and Size of Isolated Bone Mineralities Measured Using Atomic Force Microscopy." *Journal of Orthopaedic Research* 19: 1027–34.

Fenton, T.W., J.L. DeJong, and R.C. Haut. 2003. "Punched with a Fist: The Etiology of a Fatal Depressed Cranial Fracture." *Journal of Forensic Sciences* 48 (2): 227–81.

Fenton, T.W., A.E. Kendell, T.S. DeLand, and R.C. Haut. 2012. "Determination of Impact Direction Based on Fracture Patterns in Long Bones." In *Proceedings of the 64th Annual Meeting of the American Academy of Forensic Sciences*. Atlanta, GA.

Forsom, E., and M.J. Smith. 2017. “Getting to the Point: An Experimental Approach to Improving the Identification of Penetrating Projectile Trauma to Bone Caused by Medieval Arrows.” *Journal of Archaeological Science: Reports* 11: 274–86.

Frankel, V.H., and M. Nordin. 2012. “Biomechanics of Bone.” In *Basic Biomechanics of the Musculoskeletal System*, edited by M. Nordin and V.H. Frankel, 4th ed., 24–59. Baltimore, MD: Lippincott Williams & Wilkins.

Fratzl, P., H.S. Gupta, E.P. Paschalis, and P. Roschger. 2004. “Structure and Mechanical Quality of the Collagen-Mineral Nano-Composite in Bone.” *Journal of Materials Chemistry*, no. 14: 2115–23.

Frayer, D.W., and J.G. Bridgens. 1985. “Stab Wounds and Personal Identity Determined from Skeletal Remains: A Case from Kansas.” *Journal of Forensic Sciences* 30: 232–38.

Frick, S.J. 2003. “The Effects of Combined Torsion and Bending Loads on Fresh Human Cadaver Femurs.” University of Louisville, Louisville KY.

Frye v. United States. 1923, 293F, 1013.

Fung, Y.C. 1993. *Biomechanics: Mechanical Properties of Living Tissues*. 2nd ed. New York: Springer Science+Business Media.

Gaither, C. 2012. “Cultural Conflict and the Impact on Non-Adults at Puruchuco-Huaquerones in Peru: The Case for Refinement of the Methods Used to Analyze Violence against Children in the Archeological Record.” *International Journal of Paleopathology* 2 (2–3): 69–77.

Galloway, A. 1999. *Broken Bones*. Edited by A. Galloway. 1st ed. Springfield, IL: Charles C. Thomas.

Gennarelli, T.A., and E. Wodzin. 2006. “AIS 2005: A Contemporary Injury Scale.” *Injury* 37 (2): 1083–91.

Gordón, F., and L.A. Bosio. 2012. “An Experimental Approach to the Study of Interpresonal Violence in Northeastern Patagonia (Argentina), during the Late Holocene.” *Journal of Archaeological Science* 39 (3): 640–47.

Gurdjian, E.S. 1975. *Impact Head Injury*. Springfield, IL: Charles C. Thomas.

Guyomarc’h, P., M. Campagna-Vaillancourt, C. Kremer, and A. Sauvageau. 2010. “Discrimination of Falls and Blows in Blunt Head Trauma: A Multi-Criteria Approach.” *Journal of Forensic Sciences* 55 (2): 423–27.

Hall, S.J. 2012. *Basic Biomechanics*. 6th ed. New York: McGraw-Hill.

Harden, A.L., Y. Kang, K. Moorhouse, J. Stammen, and A. Agnew. 2019. “Human Rib Fracture Characteristics and Relationships with Structural Properties.” In *International Research*

Council on Biomechanics of Injury (IRCOBI), 465–74. Florence, Italy.

Hart, G.O. 2005. "Fracture Pattern Interpretation in the Skull: Differentiating Blunt Force from Ballistics Trauma Using Concentric Fractures." *Journal of Forensic Sciences* 50 (6): 1–6.

Hatze, H. 1974. "The Meaning of the Term 'Biomechanics.'" *Journal of Biomechanics* 7: 189–90.

Jones, S., H. Walsh-Haney, and R. Quinn. 2015. "Kana Tamata or Feasts of Men: An Interdisciplinary Approach for Identifying Cannibalism in Prehistoric Fiji." *International Journal of Osteoarchaeology* 25 (2): 127–45.

Jordana, X., I. Galtés, T. Turbat, D. Batsukh, C. García, A. Isidro, P.H. Giscard, and A. Malgosa. 2009. "The Warriors of the Steppes: Osteological Evidence of Warfare and Violence from Pazyryk Tumuli in the Mongolian Altai." *Journal of Archaeological Science* 36 (7): 1319–27.

Judd, M.A. 2008. "The Parry Problem." *Journal of Archaeological Science* 35 (6): 1658–66.

Judd, M.A., and R. Redfern. 2012. "Trauma." In *A Companion to Paleopathology*, edited by A.L. Grauer, 1st ed., 359–79. Blackwell Publishing Ltd.

Kanz, F., and K. Grossschmidt. 2006. "Head Injuries of Roman Gladiators." *Forensic Science International* 160 (2–3): 207–16.

Kappelman, J., R.A. Ketcham, S. Pearce, L. Todd, W. Akins, M.W. Colbert, M. Feseha, J.A. Maisano, and A. Witzel. 2016. "Perimortem Fractures in Lucy Suggest Mortality from Fall out of Tall Tree." *Nature* 537 (7621): 503–7.

Kerley, E.R. 1976. "Forensic Anthropology and Crimes Involving Children." *Journal of Forensic Sciences* 21 (2): 333–39.

Kerley, E.R. 1978. "Identification of Battered-Infant Skeletons." *Journal of Forensic Sciences* 23 (1): 163–68.

Khalil, A., D. Raymond, and E.A. Miller. 2015. "An Analysis of Butterfly Fracture Propagation." In *Proceedings of the 67th Annual Meeting of the American Academy of Forensic Sciences*.

Kieser, J. 2013. "Basic Principles of Biomechanics." In *Forensic Biomechanics*, edited by J. Kieser, M. Taylor, and D. Carr, 7–33. Chichester, West Sussex, UK: John Wiley & Sons Ltd.

Kieser, J., M. Taylor, and D. Carr. 2012. *Forensic Biomechanics*. Edited by J. Kieser, M. Taylor, and D. Carr. Chichester, West Sussex, UK: John Wiley & Sons Ltd.

King, A.I. 2015. "Introduction to and Applications of Injury Biomechanics." In *Accidental*

Injury: Biomechanics and Prevention, edited by N. Yoganandan, A.M. Nahum, and J.W. Melvin, 1–31. New York: Springer-Verlag.

Klaus, H.D. 2012. "The Bioarchaeology of Structural Violence: A Theoretical Model and a Case Study." In *The Bioarchaeology of Violence*, edited by D.L. Martin, R.P. Harrod, and V.R. Perez, 29–62. Gainesville: University of Florida Press.

Knudson, K.J., and C. Torres-Rouff. 2009. "Investigating Cultural Heterogeneity in San Pedro de Atacama, Northern Chile, through Biogeochemistry and Bioarchaeology." *American Journal of Physical Anthropology* 138 (4): 473–85.

Koester, K. J., J. W. Ager, and R. O. Ritchie. 2008. "The True Toughness of Human Cortical Bone Measured with Realistically Short Cracks." *Nature Materials* 7 (8): 672–77.

Kress, T.A., D.J. Porta, J.N. Snider, P.M. Fuller, J.P. Psihogios, W.L. Heck, S.J. Frick, and J.F. Wasserman. 1995. "Fracture Patterns of Human Cadaver Long Bones." In *Proceedings of the International Research Council on the Biomechanics of Impact (IRCOBI)*, 155–69.

Kroman, A.M. 2007. "Fracture Biomechanics of the Human Skeleton." University of Tennessee.

Kroman, A.M., T.A. Kress, and D. Porta. 2011. "Fracture Propagation in the Human Cranium: A Re-Testing of Popular Theories." *Clinical Anatomy* 24 (3): 309–18.

Kroman, A.M., and S.A. Symes. 2013. "Investigation of Skeletal Trauma." In *Research Methods in Human Skeletal Biology*, edited by E.A. DiGangi and M.K. Moore, 219–39. New York: Elsevier.

Kulin, R.M., F. Jiang, and K.S. Vecchio. 2011. "Effects of Age and Loading Rate on Equine Cortical Bone Failure." *Journal of the Mechanical Behavior of Biomedical Materials* 4 (1): 57–75.

L'Abbe, E.N., S.A. Symes, J.T. Pokines, L.L. Cabo, K.E. Stull, S. Kuo, D.E. Raymond, P.S. Randolph-Quinney, and L.R. Berger. 2015. "Evidence of Fatal Skeletal Injuries on Malapa Hominins 1 and 2." *Nature Scientific Reports* 5 (15120): 1–11.

L'Abbé, E.N., S.A. Symes, D.E. Raymond, and D.H. Ubelaker. 2019. "The Rorschach Butterfly, Understanding Bone Biomechanics Prior to Using Nomenclature in Bone Trauma Interpretations." *Forensic Science International* 299: 187–94.

Lovell, N.C. 1997. "Trauma Analysis in Paleopathology." *American Journal of Physical Anthropology* 104 (S25): 139–70.

Lovell, N.C., and A.L. Grauer. 2019. "Analysis and Interpretation of Trauma in Skeletal Remains." In *Biological Anthropology of the Human Skeleton*, edited by M.A. Katzenberg and A.L. Grauer, 3rd ed., 335–83. Hoboken, NJ: John Wiley & Sons, Inc.

Maples, W.R. 1986. “Trauma Analysis by the Forensic Anthropologist.” In *Forensic Osteology: Advances in the Identification of Human Remains*, edited by K.J. Reichs, 1st ed., 218–28. Springfield, IL: Charles C. Thomas.

Maples, W.R., B.P. Gatliff, H. Ludeña, R. Benfer, and W. Goza. 1989. “The Death and Mortal Remains of Francisco Pizarro.” *Journal of Forensic Sciences* 34: 1021–36.

Martens, M., R. van Audekercke, P. de Meester, and J.C. Mulier. 1986. “Mechanical Behaviour of Femoral Bones in Bending Loading.” *Journal of Biomechanics* 19 (6): 443–54.

Martin, D.L., and R.P. Harrod. 2015. “Bioarchaeological Contributions to the Study of Violence.” *Yearbook of Physical Anthropology* 156: 116–45.

Martin, D.L., and A.J. Osterholtz. 2016. “Broken Bodies and Broken Bones: Biocultural Approaches to Ancient Slavery and Torture.” In *New Directions in Biocultural Anthropology*, edited by M.K. Zuckerman and D.L. Martin, 471–92. New York: Wiley-Blackwell.

Martin, R.B., D.B. Burr, N.A. Sharkey, and D.P. Fyhrie. 2015. “Mechanical Properties of Bone.” In *Skeletal Tissue Mechanics*, edited by R.B. Martin, D.B. Burr, N.A. Sharkey, and D.P. Fyhrie, 355–422. New York: Springer.

Murphy, M.S., C. Gaither, E. Goycochea, J.W. Verano, and G. Cock. 2010. “Violence and Weapon-Related Trauma at Puruchuco-Huaquerones, Peru.” *American Journal of Physical Anthropology* 142 (4): 636–49.

Nagaoka, T. 2012. “Cranial Traumatic Injuries Caused by Weapons in Tokugawa Japan.” *International Journal of Osteoarchaeology* 22 (2): 138–44.

Nalla, R.K., J.W. Ager, and R.O. Ritchie. 2005. “Fracture in Human Cortical Bone: Local Fracture Criteria and Toughening Mechanisms.” *Journal of Biomechanics* 38 (7): 1517–25.

National Academy of Sciences (NAS) (2009). *Strenghtening Forensic Sciences in the Untied States: A Path Forward*. National Research Council of the National Academies, National Academies Press, Washington D.C.

Oftadeh, R., M. Perez-Viloria, J.C. Villa-Camacho, A. Vaziri, and A. Nazarian. 2015. “Biomechanics and Mechanobiology of Trabecular Bone: A Review.” *Journal of Biomechanical Engineering* 137 (1).

Özkaya, N., and D. Leger. 2012. “Introduction to Biomechanics: Basic Terminology and Concepts.” In *Basic Biomechanics of the Musculoskeletal System*, edited by M. Nordin and V.H. Frankel, 4th ed., 2–15. Baltimore, MD: Lippincott Williams & Wilkins.

Pal, S. 2014. “Mechanical Properties of Biological Materials.” In *Design of Artificial Human Joints and Organs*, edited by S. Pal, 23–40. New York: Springer Science+Business Media.

Passalacqua, N.V., and T.W. Fenton. 2012. “Developments in Skeletal Trauma: Blunt-Force Trauma.” In *A Companion to Forensic Anthropology*, edited by Dennis C Dirkmaat, 400–411. Chichester, West Sussex, UK: Blackwell Publishing, Ltd.

Pearce, A.I., R.G. Richards, S. Milz, E. Schneider, and S.G. Pearce. 2007. “Animal Models for Implant Biomaterial Research in Bone: A Review.” *European Cells and Materials* 13: 1–10.

Pérez, V.R. 2012. “The Politicization of the Dead: Violence as Performance, Politics as Usual.” In *The Bioarchaeology of Violence*, edited by D.L. Martin, R.P. Harrod, and V.R. Peréz, 13–28. Gainesville: University of Florida Press.

Peterson, J., and P.C. Dechow. 2002. “Material Properties of the Inner and Outer Cortical Tables of the Human Parietal Bone.” *Anatomical Record* 268 (1): 7–15.

Porta, D., S.J. Frick, T. Kress, and P. Fuller. 1999. “Tranvserse, Oblique, and Wedge Fracture Patterns: Variation on the Bending Theme.” *Clinical Anatomy* 12: 208.

Powell, B.J., N.V. Passalacqua, T.G. Baumer, T.W. Fenton, and R.C. Haut. 2012. “Fracture Patterns on the Infant Porcine Skull Following Severe Blunt Impact.” *Journal of Forensic Sciences* 57 (2): 312–17.

Powell, B.J., N.V. Passalacqua, T.W. Fenton, and R.C. Haut. 2013. “Fracture Characteristics of Entrapped Head Impacts Versus Controlled Head Drops in Infant Porcine Specimens.” *Journal of Forensic Sciences* 58 (3): 678–83.

Reber, S.L., and T. Simmons. 2015. “Interpreting Injury Mechanisms of Blunt Force Trauma from Butterfly Fracture Formation.” *Journal of Forensic Sciences* 60 (6): 1401–11.

Reilly, D.T., and A.H. Burstein. 1975. “The Elastic and Ultimate Properties of Compact Bone Tissue.” *Journal of Biomechanics* 8 (6): 393–405.

Rho, J.Y., R.B. Ashman, and C.H. Turner. 1993. “Young’s Modulus of Trabecular and Cortical Bone Material: Ultrasonic and Microtensile Measurements.” *Journal of Biomechanics* 26 (2): 111–1119.

Rice, J.C., S.C. Cowin, and J.A. Bowman. 1988. “On the Dependence of the Elasticity and Strength of Cancellous Bone on Apparent Density.” *Journal of Biomechanics* 21 (2): 155–68.

Robbins Schug, G., K. Gray, V. Mushrif-Tripathy, and A.R. Sankhyan. 2012. “A Peaceful Realm? Trauma and Social Differentiation at Harappa.” *International Journal of Paleopathology* 2 (2–3): 136–47.

Rockhold, L.A., and N.P. Hermann. 1999. “A Case Study of a Vehicular Hit-and-Run Fatality: Direction of Force.” In *Broken Bones: Anthropological Analysis of Blunt Force Trauma*,

edited by Alison Galloway, 287–90. Springfield, IL: Charles C. Thomas.

Roesler, H. 1987. “The History of Some Fundamental Concepts in Bone Biomechanics.” *Journal of Biomechanics* 20 (11–12): 1025–34.

Ruchonnet, A., M. Diehl, Y.H. Tang, and E.F. Kraniota. 2019. “Cranial Blunt Force Trauma in Relation to the Victim Position: An Experimental Study Using Polyurethane Bone Spheres.” *Forensic Science International* 301: 350–57.

Ruppel, M.E., L.M. Miller, and D.B. Burr. 2008. “The Effect of the Microscopic and Nanoscale Structure on Bone Fragility.” *Osteoporosis International* 19: 1241–65.

Sauer, N.J. 1984. “Manner of Death: Skeletal Evidence of Blunt and Sharp Instrument Wounds.” In *Human Identification: Case Studies in Forensic Anthropology*, edited by T.A. Rathbun and Buikst, 176–84. Springfield, IL: Thomas, Charles C.

Schiffer, M.B. 1988. “The Structure of Archaeological Theory.” *American Antiquity* 53 (3): 461–85.

Sledzik, P.S., T.W. Fenton, M.W. Warren, J.E. Byrd, C. Crowder, S.N. Drawdy, D.C. Dirkmaat, et al. 2007. “The Fourth Era of Forensic Anthropology: Examining the Future of the Discipline.” In *Proceedings of the 59th Annual Meeting of the American Academy of Forensic Sciences*. San Antonio, TX.

Smith, M.J., S. James, T. Pover, N. Ball, V. Barnetson, B. Foster, C. Guy, J. Rickman, and V. Walton. 2015. “Fantastic Plastic? Experimental Evaluation of Polyurethane Bone Substitutes as Proxies for Human Bone in Trauma Simulations.” *Legal Medicine* 17: 427–35.

Smith, O.C., H.E. Berryman, and C.H. Lahren. 1987. “Cranial Fracture Patterns and Estimation of Direction from Low Velocity Gunshot Wounds.” *Journal of Forensic Sciences* 32: 1416–21.

Smith, O.C., H.E. Berryman, S.A. Symes, and S.J. Moore. 1991. “Bone Fracture I: The Physics of Fracture.” In *Proceedings of the 43rd Annual Meeting of the American Academy of Forensic Sciences*. Anaheim, CA.

Spencer, S.D. 2012. “Detecting Violence in the Archaeological Record: Clarifying the Timing of Trauma and Manner of Death in Cases of Cranial Blunt Force Trauma among Pre-Columbian Amerindians of West-Central Illinois.” *International Journal of Paleopathology* 2 (2–3): 112–22.

Stone, P.K. 2012. “Binding Women: Ethnology, Skeletal Deformations, and Violence against Women.” *International Journal of Paleopathology* 2 (2–3): 53–60.

Scientific Working Group for Forensic Anthropology. 2011. "Trauma Analysis."

nist.gov/system/files/documents/2018/03/13/swganth_trauma.pdf

Symes, S.A., O.C. Smith, H.E. Berryman, and S.J. Moore. 1991. “Bone Fracture III: Microscopic Fracture Analysis of Bone.” In *Proceedings of the 43rd Annual Meeting of the American Academy of Forensic Sciences*. Anaheim, CA.

Symes, S.A, E.N. L’Abbé, E.N. Chapman, I. Wolff, and D.C. Dirkmaat. 2012. “Interpreting Traumatic Injury to Bone in Medicolegal Investigations.” In *A Companion to Forensic Anthropology*, edited by D.C. Dirkmaat, 340–89. Chichester, West Sussex, UK: Blackwell Publishing, Ltd.

Tersigni-Tarrant, M.A. 2015. “Blunt Force Trauma Associated with a Fall from Heights.” In *Skeletal Trauma: Case Studies in Context*, edited by N.V. Passalacqua and C.W. Rainwater, 147–55. Chichester, West Sussex, UK: John Wiley & Sons Ltd.

Torres-Rouff, C., and M.A. Costa Junqueira. 2006. “Interpersonal Violence in Prehistoric San Pedro de Atacama, Chile: Behavioral Implications of Environmental Stress.” *American Journal of Physical Anthropology* 130 (1): 60–70.

Trinkaus, E., and A.P. Buzhilova. 2012. “The Death and Burial of Sunghir 1.” *International Journal of Osteoarchaeology* 22 (6): 655–66.

Tung, T.A., and K.J. Knudson. 2008. “Social Identities and Geographical Origins of Wari Trophy Heads from Conchopata, Peru.” *Current Anthropology* 49 (5): 915–26.

Vaughan, P.E., C.C.M. Vogelsberg, J.M. Vollner, T.W. Fenton, and R.C. Haut. 2016. “The Role of Interface Shape on the Impact Characteristics and Cranial Fracture Patterns Using the Immature Porcine Head Model.” *Journal of Forensic Sciences* 61 (5): 1190–97.

Viguet-Carrin, S., P. Garnero, and P.D. Delmas. 2005. “The Role of Collagen in Bone Strength.” *Osteoporosis International* 17 (3): 319–36.

Walker, P.L. 2001. “A Bioarchaeological Perspective on the History of Violence.” *Annual Review of Anthropology* 30 (1): 573–96.

Wang, X., R.A. Bank, J.M. Tekoppele, and C.M. Agrawal. 2006. “The Role of Collagen in Determining Bone Mechanical Properties.” *Journal of Orthopaedic Research* 19 (6): 1021–26.

Wang, X., J.D. Mabrey, and C.M. Agrawal. 1998. “An Interspecies Comparison of Bone Fracture Properties.” *Bio-Medical Materials and Engineering* 8 (1): 1–9.

Wedel, V.L., A. Galloway, and L. Zephro. 2014. “Trauma Analysis: Training, Roles, and Responsibilities.” In *Broken Bones: Anthropological Analysis of Blunt Force Trauma*, edited by V.L. Wedel and A. Galloway, 2nd ed., 5–10. Springfield, IL: Charles C. Thomas.

Wheatley, B.P. 2008. “Perimortem or Postmortem Bone Fractures? An Experimental Study of Fracture Occurrences in Deer Femora.” *Journal of Forensic Sciences* 53 (1): 69–72.

Wright, T.M., and W.C. Hayes. 1976. “Tensile Testing of Bone over a Wide Range of Strain Rates: Effects of Strain Rate, Microstructure and Density.” *Medical and Biological Engineering* 14: 671–79.

Wu, X.J., L.A. Schepartz, W. Liu, and E. Trinkaus. 2011. “Antemortem Trauma and Survival in the Late Middle Pleistocene Human Cranium from Maba, South China.” *Proceedings of the National Academy of Sciences of the United States of America* 108 (49): 19558–62.

Yoganandan, N., and F.A. Pintar. 2004. “Biomechanics of Temporo-Parietal Skull Fracture.” *Clinical Biomechanics* 19 (3): 225–39.

Zephro, L., A. Galloway, and V.L. Wedel. 2014. “Theoretical Considerations in Designing Experimental Trauma Studies and Implementing Their Results.” In *Broken Bones: Anthropological Analysis of Blunt Force Trauma,* edited by V.L. Wedel and A. Galloway, 2nd ed., 73–90. Springfield, IL: Charles C. Thomas.

Zollikofer, C.P.E., M.S. Ponce de León, B. Vandermeersch, and F. Lévêque. 2002. “Evidence for Interpersonal Violence in the St. Césaire Neanderthal.” *Proceedings of the National Academy of Sciences of the United States of America* 99 (9): 6444–48.

PAPER 1: EXPERIMENTAL INVESTIGATION OF CRANIAL FRACTURE INITIATION IN BLUNT HUMAN HEAD IMPACTS

This is the peer-reviewed version of the following article: [Isa, M.I., T.W. Fenton, A.C. Goots, E.O. Watson, P.E. Vaughan, and F. Wei. 2019. "Experimental Investigation of Cranial Fracture Initiation in Blunt Human Head Impacts." *Forensic Science International* 300: 51–62.], which has been published in final form at [https://doi.org/10.1016/j.forsciint.2019.04.003].

Abstract

The relationship between the point of blunt impact and the location of cranial fracture initiation continues to be poorly understood. The current study used high-speed video to capture cranial fracture initiation and propagation in impact experiments on twelve unembalmed, intact human cadaver heads. Video footage provided direct evidence that blunt cranial impacts can produce linear fractures initiating peripheral to the impact site. Four tests produced only remote peripheral linear fractures with no damage at the known point of impact, demonstrating that the pattern of linear fractures does not necessarily indicate impact site. The range of variation observed in these experiments suggests that cranial fracture formation is more complex than it is typically described in the current literature. Differences in biomechanical and fracture results obtained with three different shaped implements provided evidence that impact surface is one important factor influencing the outcomes of blunt cranial impacts.

Introduction

Anthropologists are often asked to assess skeletal fracture patterns and provide interpretations about the circumstances involved in their production. This analysis is based on a theoretical framework that regards fracture behavior as nonrandom and subject to the laws of physics (Berryman, Berryman, and Saul 2018). Therefore, fractures can be understood as the result of interactions between extrinsic factors influencing the forces placed on bone and intrinsic factors affecting bone's ability to withstand these forces at the material, microstructural, and macrostructural levels. Anthropologists report using this framework to form hypotheses about the variables involved in producing the fracture patterns observed in forensic cases (Passalacqua and Rainwater 2015; Symes et al. 2012; Wedel and Galloway 2014; Symes et al. 2014; Kroman and Symes 2013; Berryman, Shirley, and Lanfear 2013; Berryman, Berryman, and Saul 2018; Kimmerle and Baraybar 2008; Hart 2005; Smith, Pope, and Symes 2003; Berryman and Symes 1998; Christensen et al. 2018; Isa et al. 2018). However, there are currently few scientifically validated methods available to aid assessments of specific impact variables based on fracture pattern. Before such methods can be developed and tested, it is necessary to document how fractures form under known impact conditions and to consider the biomechanically relevant extrinsic and intrinsic variables involved in fracture initiation and propagation. As such, the NIST OSAC Anthropology subcommittee identifies controlled experimental bone trauma studies as a top need in research and development (OSAC 2016).

One area in need of research is cranial fracture associated with blunt force impact. Blunt head trauma is a common finding in autopsy cases (Spitz, Spitz, and Clark 2006). Cranial fractures frequently occur in cases of fatal blunt head injuries resulting from assaults, falls, and motor vehicle accidents (Chattopadhyay and Tripathi 2010; Kiadaliri, Rosengren, and Englund

2018; Whyte et al. 2016). Because blunt cranial injuries often relate to the cause of death, they represent important areas of evaluation in medicolegal death investigations (Kranioti 2015). Despite the forensic relevance of this region, cranial fracture initiation and propagation remain poorly understood.

Neurosurgeon Dr. Elisha Gurdjian and his coworkers conducted some of the earliest experimental investigations of blunt force fracture in the human cranium (Gurdjian and Lissner 1945, 1947; Gurdjian, Lissner, and Webster 1947; Gurdjian, Webster, and Lissner 1949, 1950a, 1950b, 1953). Throughout the 1940s and 1950s, Gurdjian et al. performed a series of impact experiments on human cadaver heads. These experiments included failure-level testing aimed at producing cranial fractures and sub-failure experiments using a stress-coat technique to assess cranial deformation and infer tensile stress during impact. Gurdjian et al. report high tensile stresses remote from the known impact site in the stress-coat experiments (Gurdjian and Lissner 1945, 1947; Gurdjian, Lissner, and Webster 1947). Similarly, in failure-level experiments cranial fractures appeared to travel from these remote areas back toward the point of impact (POI) (Gurdjian, Webster, and Lissner 1949, 1950a, 1950b, 1953).

Based on these results, Gurdjian et al. report the following expectations of cranial fracture initiation and propagation: a blunt blow will cause bone to deform inward ("inbend") at the POI and deform outward ("outbend") in peripheral areas. If the blow is severe enough to cause depression at the POI, radial fractures will initiate at the POI on the inbent internal surface of the skull. However, if the blow is not severe, the inbent area at the POI rebounds without fracture and linear fractures initiate in peripheral areas of out-bending under high tensile stresses (Gurdjian, Webster, and Lissner 1950b, 336). This understanding of cranial fracture development informs influential publications in forensic pathology (Moritz 1954; DiMaio and DiMaio 2001;

Saukko and Knight 2016) and early chapters on skeletal trauma in forensic anthropology textbooks (Berryman and Symes 1998; Stewart 1979; Maples 1986; Galloway 1999).

Recent research by Dr. Anne Kroman and colleagues (Kroman 2007; Kroman, Kress, and Porta 2011) challenged Gurdjian's findings, specifically the idea that cranial fractures can initiate peripherally in areas remote from the impact site. In order to investigate the relationship between impact site and location of fracture initiation, Kroman et al. performed impact experiments on five cadaver heads using a drop tower system. Impacts were delivered to the anterior parietal region and fracture initiation and propagation were captured with high-speed video. Video footage showed linear fractures initiating at the POI and radiating outward in all experiments that produced fracture. Based on this evidence, Kroman and colleagues refute Gurdjian's findings and conclude that cranial fractures initiate only at the POI (Kroman, Kress, and Porta 2011). Kroman's work has been widely cited and as such, influences current understanding of cranial fracture formation (e.g., Passalacqua and Rainwater 2015; Wedel and Galloway 2014; Kroman and Symes 2013; Berryman, Shirley, and Lanfear 2013; Symes et al. 2012; Kimmerle and Baraybar 2008; Kranioti 2015).

However, researchers since Gurdjian have also presented evidence of peripheral fracture initiation. In experiments on human cadaver heads, Yoganandan et al. (Yoganandan et al. 1995) report fractures that were consistently wider further from the loading region. In at least one impact to the cranial vertex, fractures occurred peripherally in the frontal bone. Recent experimental research using a pediatric porcine model also provides evidence of peripheral fracture initiation (Baumer et al. 2010; Powell et al. 2013). In these studies, linear fractures consistently initiated peripheral to the impact site at adjacent sutures and often produced

multiple, unconnected linear fractures. However, it is unclear how these results apply to adult human crania.

As a result of the Gurdjian-Kroman controversy there remain uncertainties surrounding cranial fracture initiation and the relationship between impact location and fracture location. This presents not only an academic issue, but also an interpretive one. In the absence of scientifically validated methods for identifying cranial impact sites, assumptions about fracture initiation directly inform how practitioners identify the point or points of impact. If it is assumed that cranial vault fractures initiate and radiate only from impact sites, it follows that individual linear fractures represent impact sites. Clarification of the initiation issue is therefore forensically relevant because it will provide data to inform how practitioners assess location and minimum number of cranial impacts.

The purpose of the current study was to address the issue of cranial fracture initiation and propagation through impact experiments on fresh, unembalmed human cadaver heads. This study was conducted with two primary objectives: 1) to use high-speed video to investigate how fractures initiate and propagate relative to the known impact site, and 2) to document the relationship between cranial impact location and the location of fractures. For the experimentally manipulated variable of implement shape, this study aimed to document the range of variation observed in specimens subjected to *different* impact conditions, as well as *different* specimens subjected to the *same* impact conditions.

Materials and Methods

Human head specimens

The materials in the current study included 12 unembalmed, fresh-frozen human head specimens obtained from male anatomical donors. All individuals were at least 50 years of age at

the time of death. For all donors included in this study, the procurement organizations obtained consent for the use of their remains in research in accordance with the Uniform Anatomical Gift Act (UAGA). Specimens were stored at -20 °C and thawed completely at room temperature before testing. Various studies have shown that storage at this temperature is unlikely to change bone mechanical properties significantly relative to the variability that exists within a typical experimental sample (Cowin 2001; Kaye et al. 2012; van Haaren et al. 2008). Prior to experimentation the skin, muscle, and periosteum were removed from the temporoparietal region to allow for visualization of fracture initiation and propagation during impact. A small area of scalp was preserved at the impact site to account for the influence of soft tissue.

Cranial impact experiments

Cranial impact experiments were designed to simulate a blow to an upright individual. Efforts were made to allow a realistic amount of movement during the impact. First, the neck of each specimen was secured to a horizontal support plate using clamps placed between the 3rd and 6th cervical vertebra. Gross adjustments to head position were made through translation (x- and y-axes) and rotation (z-axis) of the support plate. Next, a positioning collar outfitted with breakaway tethers was affixed around the neck. The tethers were used to suspend the head in an upright posture and to provide fine adjustments of the head. These tethers, made of 4-lb fishing line, broke on impact and allowed the head to rotate about the neck.

Blunt impacts were administered to the mid-parietal bone at a location superior to the squamosal suture and halfway between the lambdoidal and coronal sutures. Most specimens were impacted on the right side of the head. Two specimens (17-0006 and 17-3757) presented with pre-existing defects in the right temporoparietal region. Therefore tests were performed on the left side in these two cases. Impacts were produced using a custom-designed pneumatic

impact system (Figure 1.1). The system controlled pressure release of compressed nitrogen gas providing the initial velocity to a guide trolley that held the impactor. As the impactor made contact with the head, the support plate holding the head slid away from the impactor along frictionless bearings.

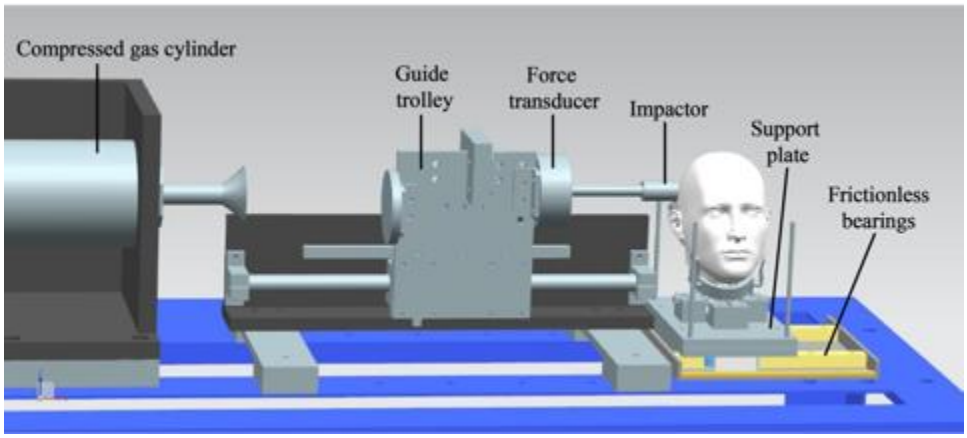

Figure 1.1: Frontal view of the customized pneumatic impact system. The impactor shown here represented the hammer shape.

Three aluminum implement shapes were selected for these experiments: the flat surface of a 1.125-inch diameter cylinder, the curved surface of a 2.5-inch long, 2.5-inch diameter hemi-cylinder, and a 3-inch diameter flat surface (Figure 1.2). These shapes were modeled after blunt surfaces that may be implicated in forensic cases: a small, focal impact surface such as the face of a hammer, a broad, curved surface such as the barrel of a baseball bat, and a large, flat surface such as the broad side of a brick, respectively. For ease of reference, this paper will refer to these implements as the "hammer," the "bat," and the "brick." However, these terms should be understood as shorthand for the impact surfaces tested in this study, and not as references to specific tools.

Because the implements were constructed from the same material and had similar masses (6.27 kg, 6.31 kg, and 6.30 kg, respectively), the primary manipulated variable in these experiments was the shape of the impact surface. Four impacts were performed with each of the

three implements. The goal of these experiments was to generate fracture initiation and propagation such that discernable fracture patterns were produced without complete destruction at the impact site.

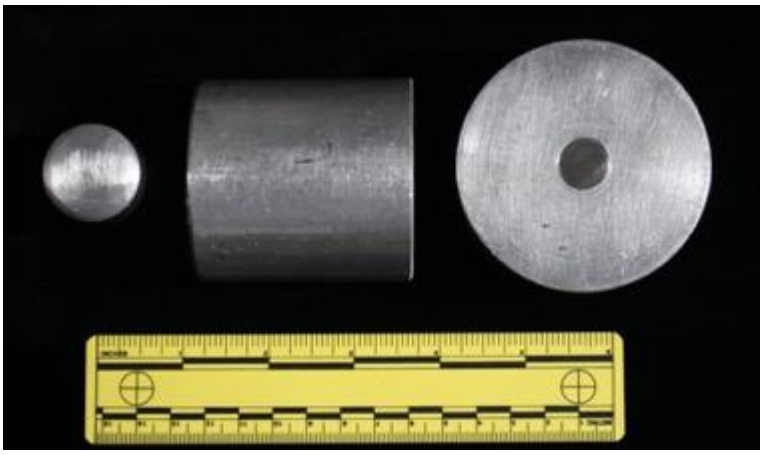

Figure 1.2: Implements used in the current experiments. From left to right: "hammer" (flat surface of a 1.125-inch diameter cylinder), "bat" (curved surface of a 2.5-inch long, 2.5-inch diameter hemi-cylinder), and "brick" (flat surface of a 3-inch diameter cylinder). The hemi-cylinder was oriented such that the 2.5-inch long curved surface was centered on the point of impact and the flat bases faced anteriorly and posteriorly.

Data collection

All impacts were filmed at 10,000 frames per second using a high-speed video camera (Fastcam Mini AX 200, Photron Ltd; Tokyo, Japan). Each head was photographed and resultant fractures were recorded on standardized cranial diagrams immediately after impact, as specimens were later used in additional experiments as part of another study. Following completion of that study, specimens were cleaned of soft tissue using hot water maceration and reconstructed using acetone soluble adhesive.

Photron software was used to generate still frames from the high-speed footage of each specimen just prior, during, and after impact. The locations of fracture initiation and propagation during the impact were assessed for each specimen using these images. Fracture photographs, diagrams and reconstructed specimens were used to confirm the video findings and assess the

relationship between impact location and fracture initiation and propagation for each impact experiment.

Impact force-time response was recorded at a sample rate of 200,000 Hz using a 10,000 lbf force transducer (model 1210AF-10K-B, Interface; Scottsdale, AZ) mounted to the guide trolley (Figure 1.1). These force data were synchronized with high-speed video for later identification of the force initiating fracture. A magnetic linear encoder (model LM15ICD50AB10F00, Renishaw Inc.; Hoffman Estates, IL), also mounted to the guide trolley, was used to collect position-time data at a sample rate of 200,000 Hz. The position-time data immediately prior to and after the impact were used to calculate the initial (v_i) and final (v_f) velocities (m/s) of the trolley. Energy absorbed by the cadaver head was determined as the kinetic energy change of the trolley during the impact based on the following equation, where E was the energy (J) absorbed and m was the mass (kg) of the trolley.

$$E = \tfrac{1}{2}m(v_{i2}-v_{f2})$$

In post-experiment data analyses, force-time data were downsampled to match the sample rate of high-speed video (10,000 Hz). Based on assessments of the synchronized video and force data, force at fracture initiation and its corresponding time were identified and documented. Contact duration was defined as the time from implement contact with the skull to initiation of cranial fracture.

Statistical analysis

General Linear Model ANOVA with Tukey post hoc test in Minitab 16 (State College, PA) was used to compare differences in energy absorbed, force at fracture initiation, and contact duration between implements, with $p<0.05$ considered significant.

Results

Throughout this section results will be presented for the "hammer," "bat," and "brick." These terms should be understood as shorthand for the three implements tested in this study, and specifically their respective impact surfaces. There exists a wide range of objects—each with multiple potential blunt impact surfaces—that may be implicated in forensic cases, making it difficult to match specific tools to blunt force trauma. Therefore, the following results are best conceptualized in terms of impact surfaces rather than specific tools.

Mechanical results

The cranial impacts were performed at an average velocity of 5.80±0.24 m/s, translating to an average input energy of 106.1±8.8 J. This energy input produced cranial fractures in all 12 experiments. Typical force-time curves for impacts with each implement are shown in Figure 1.3.

In most cases fracture initiation coincided with the first sudden drop in force-time response. Significant differences in energy absorbed ($p=0.026$), force at fracture initiation ($p=0.009$), and contact duration ($p<0.001$) were observed in impacts with the three implements. Specifically, while energy absorbed by the head in the bat impacts (56±8 J) was not significantly different from that in the hammer ($p=0.083$) or brick ($p=0.750$) impacts, the hammer delivered significantly lower energy to the head (36±6 J) than the brick (63±18 J, $p=0.027$) impacts (Figure 1.4). Furthermore, the hammer impacts required significantly lower force (2684±851 N) to initiate fracture than that required in the bat (5230±613 N, $p=0.028$) or brick (5720±1671 N, $p=0.011$) impacts, but no significant difference in force at fracture initiation was observed between the bat and brick impacts ($p=0.819$) (Figure 1.5). Finally, contact duration was significantly longer in the hammer impacts (0.8±0.1 ms) than in the bat (0.4±0.1 ms, $p=0.004$) or

brick (0.3±0.1 ms, p=0.001) impacts. However, contact duration was not found different between the bat and the brick impacts (p=0.258) (Figure 1.6).

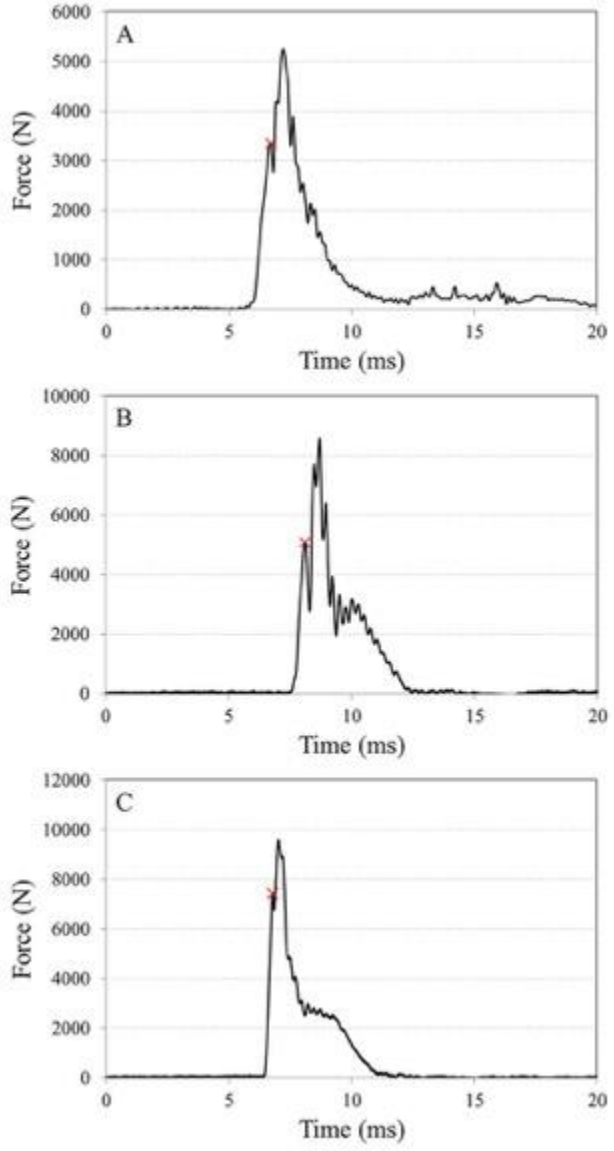

Figure 1.3: Typical force-time curves from impacts using the "hammer" (A), the "bat" (B), and the "brick" (C). Points indicated with an "x" represent forces required to initiate cranial fracture based on synchronized high-speed video footage.

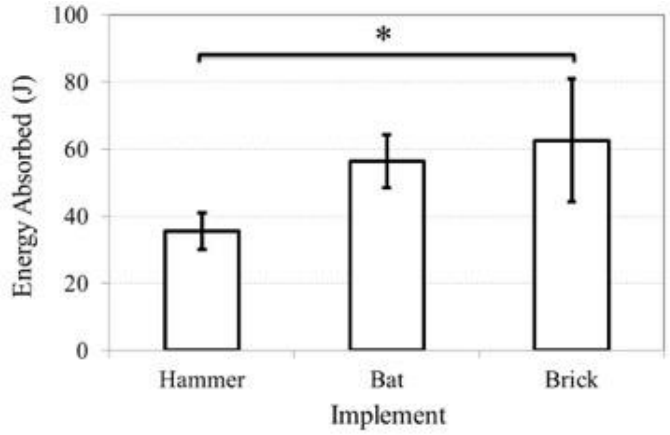

Figure 1.4: Mean energies (J ± 1 SD) absorbed during impact for different implements. *Indicates significant difference, $p < 0.05$.

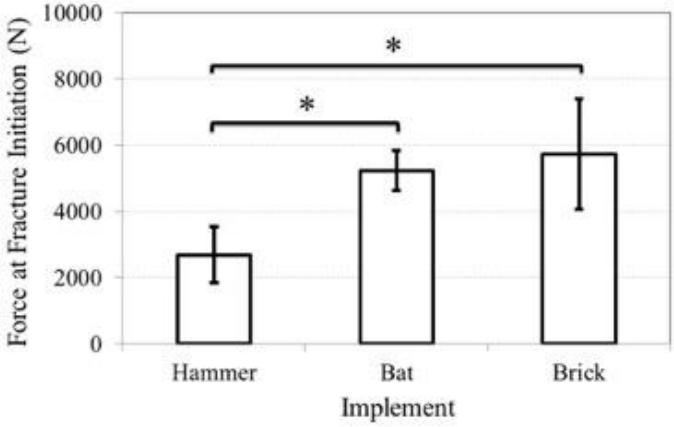

Figure 1.5: Mean forces (N ± 1 SD) required to initiate cranial fracture for different implements. *Indicates significant difference, $p < 0.05$.

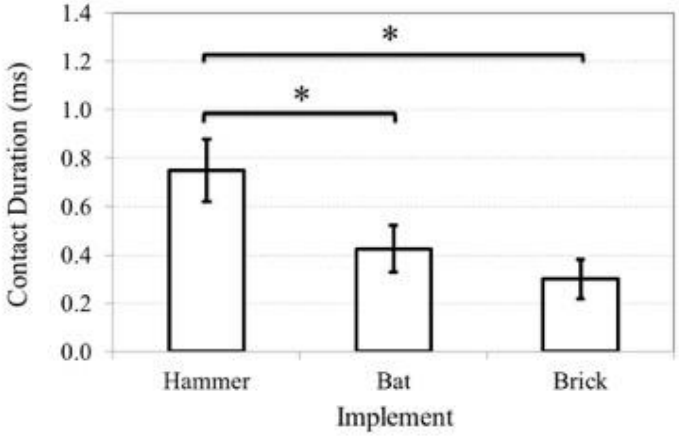

Figure 1.6.: Mean contact time (ms ± 1 SD) from implement contact with the skull to fracture initiation for different implements. *Indicates significant difference, $p < 0.05$.

Fracture initiation and propagation results

Table 1.1 summarizes the fracture initiation and propagation results for each of the 12 cranial impact experiments. The most notable finding of the current study was that the majority (10/12) of experiments, including tests with all three implements, produced peripheral linear cranial fractures initiating remote from the impact site (Figure 1.7). The following sections summarize fracture initiation and propagation results obtained with each implement.

"Hammer" (small, focal impact surface)

The only two experiments that did not produce peripheral fracture initiation were impacts with the hammer implement (Figure 1.8). One experiment (17-3827) produced only a shallow circular depression at the impact site. In the other experiment (16-3779), the first observed fracture event was a linear fracture that initiated at the POI and propagated anteriorly to the coronal suture. Ultimately, the implement penetrated the cranium at the impact site. In the remaining two hammer experiments, high-speed video showed linear fractures initiating peripheral to the POI. One hammer impact (17-0006) produced initiation both at and peripheral to the impact site (Figure 1.7). In this case, the video from this impact clearly showed a peripheral linear fracture initiated in the inferior temporal bone and propagated back toward the POI. After this fracture encircled the impact site, another linear fracture initiated at the POI and traveled anteriorly toward the coronal suture. This sequence of fractures contrasted with typical portrayals of fracture sequence wherein linear fractures radiate from the POI and then concentric fractures form between the radial fracture lines.

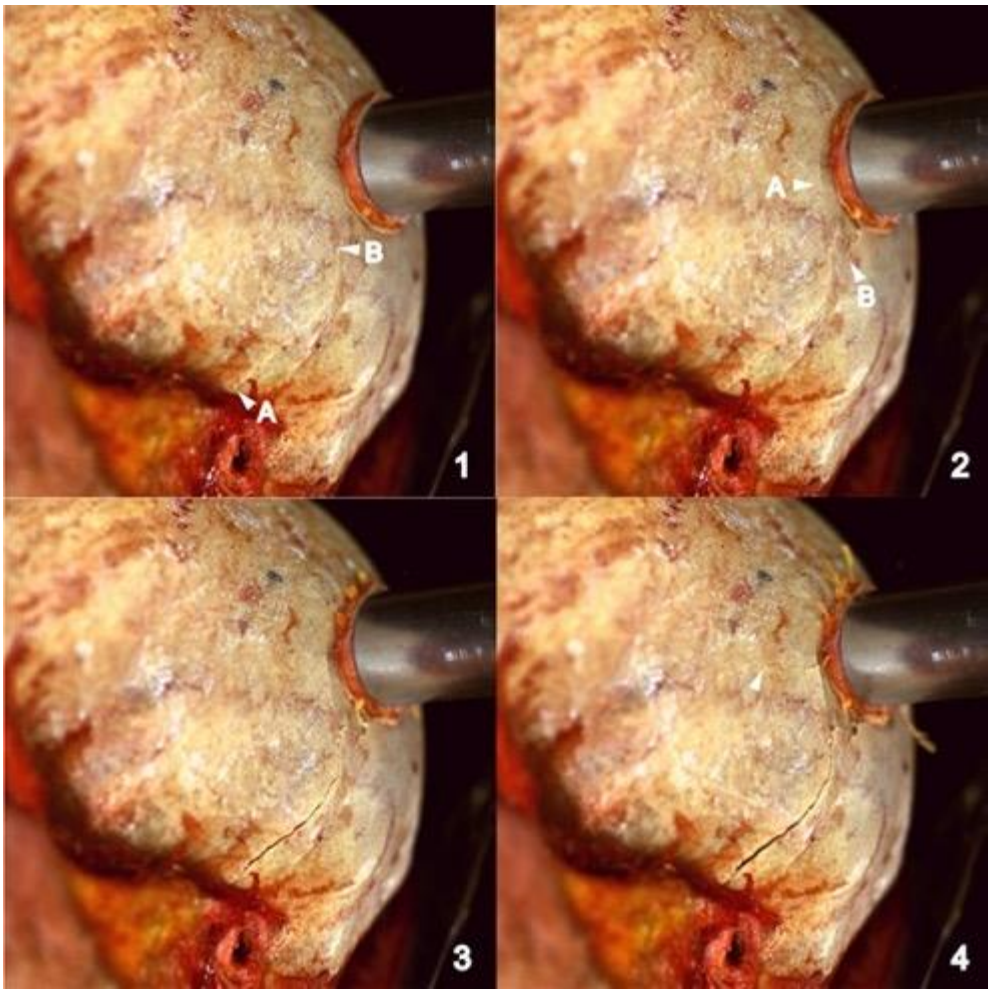

Figure 1.7: Still frames in a temporal sequence (1-2-3-4) from the hammer impact experiment 17-0006. Panel 1 shows a peripheral linear fracture initiating in the inferior temporal (A) and propagating toward the POI (B). Panel 2 shows fracture encircling the POI (A and B). Panel 3 shows the implement beginning to penetrate the bone at the impact site. Panel 4 shows a linear fracture initiating at the POI and traveling anteriorly away.

Finally, the other hammer experiment (17-3757) produced *only* peripheral linear fractures. In this experiment fractures initiated in the inferior temporal bone and propagated superiorly to the squamosal suture and parietal, and inferiorly to the external auditory meatus.

For the two specimens impacted on the left side, the effect of the pre-existing right side defects on the current results is unknown.

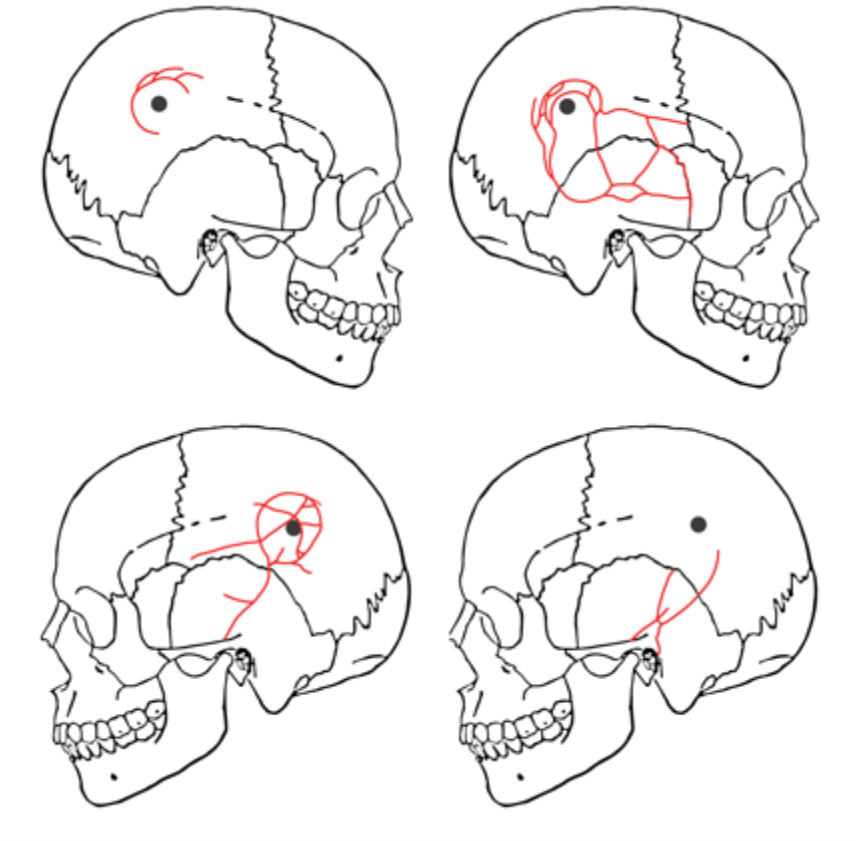

Figure 1.8: Fracture diagrams from “hammer” impact experiments. From left to right: specimens 17-3827, 16-3779, 17-0006, and 17-3757. The center of the mid-parietal impact site is indicated by a black dot.

“Bat” (broad, curved impact surface)

All four experiments with the bat implement produced peripheral fracture initiation (Figure 1.9). In these experiments fracture initiation locations and the directions of propagation after peripheral initiation varied between specimens.

One experiment (17-2067) produced initiation at two locations simultaneously. In this case a peripheral linear fracture initiated in the center of the temporal bone and traveled superiorly toward the impact site. At the same time, a linear fracture initiated at the POI and traveled anteriorly into the frontal bone. This impact also produced a hairline curvilinear fracture

partially surrounding the impact site, though this event could not be sequenced because it was obscured in the impact video.

Another experiment (16-3803) produced a peripheral linear fracture that propagated in two directions simultaneously. This fracture initiated in the anterior-inferior parietal bone and traveled both posteriorly toward and anteriorly away from the POI. The impact also produced a short curvilinear fracture at the superior aspect of the impact site, though this event could not be sequenced because it was obscured in the impact video.

The remaining two bat experiments produced multiple peripheral linear fractures. The experiment on specimen 17-3758 first produced a diastasis of the anterior squamosal suture. One peripheral linear fracture traveled superiorly from this diastasis into the parietal bone. Subsequently another peripheral linear fracture initiated at the posterior squamosal suture and traveled anteriorly into the temporal bone. In contrast, the experiment on specimen 17-4813 produced multiple peripheral linear fractures, all of which initiated from the sphenotemporal and anterior squamosal sutures. These fractures propagated in various directions into the parietal, temporal, and sphenoid bones. Examination of this specimen after impact revealed no ectocranial damage at the impact site.

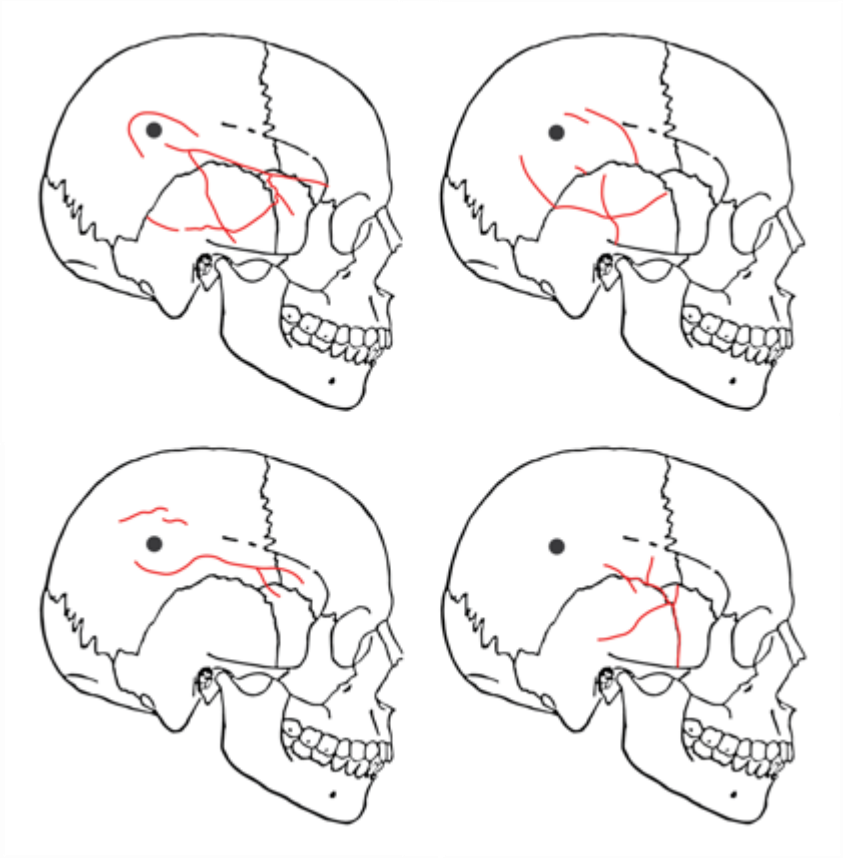

Figure 1.9: Fracture diagrams from “bat” impact experiments. From left to right: specimens 17-2067, 17-3758, 16-3803, and 17-4813. The center of the mid-parietal impact site is indicated by a black dot.

“Brick” (broad, flat impact surface)

Similar to the bat, all four experiments with the brick implement produced peripheral fracture initiation (Figure 1.10). The experiment on specimen 16-3801 produced the most complex sequence of fractures of all the impact experiments. Fracture initiation occurred at multiple sites resulting in extensive comminution of the impact site. However, the first observed fracture event was a peripheral linear fracture initiating in the anterior temporal bone. This fracture propagated in two directions, both superoposteriorly toward and inferoanteriorly away from the POI.

In the experiment on specimen 17-2035, a peripheral linear fracture extended between the sphenoid and squamosal sutures and traveled toward the impact site. The experiment also produced a hairline curvilinear fracture around the posterior and inferior aspects of the impact site, though the fracture event was obscured in the video and could not be sequenced.

Finally, the remaining two brick impact experiments produced only peripheral linear fractures with no ectocranial damage observed at the impact site. In one of these experiments (16-3805) a peripheral linear fracture initiated in the inferior temporal bone and propagated posteriorly toward the squamosal suture. The other experiment (16-3817) produced a slight diastasis of the sphenotemporal suture from which linear fractures propagated into the sphenoid bone.

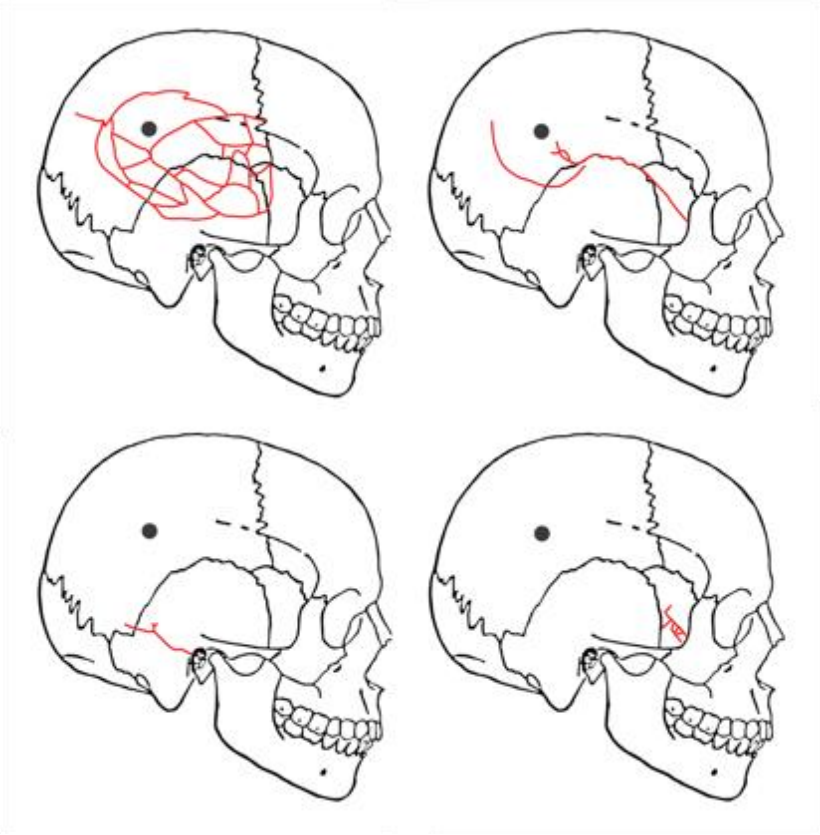

Figure 1.10: Fracture diagrams from “brick” impact experiments. From left to right: specimens 16-3801, 17-2035, 16-3805, and 16-3817. The center of the mid-parietal impact site is indicated by a black dot.

Relationship between known impact location and fracture location

In addition to the location of cranial fracture initiation, the location of resultant fracture patterns in relation to the POI was also assessed. The following sections summarize these results by implement.

"Hammer" (small, focal impact surface)

Experiments with the hammer implement produced parietal bone fractures in all (4/4) specimens (Figure 1.8). In addition to the parietal bone, 3/4 specimens also exhibited fractures in the temporal bone.

Three out of 4 hammer experiments produced circular depressed fractures at the POI, approximately the same size and shape of the implement's impact surface. Within the current set of experiments this pattern was only observed in impacts using the "hammer" implement, which had the smallest and most focal impact surface of the three implements tested. In the one experiment that produced only linear fractures (17-3757) the fracture pattern involved peripheral linear fractures intersecting in the temporal bone with no ectocranial damage at the parietal bone impact site. Only one experiment (16-3779) produced a diastatic fracture, which occurred in the sphenotemporal suture.

"Bat" (broad, curved impact surface)

Experiments with the bat implement produced parietal bone fractures in all (4/4) specimens (Figure 1.9). All four experiments produced fractures in multiple cranial bones. In addition to the parietal bone, fractures were observed in the sphenoid bone in 3/4 tests, the temporal bone in 3/4 tests, and the frontal bone in 2/4 tests. The bat was the only implement that produced fractures extending into the frontal bone.

Three out of 4 bat experiments produced curvilinear fractures partially surrounding the impact site. Unlike the hammer impacts, which produced fairly regular depressed defects at the POI, impact site fractures differed in each bat experiment. One experiment (17-2067) produced a hairline curvilinear fracture surrounding the superior aspect of the impact site. Another experiment (17-3758) produced two curvilinear fractures anterior and posterior to the impact site. The third experiment (16-3803) produced curvilinear fractures superior and inferior to the impact site. The fourth experiment (17-4813) produced only peripheral linear fractures with no fractures at the POI. Three bat impacts produced diastases of the sphenotemporal and/or anterior squamosal sutures during impact, though examination of the crania after impact revealed discernable diastatic fractures only in one specimen (17-4813).

A common feature of the bat experiments involved anteroposteriorly oriented linear fractures in the temporal bone. This result was observed in 3/4 bat experiments. Two specimens (17-3758 and 17-2067) exhibited intersecting linear fractures in the center of the temporal bone. Though these fractures appeared to radiate from a common point, they actually occurred remote from the known impact site.

"Brick" (broad, flat impact surface)

Experiments with the brick implement produced fractures of the impacted parietal bone in 3/4 tests, the sphenoid bone in 3/4 tests, and the temporal bone in 3/4 tests (Figure 1.10). All but one experiment (16-3817) produced fractures in multiple cranial bones.

Two brick impacts produced fractures at the known impact site. One experiment (16-3801) produced extensive fragmentation at the impact site, while the other (17-2035) produced a hairline curvilinear fracture surrounding the posteroinferior aspect at the POI. In contrast, the remaining two experiments produced only linear fractures remote from the impact site with no

ectocranial damage at the impact site. In specimen 16-3817 fractures occurred only in the sphenoid bone, while in specimen 16-3805 fractures occurred only in the posterior temporal and posterior parietal bones. Two brick experiments produced diastases of the sphenotemporal and anterior squamosal sutures during impact. However, examination of the crania after impact revealed discernable diastatic fractures in only one specimen (17-2035).

Discussion

The goals of the current study were to investigate cranial fracture initiation in human head impact experiments with different shaped implements and to assess the relationship between impact location and the location of fractures. High-speed videos in the current experiments showed that impacts with all three implements produced peripheral linear fractures. These fractures initiated remote from the impact site at the squamosal and sphenotemporal sutures, as well as within the body of the temporal, sphenoid, and anterior parietal bones. After initiation, peripheral linear fractures traveled back toward the POI, stayed peripheral to the POI, or both. These experiments also contributed data on the relationship between impact location and the location of resultant fracture patterns. Most mid-parietal impacts (11/12 experiments) produced fractures of the parietal bone. However, fractures of the temporal (9/12 experiments) and sphenoid (6/12 experiments) bones were also frequent and in some cases isolated from defects originating at the impact site. A key finding of this study was that as a result of peripheral initiation, four experiments (one hammer, one bat, and two brick) produced fracture patterns consisting only of linear fractures remote from the POI.

These results support the findings of Gurdjian and colleagues (Gurdjian and Lissner 1945, 1947; Gurdjian, Lissner, and Webster 1947; Gurdjian, Webster, and Lissner 1949, 1950a, 1950b, 1953), demonstrating that linear fractures *can* initiate peripherally in areas remote from

the impact site. The impact site in the current study is most similar to Gurdjian and colleagues' posterior parietal region (Gurdjian, Webster, and Lissner 1953). For impacts to this region Gurdjian et al. report the majority (86%) of fractures occurred peripherally in the temporal and inferior parietal regions (Gurdjian, Webster, and Lissner 1953). The results of the current study are comparable to Gurdjian et al. in that 10/12 (83%) of experiments generated peripherally initiating fractures and the temporal and parietal were the most frequently damaged bones.

Meanwhile, the results of the current study contrast with Kroman and colleagues' claim that cranial fractures *only* initiate at and radiate from the POI (Kroman 2007; Kroman, Kress, and Porta 2011). Our results do not necessarily refute Kroman et al., as some experiments in the study did produce linear fractures that radiated from the impact site. However, differences between our results and Kroman's require further exploration. The majority of experiments in the current study produced at least one peripherally initiating linear fracture, while Kroman et al. obtained only POI initiation. This presents the question: how did different experimental cranial impact studies produce such different findings of fracture initiation and propagation?

According to Gurdjian and colleagues (Gurdjian, Webster, and Lissner 1950b), fractures form peripherally when a blow produces areas of outbending (deformation) remote from the impact site, and at the POI when a blow produces sufficient local deformation to produce fracture at the impact site. Both extrinsic (impact-related) and intrinsic (anatomical) factors could influence whether excessive deformation occurs locally or peripherally and therefore provide potential explanations for the results obtained in the current study and those in Kroman (Kroman 2007) and Kroman et al (Kroman, Kress, and Porta 2011).

First, we can consider an explanation involving extrinsic factors. Given that both experiments were performed under laboratory conditions, most extrinsic variables are known in

both studies. One variable commonly used to explain fracture behavior is impact velocity. As a viscoelastic material, bone is stiffer when loaded rapidly than it is when loaded slowly. Therefore, under similar levels of impact energy less deformation may be expected in impacts performed at a higher velocity. Though Kroman et al. did not report impact velocity, it can be estimated using the formula $v=\sqrt{(2gh)}$ where g is the acceleration of gravity constant and h is the reported drop height. For their experimental drop heights of 1.96 m and 2.82 m, the impact velocities are approximately 6.20 m/s and 7.43 m/s, respectively. As impact velocity in the current study (5.70 m/s) was slightly lower, it is possible that the current experiments involved slightly greater bone deformations. However, Delye et al. (Delye et al. 2007) report no significant differences in specimen deformation in cranial impact experiments performed at different velocities within this range. Therefore, it seems unlikely that loading rate played a major role in the reported differences between Kroman et al. and the current study.

Another set of extrinsic variables to consider involves the implements used to generate fracture. Various researchers have reported implement effects on biomechanical parameters and fracture patterns (Hodgson and Thomas 1971, 1973; Allsop, Perl, and Warner 1991; Sulaiman et al. 2014; DeLand et al. 2016; Vaughan et al. 2016). Though Kroman and Kroman et al. report few details about the impactor, its mass (8.5 kg) is greater than that used in the current experiments (~6.3 kg). An implement of greater mass can be expected to generate more local deformation of the skull, potentially generating more POI initiation than a lighter implement. Therefore, mass could help explain the high frequency of POI fractures in the Kroman and Kroman et al. experiments.

A second key difference between the impactors used in our studies may be the shape of the impact surface. The dimensions and curvature of an object's impact surface affect the contact

area over which force is applied during an impact. An impact surface that generates a relatively small contact area can be expected to deform a similarly small area of bone and produce contact stresses localized to the impact site. However, a surface that generates a broader contact area may deform bone across a larger area, producing higher states of stress in areas distant from the center of impact. Therefore, peripheral initiation is relatively less likely in impacts involving a small contact area and more likely in impacts involving a large contact area.

Kroman et al. do not report the dimensions of their impactor. However, photographs from their study suggest they used an impactor with a square, flat impact surface similar in size to the hammer of the present study. Of all the implements in the current study, the hammer had the smallest, most focal impact surface and was the only one to produce only POI fracture initiation. In contrast, the bat and brick implements had relatively broader impact surfaces and consistently produced peripheral fracture initiation. Additionally, Gurdjian's impact experiments involved deceleration impacts onto a steel slab (Gurdjian and Lissner 1947; Gurdjian, Lissner, and Webster 1947; Gurdjian, Webster, and Lissner 1949, 1950a, 1950b, 1953). This broad, flat surface is most similar to that of the brick impact experiments in the current study. These large impact surfaces may help explain the similarly observed peripheral fracture initiation.

While impact surface dimension may have some explanatory value, it does not account for all the differences observed between studies. In the current study the hammer still produced peripheral initiation in two tests, despite its relatively small, focal impact surface. Meanwhile, Kroman et al. report no peripheral initiation using what appears to be an implement of similar surface dimension, although they used a flat square impactor versus the flat circular impactor of the current study. It is not readily clear at this point how this difference (square vs. circular) may have produced such different results.

Intrinsic factors may also be considered to help explain differences in these studies. It is assumed most intrinsic variables were essentially similar, as both studies were performed using older adult samples of unembalmed postmortem human subjects. Scalp was also retained at the impact site to account for effects of soft tissue documented in other cranial impact studies (Yoganandan and Pintar 2004; Verschueren et al. 2007; Raymond et al. 2009). However, a potential key difference between studies is that impact location differed between studies. Anatomical differences between the impact sites, including cranial curvature, the proximity to the temporal bone, and the proximity to adjacent sutures may help explain differences in fracture initiation behavior.

Kroman et al. performed impacts onto the anterior parietal bone near the parietal boss in an area of potentially increased cranial curvature. In contrast, the current experimental study avoided areas of pronounced curvature. As a result, the impact site was relatively flat in the current study and relatively curved in that of Kroman et al. Given flat impact surfaces in both studies, contact area is expected to be smaller at a more curved impact site and larger at a flatter site. Therefore, it is possible the current experiments involved larger contact areas and subsequently larger areas of bone deformation than those in Kroman et al, increasing the potential for stress generation and fracture initiation in peripheral areas.

In addition to cranial curvature, the proximity of the impact site to the temporal bone may be important. Yoganandan and Pintar (Yoganandan and Pintar 2004) note that the changing geometry between the parietal and temporal bones means that loading of one region may engage the other. In the current study impacts were performed in the mid-parietal bone, relatively closer to the temporal bone than Kroman's anterior parietal impact site. This difference in location may have involved greater engagement of the temporal bone in the current study. Additionally, the

temporal bone is weaker (exhibits lower mechanical strength) but more compliant (exhibits more deformation) than the parietal bone (Yoganandan et al. 1995). Due to the increased ability of the temporal bone to deform, greater outbending may be possible in impacts near this region compared to impacts further away. Furthermore, the squamous portion of the temporal region is much thinner than the parietal bone (Peterson and Dechow 2003). The thinness and reduced strength of the temporal bone compared to the parietal bone may help explain why some tests in the current study produced minimal or no damage at the POI, but produced peripheral linear fractures of the temporal bone.

Finally, the proximity of the impact site to adjacent sutures may also be relevant. In the current study, the impact site was relatively close to the squamosal suture, while in the Kroman et al. study the impact site appears more centered within the parietal bone. Cranial sutures absorb more energy during impact than adjacent cranial bone (Jaslow 1990). The bending strength of sutural bone is positively correlated to sutural interdigitation (Jaslow 1990; Maloul, Fialkov, and Whyne 2013), possibly because more irregular sutures provide more surface area over which energy can be released. The squamosal suture and sutures of the pterion region are typically not highly interdigitated and are therefore expected to be more susceptible to fracture. In the current study, video footage often showed slight separation (diastases) of these sutures. Although few diastatic fractures persisted after impact, linear fractures frequently initiated from these temporary diastases. This provides support for the role of sutures in absorbing energy, but also as areas of stress concentration from which linear fractures can initiate.

In summary, the authors believe differences in fracture behavior observed between the current experiments and those of Kroman and her colleagues, and between the studies of Kroman et al. and Gurdjian et al., may not actually represent contradictory results. Therefore, the current

state of the Gurdjian-Kroman controversy is that there may be no actual controversy. Both POI and peripheral initiation of linear fractures is possible, and various extrinsic and intrinsic factors may influence this process. Specifically, comparison of the methodology between the current study and that of Kroman et al. suggests that contact area between the impact surface and cranium, as well as structural variables at the anatomical location of impact, could have influenced the location of fracture initiation. However, an interesting finding of the current study was that even within tests conducted at the same location, with the same implement, and according to the same experimental protocols, there were differences between specimens in the location of fracture initiation and the resultant fracture patterns. This variation suggests that intrinsic factors unique to an individual including but not limited to bone density, skull thickness, curvature, and degree of cranial suture fusion may also play an important role in determining fracture behavior. Additional research is needed to assess the relative effects of each of the above-mentioned factors.

The mechanical results of the current study were comparable with findings in the literature and in concert with principles of mechanics. With the different shapes of implements used in the current study, it was assumed that the hammer would have the smallest contact area with the skull during impact, while the brick would have the largest contact area and the contact area for the bat would be of an intermediate surface area. Using adult monkey skulls, a study by Sulaiman et al. (Sulaiman et al. 2014) has shown that the production of cranial fractures may depend on impact intensity in combination with surface area of contact, with larger contact areas requiring a higher intensity of impact. This supports the findings in the current study that the brick delivered more energy to the head than the hammer. In addition, a study using pediatric porcine skulls dropped on variously shaped interfaces has shown that it takes less energy to

create a cranial fracture against a focal surface than a flat surface (Vaughan et al. 2016). Similarly, the results of the current study also showed a significantly lower force to initiate fracture in the hammer versus the bat or brick impacts. This may be explained by the stress, defined as the force divided by the contact area, being at the same level to initiate cranial fracture in these impact experiments. Finally, contact duration was determined in the current study to be longer in the hammer impacts than that in the bat or brick impacts, implying that more local bone deformation prior to fracture initiation might have occurred in the hammer versus the bat or brick impacts to cause more focal fracture initiation. Future studies are needed to test this hypothesis, where strain sensors can be attached to various locations of the skull for measurements of local bone deformation during blunt force impacts to the human cadaver head.

As in most experimental studies, there are limitations in the current study. Direct observation of the fracture events at the POI was limited because the impactor obscured fractures that developed directly beneath it. Therefore it was not possible to sequence fractures localized at the impact site itself. Additionally, since the experimental method involved the use of intact heads, we could not film fracture formation on the internal cranial surface. Linear fractures are expected to initiate in tension on the internal surface of the cranium directly beneath the impact site, and on the external surface of the cranium in areas of peripheral outbending. We were unable to test this expectation in the current study, nor evaluate the relative timing of such potential events. Furthermore, because the heads were later used in additional impact experiments to study the effects of multiple cranial impacts, fractures on the internal surface could not be associated with a single impact after the fact. Finally, while the older male adult sample used in this study is typical of the anatomical donor population, it does not necessarily represent a forensic sample. Age-related changes to bone may occur, including but not limited to

loss of bone density, changes in deformability, and increased fusion of the cranial sutures. As such, it is unknown whether the results obtained in the current study are typical of blunt force fracture patterns sustained by younger adults.

Conclusions

This study contributes new experimental data toward the characterization of fracture formation in blunt cranial impacts. The results demonstrate that cranial fracture initiation, propagation, and sequence of multiple fractures are more complex than typically depicted in the literature and various intrinsic and extrinsic factors may influence the process. Specimens subject to different extrinsic input parameters (namely, implement shape) exhibited differences in fracture initiation and propagation. However, the study demonstrated variation even between specimens subject to similar input parameters.

Most importantly, the study provides direct, definitive evidence that blunt cranial impacts *can* produce linear fractures initiating remote from the impact site. This finding is significant because assumptions about how fractures initiate and propagate may affect how practitioners evaluate the point and minimum number of cranial impacts in forensic cases. If practitioners assume that linear fractures initiate only from the point of impact then they must also assume that individual linear fractures represent individual impact sites. However, the current results demonstrate that cranial fractures can initiate at the point of impact, peripheral to the impact site, or at multiple locations simultaneously. The implications of these findings for forensic practice are as follows:

1. *Practitioners are likely to encounter peripheral linear fractures in forensic cases.* The majority of experiments in the current study, including impacts with three different shaped implements, produced peripherally initiating linear fractures. This suggests that at

least some forensic cases involving blunt force cranial trauma will exhibit peripherally initiating fractures. Therefore, practitioners cannot assume all linear cranial fractures to radiate from impact sites.

2. *As a result of peripheral initiation, linear fractures may occur remote from the actual impact site.* In several mid-parietal impact tests, linear fractures initiated peripherally and stayed peripheral to the impact site as they propagated. The resulting fracture patterns included one or more peripheral linear fractures in the sphenoid, temporal, and/or inferior parietal bones with no damage at the mid-parietal impact site. In these cases, traditional understanding of fracture initiation could lead practitioners to misidentify impact sites. Practitioners should be aware that one or more linear fractures in the temporoparietal region can result from a single mid-parietal impact.
3. *As a result of peripheral initiation, linear fractures may converge peripheral to the impact site.* Some mid-parietal impacts produced multiple peripherally initiating fractures that converged in the temporal, away from the impact site. In these cases traditional understanding of fracture initiation could lead practitioners to interpret the point of convergence as a separate temporal impact site. Practitioners should be aware that converging fractures in the temporal can result from a mid-parietal blunt impact and do not necessarily represent a separate temporal impact site.
4. *In summary, the assumption that cranial fractures initiate only from the point of impact is inaccurate and could lead to misidentification of the impact site or potentially, overestimation of the minimum number of impacts.*

Interface	Specimen	Initiation and Propagation Summary
Hammer	**17-3827**	Not visible on camera, the impact produced a shallow circular depression at the POI.
	16-3779	A linear fracture initiated at the POI and traveled to the coronal suture. Next, a diastatic fracture of the sphenotemporal suture formed. The implement began to penetrate the bone at the impact site, eventually producing a circular depression at the POI. Meanwhile, the initial linear fracture branched inferiorly and traveled into the temporal bone. This fracture branched within the temporal, fragmenting that bone.
	17-0006	A peripheral-linear fracture initiated in the temporal and traveled superiorly toward the POI. Then, a concentric fracture continuous with the first linear fracture encircled the POI. Next, a linear fracture initiated at the POI and propagated anteroinferiorly toward pterion. Simultaneously, the first linear fracture branched within the temporal, traveling anteriorly. Finally, the implement penetrated the bone at the impact site. Though not visible on camera, this impact also produced depression and fragmentation of the bone at the impact site and three short linear fractures extending anteriorly, posteriorly, and inferiorly from the edge of the depressed defect.
	17-3757	A peripheral-linear fracture initiated in the inferior temporal bone and propagated superiorly to the squamosal suture. Within the temporal bone, additional fractures branched from this initial fracture and traveled superiorly into the parietal and inferiorly toward the external auditory meatus.
Bat	**17-2067**	A slight diastasis of the sphenotemporal suture formed. Next, a linear fracture initiated peripherally in the center of the temporal and traveled superiorly toward the POI. Simultaneously, a linear fracture initiated at the POI and traveled inferiorly and anteriorly into the sphenoid and frontal. Finally, several linear fractures formed within the temporal bone, fragmenting that bone. Though not visible on camera, the impact also produced a hairline curvilinear fracture surrounding the superior aspect of the POI.
	16-3803	A peripheral-linear fracture initiated superior to the sphenoidal angle of the parietal and traveled in two directions, posteriorly back to the POI and anteriorly into the frontal. This fracture branched and traveled inferiorly into the sphenoid. Though not visible on camera, the impact also produced a hairline curvilinear fracture superior to the POI.

Table 1.1 Summaries of fracture initiation and propagation for each cranial impact experiment.

Table 1.1 (cont'd)

	17-3758	A diastasis of the sphenotemporal suture and anterior squamosal suture formed. A peripheral-linear fracture initiated from this diastasis and traveled superoposteriorly into the parietal anterior to the impact site. Next, a linear fracture initiated at the posterior squamosal suture and traveled anteriorly into the temporal. This fracture then branched within the temporal, fragmenting that bone. Though not visible on camera, the impact also produced a curvilinear fracture in the parietal extending between the squamosal suture and the posterior aspect of the impact site.
	17-4813	A diastatic fracture of the sphenotemporal and anterior squamosal sutures formed. Peripheral-linear fractures traveled from this diastatic fracture posteriorly and inferiorly into the temporal, superiorly into the parietal, and anteriorly into the sphenoid. Examination of the specimen revealed no ectocranial defects at the POI.
Brick	**16-3801**	Slight diastases of the sutures of the pterion region formed. A peripheral-linear fracture initiated in the anterior temporal and propagated in two directions, superoposteriorly toward the POI and inferoanteriorly away from the POI. After this point, fracture initiation and propagation was difficult to sequence due to the presence of multiple initiation sites resulting in severe comminution.
	17-2035	A peripheral linear fracture extended between the sphenoid and squamosal suture, eventually traveling posteriorly toward the POI. Though not visible on camera, examination of the specimen after impact revealed a hairline semicircular fracture surrounding the posterior aspect of the POI.
	16-3805	A peripheral linear fracture initiated in the inferior temporal, superior to the mastoid process. This fracture propagated posteriorly toward the squamosal suture. Examination of the specimen after impact showed the inferoanterior extent of the fracture was the external auditory meatus and the superoposterior extent was the posterior parietal bone, superior to the cranial landmark asterion. No ectocranial defects were present at the POI.
	16-3817	A diastasis of the sphenotemporal suture formed. Peripheral-linear fractures traveled from this suture into the sphenoid. Examination of the specimen after impact revealed no ectocranial defects at the POI.

REFERENCES

REFERENCES

Allsop, D., T.R. Perl, and C.Y. Warner. 1991. "Force/Deflection and Fracture Characteristics of the Temporo-Parietal Region of the Human Head." *Proceedings of the 35th Stapp Car Crash Conference* 35: 269–78.

Baumer, T.G., N.V. Passalacqua, B.J. Powell, W.N. Newberry, T.W. Fenton, and R.C. Haut. 2010. "Age-Dependent Fracture Characteristics of Rigid and Compliant Surface Impacts on the Infant Skull - A Porcine Model." *Journal of Forensic Sciences* 55 (4): 993–97.

Berryman, H.E., J.F. Berryman, and T.B. Saul. 2018. "Bone Trauma Analysis in a Forensic Setting: Theoretical Basis and a Practical Approach for Evaluation." In *Forensic Anthropology: Theoretical Framework and Scientific Basis*, edited by C.C. Boyd and D.C. Boyd, 213–34. Chichester, West Sussex, UK: John Wiley & Sons Ltd.

Berryman, H.E., N.R. Shirley, and A.K. Lanfear. 2013. "Low-Velocity Trauma." In *Forensic Anthropology: An Introduction*, edited by M.A. Tersigni-Tarrant and N.R. Shirley, 271–90. Boca Raton, FL: CRC Press.

Berryman, H.E., and S.A. Symes. 1998. "Recognizing Gunshot and Blunt Cranial Trauma Through Fracture Interpretation." In *Forensic Osteology: Advances in the Identification of Human Remains*, edited by Kathleen J. Reichs, 2nd ed., 333–52. Springfield, IL: Charles C. Thomas.

Chattopadhyay, S., and C. Tripathi. 2010. "Skull Fracture and Haemorrhage Pattern among Fatal and Nonfatal Head Injury Assault Victims - a Critical Analysis." *Journal of Injury & Violence Research* 2 (2): 99–103.

Christensen, A.M., J.T. Hefner, M. Smith, J. Webb, M. Bottrell, and T.W. Fenton. 2018. "Forensic Fractography of Bone." *Forensic Anthropology* 1 (1): 32–51.

Cowin, S.C. 2001. *Bone Biomechanics Handbook*. Boca Raton, FL: CRC Press.

DeLand, T.S., E.R. Niespodziewanski, T.W. Fenton, and R.C. Haut. 2016. "The Role of Interface on the Impact Characteristics and Cranial Fracture Patterns Using the Immature Porcine Head Model." *Journal of Forensic Sciences* 61 (S1): S53-59.

Delye, H., P. Verschueren, B. Depreitere, I. Verpoest, D. Berckmans, J. Vander Sloten, G. Van Der Perre, and J. Goffin. 2007. "Biomechanics of Frontal Skull Fracture." *Journal of Neurotrauma* 24 (10): 1576–86.

DiMaio, V.J., and D. DiMaio. 2001. *Forensic Pathology*. Boca Raton, FL: CRC Press.

Galloway, A, ed. 1999. *Broken Bones*. 1st ed. Springfield, IL: Charles C. Thomas.

Gurdjian, E.S., J.E. Webster, and H.R. Lissner. 1953. “Observations on Prediction of Fracture Site in Head Injury.” *Radiology* 60 (2): 226–35.

Gurdjian, E.S., J.E. Webster, and H.R. Lissner. 1949. “Studies on Skull Fracture with Particular Reference to Engineering Factors.” *The American Journal of Surgery* 78 (5): 736–42.

Gurdjian, E.S., and H.R. Lissner. 1945. “Deformation of the Skull in Head Injury: A Study with the Stresscoat Technique.” *Surgery Gynecology and Obstetrics* 81: 679–87.

Gurdjian, E.S., and H.R. Lissner. 1947. “Deformations of the Skull in Head Injury as Studied by the ‘Stresscoat’ Technic.” *The American Journal of Surgery* 73 (2): 269–81.

Gurdjian, E.S., H.R. Lissner, and J.E. Webster. 1947. “The Mechanism of Production of Linear Skull Fractures: Further Studies on Deformation of the Skull by the Stresscoat Technique.” *Surgery Gynecology and Obstetrics* 85 (2): 195–201.

Gurdjian, E.S., J.E. Webster, and H.R. Lissner. 1950a. “The Mechanism of Skull Fracture.” *Journal of Neurosurgery* 7 (2): 106–14.

Gurdjian, E.S., J.E. Webster, and H.R. Lissner. 1950b. “The Mechanism of Skull Fracture.” *Radiology* 54 (3): 313–38.

Hart, G.O. 2005. “Fracture Pattern Interpretation in the Skull: Differentiating Blunt Force from Ballistics Trauma Using Concentric Fractures.” *Journal of Forensic Sciences* 50 (6): 1–6.

Hodgson, V.R., and L.M. Thomas. 1971. “Breaking Strength of the Human Skull vs. Impact Surface Curvature.” U.S. Department of Transportation, HS-800-583, Springfield, VA.

Hodgson, V.R., and L.M. Thomas. 1973. “Breaking Strength of the Human Skull vs. Impact Surface Curvature.” DOT-HS-801-002.

Isa, M.I., T.W. Fenton, T. Deland, and R.C. Haut. 2018. “Assessing Impact Direction in 3-Point Bending of Human Femora: Incomplete Butterfly Fractures and Fracture Surfaces.” *Journal of Forensic Sciences* 63 (1): 38–46.

Jaslow, C.R. 1990. “Mechanical Properties of Cranial Sutures.” *Biomechanics* 23 (4): 313–21.

Kaye, B., C. Randall, D. Walsh, and P. Hansma. 2012. “The Effects of Freezing on the Mechanical Properties of Bone.” *Open Bone Journal* 4 (1): 14–19.

Kiadaliri, A.A., B.E. Rosengren, and M. Englund. 2018. “Fracture-Related Mortality in Southern Sweden: A Multiple Cause of Death Analysis, 1998–2014.” *Injury* 49 (2): 236–42.

Kimmerle, E.H., and J.P. Baraybar, eds. 2008. *Skeletal Trauma: Identification of Injuries Resulting from Human Rights Abuse and Armed Conflict*. Boca Raton, FL: CRC Press.

Kranioti, E. 2015. “Forensic Investigation of Cranial Injuries Due to Blunt Force Trauma: Current Best Practice.” *Research and Reports in Forensic Medical Science*, 5: 25-37.

Kroman, A.M. 2007. “Fracture Biomechanics of the Human Skeleton.” Ph.D. Dissertation, University of Tennessee, Knoxville, TN.

Kroman, A.M., T.A. Kress, and D. Porta. 2011. “Fracture Propagation in the Human Cranium: A Re-Testing of Popular Theories.” *Clinical Anatomy* 24 (3): 309–18.

Kroman, A.M., and S.A. Symes. 2013. “Investigation of Skeletal Trauma.” In *Research Methods in Human Skeletal Biology*, edited by E.A. DiGangi and M.K. Moore, 219–39. New York: Elsevier.

Maloul, A., J. Fialkov, and C.M. Whyne. 2013. “Characterization of the Bending Strength of Craniofacial Sutures.” *Journal of Biomechanics* 46 (5): 912–17.

Maples, W.R. 1986. “Trauma Analysis by the Forensic Anthropologist.” In *Forensic Osteology: Advances in the Identification of Human Remains*, edited by K.J. Reichs, 1st ed., 218–28. Springfield, IL: Charles C. Thomas.

Moritz, A.R. 1954. *The Pathology of Trauma*. Philadelphia: Lea & Febiger.

National Institute of Standards and Technology Organization of Scientific Area Committees for Forensic Sciences. 2016. “Research Needs Assessment: Controlled Experimental Bone Trauma Studies.” https://www.nist.gov/topics/organization-scientific-area-committees-forensic-science/osacresearch-and-development-needs.

Passalacqua, N.V., and C.W. Rainwater, eds. 2015. *Skeletal Trauma Analysis: Case Studies in Context*. Chichester, West Sussex, UK: John Wiley & Sons Ltd.

Peterson, J., and P.C. Dechow. 2003. “Material Properties of the Human Cranial Vault and Zygoma.” *Anatomical Record - Part A Discoveries in Molecular, Cellular, and Evolutionary Biology* 274A (1): 785–97.

Powell, B.J., N.V. Passalacqua, T.W. Fenton, and R.C. Haut. 2013. “Fracture Characteristics of Entrapped Head Impacts Versus Controlled Head Drops in Infant Porcine Specimens.” *Journal of Forensic Sciences* 58 (3): 678–83.

Raymond, D., C. Van Ee, G. Crawford, and C. Bir. 2009. “Tolerance of the Skull to Blunt Ballistic Temporo-Parietal Impact.” *Journal of Biomechanics* 42 (15): 2479–85.

Saukko, P., and B. Knight. 2016. *Knight’s Forensic Pathology*. 4th ed. Boca Raton, FL: CRC Press.

Smith, O.C., E.E. Pope, and S.A. Symes. 2003. “Look until You See: Identification of Trauma in Skeletal Material.” In *Hard Evidence: Case Studies in Forensic Anthropology*, edited by

D.W. Steadman, 138–54. Old Tappan, NJ: Pearson Education.

Spitz, W.U., D.J. Spitz, and R. Clark, eds. 2006. *Spitz and Fisher's Medicolegal Investigation of Death: Guidelines for the Application of Pathology to Crime Investigation*. 4th ed. Springfield, IL: Charles C. Thomas.

Stewart, T.D. 1979. "Judging Time and Cause of Death." In *Essentials of Forensic Anthropology Especially as Developed in the United States*, 69–81. Springfield, IL: Charles C. Thomas.

Sulaiman, N.A., K. Osman, N.H. Hamzah, and S.P.A. Amir Hamzah. 2014. "Blunt Force Trauma to Skull with Various Instruments." *Malaysian Journal of Pathology* 36 (1): 33–39.

Symes, S.A., E.N. L'Abbé, E.N. Chapman, I. Wolff, and D.C. Dirkmaat. 2012. "Interpreting Traumatic Injury to Bone in Medicolegal Investigations." In *A Companion to Forensic Anthropology*, edited by D.C. Dirkmaat, 340–89. Malden, MA: Wiley-Blackwell.

Symes, S.A., E.N. L'Abbé, K.E. Stull, M. LaCroix, and J.T. Pokines. 2014. "Taphonomy and the Timing of Bone Fractures in Trauma Analysis." In *Manual of Forensic Taphonomy*, edited by J.T. Pokines and S.A. Symes, 341–65. Boca Raton, FL: CRC Press.

van Haaren, E.H., B.C. van der Zwaard, A.J. van der Veen, I.C. Heyligers, P.I.J.M. Wuisman, and T.H. Smit. 2008. "Effect of Long-Term Preservation on the Mechanical Properties of Cortical Bone in Goats." *Acta Orthopaedica* 79 (5): 708–16.

Vaughan, P.E., C.C.M. Vogelsberg, J.M. Vollner, T.W. Fenton, and R.C. Haut. 2016. "The Role of Interface Shape on the Impact Characteristics and Cranial Fracture Patterns Using the Immature Porcine Head Model." *Journal of Forensic Sciences* 61 (5): 1190–97.

Verschueren, P., H. Delye, B. Depreitere, C. Van Lierde, B. Haex, D. Berckmans, I. Verpoest, J. Goffin, J. Vander Sloten, and G. Van der Perre. 2007. "A New Test Set-up for Skull Fracture Characterisation." *Journal of Biomechanics* 40 (15): 3389–96.

Wedel, V.L., and A. Galloway, eds. 2014. *Broken Bones: Anthropological Analysis of Blunt Force Trauma*. 2nd ed. Springfield, IL: Charles C. Thomas.

Whyte, T., T. Gibson, R. Anderson, D. Eager, and B. Milthorpe. 2016. "Mechanisms of Head and Neck Injuries Sustained by Helmeted Motorcyclists in Fatal Real-World Crashes: Analysis of 47 In-Depth Cases." *Journal of Neurotrauma* 33 (19): 1802–7.

Yoganandan, N., and F.A. Pintar. 2004. "Biomechanics of Temporo-Parietal Skull Fracture." *Clinical Biomechanics* 19 (3): 225–39.

Yoganandan, N., F.A. Pintar, A. Sances, P.R. Walsh, C.L. Ewing, D.J. Thomas, and R.G. Snyder. 1995. "Biomechanics of Skull Fracture." *Journal of Neurotrauma* 12 (4): 659–68.

PAPER 2: IDENTIFICATION OF IMPACT SITES IN MULTIPLE BLUNT FORCE CRANIAL TRAUMA

Abstract

In cases of multiple blunt force cranial trauma, identification of impact sites is the first step in assessing the minimum number and sequence of impacts. This study examines cranial fractures obtained in multiple blunt force impact experiments on 12 postmortem human subjects (PMHS). Fractures were evaluated after one, two, and three impacts to the mid-parietal region. The results suggest that the number of impacts and the impact surface may influence fracture behavior and likelihood of correct impact site identification. After initial fracture, subsequent blows required less force to fracture and more frequently produced damage at the impact site. A small, focal surface produced more circumferential and depressed defects localized to the impact site, while implements with broader surfaces produced more linear fractures and tended to extend and complicate preexisting fractures. Therefore, accurate identification of cranial impact sites will be less likely following multiple broad surface impacts to the same region.

Introduction

Blunt force cranial fractures are produced in a variety of contexts including falls, transportation accidents, assaults, child abuse, elder abuse, and human rights abuses (Galloway and Wedel 2014a; Kranioti 2015; Lee and Lathrop 2010; Gibbs 2014; Ta'ala, Berg, and Haden 2006; Fleischman 2019). Head injuries are often implicated in homicidal fatalities and may relate to the cause of death (Galloway and Wedel 2014b; Kranioti 2015). When these injuries are complex or when decomposition is advanced, the results of skeletal trauma analysis present important evidence in the death investigation. In cases of blunt force cranial trauma, questions of forensic relevance include the location, minimum number, and sequence of impacts (Symes et al. 2012; Galloway and Wedel 2014b; Kranioti 2015; Blau 2017). These assessments are all predicated on the identification of impact sites from cranial fracture patterns.

Several extrinsic factors such as impact velocity, mass, kinetic energy (a function of both mass and velocity), contact area of the impacting object, and whether a body was supported or unsupported during impact are expected to influence how bone fractures in response to the application of blunt force (Symes et al. 2012; Gurdjian, Webster, and Lissner 1950a; Gurdjian 1975; Berryman, Berryman, and Saul 2018; Yoganandan and Pintar 2004; Bass and Yoganandan 2015; Hamel et al. 2013; Motherway et al. 2009). Additionally, intrinsic factors such as cortical and diploic bone thicknesses and densities, the radius of curvature at the impact site, the degree of cranial suture closure, and the presence of defects or irregularities in the bone are all thought to affect cranial fracture formation (Symes et al. 2012; Gurdjian 1975; Gurdjian, Webster, and Lissner 1953; Berryman, Berryman, and Saul 2018; Bass and Yoganandan 2015; Hamel et al. 2013). Due to these myriad sources of variation, the appearance of blunt force cranial impact sites is variable, particularly compared to gunshot impact sites (Hart 2005).

Expectations for how fractures form in response to a blunt force impact directly inform the interpretation of cranial fractures. The foundational research on the mechanism of cranial fracture was performed in the 1940s and 1950s by Gurdjian and colleagues (Gurdjian and Lissner 1945, 1947; Gurdjian, Lissner, and Webster 1947; Gurdjian, Webster, and Lissner 1949, 1950a, 1950b, 1953). Gurdjian et al. used sub-failure stresscoat experiments to assess how the cranium deforms after impact. They found that an impact causes bone to inbend (deform inward) at the point of impact (POI), generating tensile stress on the inner table. Meanwhile, inbending at the POI also causes noncontinuous areas peripheral to the POI to outbend (deform outward) generating tensile stresses on the outer table (Gurdjian and Lissner 1945; Gurdjian, Lissner, and Webster 1947; Gurdjian and Lissner 1947). In failure-level experiments, cranial fractures formed in these same areas of high tensile stress (Gurdjian, Webster, and Lissner 1950a, 1950b, 1953).

Based on these findings, Gurdjian and colleagues predict how cranial fractures form relative to an impact site (Gurdjian, Webster, and Lissner 1950a, 1953; Gurdjian 1975). If impact energy is insufficient, the inbent area at the POI will rebound without fracture. In this case, linear fractures will initiate peripherally on the outer table and propagate toward areas of stress concentration: the impact site, which becomes a region of tensile stress as it rebounds, and/or structural discontinuities such as foramina or sutures. However, given sufficient energy, fractures will form at the POI. Depressed fractures may form at the boundary of the inbent area underlying the point of impact (Gurdjian, Webster, and Lissner 1953). Linear fractures may initiate internally within the inbent area at the impact site and radiate externally. Additionally, semicircular or curvilinear fractures may form at various distances from the POI. These fractures initiate externally at the junction of inbent and not-inbent bone and propagate internally (Gurdjian, Webster, and Lissner 1950a). Moritz (Moritz 1954), a forensic pathologist and

another historically influential source on the mechanism of skull fracture, presents a largely similar description of cranial fracture formation.

Until recently there was some question as to whether linear fractures could initiate in areas peripheral to the POI as Gurdjian and colleagues describe. Kroman et al. (Kroman, Kress, and Porta 2011) performed impact experiments on intact heads from postmortem human subjects (PMHS) in order to test this finding using modern methods. In a series of parietal impact experiments, they report all fractures initiated at the POI and radiated outward. However, in a more recent study of mid-parietal impacts, Isa et al. (Isa et al. 2019) demonstrated linear fractures of the cranial vault can form both at and peripheral to the POI. This result suggested that linear fractures in the absence of other features are unreliable indicators of impact site.

The mechanism of skull fracture as presented by Gurdjian and colleagues (Gurdjian, Webster, and Lissner 1949, 1950a, 1950b, 1953; Gurdjian 1975) and Moritz (Moritz 1954) is frequently referenced in forensic anthropology texts. As a result, these texts contain similar descriptions of cranial fracture formation and expectations for the appearance of blunt force impact sites (E.H. Kimmerle and Baraybar 2011; Stewart 1979; Berryman and Symes 1998; Galloway 1999; Hart 2005; D.A. Komar and Buikstra 2008; Smith, Pope, and Symes 2009; Maples 1986; Symes et al. 2012; Galloway and Wedel 2014b; Christensen, Passalacqua, and Bartelink 2014; Love 2015; Blau 2017; Lovell and Grauer 2019). Linear fractures are expected to radiate from a central point at the point of impact, followed by semicircular or curvilinear fractures circumscribing the impact site. Therefore, "…identifiable points of impact are determined by noting areas of fracture with surrounding (hoop) or radiating fracture lines" (Byers 2017, 316). Additionally, depressed fractures are expected to be localized at and around the point of impact.

These features form the basis for interpreting blunt force impact sites in the cranial vault. However, they have yet to be assessed systematically in cases of multiple blunt force cranial trauma in which the impacting object as well as the number, locations, and sequence of impact sites are precisely known.

Following identification of cranial impact sites, determination of impact sequence is also of forensic relevance. Sequencing is typically discussed in terms of Puppe's rule (Symes et al. 2012; E.H. Kimmerle and Baraybar 2011; Berryman and Symes 1998; Madea and Staak 1988; D.A. Komar and Buikstra 2008; Lovell and Grauer 2019; Spitz 1993; Christensen, Passalacqua, and Bartelink 2014; Saukko and Knight 2016; Smith, Pope, and Symes 2009). Puppe's rule states that fractures from subsequent impacts will be arrested at fracture lines generated during previous impacts (Madea and Staak 1988). Preexisting fractures are expected to dissipate energy such that new fractures do not cross them. Puppe's rule has been applied to sequence fractures associated with gunshot entrance and exit wounds in forensic cases (Madea and Staak 1988; Smith, Berryman, and Lahern 1987; Dixon 1984). The rule has also been tested experimentally in blunt force experiments to human crania (Schüttrumpf 1966). Puppe's rule was verified in experiments involving two sequential impacts with a round mallet (25 cm^2 in area). However, the application of Puppe's rule in cases involving more than two blunt force impacts and with different surface shapes should also be explored.

To address the issues of cranial site identification and sequence, this study assesses fracture patterns produced in experimental multiple blunt force cranial impacts. Isa et al. (Isa et al. 2019) previously described cranial fracture formation for a series of single impacts to twelve unembalmed heads. The current research builds on this work, assessing fracture patterns after two additional impacts to the same crania. The goals of this study were: 1) to document cranial

fracture behavior after one, two, and three impacts, 2) to compare the appearance and severity of fractures produced in impacts 1, 2, and 3, and 3) to compare the appearance and severity of fractures produced in experiments with three different blunt surfaces. It was hypothesized that commonly described impact site features would be more frequent with a focal impact surface compared to broader surfaces, and that subsequent impacts would produce more severe fracture than initial impacts.

Materials and Methods

Specimens

The experimental sample includes twelve intact heads from unembalmed PMHS acquired from outside procurement agencies (university anatomy departments). These agencies obtained permissions for research according to the Uniform Anatomical Gift Act. The twelve heads in this sample were the subject of a recent study by Isa et al. (Isa et al. 2019) investigating single impacts to the mid-parietal. Immediately after that initial impact, two additional impacts were delivered to the same heads. For the purposes of the original study, soft tissue was removed from areas adjacent the impact site to allow for video documentation of fracture initiation and propagation following impact. For subsequent impacts a patch of skin from the area corresponding to the impact site was replaced prior to experimentation.

Impact experiments

The method of impact delivery has previously been described in detail (Isa et al. 2019). In brief, impacts were designed to simulate blows to an upright individual while allowing for a reasonably realistic degree of post-impact movement. Impacts were administered using a pneumatic system (Figure 1.1). Controlled pressure release of nitrogen gas provided the initial

velocity to the guide trolley holding the impactor. After impact, the support plate, to which the head was mounted, was free to slide along frictionless bearings away from the impactor.

To investigate impact surface effects, three aluminum impactors of different surface shapes were chosen for these experiments (Figure 1.2). These included a flat surface of a 1.125-inch diameter cylinder (6.27 kg), a curved surface of a 2.5-inch diameter, 2.5-inch long cylinder (6.31 kg), and a flat surface of a 3-inch diameter circular implement (6.30 kg). These shapes were selected to represent blunt surfaces within the range of those implicated in forensic cases: a small, focal impact surface (e.g., the face of a hammer), a broad, curved surface (e.g., the barrel of a baseball bat), and a broad, flat surface (e.g., the broad side of a brick), respectively. The terms "hammer," "bat," and "brick" will be used to refer to these implements. However, these should be understood only as shorthand references to impact surfaces investigated in this study and not as specific tools.

Three sequential impacts were administered to each of the twelve heads, for a total of 36 experiments. The same implement was used for all three impacts to a single subject, and each implement was tested on four subjects. Blows were delivered at the following locations: first to the low mid-parietal bone between the squamosal suture and the parietal boss; second to a point halfway between the first impact and the coronal suture; and third to a point halfway between the first impact and the lambdoidal suture. Heads were positioned such that all impactors contacted the cranium at an angle normal (perpendicular) to the impact site.

Data collection

A 10,000 lbf force transducer (model 1210AF-10K-B, Interface; Scottsdale, AZ) attached to the guide trolley recorded impact force-time response at a sample rate of 200,000 Hz. Position-time data was recorded at a sample rate of 200,000 Hz using a magnetic linear encoder

(model LM15ICD50AB10F00, Renishaw Inc.; Hoffman Estates, IL), also attached to the guide trolley. Position-time data at the moments immediately before and after the impact were used to calculate the initial (v_i) and final (v_f) velocities (m/s) of the guide trolley. The energy absorbed by the head was then calculated as the change in kinetic energy of the trolley. Based on previous studies of cranial trauma by this research team, including Isa et al. (Isa et al. 2019), the energy absorbed by a PMHS is a critical parameter that may help determine the initiation of a fracture. As a result, in the current study initial velocity of the guide trolley was carefully controlled and selected to ensure that the energy absorbed was (1) sufficient to initiate cranial fracture, and (2) within the same level across the three implements.

Fracture patterns were documented with photographs and diagrams after each impact (Figure 2.1). Following the third and final impact, heads were cleaned of soft tissue using hot water maceration and reconstructed using an acetone-soluble adhesive. Additionally, the opposing side of the cranial vault was removed using a bone saw to allow for visualization of endocranial fractures (Figure 2.2).

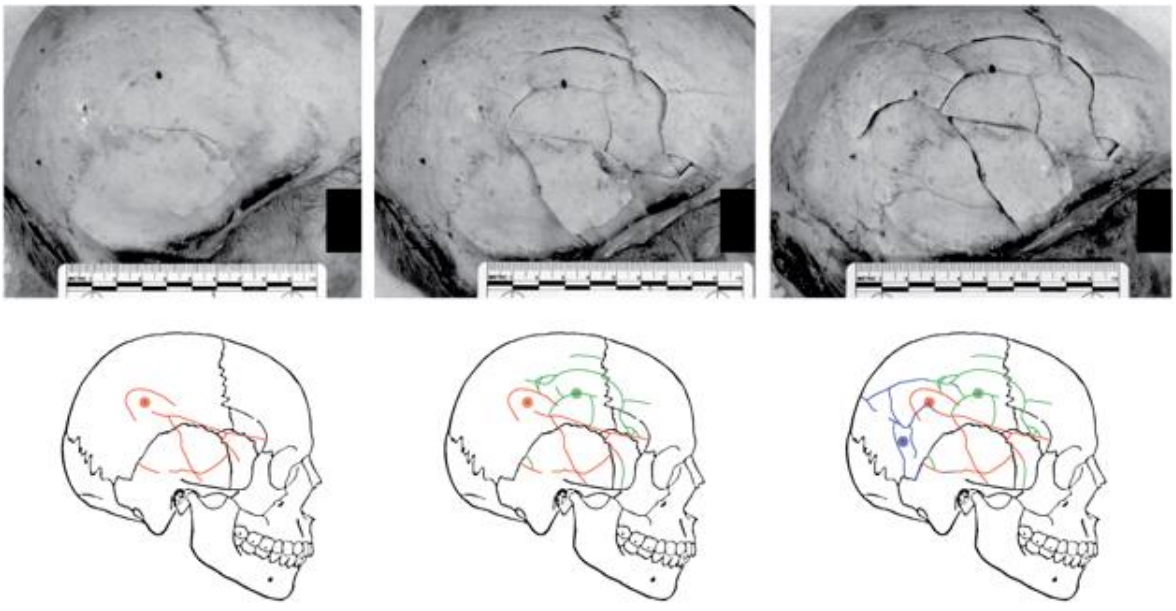

Figure 2.1: Impact photos and diagrams from experiments with specimen 16-2067. From left to right: impact 1, impact 2, and impact 3.

The presence and appearance of fractures were assessed for each impact site. Special attention was given to the presence of commonly described impact site characteristics: radiating linear fractures, circumferential fractures, and depressed fractures. Two types of radiating linear fractures were scored: primary radiating linear fractures (rad1) were scored as present if multiple fractures extended from and/or converged at a common point at the center of impact on either the inner or outer table. Secondary radiating linear fractures (rad2) were scored as present if fractures extended from the edge of a circumferential or depressed fracture. Circumferential fractures (circ) were scored as present if semicircular or curvilinear fractures circumscribed the impact site, either completely or incompletely. Depressed fractures (depr) were scored as present if the impact caused localized internal displacement of bone. Additionally, fracture characteristics associated with severity including depression, comminution (comm) and delamination of the outer and/or inner table (delam) were assessed. None of these features was considered exclusive and multiple features could be marked present for the same impact site. Finally, photos and diagrams recorded after each impact were used to assess how new fractures behaved in relation to preexisting ones.

Figure 2.2: Reconstructed cranium 17-0006 (left) and internal view (right).

Statistical Analysis

Two-way factorial ANOVA with Tukey post hoc test was used to compare the main effects of implement shape (factor one) and impact number (factor two), and their interaction effects on energy absorbed (E_a) and peak force. Results were considered significant at $p<0.05$. For each fracture type, Fisher's exact tests were used to assess the significance of associations between implement and fracture type, and between impact number and fracture type, with $p<0.05$ considered significant.

Multiple correspondence analysis (MCA) was used to visualize associations among variables assessed in this study. MCA is an extension of correspondence analysis (CA) that allows for the exploration of relationships among multiple dependent categorical variables (Abdi and Valentin 2007). MCA applies standard CA to an indicator matrix where the rows represent individuals and the columns are dummy variables representing nominal variable categories. Row and column factor scores are represented graphically as points in n-dimensional space where dimensions represent linear combinations of the variables of a data table. Interpretations of the

resulting factor maps are based on the distances between points and on the distribution of points along each dimension. Individuals with more similar profiles are closer together, while individuals with more dissimilar profiles are further apart. Likewise, categories with similar profiles are closer together, and dissimilar categories are further apart (Abdi and Valentin 2007).

Factor maps were used to visualize patterns within the dataset. Fracture characteristic variables were treated as active variables and were used in the MCA. Experimental input variables *number* (categories: impact 1, impact 2, impact 3) and *implement* (categories: hammer, bat, brick) were treated as supplemental (illustrative) variables, meaning they did not participate in the MCA and were projected onto the analysis. This projection was used to visualize how impact number and implement relate to the distribution of fracture characteristic variables.

All statistical analyses were conducted in R (R Core Team 2020). The MCA was conducted using the FactoMineR package (Lê, Josse, and Husson 2008).

Results

Mechanical results

Impact experiments were performed at an average initial velocity (v_i) of 5.70±0.51 m/s, translating to an average input energy (E_i) of 103.15±17.45 J. This input produced cranial fractures in all experiments. Energy absorbed by the head (E_a) ranged from 17.31–77.66 J (mean= 53.7±13.9 J). The main effects for impact number ($F_{(2,33)}$=1.07, p=.36) and implement ($F_{(2,33)}$=2.23, p=.12) were not significant. The interaction effect was also nonsignificant ($F_{(4,27)}$=0.43, p=.78). Peak force ranged from 1786.4–10855.6 N (mean=5258.70±2018.53 N). The main effect for impact number was significant ($F_{(2,33)}$=3.87, p=.03). Peak force was significantly higher in impact 1 (6415.82±2155.92N) than in impact 2 (4326.58±1588.03 N); however, peak force in impact 3 (5033.70±1825.01N) was not significantly different from

impact 1 or 2. The main effect of implement ($F_{(2,33)}$=0.24, p=.79) and the interaction effect of implement and number ($F_{(4,27)}$=0.33, p=.86) were not significant.

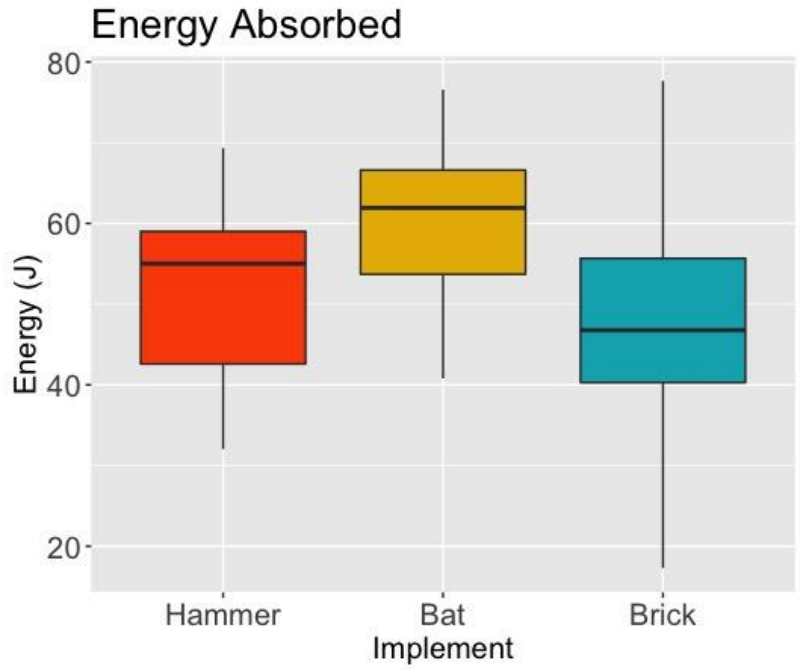

Figure 2.3: Energy absorbed by implement.

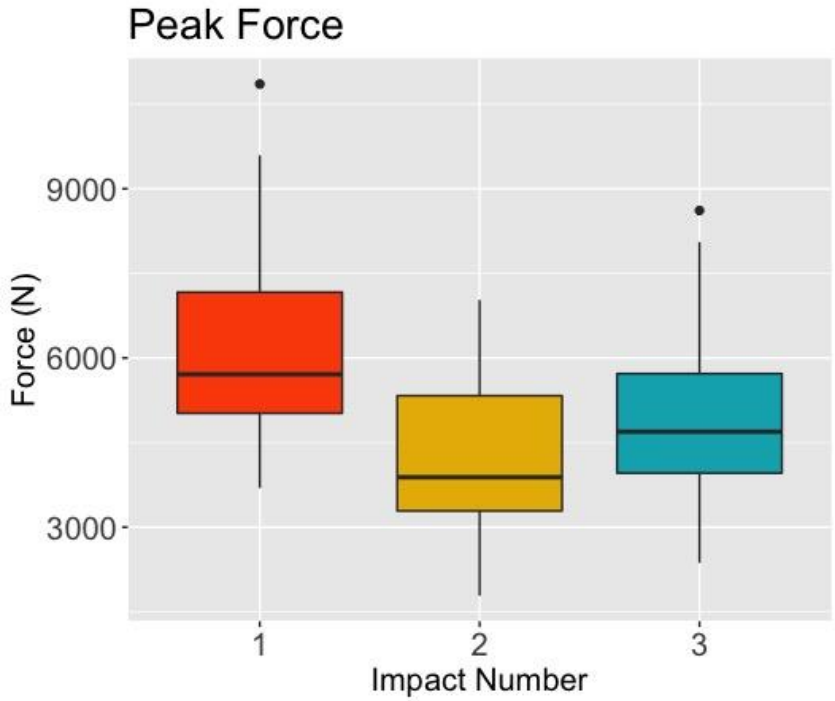

Figure 2.4: Peak force by impact number.

Impact site features

Twenty-eight of the 36 impact sites displayed at least one of the features under investigation. Radiating linear fractures were observed in association with 19/36 impact sites (rad1=12, rad2=13, both=6). Primary radiating fractures were typically longer internally than externally, consistent with initiation on the endosteal surface. Circumferential fractures were produced at 23/36 impact sites. In ten cases, circumferential fractures affected only the outer table of bone. In the other 13 cases, circumferential fractures penetrated both tables. Most of these beveled (widened) internally (Figure 2.5). This is consistent with fractures initiating in tension on the outer table and propagating internally and away from the impact site. Circumferential fractures are often described as forming secondary to radiating linear fractures. In this scenario, radial fractures emanating from a central point ("primary radiating linear fractures" in this study) are expected to form first, and circumferential fracture arcs are expected to form perpendicularly between these. However, in some of the current experiments, circumferential fractures formed in the absence of primary radiating linear fractures. In other cases, radiating and circumferential fractures did not intersect on either the inner or outer table. Finally, in some cases, primary radiating linear fractures were arrested at circumferential fractures, indicating the circumferential fractures formed or were completed first. These results suggest circumferential and radiating fractures form independently and in a variety of sequences.

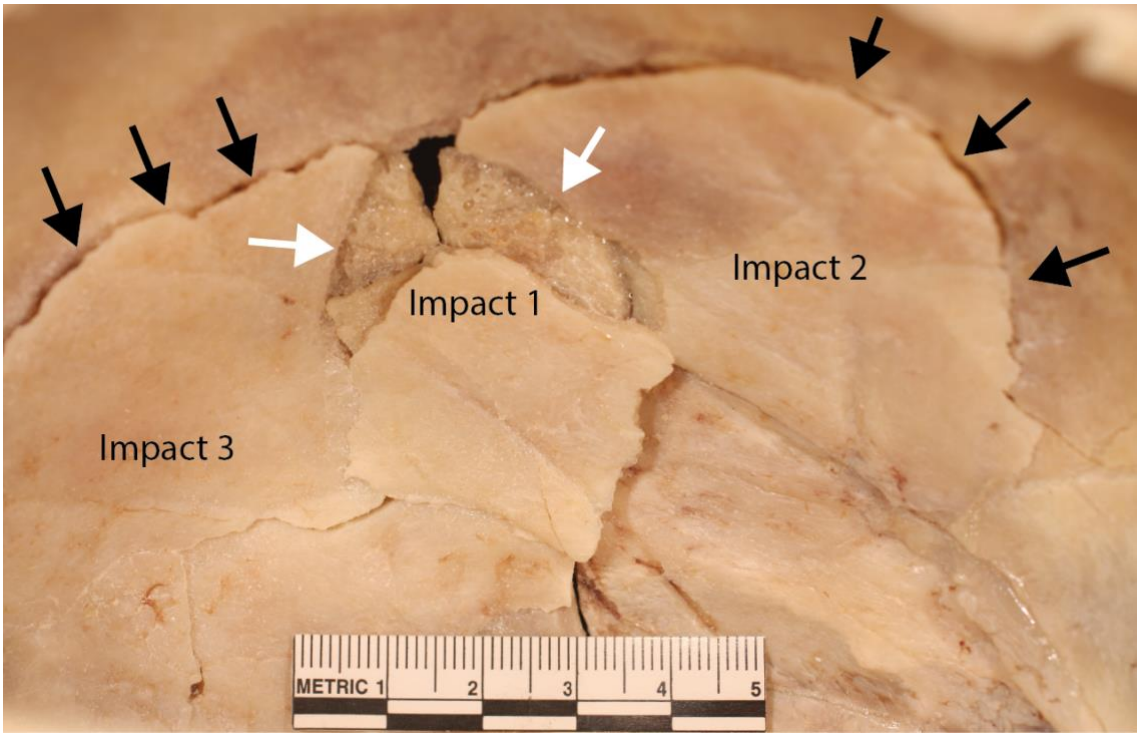

Figure 2.5: Internal view of cranium 17-0006. White arrows indicate delamination at impact site 1. Black arrows indicate internal beveling at impact sites 2 and 3.

Depressed fractures occurred at 15/36 impact sites. A one-way ANOVA was conducted to assess whether group means for peak force differed when depressed fractures were produced vs. when they were not produced. There were significant differences in peak force to fracture between groups ($F_{(1,34)}=16.77$, $p<.0003$). Peak force was lower in the group with depressed fractures present (mean=3905.33±1235.56 N) compared to the group with depressed fractures absent (mean=6225.39±1925.30 N) (Figure 2.6).

Eight out of 36 impact sites did not exhibit any of the features under investigation. This occurred when linear fractures formed peripheral to the impact site, when single linear fractures formed at the impact site, and/or when new fractures formed between preexisting ones, complicating the overall fracture pattern.

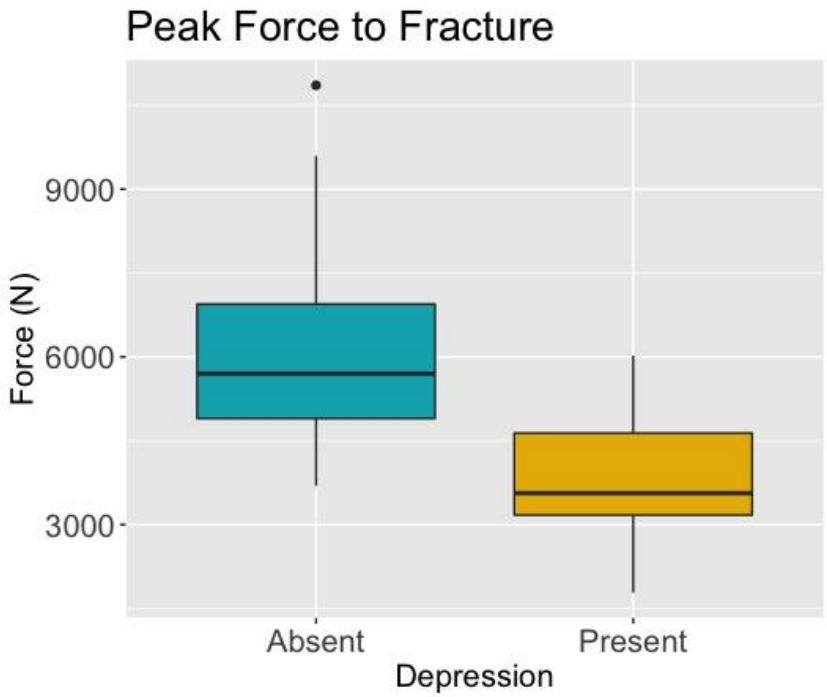

Figure 2.6: Peak force to fracture in impacts that did not produce depressed fractures (absent) vs. impacts that produced depressed fractures (present).

Fracture sequence

After impact 1 produced fracture, new fractures from impact 2 were arrested at preexisting fractures (10/12 experiments) and/or extended preexisting fractures (7/12 experiments). Fractures from impact 3 were arrested at preexisting fractures in 10/12 experiments and extended preexisting fractures in 8/12 experiments. When a prior impact produced fractures that did not penetrate both tables of cranial bone, new fractures from subsequent impacts occasionally crossed these hairline fractures. This occurred in 2/12 impact 2 experiments and 3/12 impact 3 experiments. Hairline fractures never crossed complete fractures.

Impact number

As previously reported (Isa et al. 2019), impact 1 produced peripheral linear fracture without damage at the impact site in 4/12 experiments. In contrast, all impacts 2 and 3 produced impact site damage. Statistical analyses (two-sided Fisher's exact tests) were applied to assess

whether the frequencies of each feature under investigation differed by impact number. None of these differences was significant. However, depressed fractures were more frequent in impact 2 (6/12) and impact 3 (6/12) than impact 1 (3/12) experiments ($p=0.42$). Considering only impacts 2 and 3 ($n=24$), depressed fractures were produced more frequently when a prior impact produced depressed fracture than when there was not a preexisting depressed fracture ($p=0.01$). In the three subjects for which impact 1 produced depressed fractures, both subsequent impacts to the same subject also produced depressed fractures.

The results show a slight trend toward increased severity of fracture with subsequent impacts. In addition to depressed fractures, the presence of comminuted fractures was more frequent in impact 2 (6/12) and impact 3 (5/12) than impact 1 (3/12). Similarly, the presence of delamination was more frequent in impact 2 (4/12) and impact 3 (4/12) than impact 1 (2/12). However, these differences were not significant.

Some patterns emerged in the relationship between impact number and fracture location. Frontal fractures were more frequent in impact 2 (7/12) than impact 1 (2/12) and impact 3 (1/12) experiments ($p=0.04$). Diastatic fractures of the sphenofrontal and coronal sutures were only observed in impact 2 experiments. In contrast, occipital fractures and diastatic fractures of the occipitomastoid and lambdoidal sutures were only observed in impact 3 experiments. These results likely reflect the location rather than the sequence of impact; impact 2 experiments were administered to the anterior parietal and impact 3 experiments to the posterior parietal.

Implement

Two-sided Fisher's exact tests were conducted to assess whether the frequencies of each fracture type differed by implement. None of these differences were significant. However, secondary radiating linear fractures, circumferential fractures, and depressed fractures were most frequent in impacts with the hammer (small, focal implement), least frequent in impacts with the

brick (broad, flat implement), and intermediate in impacts with the bat implement (broad, curved implement). Additionally, hammer impacts tended to produce more severe fractures than the bat and brick including a higher frequency of depression, comminution, and delamination.

The results of sequential hammer (small, focal) impact experiments are shown in Figure 2.7. Hammer impacts typically produced circumferential (9/12) and/or depressed fractures (7/12) localized at the impact site. These remained distinct even after multiple impacts. Primary radiating linear fractures were produced in 5/12 hammer impacts and secondary radiating linear fractures in 7/12 hammer impacts. Half of the impact sites (6/12) featured delamination.

The results of sequential bat (broad, curved) impact experiments are shown in Figure 2.8**.** The majority of bat impacts produced circumferential fractures partially surrounding the impact site (7/12). Primary radiating linear fractures were produced in 5/12 impacts, and secondary radiating linear fractures in 4/12 impacts. Depressed fractures were obtained at 5/12 impact sites; three of these sites also featured delamination. None of the impact 1 bat experiments produced depressed fractures; depressed fractures were obtained only in impacts 2 and 3. Similarly, comminuted fractures were only obtained in impacts 2 and 3 with the bat. Generally, the bat produced more diffuse fracture patterns than those obtained with the hammer. Impacts 2 and 3 tended to extend or complicate pre-existing fracture patterns, particularly when they produced comminution.

The results of sequential brick (broad, flat) impact experiments are shown in Figure 2.9. Brick impacts produced circumferential fractures in 5/12 impacts, primary radiating linear fractures in 2/12 impacts, and secondary radiating linear fractures in 2/12 impacts. These experiments generally produced more linear fractures and less destruction of the cranial vault than the bat and hammer experiments, with one exception. The first impact to subject 16-3801

produced a large comminuted depressed fracture. Subsequent impacts extended and further fragmented this area of depression. This subject accounts for all three depressed fractures, all cases of delamination, and all but one of the comminuted fractures produced in brick experiments. As in the bat experiments, brick impacts 2 and 3 tended to produce fractures that extended, complicated, or joined pre-existing fracture patterns.

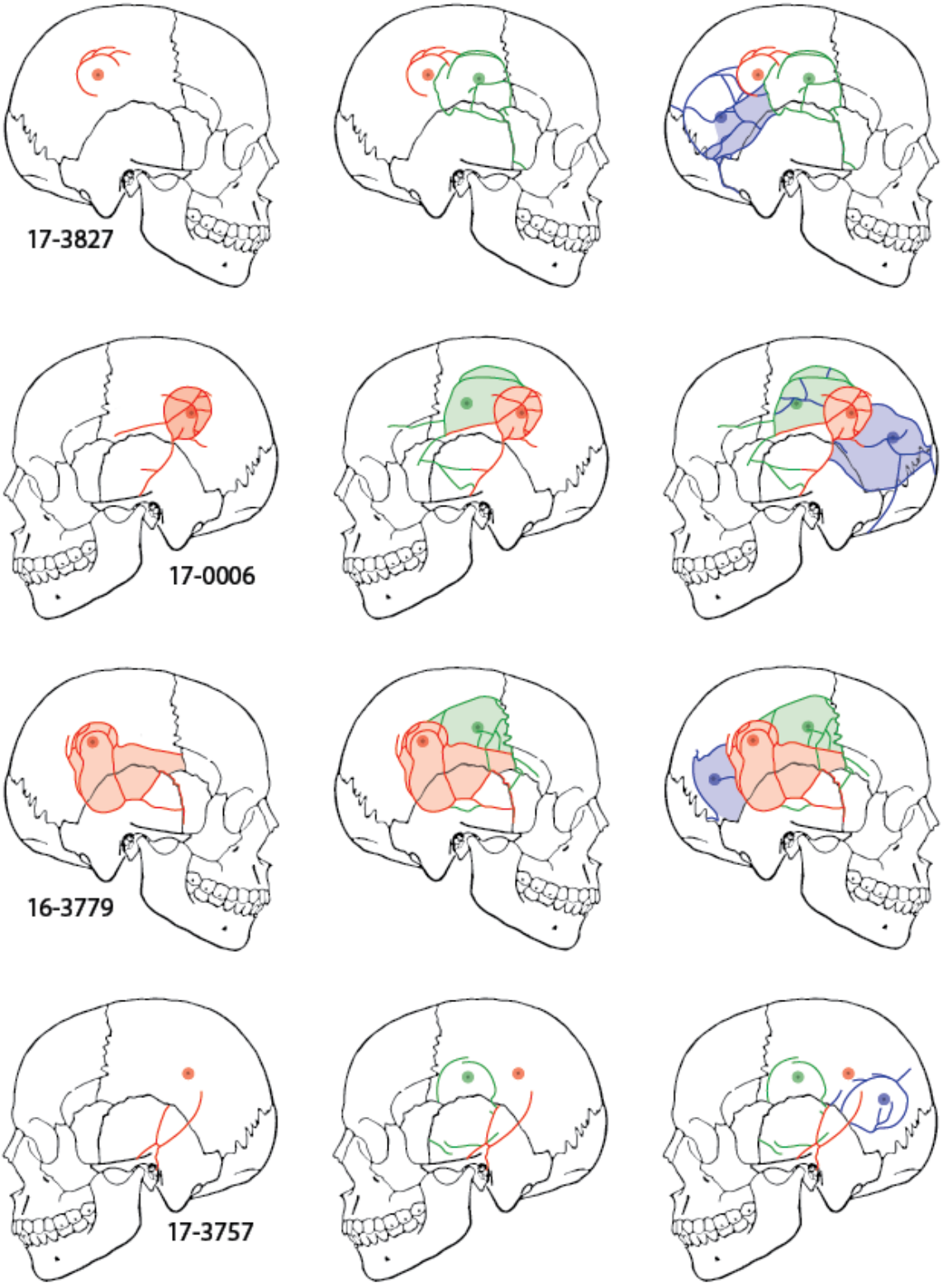

Figure 2.7: Fracture patterns after 1, 2, and 3 impacts with the hammer (small, focal) implement. Fractures from impact 1 are shown in red, impact 2 in green, and impact 3 in blue. Shaded areas represent areas of depression.

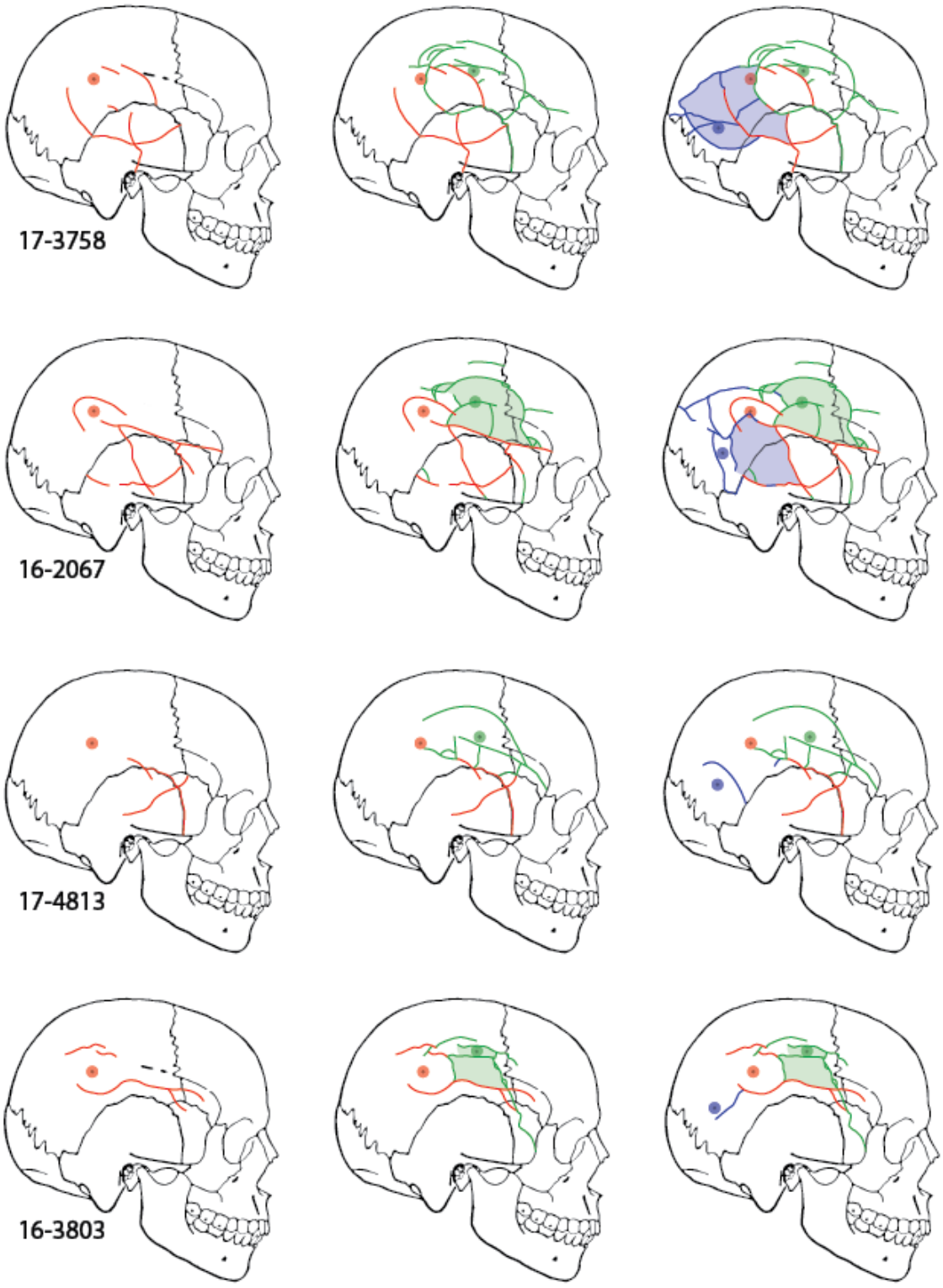

Figure 2.8: Fracture patterns after 1, 2, and 3 impacts with the bat (broad, curved) implement. Fractures from impact 1 are shown in red, impact 2 in green, and impact 3 in blue. Shaded areas represent areas of depression.

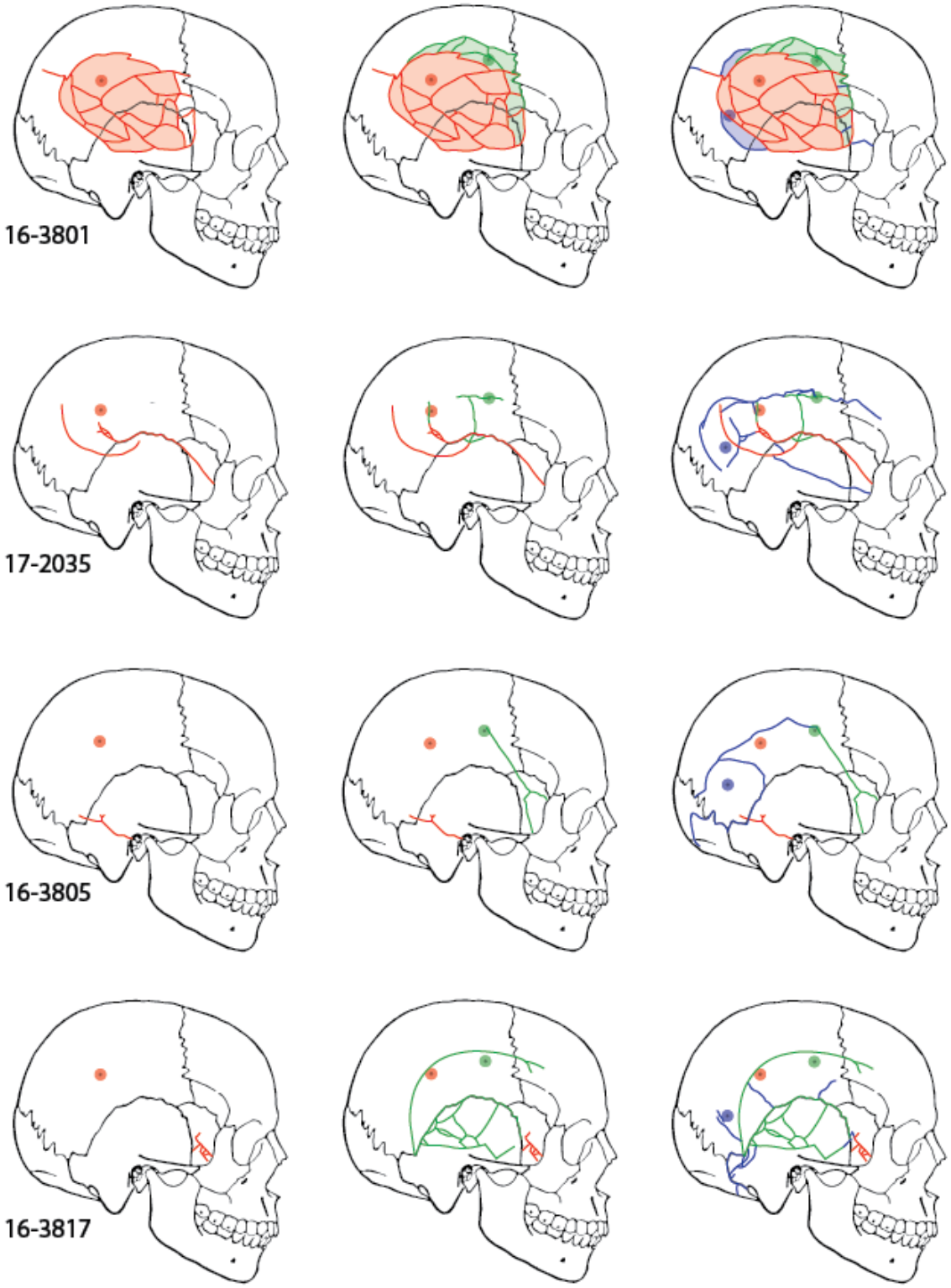

Figure 2.9: Fracture patterns after 1, 2, and 3 impacts with the brick (broad, flat) implement. Fractures from impact 1 are shown in red, impact 2 in green, and impact 3 in blue. Shaded areas represent areas of depression.

Multiple correspondence analysis

Multiple correspondence analysis (MCA) assists in visualizing these results (Figure 2.10). MCA reduced the data such that the first two dimensions retain 76% of the total inertia (variation) in the dataset. Dimension 1 has the most inertia (55%) and therefore contributes most of the variation. All variables under investigation contributed to dimension 1 including (in order of squared correlation r_2) depressed, delamination, secondary radiating linear, comminuted, primary radiating linear, and circumferential. These variables are distributed such that the presence categories cluster on the positive side of dimension 1 while absence categories cluster on the negative side. Dimension 2 retains 21% of the inertia. The variables of dimension 2 are circumferential, primary radiating linear, and depressed. The absence of circumferential and primary radiating features and presence of depressed fractures cluster on the positive side of this axis, while the opposite categories cluster on the negative side.

Projection of supplementary elements onto the model provides insights about the relationships between implement, impact number, and fracture characteristics. MCA results indicate that brick and hammer impacts are dissimilar. On dimension 1, hammer impacts are on the positive side of the axis, which is associated with the presence of impact site features and features associated with more severe cranial vault damage. Brick impacts are on the negative side, which is associated with the absence of these features. On dimension 2, hammer impacts are on the negative side of the axis (presence categories) while brick impacts are on the positive side (absence categories). These results are consistent with the observation that hammer impacts more frequently produced significant localized damage, while brick impacts more frequently produced diffuse linear fractures with less destruction of the cranial vault. The placement of the

bat is not well described by the model. This, too, is consistent with data showing bat impacts produced fracture characteristics at a frequencies intermediate between the hammer and brick.

MCA results also suggest that impact 1 is dissimilar from impacts 2 and 3, while impacts 2 and 3 are similar. Specifically, impact 1 is on the negative side of dimension 1 (absence categories) and impacts 2 and 3 on the positive side (presence categories). This is consistent with the finding that impact 1 tended to produce fewer impact site features and less severe fractures than impacts 2 and 3.

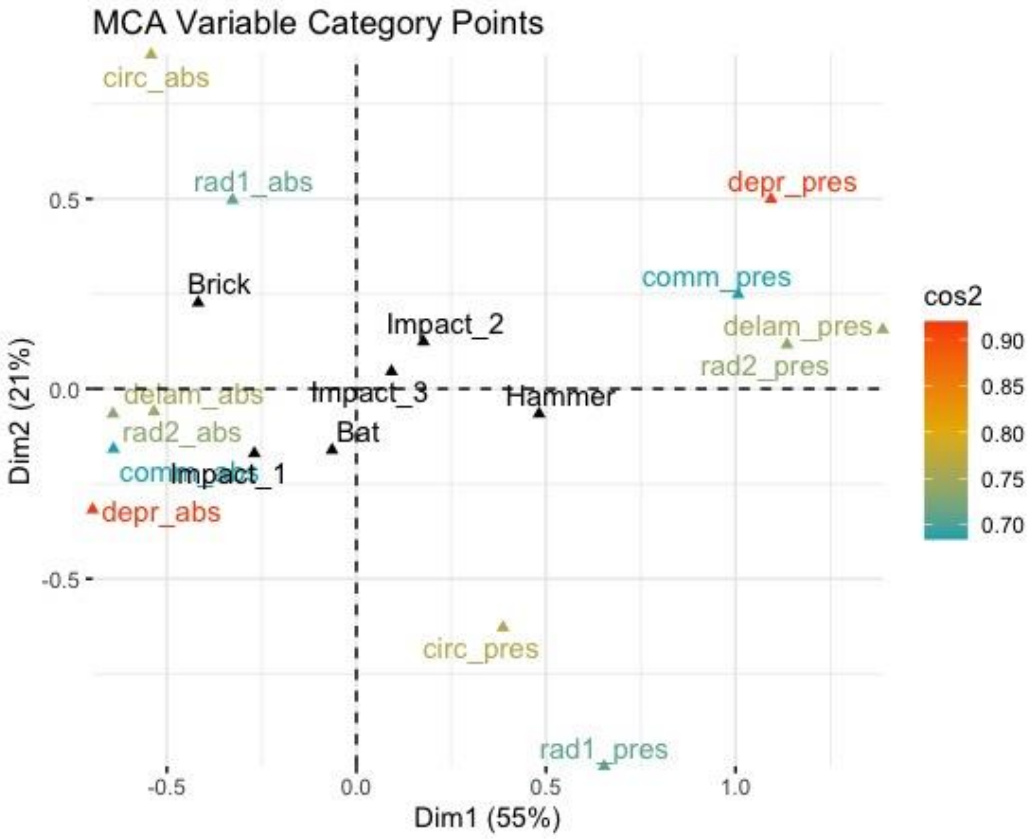

Figure 2.10: Results of the MCA where the plot of category points for the first two dimensions shows the associations between fracture characteristics, implement, and impact number. The squared cosine (cos2) value measures the degree of association between variable categories and dimensions, with values closer to 1 indicating stronger associations. High cos2 values indicate that the variable categories are well represented by the two dimensions presented in this model.

Discussion

The goals of the current study were to investigate cranial fracture behavior in multiple impact experiments with different shaped implements and to assess the appearance of and relationships between cranial impact sites. Most impact sites (78% or 28/36) featured at least one of the following: depressed fractures, circumferential fractures, and/or radiating linear fractures. However, 22% (8/36) of impact experiments produced none of these features. In these cases, linear fractures formed peripheral to the impact or formed between and extended preexisting fracture lines, complicating the overall fracture pattern. These impact sites would likely be unidentifiable in a forensic context. Multiple correspondence analysis provided visual confirmation of the descriptive results regarding the effects of impact number and surface on the appearance and severity of fracture patterns. An initial impact causing fracture (impact 1) produced fracture patterns dissimilar to subsequent impacts (impacts 2 and 3), and a broad, flat impact surface produced fracture patterns dissimilar to a small, focal surface. Finally, in the current study, all subsequent impacts produced cranial fractures that extended, initiated from, or were arrested at fracture lines generated in previous impacts. New fractures only crossed preexisting hairline fractures that had not perforated both tables of cranial bone. These results support the use of Puppe's rule to sequence cranial impacts.

A key finding of this research is that the number of impacts may affect fracture behavior, and therefore the ability of analysts to identify and sequence impact sites. Specifically, the results indicate that an initial impact causing damage to the cranial vault makes the bone more susceptible to damage by subsequent impacts. In the current experiments, peak force was lower in impacts 2 and 3 than in impact 1. This suggests is that the introduction of a discontinuity in bone lowers the force required to produce additional fracture. Furthermore, whereas an initial

impact to the mid-parietal region did not always produce impact site fracture, all subsequent impacts produced damage at the impact site. Gurdjian et al. (Gurdjian, Webster, and Lissner 1950a, 1950b) suggest that linear fractures form peripherally when the impact site rebounds without fracture. As a result of lowered fracture force, cranial bone is potentially less likely to rebound without damage in subsequent impacts to the same region. Additionally, a preexisting fracture presents a discontinuity in bone, which in turn produce stress concentrations. New fractures are likely to initiate from or be directed toward these areas of high stress. Because impacts 2 and 3 were administered adjacent to the first impact site, the presence of fractures at the first impact site likely directed and helped localize the formation of new fractures from subsequent impacts.

Depressed fractures were also more frequent in impact 2 and 3 than in impact 1 experiments. They were significantly more frequent when a prior impact produced depressed fracture. These results suggest that production of a depressed fracture in one impact may increase susceptibility to depressed fracture in subsequent impacts; alternatively, certain individual crania may be at increased risk to depressed fracture as a result of intrinsic factors. Variables such as cortical and overall skull thickness, cortical rigidity, cortical density, cranial bossing, and cranial location have been shown to affect fracture susceptibility (Hamel et al. 2013; Ruan and Prasad 2001; Hodgson and Thomas 1971; Motherway et al. 2009).

The results of the study also suggest potential relationships between impact surface shape and fracture behavior. This is consistent with findings reported in other studies (Hodgson and Thomas 1971, 1973; Allsop, Perl, and Warner 1991; Hamel et al. 2013; Sulaiman et al. 2014; Vaughan et al. 2016). Among the three implements tested, depressed fractures, circumferential fractures, and secondary radiating fractures were most frequent in experiments with the small,

focal “hammer” implement and least frequent in experiments with the broad, flat “brick” implement. Conversely, impacts with the brick produced simple linear fractures more frequently than impacts with the hammer or the broad, curved “bat” implement. With the focal implement, impacts 2 and 3 produced fractures that tended to remain localized to the impact site. With the two broader implements, impacts 2 and 3 produced fractures that tended to intersect or extend pre-existing fractures.

The shape of an object and particularly the dimensions and curvature of its impact surface may influence the contact area over which the force of an impact is applied. An impact generating a relatively small contact area can be expected to deform a small area of bone. In this case, contact stresses remain localized at the impact site. This is consistent with the more focal distribution of fractures and higher frequency of depressed fractures in hammer impacts. In contrast, an impact generating a relatively broad contact area can be expected to deform a larger area of bone, producing stresses both at and remote from the impact site. This is consistent with the more diffuse distribution of fractures observed in brick and, to a lesser extent, bat impacts.

There are a few limitations to the current study that merit discussion. First, the current study was limited to the mid-parietal region. Different cranial regions and even different regions of the same cranial bone are associated with different cortical thicknesses, densities, and elastic properties (Peterson and Dechow 2003, 2002). All of these represent variables that may affect fracture behavior. Future research is needed to assess multiple impacts in other regions of the cranium. Second, impacts were performed at the same locations and in the same sequence in each set of experiments. Effects of impact number therefore cannot be separated entirely from the effects of impact location. Of particular interest is the fact that composition (relative thicknesses of the inner and outer cortical tables) differs between the anterior and posterior

parietal, the locations of impacts 2 and 3, respectively (Peterson and Dechow 2002). Third, the results of the current study suggest that the type of fracture produced in an initial impact may affect the type of fracture produced in subsequent impacts. Any experiment that involves administering multiple impacts to the same head compounds variation with each impact.

As discussed in the introduction, understanding of the mechanism of cranial fracture formation is directly relevant to the identification and interpretation of impact sites. Gurdjian et al. (Gurdjian, Webster, and Lissner 1950a, 1950b, 1953; Gurdjian 1975) and others present expectations for how cranial fractures form on both the outer and inner table. Because this study used intact crania, it was not possible to record endocranial fracture patterns after each impact. Therefore, endocranial fractures – particularly linear fractures – could not always be confidently associated with impact 1, 2, or 3. Future research is needed to shed light on the relationship between cranial fracture formation on the inner and outer table.

Finally, the sample of PMHS in the current study consists of older adult males, a demographic that is not representative of a forensic sample. Fusion of the cranial sutures, losses in bone density, and changes in cortical thickness may occur with age and potentially affect the cranium's response to impact. Future studies are needed to assess whether the results presented here are typical of fracture patterns seen in younger adults.

Conclusions

The current study contributes new experimental data characterizing fracture behavior in multiple blunt force cranial trauma to PMHS heads. Fracture patterns, specifically those related to the appearance of impact sites, were evaluated after one, two, and three impacts to known locations in the mid-parietal region in experiments with three differently shaped blunt implements. Impact site identification is the first step in conducting forensically relevant

analyses including assessment of minimum number and sequence of impacts. The implications of this study for assessing impact site in unknown cases of trauma are as follows.

Depressed fractures and circumferential fractures occur only at known points of impact and are typically unambiguous. These features are therefore useful for identifying impact sites in cases involving multiple blunt force trauma. Linear fractures also radiate from known impact sites, however, peripherally-initiating linear fractures may also intersect in areas remote to the impact site, particularly in the temporal squama (Isa et al. 2019). Furthermore, repeated impacts complicate the appearance of radiating fractures. Therefore, intersecting linear fractures in the absence of circumferential and/or depressed fractures are unreliable indicators of impact sites.

The current experiments provide evidence that Puppe's rule can be used to sequence fractures from multiple blunt force impacts. New fractures from subsequent impacts initiated from, were arrested at, or extended preexisting fracture lines. New fractures only crossed hairline fractures (i.e., those affecting only the outer table) produced in previous impacts. Because multiple blunt force impacts to the same region produce complex fracture patterns, using circumferential or depressed fractures rather than radiating linear fractures to establish sequence would provide a more conservative assessment.

The number of impacts will likely influence impact site identification and sequencing in cases involving multiple impacts. After an initial impact produces cranial fracture, subsequent impacts require less force to fracture and are more likely to produce fractures at the impact site. Production of a depressed fracture, in particular, may increase the likelihood of additional depressed fractures useful for identifying impact sites. However, impact sites become more complex and may be less identifiable after multiple blows to the same region.

Implement shape is also likely to influence site identification and sequencing in cases involving multiple impacts. Impacts with a focal surface can be expected to produce circumferential and depressed defects localized to the impact site. Broader surfaces can be expected to produce more linear fractures and to extend and complicate pre-existing fractures. Therefore, impact sites will likely be identifiable even after multiple impacts with a more focal implement, but may not be identifiable after multiple impacts with a broader implement.

REFERENCES

REFERENCES

Abdi, H., and D. Valentin. 2007. "Multiple Correspondence Analysis." In *Encyclopedia of Measurement and Statistics*, edited by NJ Salkind, 651–57. Thousand Oaks, CA: Sage Publications.

Allsop, D., T.R. Perl, and C.Y. Warner. 1991. "Force/Deflection and Fracture Characteristics of the Temporo-Parietal Region of the Human Head." *Proceedings of the 35th Stapp Car Crash Conference* 35: 269–78.

Bass, C.R., and N. Yoganandan. 2015. "Skull and Facial Bone Injury Biomechanics." In *Accidental Injury: Biomechanics and Prevention*, edited by N. Yoganandan, A.M. Nahum, and J.W. Melvin, 203–20. New York: Springer-Verlag.

Berryman, H.E., J.F. Berryman, and T.B. Saul. 2018. "Bone Trauma Analysis in a Forensic Setting: Theoretical Basis and a Practical Approach for Evaluation." In *Forensic Anthropology: Theoretical Framework and Scientific Basis*, edited by C.C. Boyd and D.C. Boyd, 213–34. Chichester, West Sussex, UK: John Wiley & Sons Ltd.

Berryman, H.E., and S.A. Symes. 1998. "Recognizing Gunshot and Blunt Cranial Trauma Through Fracture Interpretation." In *Forensic Osteology: Advances in the Identification of Human Remains*, edited by Kathleen J. Reichs, 2nd ed., 333–52. Springfield, IL: Charles C. Thomas.

Blau, S. 2017. "How Traumatic: A Review of the Role of the Forensic Anthropologist in the Examination and Interpretation of Skeletal Trauma." *Australian Journal of Forensic Sciences*.

Byers, S.N. 2017. *Introduction to Forensic Anthropology*. *Introduction to Forensic Anthropology*. 5th ed. New York, NY: Routledge.

Christensen, A.M., N.V. Passalacqua, and E.J. Bartelink. 2014. *Analysis of Skeletal Trauma*. *Forensic Anthropology*.

Dixon, D.S. 1984. "Pattern of Intersecting Fractures and Direction of Fire." *Journal of Forensic Sciences* 29 (2): 651–54.

Fleischman, J. 2019. "Analysis of Skeletal Demographics and Traumatic Injuries from the Khmer Rouge–Period Mass Gravesite of Choeung Ek, Cambodia." *Forensic Anthropology* 2 (4): 347–65.

Galloway, A. 1999. *Broken Bones*. Edited by A. Galloway. 1st ed. Springfield, IL: Charles C. Thomas.

Galloway, A., and V. Wedel. 2014a. “Common Circumstances of Blunt Force Trauma.” In *Broken Bones: Anthropological Analysis of Blunt Force Trauma*, edited by Vicki L. Wedel and Alison Galloway, 2nd ed., 91–130. Springfield, IL: Charles C. Thomas.

Galloway, A., and V.L. Wedel. 2014b. “Bones of the Skull, the Dentition, and Osseous Structures of the Throat.” In *Broken Bones: Anthropological Analysis of Blunt Force Trauma*, edited by V.L. Wedel and A. Galloway, 2nd ed., 133–60. Springfield, IL: Charles C. Thomas.

Gibbs, L.M. 2014. “Understanding the Medical Markers of Elder Abuse and Neglect: Physical Examination Findings.” *Clinics in Geriatric Medicine* 30 (4): 687–712.

Gurdjian, E. S., J. E. Webster, and H. R. Lissner. 1953. “Observations on Prediction of Fracture Site in Head Injury.” *Radiology* 60 (2): 226–35.

Gurdjian, E. S., John E. Webster, and Herbert R. Lissner. 1949. “Studies on Skull Fracture with Particular Reference to Engineering Factors.” *The American Journal of Surgery* 78 (5): 736–42.

Gurdjian, E.S. 1975. *Impact Head Injury*. Springfield, IL: Charles C. Thomas.

Gurdjian, E.S., and H.R. Lissner. 1945. “Deformation of the Skull in Head Injury: A Study with the Stresscoat Technique.” *Surgery Gynecology and Obstetrics* 81: 679–87.

Gurdjian, E.S., and H.R. Lissner. 1947. “Deformations of the Skull in Head Injury as Studied by the ‘Stresscoat’ Technic.” *The American Journal of Surgery* 73 (2): 269–81.

Gurdjian, E.S., H.R. Lissner, and J.E. Webster. 1947. “The Mechanism of Production of Linear Skull Fractures: Further Studies on Deformation of the Skull by the Stresscoat Technique.” *Surgery Gynecology and Obstetrics* 85 (2): 195–201.

Gurdjian, E.S., J.E. Webster, and H.R. Lissner. 1950a. “The Mechanism of Skull Fracture.” *Radiology* 54 (3): 313–38.

Gurdjian, E.S., J.E. Webster, and H.R. Lissner. 1950b. “The Mechanism of Skull Fracture.” *Journal of Neurosurgery* 7 (2): 106–14.

Hamel, A., M. Llari, M.D. Piercecchi-Marti, P. Adalian, G. Leonetti, and L. Thollon. 2013. “Effects of Fall Conditions and Biological Variability on the Mechanism of Skull Fractures Caused by Falls.” *International Journal of Legal Medicine* 127 (1): 111–18.

Hart, G.O. 2005. “Fracture Pattern Interpretation in the Skull: Differentiating Blunt Force from Ballistics Trauma Using Concentric Fractures.” *Journal of Forensic Sciences* 50 (6): 1–6.

Hodgson, V.R., and L.M. Thomas. 1971. “Breaking Strength of the Human Skull vs. Impact Surface Curvature.” DOT-HS-800-583.

Hodgson, V.R., and L.M. Thomas. 1973. “Breaking Strength of the Human Skull vs. Impact Surface Curvature.” DOT-HS-801-002.

Isa, M.I., T.W. Fenton, A.C. Goots, E.O. Watson, P.E. Vaughan, and F. Wei. 2019. “Experimental Investigation of Cranial Fracture Initiation in Blunt Human Head Impacts.” *Forensic Science International* 300: 51–62.

Kimmerle, E.H., and J.P. Baraybar. 2011. “Blunt Force Trauma.” In *Skeletal Trauma: Identification of Injuries Resulting from Human Rights Abuse and Armed Conflict*, edited by Erin H. Kimmerle and José Pablo Baraybar, 151–99. Boca Raton, FL: CRC Press.

Komar, D.A., and J.E. Buikstra. 2008. “Pathology and Trauma Assessment.” In *Forensic Anthropology: Contemporary Theory and Practice*, edited by Debra A. Komar and Jane E. Buikstra, 154–88. New York: Oxford University Press, Inc.

Kranioti, Elena. 2015. “Forensic Investigation of Cranial Injuries Due to Blunt Force Trauma: Current Best Practice.” *Research and Reports in Forensic Medical Science* 5: 25–37.

Kroman, A.M., T.A. Kress, and D. Porta. 2011. “Fracture Propagation in the Human Cranium: A Re-Testing of Popular Theories.” *Clinical Anatomy* 24 (3): 309–18.

Lê, S., J. Josse, and F. Husson. 2008. “FactoMineR: An R Package for Multivariate Analysis.” *Journal of Statistical Software* 25 (1): 1–18.

Lee, C.K., and S.L. Lathrop. 2010. “Child Abuse-Related Homicides in New Mexico: A 6-Year Retrospective Review.” *Journal of Forensic Sciences* 55 (1): 100–103.

Love, J.C. 2015. “Neurocranial Fractures.” In *Skeletal Trauma: Case Studies in Context*, edited by Nicholas V. Passalacqua and Christopher W. Rainwater, 130–46. Chichester, West Sussex, UK: John Wiley & Sons Ltd.

Lovell, N.C., and A.L. Grauer. 2019. “Analysis and Interpretation of Trauma in Skeletal Remains.” In *Biological Anthropology of the Human Skeleton*, edited by M.A. Katzenberg and A.L. Grauer, 3rd ed., 335–83. Hoboken, NJ: John Wiley & Sons, Inc.

Madea, B., and M. Staak. 1988. “Determination of the Sequence of Gunshot Wounds of the Skull.” *Journal of the Forensic Science Society* 28: 321–28.

Maples, W.R. 1986. “Trauma Analysis by the Forensic Anthropologist.” In *Forensic Osteology: Advances in the Identification of Human Remains*, edited by K.J. Reichs, 1st ed., 218–28. Springfield, IL: Charles C. Thomas.

Moritz, A.R. 1954. *The Pathology of Trauma*. Philadelphia: Lea & Febiger.

Motherway, J.A., P. Verschueren, G. Van der Perre, J. Vander Sloten, and M.D. Gilchrist. 2009. “The Mechanical Properties of Cranial Bone: The Effect of Loading Rate and Cranial

Sampling Position." *Journal of Biomechanics* 42 (13): 2129–35.

Peterson, J., and P.C. Dechow. 2002. "Material Properties of the Inner and Outer Cortical Tables of the Human Parietal Bone." *Anatomical Record* 268 (1): 7–15.

Peterson, J., and P.C. Dechow. 2003. "Material Properties of the Human Cranial Vault and Zygoma." *Anatomical Record - Part A Discoveries in Molecular, Cellular, and Evolutionary Biology* 274 (1): 785–97.

R Core Team. 2020. "R: A Language and Environment for Statistical Computing." Vienna, Austria: R Foundation for Statistical Computing. https://www.r-project.org/.

Ruan, J., and P. Prasad. 2001. "The Effects of Skull Thickness Variations on Human Head Dynamic Impact Responses." *SAE Technical Papers* 45 (395–414).

Saukko, P., and B. Knight. 2016. *Knight's Forensic Pathology*. 4th ed. Boca Raton, FL: CRC Press.

Schüttrumpf, G. 1966. "Untersuchungen Über Die Priorität Der Schädelbrüche." *Deutsche Zeitschrift Für Die Gesamte Gerichtliche Medizin* 58: 94–100.

Smith, O.C., H.E. Berryman, and C.H. Lahern. 1987. "Cranial Fracture Patterns and Estimate of Direction of Low Velocity Gunshot Wounds." *Journal of Forensic Sciences* 32 (5): 1416–21.

Smith, O.C., E.J. Pope, and S.A. Symes. 2009. "Look Until You See: Identification of Trauma in Skeletal Material." In *Hard Evidence: Case Studies in Forensic Anthropology*, edited by D.W. Steadman, 190–204. Upper Saddle River, NJ: Pearson Education.

Spitz, Werner U. 1993. "Blunt Force Injury." In *Spitz and Fisher's Medicolegal Investigation of Death: Guidelines for the Application of Pathology to Crime Investigation*, edited by Werner U. Spitz, 3rd ed., 199–251. Springfield, IL: Charles C. Thomas.

Stewart, T.D. 1979. "Judging Time and Cause of Death." In *Essentials of Forensic Anthropology Especially as Developed in the United States*, 69–81. Springfield, IL: Charles C. Thomas.

Sulaiman, N.A., K. Osman, N.H. Hamzah, and S.P.A. Amir Hamzah. 2014. "Blunt Force Trauma to Skull with Various Instruments." *Malaysian Journal of Pathology* 36 (1): 33–39.

Symes, S.A, E.N. L'Abbé, E.N. Chapman, I. Wolff, and D.C. Dirkmaat. 2012. "Interpreting Traumatic Injury to Bone in Medicolegal Investigations." In *A Companion to Forensic Anthropology*, edited by D.C. Dirkmaat, 340–89. Chichester, West Sussex, UK: Blackwell Publishing, Ltd.

Ta'ala, S.C., G.E. Berg, and K. Haden. 2006. "Blunt Force Cranial Trauma in the Cambodian Killing Fields." *Journal of Forensic Sciences* 51 (5): 996–1001.

Vaughan, P.E., C.C.M. Vogelsberg, J.M. Vollner, T.W. Fenton, and R.C. Haut. 2016. “The Role of Interface Shape on the Impact Characteristics and Cranial Fracture Patterns Using the Immature Porcine Head Model.” *Journal of Forensic Sciences* 61 (5): 1190–97.

Yoganandan, N., and F.A. Pintar. 2004. “Biomechanics of Temporo-Parietal Skull Fracture.” *Clinical Biomechanics* 19 (3): 225–39.

PAPER 3: EFFECTS OF IMPACT SURFACE AND ENERGY ON CRANIAL FRACTURE PATTERNS

Abstract

This study contributes data documenting the effects of impact surface and energy on human cranial fracture patterns. Using previously reported impact experiments (Isa et al. 2019) as a baseline, a 67% increase in input energy was achieved for the current experiments (n=12). Present and previous results were compared to evaluate three impact surfaces and two levels of input energy. A small, focal surface produced smaller defects and less variation in fracture patterns than a broad, flat impact surface. Two surfaces tested (small, focal and broad, curved) produced more severe fractures in higher energy compared to lower energy impacts. However, a broad, flat surface produced similar fracture severity at both energy levels. As reported for lower energy experiments, remote cranial fracture initiation was also observed in the current higher energy experiments. This provides additional evidence that multiple linear fractures in the temporoparietal region do not necessarily reflect multiple impacts.

Introduction

Blunt force trauma (BFT) involves a relatively low-velocity impact from a blunt object or surface (Passalacqua and Fenton 2012). BFT to the skull is of particular concern in a forensic context. Skull fractures are associated with increased severity of injury and fatality in assaults and accidents and therefore may reflect evidence relevant to the cause of death (Chattopadhyay and Tripathi 2010; Kranioti 2015; Galloway and Wedel 2014a). Several variables are thought to influence cranial fracture patterns including the magnitude and duration of the force applied, the mass and velocity of the impact, and the contact area between impact and target surface (Gurdjian, Webster, and Lissner 1950a; Gurdjian 1975; Berryman and Symes 1998; E.H. Kimmerle and Baraybar 2011; Symes et al. 2012; Berryman, Berryman, and Saul 2018; Galloway and Wedel 2014b). An assumption of skeletal trauma analysis is that these variables can be inferred from fracture patterns in order to address questions relevant to the death investigation. To some degree, these relationships can be theorized using thought experiments (Berryman, Berryman, and Saul 2018). However, experimental data provides an important link between known impact variables and fracture patterns.

To date, most experimental studies of blunt force cranial trauma using postmortem human subjects (PMHS) have been undertaken in the field of biomechanics within the context of the automotive industry (Bass and Yoganandan 2015). This research has primarily aimed to document impact force-deflection curves and acceleration-time histories in order to derive head injury criteria relevant to vehicle safety testing. Because fracture patterns are rarely the focus of these studies, they often provide limited data regarding fracture formation, fracture type, or defect size of interest to forensic practitioners. Recent experimental studies have aimed to fill this gap using animal models to investigate the relationship between different manipulated

variables and fracture patterns (Otero and Béguelin 2019; Sharkey et al. 2012; Sulaiman et al. 2014; Baumer et al. 2010; Powell et al. 2012, 2013; Vaughan et al. 2016; Mole, Heyns, and Cloete 2015). Given structural differences between human and nonhuman crania, it is yet unclear how these results apply to humans. PMHS studies present the closest analogues to forensic cases and therefore provide important comparative data. However, the availability of this type of data is currently limited.

One relevant question in a death investigation may include "what object caused the injury?" It is likely impossible to determine specific tools or objects based on blunt force fracture patterns (Dirkmaat et al. 2008; Symes et al. 2012; Berryman and Symes 1998). There exists a wide range of blunt objects, each of which may present multiple potential impact surfaces. Additionally, the cranium varies in shape and structure depending on the location and individual in question (Peterson and Dechow 2003, 2002; Got et al. 1983). However, it is assumed possible that general interpretations can be made about whether fracture patterns are consistent with a given impact surface (Symes et al. 2012; Berryman and Symes 1998).

Contact area between impact and target surface has been shown to be important in fracture response (Bass and Yoganandan 2015; Yoganandan and Pintar 2004). In the temporoparietal region, lower fracture forces are reported with smaller impact surfaces (Melvin et al. 1969; Nahum et al. 1968; Schneider and Nahum 1972; Allsop, Perl, and Warner 1991) compared to larger, flat surfaces (Allsop, Perl, and Warner 1991; Hodgson and Thomas 1971). Recent experimental studies using animal models also suggest differences in fracture patterns obtained with different impact surfaces. Otero and Béguelin performed impact experiments on adult pig heads and report identifiable differences in fracture types and defect sizes obtained with

four different objects. Similarly, Vaughan et al. (Vaughan et al. 2016) report differences in fracture types obtained with broader vs. more focal impact surfaces in a juvenile porcine model.

Another relevant question in a death investigation may include "how hard was the blow administered?" There are various means of quantifying input, including force and energy. Force is a mechanical disturbance that can move or deform an object. The transfer of energy required to move an object with a given force is called work, and energy is the ability to do work (Kieser 2013). An impact transmits forces to the skull, which produce deformations (strains) across the skull and subsequent fracture at critical levels of strain. The magnitude of the force depends on the relative velocities and properties of the hitting object and target surfaces (Melvin and Evans 1971) and is measured at the impact surface. Meanwhile, the magnitude of the input energy is independent from surface properties, geometries, and contact areas between surfaces (Siegenthaler et al. 2018) and is therefore more convenient to manipulate experimentally. Input energy is often measured as kinetic energy, a function of mass and velocity.

Studies specifically focusing on the relationship between input energy or force and fracture patterns are limited in human subjects, but have been explored in animal models including pig (Mole, Heyns, and Cloete 2015; Powell et al. 2012; Sharkey et al. 2012) and macaque (Sulaiman et al. 2014). Generally, increased inputs produce higher frequencies of fracture (Baumer et al. 2010; Sharkey et al. 2012; Sulaiman et al. 2014). However, an interaction with impact surface may affect specific results (Sharkey et al. 2012; Sulaiman et al. 2014).

Experimental investigations of blunt force cranial fracture in PMHS have focused primarily on how and where cranial fractures form relative to the impact site. Gurdjian et al. were among the first to investigate the mechanism of cranial fractures using stresscoat experiments on PMHS (Gurdjian and Lissner 1947; Gurdjian, Webster, and Lissner 1949, 1950a,

1950b, 1953). Performing head drop experiments onto a flat surface, they report deformation and failure occurred first in areas peripheral to the point of impact (POI), and with additional input energy, in secondary and tertiary areas at and surrounding the POI (Gurdjian, Webster, and Lissner 1950a, 1950b). However, as they used dry skulls and embalmed heads to perform experiments, it was unclear how these results apply to the formation of fracture in biomechanically fresh bone.

More recently, Kroman et al. (Kroman, Kress, and Porta 2011) investigated cranial fracture formation using modern methods and unembalmed, intact PMHS heads. Using a focal impact surface of unknown dimensions, they obtained failure only at the POI. However, this study did not account for the influence of impact surface. In order to account for impact surface effects, we previously performed experiments on 12 PMHS using three blunt surfaces with different expected contact areas (Isa et al. 2019). These experiments provided evidence that fractures can form peripheral to the impact site and indicated that impact surface is one variable influencing fracture formation.

The current study builds on this work. New impact experiments were performed using the previous sample (Isa et al. 2019) as a baseline for investigating the effects of both input energy and impact surface on fracture behavior. The goals of the current study were 1) to deliver cranial impacts at a higher kinetic energy than that assessed in the previous study (Isa et al. 2019); 2) to report mechanical response, fracture initiation, and fracture pattern data for these experiments; 3) to compare results obtained at different input energies, and 4) to compare results obtained with different implements. It was hypothesized that different impact surfaces would produce different cranial fracture types and defect sizes, and that higher energy impacts would produce more severe fracture than lower energy impacts.

Materials and Methods

Specimens

The current experimental sample included 12 male adult PMHS heads. Heads were stored at a temperature of -20°C and allowed to thaw completely before testing began. Storage of specimens at this temperature is understood to have minimal effects on the biomechanical properties of bone (Cowin 2001; van Haaren et al. 2008; Kaye et al. 2012; Torimitsu et al. 2014). Prior to experimentation, the skin, muscle, and periosteum were removed from the parietal region in order to allow for visualization of cranial fracture initiation and propagation during and after impact. A small area of scalp was retained at the impact site to account for soft tissue effects. The results of the current experiments were compared to the previously reported results of experiments performed on another 12 male adult PMHS heads (Isa et al. 2019).

Impact experiments

The impact methodology is described in detail in a previous publication (Isa et al. 2019). Experiments were designed to approximate a blow to an upright individual and to allow for rotation of the head about the neck and translation of the head away from the impactor after contact. Impacts were administered to the parietal at a location superior to the squamosal suture and halfway between the coronal and lambdoidal sutures. The impact system used in these experiments is shown in Figure 1.1.

In order to allow for comparison with previous work (Isa et al. 2019), the current study evaluated the same three aluminum impactors (Figure 1.2). These included a small, focal surface (the base of a 1.125-inch diameter cylinder); a broad, curved surface (the curved surface of a horizontally oriented 2.5-inch diameter, 2.5-inch long cylinder); and a broad, flat surface (3-inch diameter). These impactors were selected to represent a range of blunt surfaces implicated in

forensic cases, such as the face of a hammer, the barrel of a baseball bat, and a flat surface such as the broad side of a brick, respectively. The current and previous studies refer to the impactors as the "hammer," "bat," and "brick." However, these are intended as shorthand references and are not meant to implicate specific tools.

Input energy in this study was increased relative to the previous experiments. This was accomplished primarily by increasing the mass of the impact. Weighted plates were added to the guide trolley that held and travelled with the impactor, so that an increase of the mass by a factor of approximately 1.5 compared to the previous (Isa et al. 2019) experiments was achieved. The masses used in the current experiment were 9.41 kg, 9.61 kg, and 9.60 kg for the hammer, bat, and brick, respectively. The input energy (E_i) was calculated from the mass (m) and initial velocity (v_i) using the formula:

$$E_i = \frac{1}{2}mv_{i2}$$

This paper will refer to the previous experiments as "low energy" and the current experiments as "high energy" impacts. However, the designations of low and high are relative terms used to describe the experimental samples assessed in this study and should not be considered absolute measures.

Data collection

Force-time and position-time data was collected at a sample rate of 200,000 Hz as described by Isa et al. (Isa et al. 2019). Position-time data pre- and post-impact were used to calculate the initial (v_i) and final (v_f) velocities of the guide trolley, which in turn were used to calculate the initial and final kinetic energy of the trolley based on the above formula. The energy absorbed by the head (E_a) was calculated as the change in kinetic energy pre- and post-impact.

Each impact was filmed at a rate of 10,000 frames per second using a high-speed camera (Fastcam Mini AX 200, Photron Ltd; Tokyo, Japan). Photron software was used to examine footage frame by frame in order to evaluate the location of fracture initiation and sequence of propagation in each experiment. Immediately after each impact, photographs were taken and fracture patterns were documented.

The heads were later used in additional experiments aimed at examining the effect of multiple high energy impacts on cranial fracture patterns. After these experiments, heads were cleaned of remaining soft tissue using hot water maceration. If necessary, cranial fragments were reconstructed using acetone soluble adhesive. Additionally, the side of the cranial vault opposing the impact was removed in order to allow for visualization of endocranial fracture patterns (Figure 2.2). Characteristics related to the location of fracture relative to the impact site and the complexity and severity of fracture were assessed for each experiment. The following were scored as present or absent: damage at the point of impact (poi), primary radiating linear fractures (rad1), secondary radiating linear fractures (rad2), circumferential fractures (circ), depressed fractures (depr), comminuted fractures (comm), and delamination (delam). If circumferential or depressed defects were present, the maximum defect diameter was measured with sliding digital calipers. The diameter of the defect perpendicular to the maximum was also measured.

Statistical analysis

One-way ANOVA was used to verify differences in input energy (E_i) between low and high energy experiments. Two-way factorial ANOVA with Tukey post hoc test was used to assess the main and interaction effects of energy group (factor 1) and impact surface (factor 2) on

energy absorbed by the head (E_a), peak force, maximum defect diameter (MDD), and perpendicular defect diameter (PDD). Results were considered significant at $p<0.05$.

Multiple correspondence analysis (MCA) was used to explore associations among variable categories assessed in this study. MCA is a technique for visualizing and summarizing datasets involving multiple dependent categorical variables. Nominal data are represented graphically as points in n-dimensional space where each dimension represents a linear combination of the variables and each point represents a factor score for an individual or variable category. The resulting factor maps are interpreted based on the distances between points and on the distribution of points along each dimension. The distance between points represents a measure of their similarity such that individuals (or categories) with more similar profiles are closer together, while individuals (or categories) with more dissimilar profiles are further apart (Abdi and Valentin 2007).

Factor maps were used to visualize patterns within the current dataset. Fracture characteristics were treated as active variables and were used in the MCA. Experimental input variables *energy* (categories: high, low) and *implement* (categories: hammer, bat, brick) were treated as supplemental (illustrative) variables, meaning they did not participate in the MCA and were projected onto the analysis after the fact. This projection was used to visualize how implements and energy levels relate to the distribution of fracture characteristics.

All statistical analyses were conducted in R (R Core Team 2020). The MCA was conducted using the FactoMineR package (Lê, Josse, and Husson 2008).

Results

Mechanical results

High energy experiments were performed at an average v_i of 6.13±0.42 m/s, translating to an average E_i of 180.07±23.02 J. The current experiments achieved a significantly higher E_i than the previous lower energy experiments (106.11±8.80 J, $F_{(2,22)}$=108, p=.60e^{-10}), increasing the average E_i by a factor of approximately 1.67.

In high energy experiments, E_a ranged from 40.47 J to 130.27 J (mean=86.31±25.31 J). At this energy level, differences between impact surfaces approached significant ($F_{(2,9)}$=3.70, p=.067). The bat (100.31±20.42 J) and brick (95.01±23.47 J) delivered more energy than the hammer (E_a: 63.50±17.91 J).

The main effect of energy was significant for E_a ($F_{(1,22)}$=15.52, p=.0007). As expected, heads absorbed more energy in high (mean=86.31±25.31 J) compared to low (mean=55.21±10.35 J) energy impacts (Figure 3.1). The main effect of implement ($F_{(2,21)}$=1.34, p=.28) and the interaction effect of implement and energy ($F_{(2,18)}$=2.88, p=.08) were not significant for E_a. Because the interaction approached significant, these results were explored further. High energy bat and brick impacts delivered significantly higher energy than low energy hammer, bat, and brick impacts (p<.05). However, there was no significant difference between the high energy hammer and any of the low energy impacts (p>.90).

In high energy experiments, peak force ranged from 4178.3 N to 10806.8 N (mean=6980.8±2036.9 N). At this energy level, differences between hammer (6121.90±1372.64 N), bat (6458.56±1524.77 N) and brick (8361.81±2667.13 N) impacts were not significant ($F_{(2,9)}$=1.55, p=.27).

When high and low energy experiments were considered together, the main effect of energy on peak force was not significant ($F_{(2,22)}$=0.44, p=.52). This indicates similar peak forces obtained at both energy levels tested (6415.82±2155.92 N). The main effect of implement on peak force was also nonsignificant ($F_{(2,21)}$=0.53, p=.60), indicating no differences between hammer (6501.44±2000.41 N), bat (6281.53±1535.68 N), and brick (7311.89±2657.87 N) impacts. The interaction effect of energy and implement was not significant for peak force ($F_{(2,18)}$=0.89, p=.43).

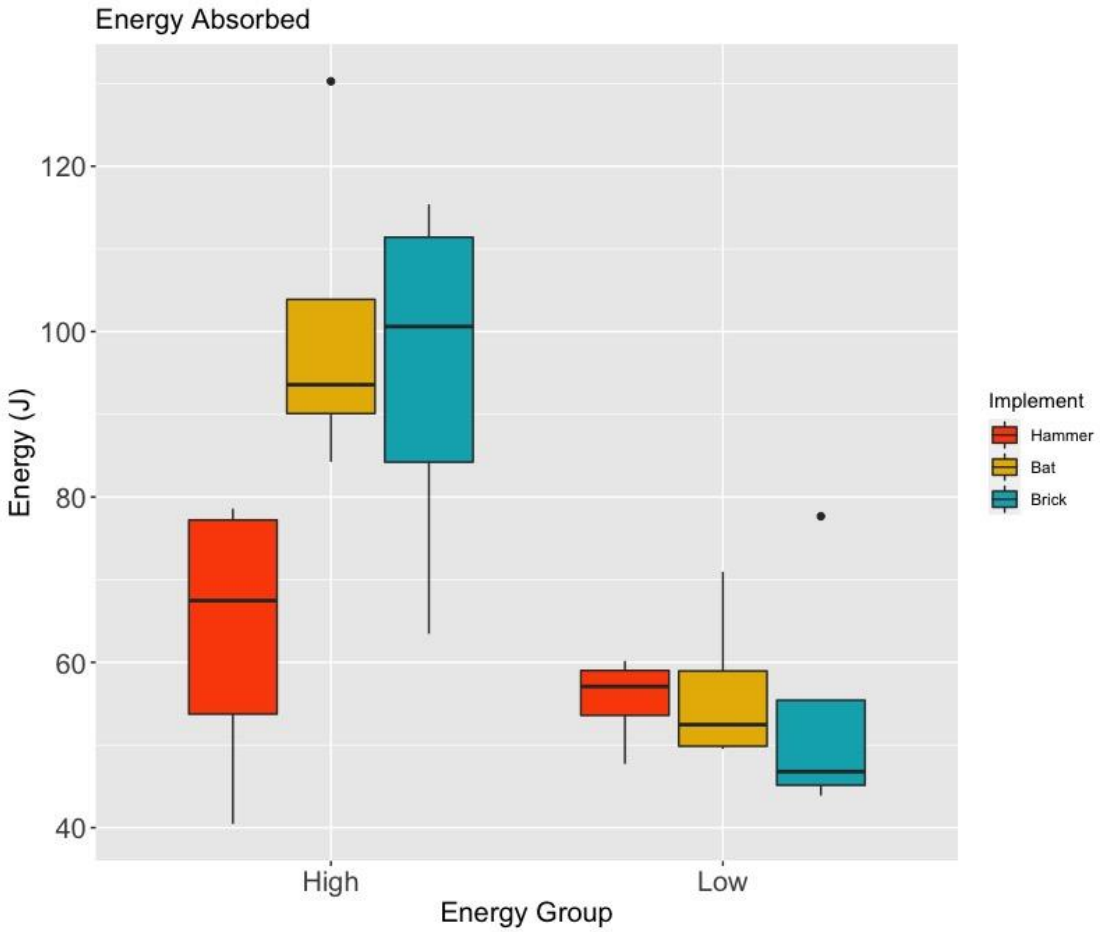

Figure 3.1: Energy absorbed by the head (E_a) in high energy (current) experiments compared to low energy (Isa et al. 2019) experiments.

Fracture initiation and propagation results

Fracture initiation and propagation results of the current cranial impact experiments were summarized in Table 3.1 and in Figures 3.2-3.5. Most high energy experiments produced failure at the impact site. However, videos also indicated peripheral deformation and failure with all three surfaces tested. When present, peripherally initiating linear fractures traveled back toward the POI. The following sections summarize results obtained with each impact surface.

"Hammer" (small, focal impact surface)

In the current experiments, the hammer generally produced circular depressed fractures at the POI (Figure 3.2). Impact video also showed peripheral deformation and failure in three of four experiments. Two of these (17-2075 and 17-2082) produced depressed fractures at the POI and diastatic fractures peripheral to the impact site. In 17-2082, a diastasis of the squamosal suture continued as a linear fracture toward the POI. In the third experiment (17-2071), the first observed failure event was a peripheral linear fracture that initiated in the temporal and traveled back to the POI (Figure 3.3). Next, a circumferential fracture formed around the POI. Several linear fractures initiated at the edge of this circumferential fracture and traveled both toward and away from the impact center. As the impact progressed, the bone at the impact site was displaced inwardly and fragmented, producing a comminuted depressed fracture. The fourth experiment (18-2359) produced only POI fracture. Radiating linear fractures traveled away from the POI. The implement then completely penetrated the cranial vault.

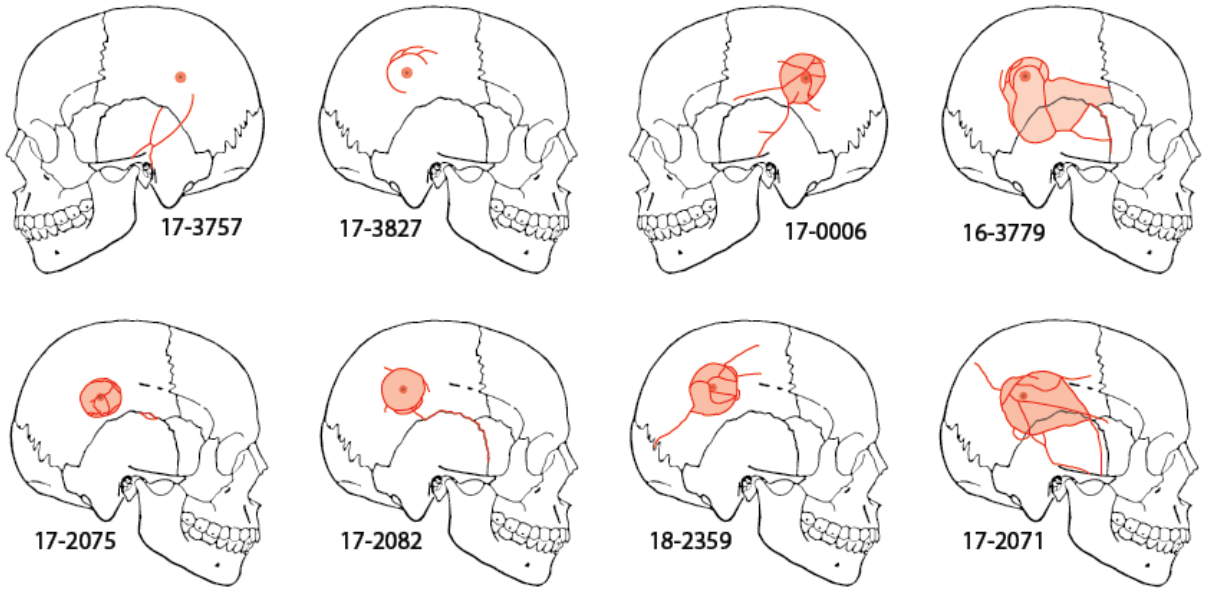

Figure 3.2: Impacts with the small, focal "hammer" implement. Top row: Low energy impacts. Bottom row: Current, high energy impacts. Areas of depression are shaded. Three of the high energy experiments produced circular depressed fractures at the POI, approximately the same size and shape of the impact surface. Two of these experiments (17-2075 and 17-2082) also produced diastases of the squamosal suture. The fourth experiment (17-2071) produced an irregularly shaped comminuted depressed fracture larger in area than the impact surface.

"Bat" (broad, curved impact surface)

All four experiments with the bat produced circumferential fractures surrounding the POI (Figure 3.4). Impact videos indicate areas of peripheral deformation and failure in three out of four experiments. Experiment 18-0386 produced one POI linear fracture and one peripheral linear fracture, as well as circumferential fractures partially encircling the POI. Experiment 17-2081 produced a POI linear fracture, a circumferential fracture around the POI, and diastatic fractures peripheral to the impact site. Experiment 18-0364 produced a peripheral linear fracture in the anterior temporal and several POI linear fractures. This experiment also produced a circumferential fracture. This area of bone was then displaced inward at the impact site, producing a comminuted depressed fracture. The fourth experiment (17-2118) produced several

POI linear fractures and a comminuted depressed fracture similar to 18-0364. However, there was no evidence peripheral engagement in this case.

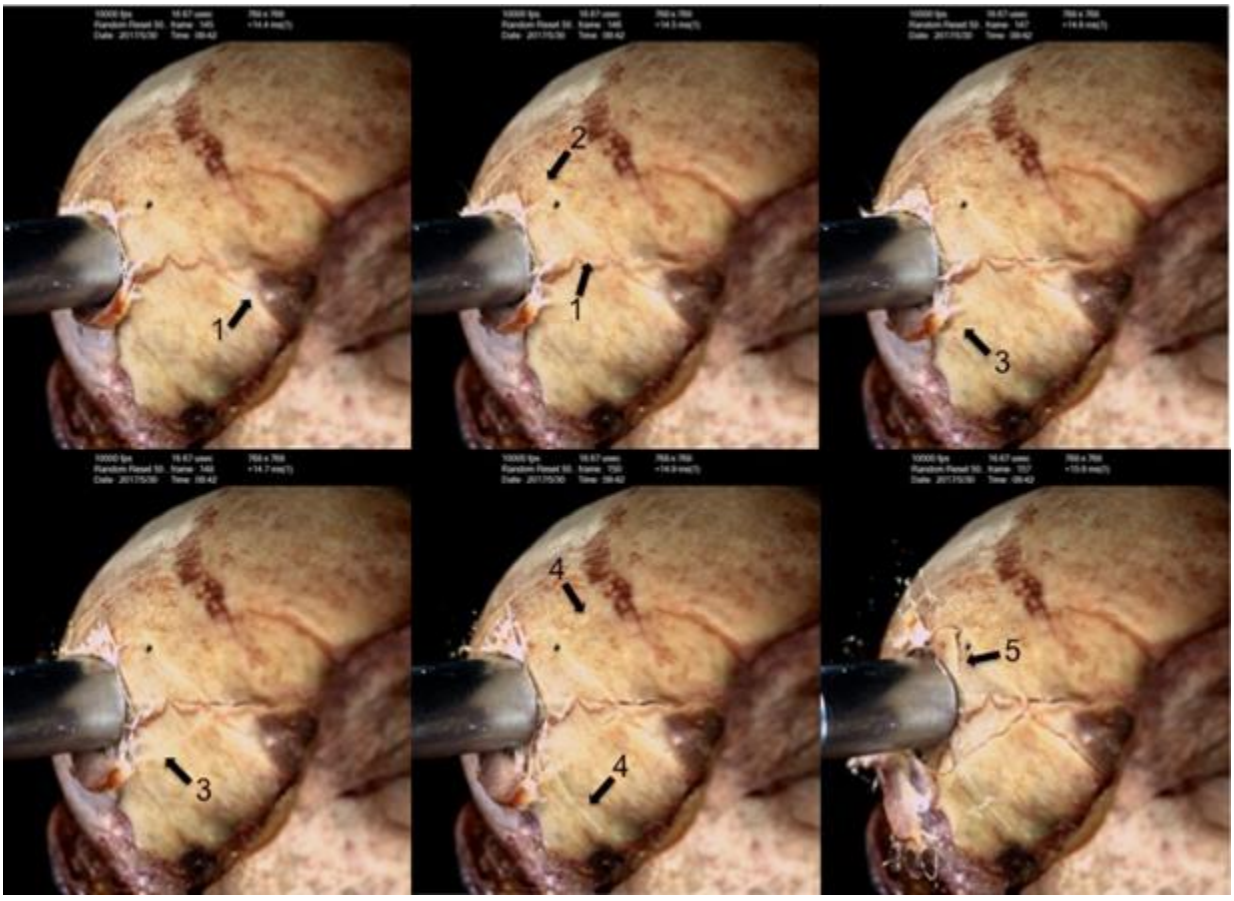

Figure 3.3: Fracture initiation and propagation in hammer experiment 17-2071. Fracture initiates peripherally in the temporal and travels back toward the POI (1). A circumferential fracture forms around the impact site (2-3). Linear fractures initiate from the edge of the circumferential fracture and travel away (4). Linear fractures initiate from the edge of the circumferential fracture and travel back to the impact center (5).

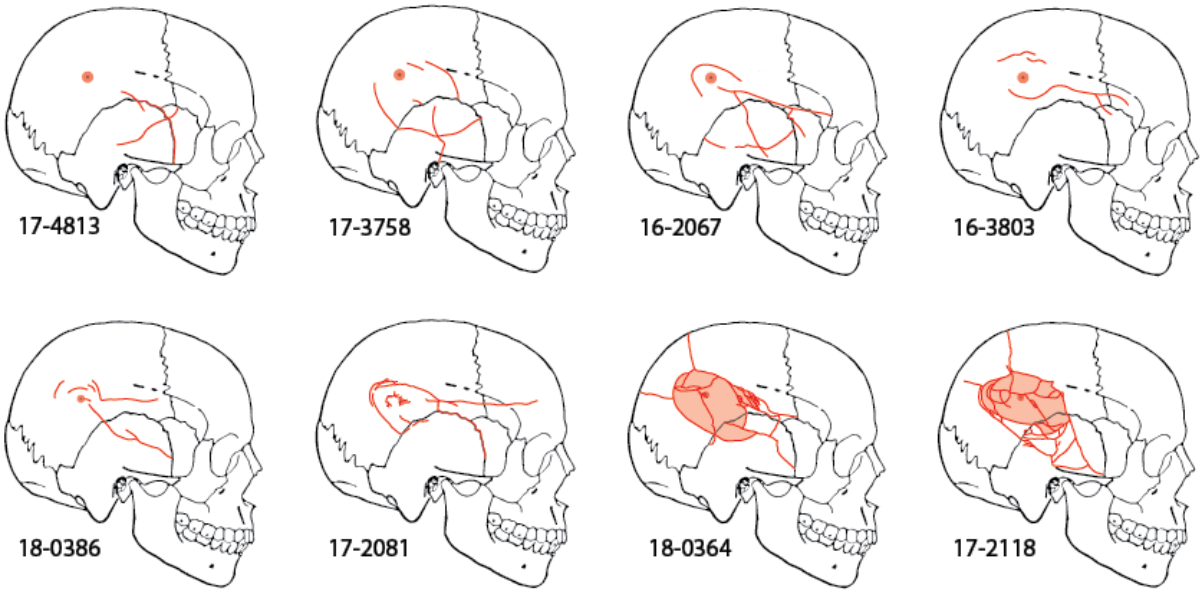

Figure 3.4: Impacts with the broad, curved "bat" implement. Top row: Low energy impacts. Bottom row: Current, high energy impacts. Areas of depression are shaded. All four high energy bat experiments produced circumferential fractures partially or completely encircling the POI. In two experiments (18-0364 and 17-2118) the area of bone at the impact site was displaced inward, producing comminuted depressed fractures. These two experiments also produced radiating linear fractures that crossed the midline and extended into the left parietal.

"Brick" (broad, flat impact surface)

Impacts with the brick produced the most variation in fracture initiation and propagation results (Figure 3.5). One experiment (18-0361) produced only peripheral linear fractures in the temporal and posterior parietal. Two experiments produced primarily POI fractures. In one case (17-2132), the impact produced several POI linear fractures that traveled inferiorly into the temporal. The second case (17-2095) exhibited a similar sequence, however this impact also produced a circumferential fracture partially encircling the POI. The fourth experiment (18-0300) produced both POI and peripheral fractures. In this experiment, a peripheral linear fracture formed in the sphenoid as a circumferential fracture formed around the POI. Several linear fractures initiated at the POI and radiated away from the impact site. As the impact progressed the bone at the impact site was displaced inward, forming a comminuted depressed fracture.

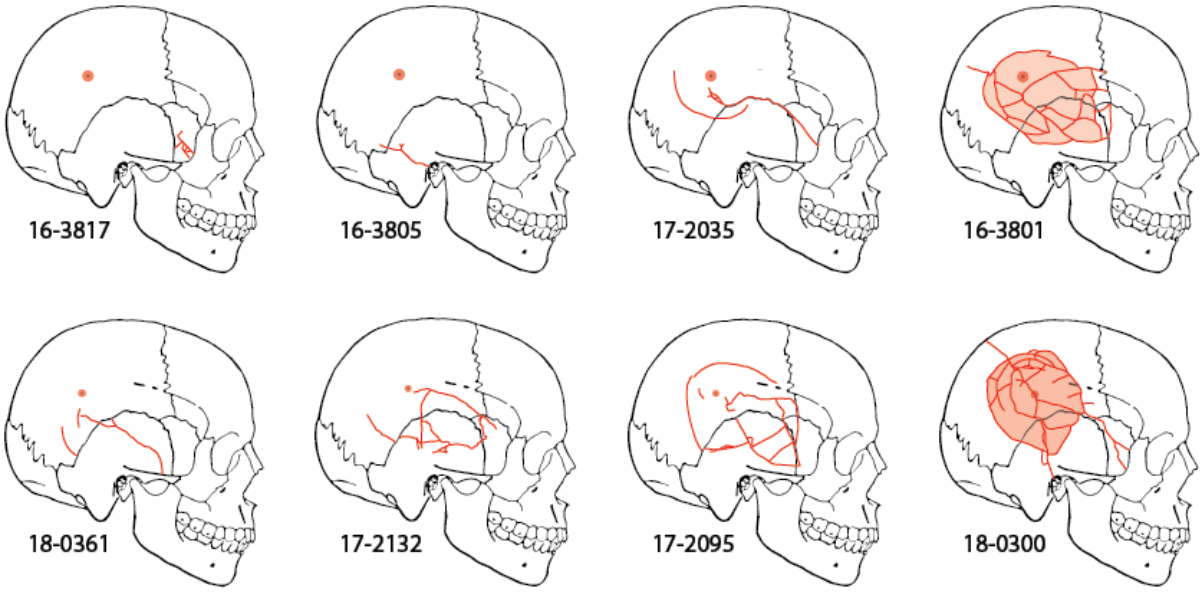

Figure 3.5: Impacts with the broad, flat "brick" implement. Top row: Low energy impacts. Bottom row: Current, high energy impacts. Areas of depression are shaded. Brick impacts produced two general patterns of fracture in the high energy impacts. Two experiments (18-0361 and 17-2132) produced primarily linear fractures of the inferior parietal and temporal. The other two experiments (17-2095 and 18-0300) produced large circumferential fractures around the POI. Bone fragments were displaced inwardly in 18-0300, forming a comminuted depressed fracture. In this case, a radiating linear fracture crossed the midline into the left parietal.

Comparison of fracture patterns in low and high energy impacts (n=24)

The appearance and severity of fractures observed in low and high energy experiments were compared in order to investigate potential effects of energy and implement on cranial fracture patterns.

Energy effects

Generally, high energy impacts tended to completely fracture both tables of bone, while low energy impacts often produced fractures affecting only the outer table. Assessment of fracture patterns generated in these experiments demonstrate greater severity in higher energy impacts. High energy impacts more frequently produced circumferential fractures (high: 9/12, low: 7/12), depressed fractures (high: 7/12, low: 3/12) and comminuted fractures (high: 6/12,

low: 3/12) than lower energy impacts. High energy impacts also produced delamination more frequently than low energy impacts (E2: 7/12, E1: 2/12). Additionally, only impacts performed at the higher energy level produced fractures crossing the midline (high: 3/12, low: 0/12). While these results suggest general trends, none of these differences was statistically significant (Fisher's exact test, $p>.05$).

High energy impacts produced larger average maximum defect diameters (51.03±17.39 mm) than low energy impacts (39.73±16.03 mm, $F_{(1,16)}=2.01$, $p=.18$). Similarly, high energy impacts produced larger average perpendicular defect diameters (38.31±16.97 mm) than low energy impacts (28.93±13.30 mm, $F_{(1,16)}=.1.63$, $p=.22$). However, these differences were not statistically significant and likely reflect the higher frequency of measurable defects produced with broader implements at the higher compared to the lower energy level.

Impact surface effects

The results suggest some trends in fracture patterns obtained with different impact surfaces. Depressed fractures were more frequent in hammer (6/8) than in bat (2/8) or brick (2/8) experiments. Circumferential fractures were more frequent in bat (7/8) and hammer (7/8) than in brick (4/8) experiments. Finally, brick experiments more frequently produced patterns involving only linear fractures (hammer: 1/8, bat 1/8, brick 4/8). Despite these trends, none of these differences was statistically significant (Fisher's exact test, $p>.05$). Similar frequencies of delamination (hammer: 4/8, bat: 3/8, brick: 2/8) and comminution (hammer: 4/8, bat: 2/8, brick: 3/8) were obtained across impact surfaces.

The results also suggest relationships between impact surface and defect diameter. There was a significant relationship between impact surface and MDD (Figure 3.6, $F_{(2,15)}=4.98$, $p=.02$). Specifically, MDD was smaller in hammer (35.02±10.25 mm) than in brick defects (63.15±7.21

mm, p=.02). MDD in bat defects (47.21±19.45 mm) was not significantly different from hammer or brick defects and exhibited a wide range. There was also a significant relationship between impact surface and PDD (Figure 3.7, $F_{(2,15)}$=4.09, p=.04). PDD in brick defects (51.44±22.78 mm) was significantly larger than PDD in bat defects (28.91±10.44 mm, p=.04) and nearly significantly larger than hammer defects (29.66±9.32 mm, p=.06). The difference between hammer and bat impacts was not significant (p=.99).

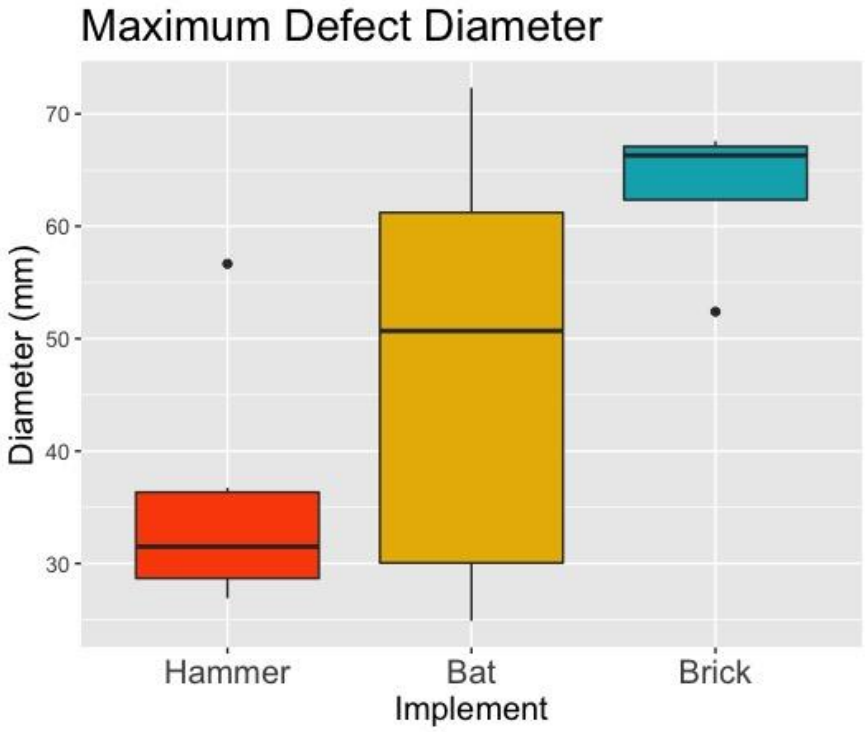

Figure 3.6: Maximum defect diameters obtained with the three implements tested.

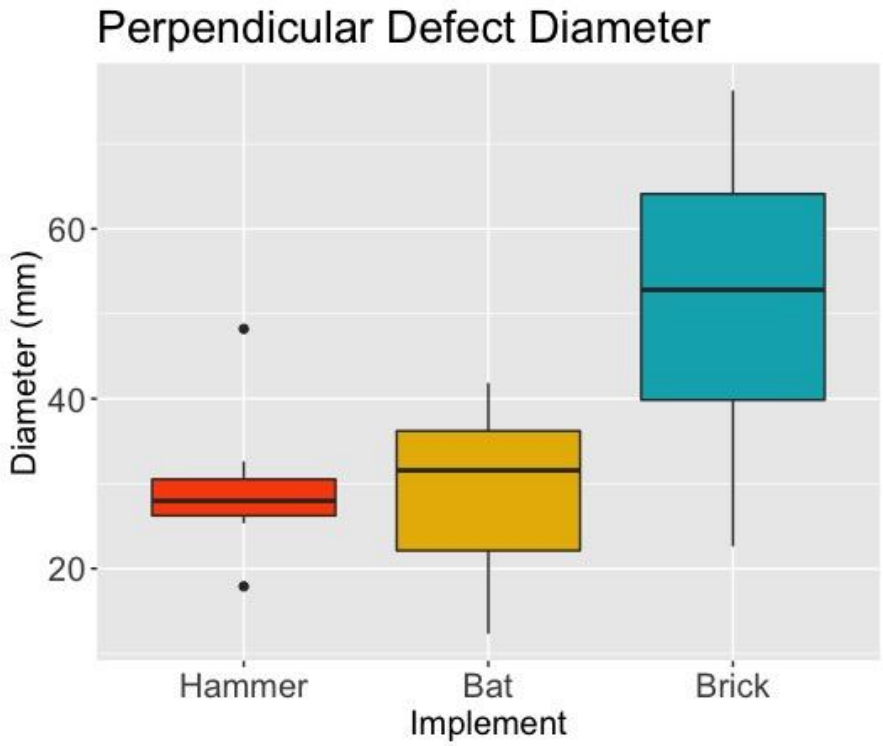

Figure 3.7: Perpendicular defect diameters obtained with the three implements tested.

Multiple Correspondence Analysis (MCA)

Multiple correspondence analysis (MCA) helps to visualize and summarize these results (Figure 3.8). MCA reduced the data such that the first two dimensions retain 73.2% of the inertia (variation) in the sample. Dimension 1 has the most inertia (58.6%) and therefore accounts for most of the variation. All variables under investigation contributed to dimension 1 including (in order of squared correlation r_2) depressed, secondary radiating, comminuted, circumferential, primary radiating, delamination, and POI damage. The presence of these features cluster on the negative side of this axis while the absence of these features cluster on the positive side. Dimension 2 accounts for 14.6% of the variation. This dimension can be understood as the appearance of the impact site. The variables contributing to dimension 2 are POI damage and circumferential fractures. The presence of these features cluster on the negative side of this axis while their absence cluster on the positive side.

Projection of the supplementary elements onto the model provides insights as to the relationships between fracture characteristics, energy, and implement. MCA results indicate high energy and low energy impacts are dissimilar. The differences between high and low energy can be described almost entirely along dimension 1. On this dimension, high energy is on the negative side of the axis, which is associated with the presence of features related to the complexity and severity of fracture. In contrast, low energy impacts are on the positive side of the dimension 1 axis, which is associated with the absence of these features. This is consistent with the finding that high energy impacts generally produced more damage at the impact site than low energy impacts.

The MCA results also suggest differences by implement. The distribution of hammer, bat, and brick can be described along two dimensions. The placement of the hammer on the negative side of dimension 1 (presence of features) and the brick on the positive side (absence of features) is consistent with the finding that hammer impacts more frequently produced complex (non-linear) fractures at the impact site with significant damage (e.g., depression, comminution, delamination) to the cranial vault. In comparison, brick impacts more frequently produced linear fractures and minimal damage to the cranial vault. Bat impacts are not well described by dimension 1, but are projected onto the negative side of dimension 2 (presence of circumferential fractures and POI damage). This is consistent with the finding that nearly all bat impacts produced nonlinear impact site fractures, but the severity varied by individual and energy level.

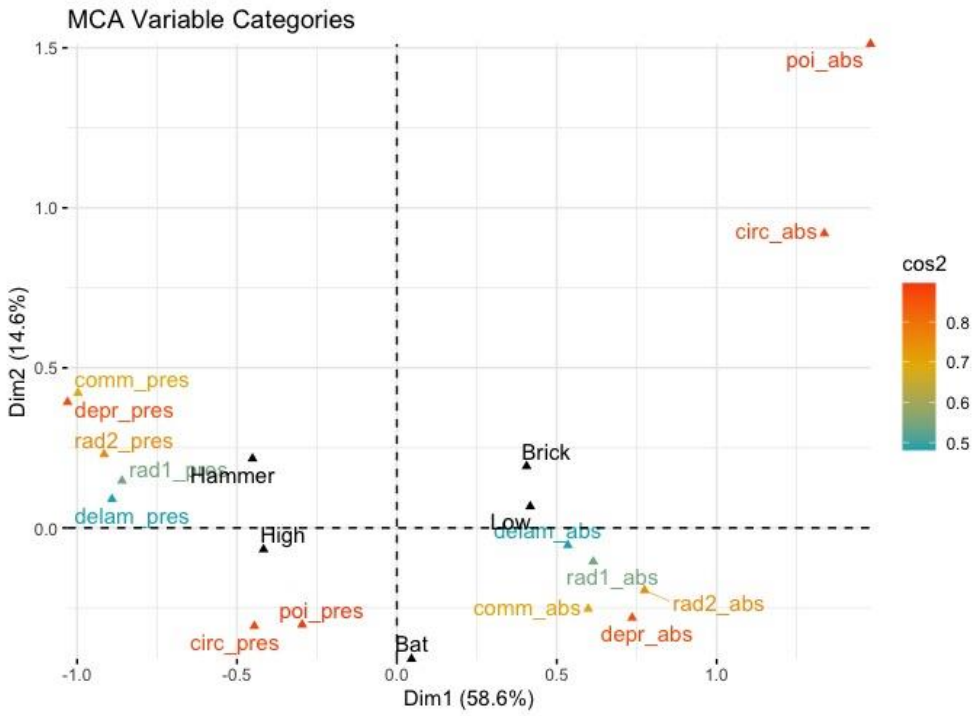

Figure 3.8: Results of the MCA where the plot of category points for the first two dimensions shows the associations between fracture characteristics, energy, and implement. The squared cosine (cos2) value measures the degree of association between variable categories and dimensions, with values closer to 1 indicating stronger associations. High cos2 values indicate that most of the variable categories are well represented by the two dimensions presented in this model, in particular the presence and absence of POI damage, depression, and circumferential fractures.

Discussion

The goals of this study were to perform blunt force cranial impacts at a higher input kinetic energy than in previously reported experiments (Isa et al. 2019), and to evaluate potential effects of input energy and impact surface on mechanical response, fracture initiation, and fracture patterns. The current experiments attained significantly higher input energy than the previous study. A 67% increase in energy was achieved primarily through the addition of mass to the impactor. Comparison of results obtained in the current and previous study suggest some effects of energy and implement on the parameters investigated.

The results demonstrate that given a higher input energy, more energy is absorbed by the head. However, the impact surface may limit the amount of energy absorbed. In the current study, E_a was lower in experiments with a more focal impact surface compared to the two broader surfaces tested. This is consistent with the results of the previous study conducted at a lower input energy (Isa et al. 2019). The current study found no significant differences in peak force based on input energy or impact surface. This contrasts with the previous study, in which the hammer (small, focal surface) required significantly lower force to initiate fracture than the bat or brick (broad surfaces). Various studies in human and non-human material have reported lower force to fracture in impacts with smaller contact surfaces (Allsop, Perl, and Warner 1991; Hodgson and Thomas 1971; Vaughan et al. 2016; Yoganandan and Pintar 2004; Bass and Yoganandan 2015; Sulaiman et al. 2014).

The current study provides additional evidence that cranial fractures initiate both at the POI and in peripheral areas. These results are consistent with the findings of Gurdjian et al. (Gurdjian, Webster, and Lissner 1950a, 1950b) and with the results obtained in lower energy impacts (Isa et al. 2019). However, nearly all of the current higher energy impact experiments produced failure at the impact site. Even when linear fractures formed peripherally, they tended to travel toward the POI. In contrast, a third of lower energy impacts produced peripheral linear fractures with no damage at the impact site.

In the current experiments, energy was increased primarily through the addition of mass. Impacts involving greater mass can be expected to generate more local deformation, and subsequently more local failure, than impacts involving less mass. In the previous experiments, the impact mass was approximately 6.3 kg. We previously hypothesized that the greater mass (8.5 kg) used in the Kroman et al. (Kroman, Kress, and Porta 2011) experiments may be one

factor explaining why they obtained only POI fracture in their study. The current study used masses of approximately 9.5 kg and produced more POI failure; however, fractures also initiated peripherally in the majority of experiments. This supports the hypothesis that intrinsic factors such as the anatomical location of impact also influence fracture formation (Isa et al. 2019). Specifically, an impact to the inferior parietal may involve engagement of the adjacent temporal bone, which is more compliant than the parietal and thus has a greater ability to deform and produce outbending (Yoganandan et al. 1995). This impact location also appears to engage adjacent sutures, which are known to absorb energy and are potentially more susceptible to fracture than surrounding cranial bone (Maloul, Fialkov, and Whyne 2013; Jaslow 1990).

The results suggest effects of input energy on the appearance and severity of cranial fractures. Descriptive results and the results of multiple correspondence analysis suggest that high energy impacts and low energy impacts produce dissimilar fracture patterns, with the former producing more severe, localized fractures than the latter. This is consistent with animal and human studies that have reported increased frequency and complexity of fracture with increased energy (Powell et al. 2012; Sharkey et al. 2012; McIntosh et al. 1993; Yoganandan et al. 1993; Delye et al. 2007; Raymond et al. 2009). However, there were similarities in fracture patterns obtained in higher and lower energy experiments. In particular, impacts with the broad, flat (brick) impact surface produced similar fracture patterns at both energy levels. In both lower and higher energy impacts, fracture patterns ranged from peripheral linear with minimal damage, to comminuted depressed with destruction of the cranial vault. This suggests that the severity of fractures obtained in impacts with broader surfaces may be more strongly influenced by properties of individual crania.

While the current experiments examined the effects of increased input energy attained via increase in mass, most other studies report on the effects of increased energy attained via increased velocity (Delye et al. 2007; McIntosh et al. 1993; Yoganandan et al. 1993; Raymond et al. 2009; Mole, Heyns, and Cloete 2015; Powell et al. 2012). On the one hand, the current results contribute unique data regarding the effect of increased mass on resultant fracture patterns. However, future experiments should also evaluate the effect of increased velocity on fracture results in PMHS.

Descriptive results and multiple correspondence analysis highlighted differences between the three impact surfaces tested. A small, focal surface (hammer) and a broad, curved surface (bat) produced impact site features more frequently than a broad, flat surface (brick). Meanwhile, severe fractures were most frequent with a small, focal surface, least frequent with the broad, flat surface, and intermediate with the broad, curved surface.

The results also indicate differences in the size of defects obtained with different impact surfaces. A broad, flat surface produced larger defect diameters than impacts with a focal, flat surface, while impacts with a broad, curved surface produced a wide range of variation. However, all three impact surfaces produced defects that were either larger or smaller than the actual impact surface. Overlap in fracture types and defect sizes obtained with different impact surfaces has also been reported in animal models (Sharkey et al. 2012; Vaughan et al. 2016; Otero and Béguelin 2019; Sulaiman et al. 2014). In experiments on pig crania, Otero and Béguelin (Otero and Béguelin 2019) also report greater variation in larger and more irregular impact surfaces compared to smaller and more regular surfaces.

The increased variation in fracture type and size with increased impact surface size is likely due to individual differences in contact area between the head and the impact surface. For

a more focal implement like the hammer, the entire impact surface is likely to contact the head. This impact surface can therefore be expected to produce relatively similar localized areas of deformation and contact stresses even in different individuals. For broader implements like the brick and curved implements like the bat, the entire surface does not contact the head during impact. Contact area in these cases is more dependent on the curvature of the head and likely varies more between individuals. Additionally, surfaces that generate broader contact areas may distribute deformations across a larger area. The location of fractures may therefore be more strongly influenced by stress concentrations developed at local irregularities (e.g. foramina, sutures, areas of relatively thick or thin bone) that differ between individuals.

Variation in contact area could also explain the overlap in fracture patterns and defect sizes obtained with different impact surfaces in this study. While the three blunt surfaces tested have different expected contact areas, they may produce similar effective contact areas on different specimens due to individual variation in cranial curvature. A limitation of the current study is that actual contact area was not directly measured during impact experiments. Future research should investigate the correlation between defect size and shape and the size and shape of the measured contact area.

Finally, a limitation of this research is that it is restricted to investigating the effects of two extrinsic variables – input energy and impact surface – on fracture behavior. Experiments on PMHS are valuable in that they demonstrate a known range of potential outcomes for a given set of applied variables. This data is useful for comparison to unknown cases, and for demonstrating limits to interpretations that can be made from fracture patterns. However, differences in fractures obtained in similar impacts and similarities in fractures produced under different conditions demonstrate the likely important role of intrinsic factors in influencing fracture

patterns. Previous studies have investigated the effect of individual variation on impact and fracture response (e.g., Got et al. 1983). Future research is needed to assess the effects of different aspects of individual variation on fracture patterns. This will require large sample sizes and investigation of a narrow set of extrinsic variables.

Conclusions

This study contributes new data on blunt force impacts performed at a higher input energy than those reported in our previous work (Isa et al. 2019). Results are presented from impacts with three known surfaces and two levels of input energy. As these experiments were performed on human material, they may provide a useful comparative sample for unknown human cases.

As reported in previous experiments, the current higher energy experiments also produced linear fractures initiating both at the point of impact and in areas peripheral to the impact site. This provides further evidence that isolated linear fractures in the temporoparietal region cannot be considered separate impact sites. However, current higher energy impacts more frequently produced impact site damage and depressed fractures than lower energy impacts. This may imply that impact sites are more likely to be accurately identified in higher energy impacts compared to similar lower energy impacts.

Impacts performed at a higher energy produced more damage at the impact site and across the cranial vault than that from impacts performed at a lower energy. This was evidenced by the increasing complexity and depth of fractures, as well as the distance traveled by radiating fractures. Overlap in the results obtained between the two studies suggests the degree of damage likely involves both individual properties of the cranium and the forces generated by input energy, particularly for broader impact surfaces. However, radiating fractures crossing the

midline were only obtained in higher energy impacts and may represent stronger evidence of higher input energy.

Finally, implement size correlated with defect size such that a more focused implement produced smaller, more consistent defects than those produced by broader implements. This suggests that general conclusions about contact area may be made based on the appearance and size of defects obtained. Focal, penetrating depressed fractures are associated with similarly focal contact areas. Defects are similar in size, though may be larger, than the impact surface. While larger circumferential and depressed fractures likely indicate broader impacts, the relationship between impact surface and defect size can be highly variable, are more dependent on cranial curvature, and therefore probably cannot be reconstructed.

Interface	Specimen	Initiation
Hammer (n=4)	17-2075	The impact produced a diastatic fracture of the squamosal suture and a depressed fracture at the POI.
	17-2082	The impact produced a diastatic fracture of the squamosal and sphenotemporal sutures. A short peripheral linear fracture traveled from the suture toward the POI. The impact also produced a depressed fracture at the POI.
	18-2359	Linear fractures initiated at the POI and traveled anteriorly toward the coronal suture and posteriorly to the lambdoidal suture. The impactor penetrated the cranial vault.
	17-2071	A peripheral linear fracture initiated in the temporal and propagated back to the POI. Next, a circumferential fracture formed around the POI. Finally, several linear fractures initiated at this circumferential fracture and traveled both toward and away from the POI.
Bat (n=4)	18-0386	A peripheral linear fracture initiated at the sphenotemporal suture and traveled back toward the POI. Another linear fracture initiated at the POI and traveled anteriorly toward the coronal suture. The impact also produced circumferential fractures partially encircling the POI.
	17-2081	A linear fracture initiated at the POI and traveled anteriorly into the frontal. The impact also produced a circumferential fracture around the POI and diastatic fractures of the squamosal and sphenotemporal sutures.
	18-0364	A peripheral linear fracture initiated in the anterior temporal and propagated in two directions, back to the POI and inferiorly to the sphenotemporal suture. Several linear fractures traveled posteriorly, superiorly, and anteriorly away from the POI. The impact also produced a circumferential fracture around the POI. As the impact progressed the bone at the impact site was displaced inwardly, producing depression.
	17-2118	Several linear fractures initiated at the POI and traveled posteriorly, superiorly, and inferiorly. This impact also produced a circumferential fracture around the POI. As the impact progressed the bone at the impact site was displaced inwardly, producing depression.
Brick (n=4)	18-0361	A peripheral linear fracture initiated in the inferior temporal and propagated superiorly toward the POI. Another short, peripheral linear fracture initiated at the squamosal suture, anterior to asterion, and propagated superiorly.

Table 3.1: Initiation results from the high energy impact experiments.

Table 3.1 (cont'd)

17-2132	Linear fractures initiated at the POI and propagated toward pterion. Additional linear fractures traveled from the POI to the temporal.
17-2095	Linear fractures initiated at the POI and propagated toward pterion. Additional linear fractures traveled from the POI into the temporal, fragmenting the bone. The impact also produced a circumferential fracture partially encircling the POI.
18-0300	The impact produced separation of the sphenofrontal suture that did not persist as a diastatic fracture. A peripheral linear fracture formed in the sphenoid as a circumferential fracture formed around the POI. Several linear fractures traveled from the POI inferiorly, anteriorly, and superiorly, resulting in extensive fragmentation of the parietal and temporal. As the impact progressed the bone at the impact site was displaced inwardly, producing depression.

REFERENCES

REFERENCES

Allsop, D., T.R. Perl, and C.Y. Warner. 1991. "Force/Deflection and Fracture Characteristics of the Temporo-Parietal Region of the Human Head." *Proceedings of the 35th Stapp Car Crash Conference* 35: 269–78.

Bass, C.R., and N. Yoganandan. 2015. "Skull and Facial Bone Injury Biomechanics." In *Accidental Injury: Biomechanics and Prevention*, edited by N. Yoganandan, A.M. Nahum, and J.W. Melvin, 203–20. New York: Springer-Verlag.

Baumer, T.G., N.V. Passalacqua, B.J. Powell, W.N. Newberry, T.W. Fenton, and R.C. Haut. 2010. "Age-Dependent Fracture Characteristics of Rigid and Compliant Surface Impacts on the Infant Skull - A Porcine Model." *Journal of Forensic Sciences* 55 (4): 993–97.

Berryman, H.E., J.F. Berryman, and T.B. Saul. 2018. "Bone Trauma Analysis in a Forensic Setting: Theoretical Basis and a Practical Approach for Evaluation." In *Forensic Anthropology: Theoretical Framework and Scientific Basis*, edited by C.C. Boyd and D.C. Boyd, 213–34. Chichester, West Sussex, UK: John Wiley & Sons Ltd.

Berryman, H.E., and S.A. Symes. 1998. "Recognizing Gunshot and Blunt Cranial Trauma Through Fracture Interpretation." In *Forensic Osteology: Advances in the Identification of Human Remains*, edited by Kathleen J. Reichs, 2nd ed., 333–52. Springfield, IL: Charles C. Thomas.

Chattopadhyay, S., and C. Tripathi. 2010. "Skull Fracture and Haemorrhage Pattern among Fatal and Nonfatal Head Injury Assault Victims - a Critical Analysis." *Journal of Injury & Violence Research* 2 (2): 99–103.

Cowin, S.C. 2001. *Bone Biomechanics Handbook*. Boca Raton, FL: CRC Press.

Delye, H., P. Verschueren, B. Depreitere, I. Verpoest, D. Berckmans, J. Vander Sloten, G. Van Der Perre, and J. Goffin. 2007. "Biomechanics of Frontal Skull Fracture." *Journal of Neurotrauma* 24 (10): 1576–86.

Dirkmaat, D.C., L.L. Cabo, S.D. Ousley, and S.A. Symes. 2008. "New Perspectives in Forensic Anthropology." *American Journal of Physical Anthropology* 137 (S47): 33–52.

Galloway, A., and V. Wedel. 2014a. "Common Circumstances of Blunt Force Trauma." In *Broken Bones: Anthropological Analysis of Blunt Force Trauma*, edited by Vicki L. Wedel and Alison Galloway, 2nd ed., 91–130. Springfield, IL: Charles C. Thomas.

Galloway, A., and V.L. Wedel. 2014b. "Bones of the Skull, the Dentition, and Osseous Structures of the Throat." In *Broken Bones: Anthropological Analysis of Blunt Force Trauma*, edited by V.L. Wedel and A. Galloway, 2nd ed., 133–60. Springfield, IL: Charles

C. Thomas.

Got, C., F. Guillon, A. Patel, and P. Mack. 1983. “Morphological and Biomechanical Study of 146 Human Skulls Used in Experimental Impacts in Relation with the Observed Injuries.” *Proceedings of the 27th Stapp Car Crash Conference*, 241–59.

Gurdjian, E. S., J. E. Webster, and H. R. Lissner. 1953. “Observations on Prediction of Fracture Site in Head Injury.” *Radiology* 60 (2): 226–35.

Gurdjian, E. S., John E. Webster, and Herbert R. Lissner. 1949. “Studies on Skull Fracture with Particular Reference to Engineering Factors.” *The American Journal of Surgery* 78 (5): 736–42.

Gurdjian, E.S. 1975. *Impact Head Injury*. Springfield, IL: Charles C. Thomas.

Gurdjian, E.S., and H.R. Lissner. 1947. “Deformations of the Skull in Head Injury as Studied by the ‘Stresscoat’ Technic.” *The American Journal of Surgery* 73 (2): 269–81.

Gurdjian, E.S., J.E. Webster, and H.R. Lissner. 1950a. “The Mechanism of Skull Fracture.” *Radiology* 54 (3): 313–38.

Gurdjian, E.S., J.E. Webster, and H.R. Lissner. 1950b. “The Mechanism of Skull Fracture.” *Journal of Neurosurgery* 7 (2): 106–14.

Haaren, E.H. van, B.C. van der Zwaard, A.J. van der Veen, I.C. Heyligers, P.I.J.M. Wuisman, and T.H. Smit. 2008. “Effect of Long-Term Preservation on the Mechanical Properties of Cortical Bone in Goats.” *Acta Orthopaedica* 79 (5): 708–16.

Hodgson, V.R., and L.M. Thomas. 1971. “Breaking Strength of the Human Skull vs. Impact Surface Curvature.” DOT-HS-800-583.

Isa, M.I., T.W. Fenton, A.C. Goots, E.O. Watson, P.E. Vaughan, and F. Wei. 2019. “Experimental Investigation of Cranial Fracture Initiation in Blunt Human Head Impacts.” *Forensic Science International* 300: 51–62.

Jaslow, C.R. 1990. “Mechanical Properties of Cranial Sutures.” *Biomechanics* 23 (4): 313–21.

Kaye, B., C. Randall, D. Walsh, and P. Hansma. 2012. “The Effects of Freezing on the Mechanical Properties of Bone.” *Open Bone Journal* 4 (1): 14–19.

Kieser, J. 2013. “Basic Principles of Biomechanics.” In *Forensic Biomechanics*, edited by J. Kieser, M. Taylor, and D. Carr, 7–33. Chichester, West Sussex, UK: John Wiley & Sons Ltd.

Kimmerle, E.H., and J.P. Baraybar. 2011. “Blunt Force Trauma.” In *Skeletal Trauma: Identification of Injuries Resulting from Human Rights Abuse and Armed Conflict*, edited by

Erin H. Kimmerle and José Pablo Baraybar, 151–99. Boca Raton, FL: CRC Press.

Kranioti, Elena. 2015. “Forensic Investigation of Cranial Injuries Due to Blunt Force Trauma: Current Best Practice.” *Research and Reports in Forensic Medical Science* 5: 25–37.

Kroman, A.M., T.A. Kress, and D. Porta. 2011. “Fracture Propagation in the Human Cranium: A Re-Testing of Popular Theories.” *Clinical Anatomy* 24 (3): 309–18.

Maloul, A., J. Fialkov, and C.M. Whyne. 2013. “Characterization of the Bending Strength of Craniofacial Sutures.” *Journal of Biomechanics* 46 (5): 912–17.

McIntosh, A.S., D. Kallieris, R. Mattern, and E. Miltner. 1993. “Head and Neck Injury Resulting from Low Velocity Direct Impact.” *SAE Technical Paper 933112*.

Melvin, J.W., and F.G. Evans. 1971. “A Strain Energy Approach to the Mechanics of Skull Fracture.” *Proceedings of the 15th Stapp Car Crash Conference*, 666–85.

Melvin, J.W., P.M. Fuller, R.P. Daniel, and G.M. Pavliscak. 1969. “Human Head and Knee Tolerance to Localized Impacts.” *SAE Technical Paper* 690477.

Mole, C.G., M. Heyns, and T. Cloete. 2015. “How Hard Is Hard Enough? An Investigation of the Force Associated with Lateral Blunt Force Trauma to the Porcine Cranium.” *Legal Medicine* 17 (1): 1–8.

Nahum, A.M., J.D. Gatts, G.W. Gadd, and J. Danforth. 1968. “Impact Tolerance of the Skull and Face.” *SAE Technical Paper 680785*.

Otero, F., and M. Béguelin. 2019. “Experimental Study of Cranial Injuries Due to Blunt Force Trauma : Sus Scrofa Domestica Model.” *Journal of Forensic Sciences and Criminal Investigation* 13 (2): 1–8.

Passalacqua, N.V., and T.W. Fenton. 2012. “Developments in Skeletal Trauma: Blunt-Force Trauma.” In *A Companion to Forensic Anthropology*, edited by Dennis C Dirkmaat, 400–411. Chichester, West Sussex, UK: Blackwell Publishing, Ltd.

Peterson, J., and P.C. Dechow. 2002. “Material Properties of the Inner and Outer Cortical Tables of the Human Parietal Bone.” *Anatomical Record* 268 (1): 7–15.

Peterson, J., and P.C. Dechow. 2003. “Material Properties of the Human Cranial Vault and Zygoma.” *Anatomical Record - Part A Discoveries in Molecular, Cellular, and Evolutionary Biology* 274 (1): 785–97.

Powell, B.J., N.V. Passalacqua, T.G. Baumer, T.W. Fenton, and R.C. Haut. 2012. “Fracture Patterns on the Infant Porcine Skull Following Severe Blunt Impact.” *Journal of Forensic Sciences* 57 (2): 312–17.

Powell, B.J., N.V. Passalacqua, T.W. Fenton, and R.C. Haut. 2013. “Fracture Characteristics of Entrapped Head Impacts Versus Controlled Head Drops in Infant Porcine Specimens.” *Journal of Forensic Sciences* 58 (3): 678–83.

R Core Team. 2020. “R: A Language and Environment for Statistical Computing.” Vienna, Austria: R Foundation for Statistical Computing. https://www.r-project.org/.

Raymond, D., C. Van Ee, G. Crawford, and C. Bir. 2009. “Tolerance of the Skull to Blunt Ballistic Temporo-Parietal Impact.” *Journal of Biomechanics* 42 (15): 2479–85.

Schneider, D.C., and A.M. Nahum. 1972. “Impact Studies of Facial Bones and Skull.” *Proceedings of the 16th Stapp Car Crash Conference* 16: 186–203.

Sharkey, E. J., M. Cassidy, J. Brady, M. D. Gilchrist, and N. NicDaeid. 2012. “Investigation of the Force Associated with the Formation of Lacerations and Skull Fractures.” *International Journal of Legal Medicine* 126 (6): 835–44.

Siegenthaler, L., F.D. Sprenger, B.P. Kneubuehl, and C. Jackowski. 2018. “Impact Energy of Everyday Items Used for Assault.” *International Journal of Legal Medicine* 132 (1): 211–17.

Sulaiman, N.A., K. Osman, N.H. Hamzah, and S.P.A. Amir Hamzah. 2014. “Blunt Force Trauma to Skull with Various Instruments.” *Malaysian Journal of Pathology* 36 (1): 33–39.

Symes, S.A, E.N. L’Abbé, E.N. Chapman, I. Wolff, and D.C. Dirkmaat. 2012. “Interpreting Traumatic Injury to Bone in Medicolegal Investigations.” In *A Companion to Forensic Anthropology*, edited by D.C. Dirkmaat, 340–89. Chichester, West Sussex, UK: Blackwell Publishing, Ltd.

Torimitsu, S., Y. Nishida, T. Takano, Y. Koizumi, M. Hayakawa, D. Yajima, G. Inokuchi, et al. 2014. “Effects of the Freezing and Thawing Process on Biomechanical Properties of the Human Skull.” *Legal Medicine* 16 (2): 102–5.

Vaughan, P.E., C.C.M. Vogelsberg, J.M. Vollner, T.W. Fenton, and R.C. Haut. 2016. “The Role of Interface Shape on the Impact Characteristics and Cranial Fracture Patterns Using the Immature Porcine Head Model.” *Journal of Forensic Sciences* 61 (5): 1190–97.

Yoganandan, N., and F.A. Pintar. 2004. “Biomechanics of Temporo-Parietal Skull Fracture.” *Clinical Biomechanics* 19 (3): 225–39.

Yoganandan, N., F.A. Pintar, J. Reinartz, and A. Sances. 1993. “Human Facial Tolerance to Steering Wheel Impact: A Biomechanical Study.” *Journal of Safety Research* 24 (2): 77–85.

Yoganandan, N., F.A. Pintar, A. Sances, P.R. Walsh, C.L. Ewing, D.J. Thomas, and R.G. Snyder. 1995. “Biomechanics of Skull Fracture.” *Journal of Neurotrauma* 12 (4): 659–68.

PAPER 4: ASSESSING IMPACT DIRECTION IN 3-POINT BENDING OF HUMAN FEMORA: INCOMPLETE BUTTERFLY FRACTURES AND FRACTURE SURFACES

Abstract

Current literature associates bending failure with butterfly fracture, in which fracture initiates transversely at the tensile surface of a bent bone and branches as it propagates toward the impact surface. The orientation of the resulting wedge fragment is often considered diagnostic of impact direction. However, experimental studies indicate bending does not always produce complete butterfly fractures, or produces wedge fragments variably in tension or compression, precluding their use in interpreting directionality. The present study reports results of experimental 3-point bending tests on thirteen unembalmed human femora. Complete fracture patterns varied following bending failure, but incomplete fractures and fracture surface characteristics were observed in all impacted specimens. A flat, billowy fracture surface was observed in tension, while jagged, angular peaks were observed in compression. Impact direction was accurately reconstructed using incomplete tension wedge butterfly fractures and tension and compression fracture surface criteria in all thirteen specimens.

Introduction

Direction of blunt force impact is often a factor of interest in forensic death investigations. In the absence of soft tissue evidence, forensic anthropologists may be asked to assist forensic pathologists by assessing skeletal fractures and interpreting injury mechanisms. Anthropologists draw on basic principles of biomechanics and bone strength asymmetry to analyze blunt injuries in terms of failure in tension and compression. From this understanding, it is possible to infer the direction of impact (Passalacqua and Fenton 2012; Symes et al. 2012). One pattern of injury often discussed in these terms is the butterfly fracture (Passalacqua and Fenton 2012; Symes et al. 2012; Smith, Pope, and Symes 2003; Berryman, Shirley, and Lanfear 2013).

Biomechanical and anthropological literature associates butterfly fracture with long bone bending (Smith, Pope, and Symes 2003; Gozna, Harrington, and Evans 1982; Nordin and Frankel 2012; Kimmerle and Baraybar 2008). When a bone is bent, maximum compressive stress is generated on the concave impact surface and maximum tensile stress on the opposing convex surface. Because cortical bone is weaker in tension than compression, failure initiates in tension opposite the impact (Gozna, Harrington, and Evans 1982). As the initial fracture crack approaches the compressed side of the neutral axis, it has been suggested that shear stresses exceed the bone's shear strength and cause the crack to bifurcate along 45-degree planes of maximum shear (Martin et al. 2015). The expected result of bending failure is thus a "butterfly" fracture consisting of a transverse segment on the tension side of the neutral axis and a triangular wedge fragment formed by the propagation of oblique fractures on the compression (impact) side (Smith, Pope, and Symes 2003; Berryman, Shirley, and Lanfear 2013; A. Galloway 1999). This pattern of fracture is also known as a "tension wedge" because the wedge forms with the apex

toward the side of the bone in tension (Kress 1996). Based on this understanding of butterfly fracture production, wedge orientation is often regarded as diagnostic of impact direction (Smith, Pope, and Symes 2003; Rockhold and Hermann 1999; Ubelaker and Adams 1995; Kroman and Symes 2013; Emanovsky 2015).

Research validating this understanding of butterfly fracture suggests that the relationship between long bone bending and butterfly fractures is more variable than typically presented in the literature (Kress 1996; Teresinski and Madro 1999; Martens et al. 1986; Fenton et al. 2012; Reber and Simmons 2015; Thomas and Simmons 2011; Khalil, Raymond, and Miller 2015). In a key engineering study, Kress (Kress 1996) reports several complete fracture types generated in bending in a large sample of human femora and tibiae. Tension wedge butterfly fractures and oblique fractures were most prevalent, but bending also generated transverse and comminuted fractures. Additionally, some butterfly fractures occurred in a "compression wedge" orientation with the apex pointing toward the compression side of the bone. Similarly, in an actualistic study of femur and tibia fractures in pedestrian-vehicular impacts, Teresinski and Madro (Teresinski and Madro 1999) report butterfly fractures occurring in both tension and compression wedge orientations.

Other experimental studies provide different reports on the expected prevalence of complete fracture types following bending failure, and on the circumstances surrounding the production of compression wedge butterfly fractures (Martens et al. 1986; Fenton et al. 2012; Reber and Simmons 2015; Thomas and Simmons 2011; Khalil, Raymond, and Miller 2015). Martens et al. (Martens et al. 1986) report 4-point bending of posterior-loaded human femora produced only oblique or compression wedge butterfly fractures. Fenton et al. (Fenton et al. 2012) report no complete butterfly fractures of either wedge orientation in 3-point bending of

anterior- and posterior-loaded dry human femora. In the Fenton et al. study, complete fracture patterns involved 60% oblique fractures, 27% transverse fractures, and 13% comminuted fractures. In 3-point bending experiments on sheep femora, Reber and Simmons (Reber and Simmons 2015) report butterfly fractures in about half the sample; of these 60% were tension wedges and 40% were compression wedges. Even in synthetic bone, Khalil et al. (Khalil, Raymond, and Miller 2015) report variation in complete fracture patterns. Three-point bending experiments in the Khalil et al. study produced some tension wedges, but no compression wedge butterfly fractures.

The inconsistency in the presence and orientation of complete butterfly fractures generated in experimental studies indicate this fracture pattern may be an unreliable indicator of directionality in forensic cases. L'Abbé and colleagues (L'Abbé et al. 2014) caution that simple recognition of a butterfly fracture does not necessarily lead to successful interpretation of injuries. In response to this problem, Fenton et al. (Fenton et al. 2012) investigated the presence and orientation of four incomplete fracture characteristics, drawn from the anthropological literature (particularly from Symes, Berryman, and their colleagues (Symes et al. 2012; Berryman et al. 1991; Symes et al. 1996; Berryman 2014)), in dry human femora failed under 3-point bending. These characteristics appeared frequently, in up to 80% of the sample, and could be used to reconstruct loading direction accurately in most specimens. However, it was unclear how these results might apply to the evaluation of perimortem trauma because the materials used in the experiments (dry bones) were outside the perimortem interval.

In addition to incomplete fractures, Symes and colleagues (Symes et al. 2012; Berryman et al. 1991; Symes et al. 1996) and Berryman (Berryman 2014) cite fracture surface morphology as indicative of failure in tension vs. compression for blunt trauma to long bones. In tension,

Symes et al. (Symes et al. 1996) describe “bone tears,” a fracture surface with a “pulled apart” appearance also described as mottled, billowy, and similar in appearance to an unfused epiphysis. In compression, the presence of “dog-eared notches” delineates corresponding “breakaway spurs” (Symes et al. 1996). Compression surfaces are described as splintery, macroscopically jagged, angular, and irregular, with longitudinal alignment with the grain of the bone (Rockhold and Hermann 1999; Symes et al. 1996; Berryman 2014). Rockhold and Hermann (Rockhold and Hermann 1999) report using these fracture surfaces to reconstruct failure in tension and compression and subsequently infer impact directionality in a case involving a vehicular hit-and-run fatality. Problematically, assertions about fracture surface morphology appear to originate largely from the authors’ (e.g. Symes et al. (Symes et al. 1996) and Berryman (Berryman 2014)) forensic anthropology case experience and have not been validated through controlled experimentation on human material.

The purpose of the current study was to perform controlled 3-point bending impact experiments on fresh human femora and document the incidence and patterns of complete fractures, incomplete fractures, and fracture surface characteristics. The study was conducted with two primary objectives. The first objective was to test whether the incomplete fracture characteristics Fenton et al. (Fenton et al. 2012) documented in dry material also apply to reconstructing loading direction in fresh human bone. The second objective was to determine if fracture surface characteristics, as discussed by Berryman (Berryman 2014), Symes (Symes et al. 2012, 1996), and others (e.g., Rockhold and Hermann (Rockhold and Hermann 1999)), are useful for interpreting loading direction in bones failed in laboratory-controlled impact experiments.

Materials and Methods

Impact experiments

Three-point bending experiments were conducted to simulate a transverse impact to the lower limb of a standing subject (methods also described in DeLand's thesis (DeLand 2013)). Thirteen fresh, unembalmed femora from seven male cadavers ranging in age between 52 and 66 years (mean age at death 57.2±4.9 years) were selected for the study. All specimens were stored at -20°C and thawed at room temperature for two days before testing. Prior to impact, the skin and muscle was excised from each femur in order to facilitate manipulation of the specimens in the impact fixture and ensure consistent anatomical orientation. The proximal and distal ends of the femur were left intact and potted in polyester resin (Martin Senour Fibre Strand Plus 6371, Sherwin-Williams; Cleveland, OH) to create attachment points for installing the bone into the fixture (Figure 4.1). At the distal end, a cup was attached at a point just above the knee as the knee joint itself, including the distal femur, was later used in a different set of experiments.

Mechanical testing was performed using a 3-point bending fixture mounted on a servohydraulic materials testing machine (MTS; Eden Prairie, MN). Femora were installed into the fixture using the resin pots as attachment points. The fixture allowed both ends of the bone to pivot freely, while an X-Y table allowed planar translation of the distal end. Springs at both ends of the bone were used to apply a static axial compressive preload of 450 N, to approximately simulate one leg supporting one half of normal body weight. Impacts were performed using a 30 mm-diameter solid steel cylinder anvil oriented perpendicular to the bone's long axis. A preload of 50 N was applied mid-diaphysis to eliminate any potential residual system compliance.

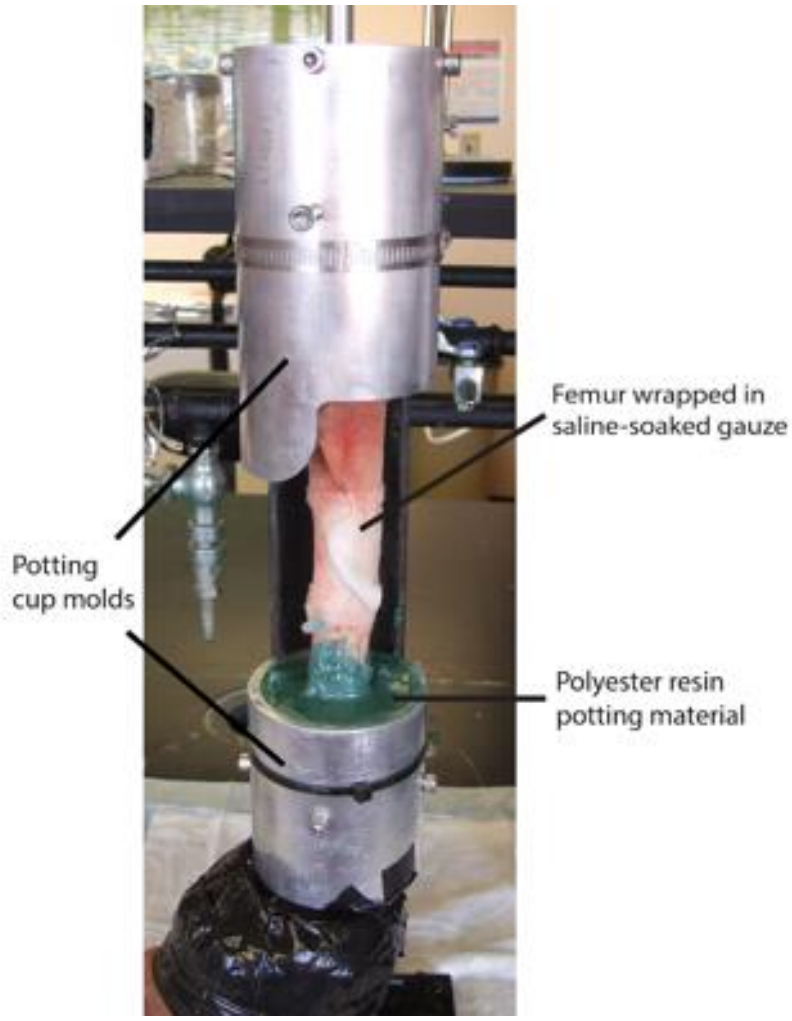

Figure 4.1: Potting the proximal and distal ends of a femur.

Failure was induced via a position-controlled 2 Hz 30 mm haversine displacement of the impact anvil into the bone. Force and displacement data were recorded at 10,000 Hz by an actuator-mounted load transducer (3210AF-5K, 5000 lb capacity, Interface; Scottsdale, AZ) and a linear variable differential transformer (LMT-711P35, ±3.5" stroke, G.L. Collins Corporation; Long Beach, CA). Energy to failure was calculated as the area under the load-displacement curve up to the peak load. Figure 4.2 shows the impact setup with one of the specimens in the materials testing machine. Paired impacts were performed to account for potential influences of impact surface geometry (such as the linea aspera on the posterior femur) on fracture results. The

left femur of each individual was impacted on the anterior surface (anterior to posterior or A-P bending), while the right femur was loaded on the posterior surface (posterior to anterior or P-A bending).

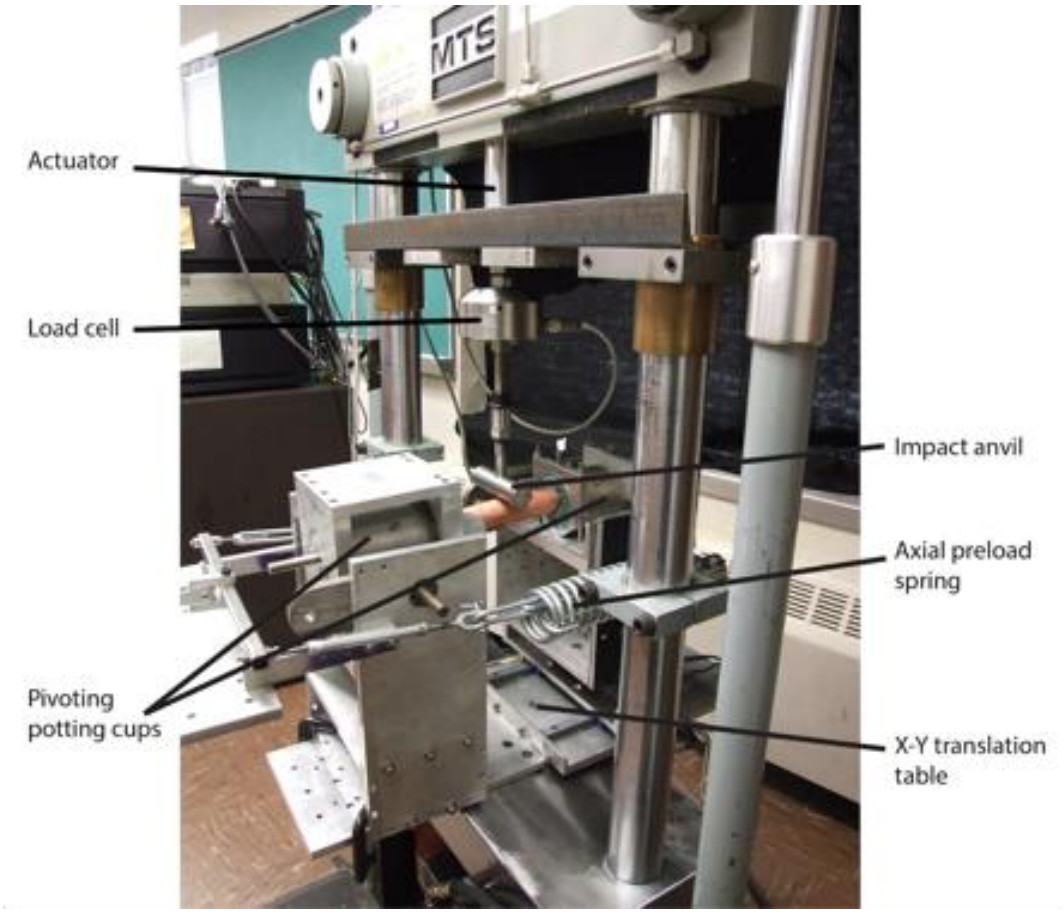

Figure 4.2: Impact setup with a femur installed in the 3-point bending fixture on the materials testing machine.

High-speed video was recorded of one impact experiment to document fracture initiation and propagation. Fracture was recorded at 40,000 frames per second, allowing for observation of fracture from initiation to complete failure of the bone.

Fracture analysis

Following impact, any remaining adhering soft tissue was removed using warm water maceration (Fenton, Birkby, and Cornelison 2003). Subsequently, specimens were examined

macroscopically for the presence of complete fractures, incomplete fractures, and fracture surface features. Each specimen was reconstructed from its constituent bone fragments to allow for the photographic and diagrammatic documentation of complete and incomplete fracture outlines. Medial and lateral views were recorded to account for potential asymmetry.

Specimens were first assessed for complete fractures. Complete fractures were classified as "transverse" (running approximately perpendicular to the bone's long axis), "oblique" (running diagonal to the bone's long axis), or "comminuted" (dividing the bone into more than two pieces) (Galloway 1999). Fractures classified as comminuted were further examined for the presence of triangular-shaped fragments. If present, these were further classified as "tension wedge" or "compression wedge" butterfly fractures.

Each specimen was reconstructed, then assessed for the presence of four fracture characteristics previously described by Fenton et al. (Fenton et al. 2012) (Figure 4.3):

1) A *transverse crack* at initiation;
2) *Incomplete tension wedge butterfly fractures* formed as incomplete fracture lines branch off the main crack at approximately 45-degree angles;
3) *Failure angle shifts* occurring as fracture branches shift to run parallel to the bone's long axis; and
4) A *breakaway spur* in which the fracture angle sharply changes direction just prior to fracture completion.

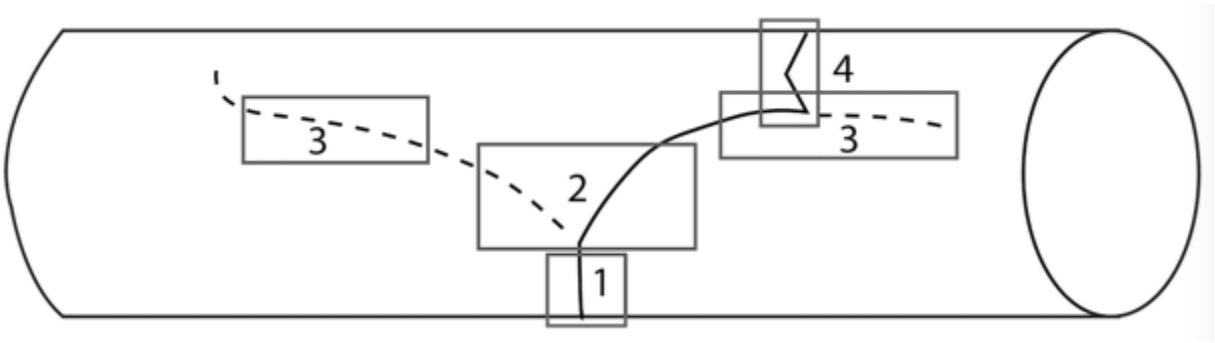

Figure 4.3: Incomplete fracture features. 1: Transverse crack. 2: Incomplete tension wedge butterfly fracture. 3: Failure angle shift. 4: Breakaway spur.

Prior to reconstruction, the fracture surfaces of each bone fragment were assessed for characteristics described in the literature (Symes et al. 2012; Rockhold and Hermann 1999; Symes et al. 1996; Berryman 2014). Surfaces were categorized as 1) relatively flat with shallow topography and a "pulled apart," mottled, billowy appearance similar to an unfused epiphysis; or 2) angular, jagged or irregular peaks with steep topography and longitudinal alignment with the grain of the bone. The presence and anatomical location of these surfaces were noted for each specimen.

Results

Load-displacement plots to failure showed a linear response of each bone with abrupt failure in all cases (Figure 4.4). Failure loads ranged from 399 to 920 N. No significant differences were observed between failure loads recorded for anterior impacts (576±118 N) and posterior impacts (644±216 N). Anvil displacement prior to failure ranged from 5.8 mm to 13.2 mm. No significant differences were observed between anterior impacts (8.83±2.67 mm) and posterior impacts (10.21±1.57 mm). Input energy to failure ranged from 15.0 to 66.3 J. While the energy was generally higher for posterior impacts (39.4 ±18.4 J) than anterior impacts (29.0±11.7 J), the difference was also non-significant.

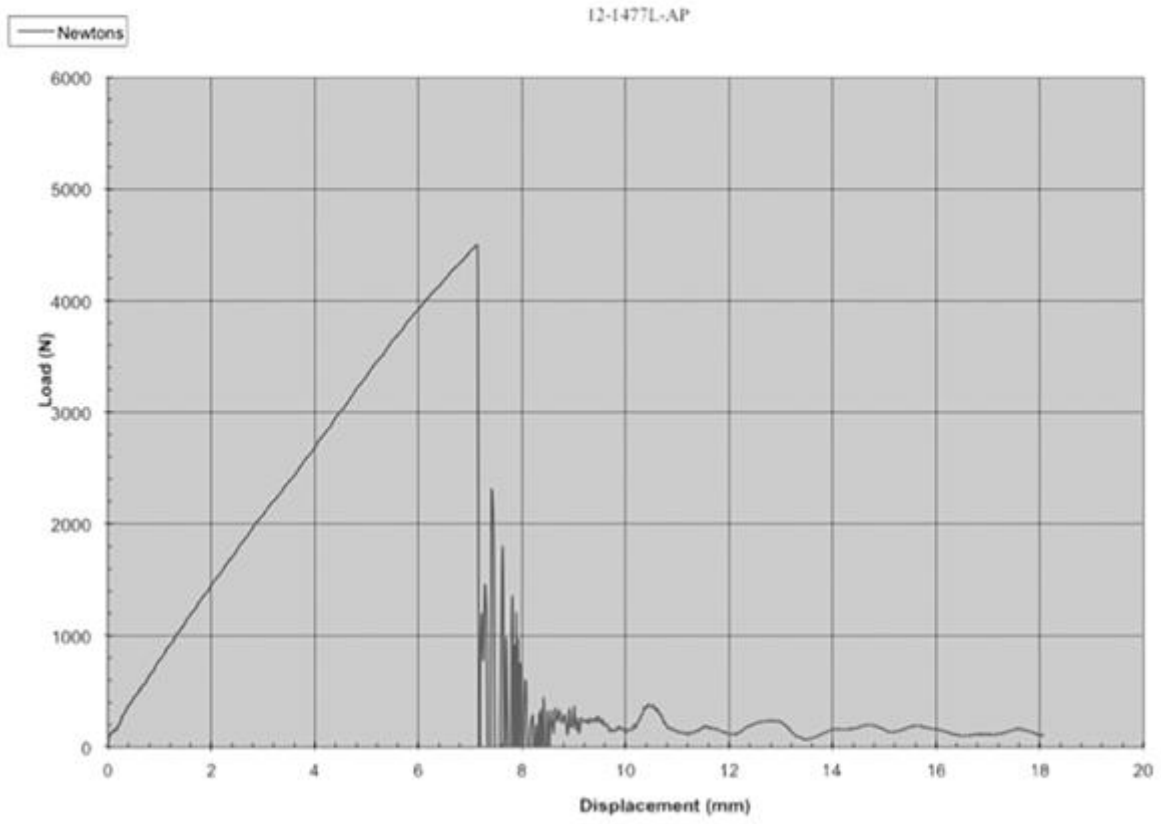

Figure 4.4: Load-displacement graph of one impact experiment.

Complete fracture characteristics

Controlled 3-point bending experiments produced complete fracture in 100% (13/13) of anterior- and posterior-impacted human femora. Several complete fracture types were observed including transverse fractures in 6/13 (46.2%) impacts, oblique fractures in 3/13 (23.1%) impacts, and comminuted fractures in 4/13 (30.8%) impacts. No complete butterfly fractures were observed in any impact. Anterior impacts produced transverse fractures in 3/6 (50%) specimens, oblique fractures in 2/6 (33.3%) specimens, and comminuted fractures in 1/6 (16.7%) specimens. Posterior impacts produced transverse fractures in 3/7 (42.9%) specimens, oblique fractures in 1/7 (14.3%) specimens, and comminuted fractures in 3/7 (42.9%) specimens. These results support previous experimental studies of long bone bending that report high incidences of oblique and transverse fractures (Kress 1996; Fenton et al. 2012).

Interestingly, the results demonstrate that complete fracture types vary both between subjects loaded in the same direction and within subjects with femur pairs loaded in different directions. In each of the paired impact experiments the anterior-loaded left femur exhibited a different complete fracture type than the corresponding posterior-loaded right femur. However, no consistent, significant difference in complete fracture type was observed between anterior and posterior impacts (p=.633).

Incomplete fracture characteristics

While complete fracture types varied across impact experiments, the presence and orientation of incomplete fractures were consistent across impact experiments (Figures 4.5, 4.6). The four features investigated by Fenton et al. (Fenton et al. 2012) in dry femora were consistently observed in this sample in a particular sequence and location relative to the impact. Transverse cracks were present in 100% (13/13) of impacted specimens. In each case this feature was observed on the tensile side of the bone opposite the applied load, that is, anteriorly in posterior-loaded femora and posteriorly in anterior-loaded femora. Contrasting with conventional depictions of butterfly fracture in the literature, the transverse cracks were short in this experimental set. Incomplete butterfly fractures formed through the branching of incomplete fractures off the main crack occurred in 13/13 (100%) impacts. The number and location of branch points varied between specimens, but branching began from the tension side in each case. Branch points occurred on the anterior side in all posterior impacts and the posterior side in all anterior impacts. Failure angle shifts were also observed in 13/13 (100%) impacts. These were observed most often in incomplete fracture branches. Finally, clear breakaway spurs were observed in 11/13 (84.6%) impacts. This includes 6/6 (100%) A-P impacts and 5/7 (71.4%) P-A

impacts. For each case in which breakaway spurs were present, they were observed on the compression (impact) side of the bone.

When medial and lateral views were compared, some asymmetry was observed within specimens. Only incomplete butterfly fractures were easily identified in both medial and lateral views in all thirteen A-P and P-A impacts. Failure angle shifts were observed in both medial and lateral views in 6/6 (100%) A-P specimens, but only 5/6 (83.3%) P-A specimens. Transverse cracks were visible in both medial and lateral views in 5/6 (83.3%) A-P specimens and 5/7 (71.4%) P-A specimens. Breakaway spurs exhibited the most asymmetry within specimens. These were visible in both views in only 2/6 (33.3%) A-P specimens. Of the P-A specimens, breakaway spurs were observed in both medial and lateral views in all five of seven cases in which they were present (71.4%). This asymmetry underscores the importance of viewing incomplete fractures carefully across all surfaces of the bone.

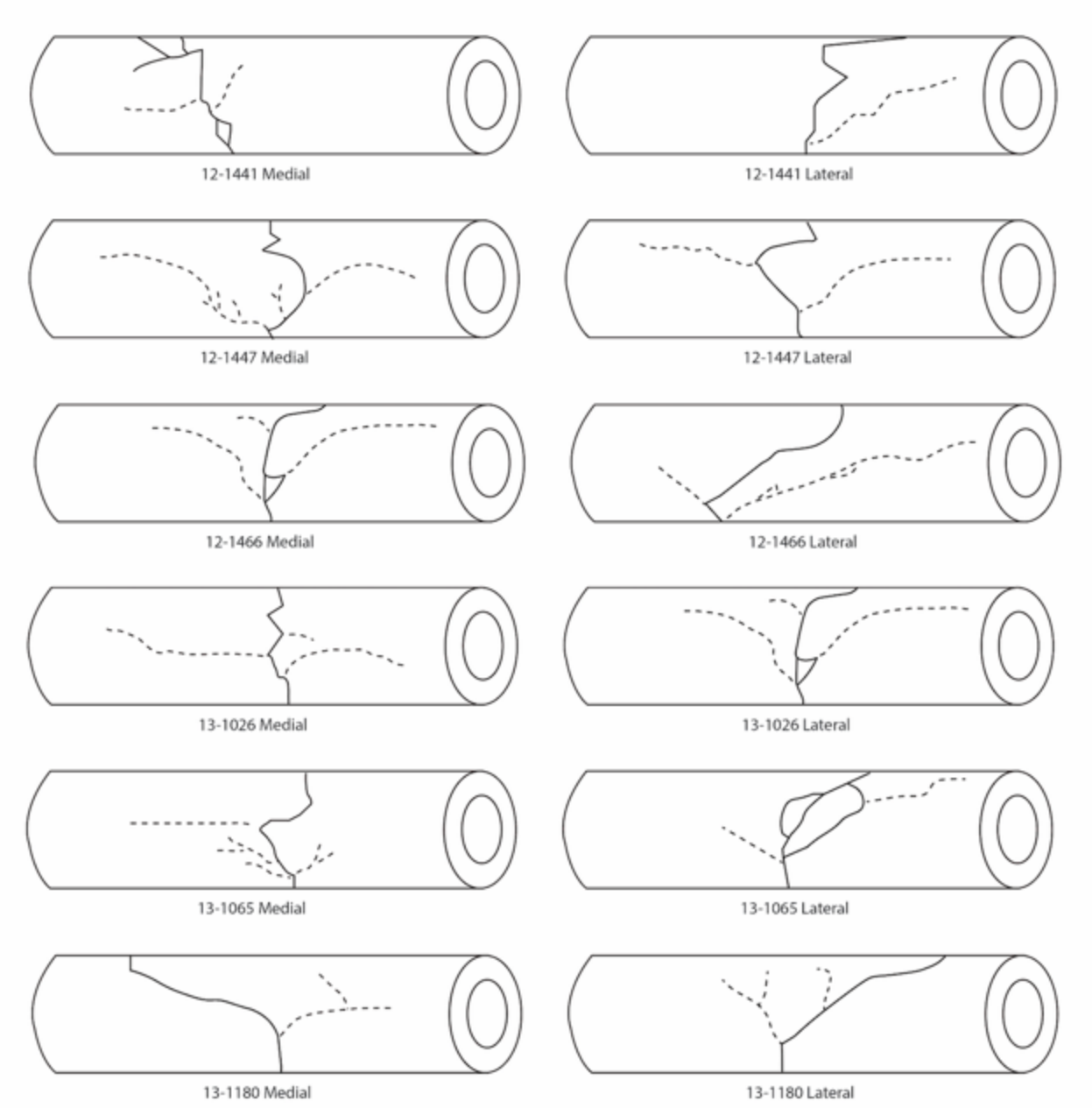

Figure 4.5: Results of anterior (A-P) impacts to left femora; impact side is up. Solid lines represent complete fractures and dotted lines represent incomplete fractures.

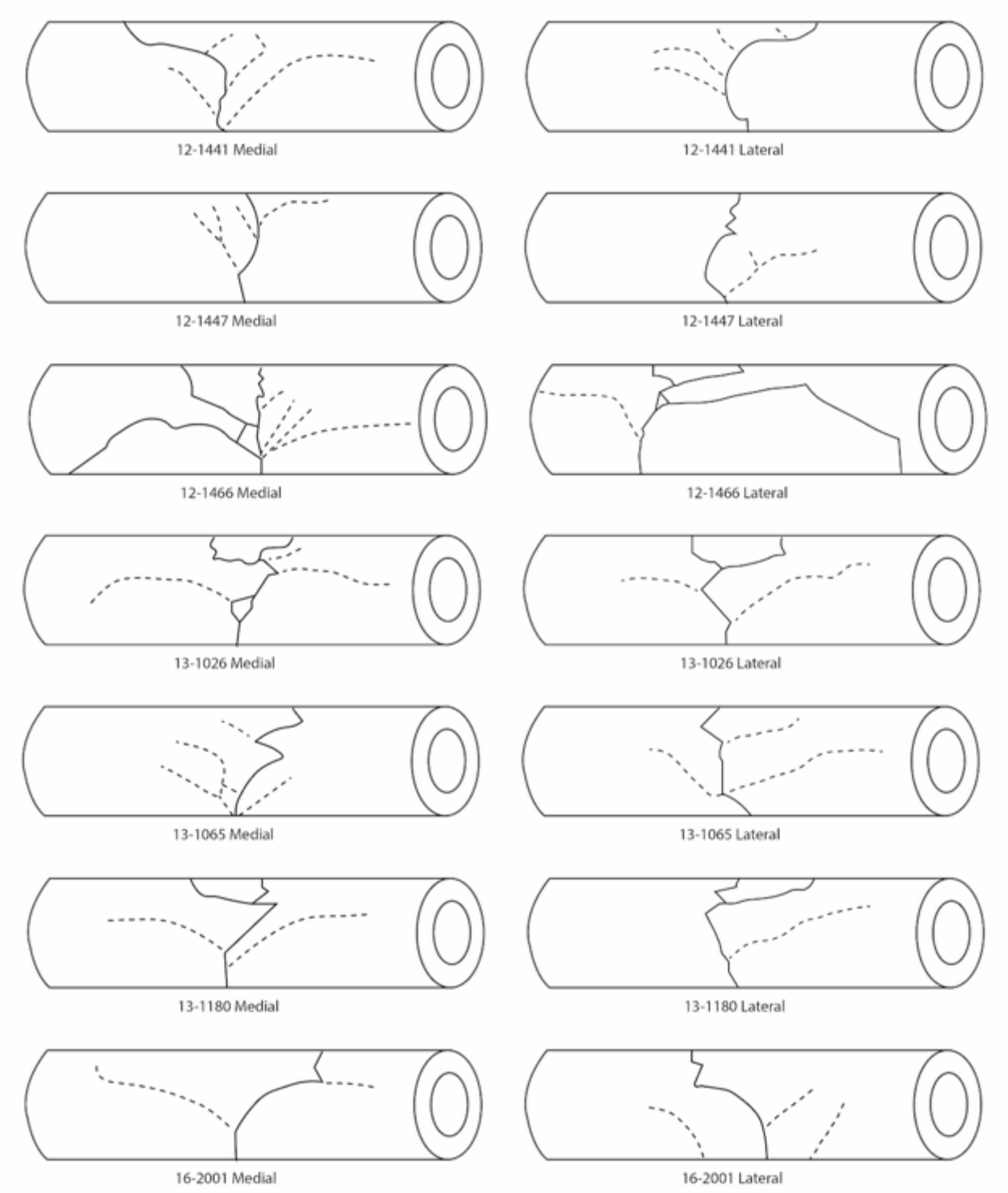

Figure 4.6: Results of posterior (P-A) impacts to right femora; impact side is up. Solid lines represent complete fractures and dotted lines represent incomplete fractures.

High-speed video: production of incomplete butterfly fractures

High-speed video footage of one 3-point bending experiment may exhibit how fractures initiate and propagate during failure in bending. In the video, production of the four incomplete fracture characteristics (Figure 4.3) was observed as four "events" or directional changes the fracture takes during propagation (Figure 4.7). The video showed the fracture initiating as a short transverse crack on the side of the bone opposite impact. This supported the prediction based on basic principles of biomechanics and bone anisotropy that bent bone will fail initially in tension on the side opposite impact. However, fracture initiation did not occur directly opposite the impact site. This suggests the location of initial tensile failure does not necessarily reflect the location of impact along the shaft. Immediately following initial failure, a secondary incomplete fracture branched off the initial transverse crack. This branching began on the tension side of the bone. As they propagated toward the impact (compression) side, both complete and incomplete fractures shifted to parallel the bone's long axis (failure angle shifts). The incomplete fracture terminated in this position. Meanwhile, the primary complete fracture sharply shifted directions as it propagated toward the impact (compression) side, resulting in a short fracture segment (breakaway spur) that reached completion on the impact side of the bone.

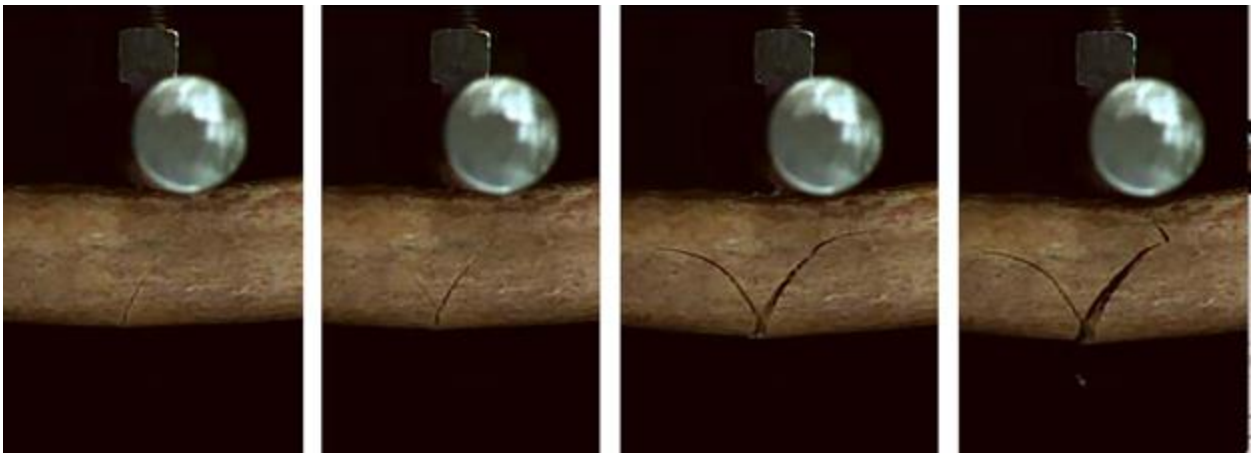

Figure 4.7: Stills from high-speed video of impact experiment 16-2001. Frame 1: tensile initiation. Frame 2: branching of incomplete and complete fractures. Frame 3: failure angle shifts. Frame 4: formation of breakaway spur.

Fracture surface characteristics

The appearance and location of two distinct fracture surface features were consistent across all anterior and posterior impacts. In all thirteen (100%) specimens, the tension surface was relatively flat and epiphysis-like with shallow billowing and was observed on the non-impact side. In 6/6 (100%) of A-P impacts the tension surface was observed on the posterior portion of the bone, and in 7/7 (100%) of P-A impacts the tension surface was observed on the anterior portion. Similarly, the compression surface was macroscopically jagged with angular, longitudinally oriented peaks and steep topography on the impact side in all thirteen specimens. In 6/6 (100%) of A-P impacts the compression surface was observed on the anterior portion of the bone, and in 7/7 (100%) of P-A impacts it was observed on the posterior portion (Figures 4.8 and 4.9). Assessment of the fracture surfaces in some cases helped to differentiate between the transverse crack and the breakaway spur; the transverse crack was associated with the flat, billowy surface while the breakaway spur was associated with the jagged, peaked surface.

When viewing the fracture surface looking down the medullary cavity, the tension feature occupied most of the fracture surface in all specimens. Jagged compression features were most

pronounced close to the impact surface. When the complete fracture type was oblique, the compression surface was sometimes observed as a single peak on one portion of the bone and a notch on the corresponding surface. The transition of surface morphology from tension to compression characteristics was typically abrupt. A line demarcating between the two surfaces could often be drawn across the medullary cavity from medial to lateral, roughly perpendicular to the direction of the applied load.

Figure 4.8: Fracture surface in an A-P impacted specimen (13-1026). The compression surface occurs on the anterior side of the bone (image right). The tension surface occurs on the posterior side of the bone (image left).

Figure 4.9: Fracture surface in a P-A impacted specimen (12-1466). The compression surface occurs on the posterior side of the bone (image left). The tension surface occurs on the anterior side of the bone (image right).

Discussion

The current experimental study of thirteen cases of controlled 3-point bending in the human femur demonstrated the expected range of variation in fracture characteristics that have been discussed previously in the trauma literature. While the results did show considerable variation in complete fractures, there was a consistency in the incidence and location of incomplete fractures and fracture surface characteristics.

The current results support previous experimental research (Kress 1996; Fenton et al. 2012; Reber and Simmons 2015) demonstrating that long bone bending produces a variety of complete fracture patterns. This complicates the simple relationship between long bone bending and butterfly fractures often presented in the literature (e.g., (Passalacqua and Fenton 2012; Symes et al. 2012; Smith, Pope, and Symes 2003; Berryman, Shirley, and Lanfear 2013)). The results also highlight the limitations of relying on butterfly fracture wedge orientation to diagnose impact direction (Smith, Pope, and Symes 2003; Rockhold and Hermann 1999; Ubelaker and Adams 1995; Berryman 2014), as the present study demonstrates bending may not produce complete butterfly fractures. Because none of the specimens in the current study exhibited complete butterfly fractures, these results neither support nor contradict the results of previous investigators (Martens et al. 1986; Reber and Simmons 2015) that complete butterfly fragments are more likely to occur on the posterior femur, regardless of impact direction. In the present study, incomplete butterfly fractures occurred exclusively as tension wedges with no fracture patterns suggestive of compression wedges. The incomplete wedge fragment occurred on the impact side in both anterior- and posterior-loaded specimens. Bending experiments in the present study did produce different complete fracture patterns in paired femora loaded on the

anterior vs. the posterior surface. However, the relationship between loading surface and complete fracture type was non-significant in this experimental set.

The four incomplete fracture characteristics Fenton et al. (Fenton et al. 2012) report in dry bones were also observed in the present set of fresh, unembalmed human femora. As observed in high-speed video footage, incomplete fracture characteristics appear to reflect directional changes in the fracture as it propagates from initiation on the tension side to completion on the compression side of the long bone. Although video footage was not taken of all impact experiments, the incomplete fractures in the filmed impact appear similar to those observed in the experiments not filmed. Transverse cracks were consistently observed where the bone was initially in tension. In all specimens, incomplete butterfly fracture branches began closer to the side of fracture initiation and widened as they propagated toward the compression side of the bone. Failure angle shifts tended to occur toward the compression side, and breakaway spurs were consistently observed on the impact side where the bone was initially in compression. Understanding incomplete fractures as artifacts of fracture propagation from tension to compression allowed for an accurate interpretation of impact directionality in the current experimental set.

Incomplete fracture characteristics were observed more consistently in the current sample of fresh bones than in dry bones failed under the same loading conditions. Transverse cracks, incomplete tension wedge butterfly fractures, and failure angle shifts occurred in 100% of fresh specimens in the present study, but only in 80-87% of dry bone specimens reported by Fenton et al. (Fenton et al. 2012). In both fresh and dry specimens, however, breakaway spurs were observed less frequently than the other three features. The lower incidence of incomplete fracture characteristics in dry material may indicate that postmortem changes in bone material properties

affect the production of incomplete fracture characteristics. Effects of postmortem drying on fracture results have been reported in some experimental studies (Wieberg and Wescott 2008; Wheatley 2008). Bone moisture content has been shown to decrease rapidly in the months after death (Wieberg and Wescott 2008). Wieberg and Wescott (Wieberg and Wescott 2008) report a low, but significant correlation between moisture content and some fracture characteristics. Of note, wet bones tend to exhibit more fracture lines than dry bones. This may help explain why incomplete tension wedges, formed by the branching of two or more fracture lines, were observed more frequently in the current fresh bone sample than in the dry bone sample. Additionally, wet bone fractures tend to exhibit more curved or V-shaped outlines than dry bone fractures, which tend toward transverse outlines (Wheatley 2008). Two incomplete fracture characteristics relevant to the current study, incomplete tension wedges and failure angle shifts, are the direct results of changes in fracture angle and curvature away from the transverse.

The current three-point bending experiments generated fracture surface features consistent with those described by Symes (Symes et al. 1996), Berryman (Berryman 2014), and others (Rockhold and Hermann 1999; Emanovsky 2015). Flat, shallow, epiphysis-like billowing was observed opposite the impact where the bone was in tension in all specimens regardless of loading surface. Jagged, angular peaks were consistently observed on the impact (compression) side. These results lend support to the validity of fracture surfaces described in the literature and indicate the transition of fracture surfaces from flat to jagged likely reflects a transition from initial failure in tension to failure on the compression side of the bone.

As these bending experiments were performed in a laboratory setting, there were some limitations to the study. The current study reflects a small sample of bones that failed under a particular set of loading conditions (3-point bending with axial compression). The effect of

different impact variables, including loading rate, implement type, or different loading configurations, on the incomplete fractures and fracture surface characteristics described here is yet untested. Still, consistency in the incidence and orientation of incomplete fractures and fracture surfaces observed in this experimental set suggest these features may make more reliable units of analysis than complete butterfly fractures.

For the current study the authors found the following steps most useful for assessing fracture and reconstructing loading direction. In the experimental set, fracture surface morphology was found to be reliable for reconstructing failure on the tension vs. compression side of the bone, and subsequently accurately reconstructing loading direction. To best observe these features, the authors focused on the fractured cortical surfaces surrounding the medullary cavity and noted the presence and anatomical location of the two surface textures. The relatively flat surface characterized by shallow billowing occurred on the tension side and the jagged surface, consisting of sharp, angular peaks, occurred on the compressed side in the current study. Typically, the abrupt transition between these two contrasting surfaces could be demarcated with a line across the medullary cavity, approximately perpendicular to the direction of loading.

Next, the bone was reconstructed to best observe incomplete fractures. The anatomical location and orientation of the branch points of the incomplete butterfly fractures were noted. While all four incomplete fracture characteristics were observed consistently in this experimental set, branching of incomplete butterfly fractures was the single most reliable and unambiguous of these features to identify and interpret. In all experimental cases, incomplete or complete secondary fractures branched off the primary complete fracture line and formed branch points whose apex pointed toward the tension side of the bone. The other incomplete fracture features helped confirm direction of impact. The location of the transverse crack helped identify the

tension side of the bone, while the breakaway spur helped identify the compressed side. Failure angle shifts were typically observed as the fracture progressed to the compressed side of the bone, which provided further evidence of directionality. When the anatomical orientation of the incomplete butterfly fracture and the anatomical orientation of the tension and compression fracture surfaces agreed, this provided a good indication of the impact direction. Using these steps the authors reconstructed impact direction accurately in 100% of cases.

These features were useful in the present sample of specimens failed under 3-point bending with axial loading. However, this data cannot confirm whether the same incomplete fractures and fracture surfaces will be present or equally useful for estimating loading direction in human long bones when impact conditions involve other variables. The method presented here should be blind tested on external samples with known impact direction in order to establish error rates. Until then, practitioners should remain cautious about applying this method for estimating loading direction in forensic cases.

Conclusion

This study of controlled 3-point bending using fresh human bone responds directly to the "Current Needs in Forensic Anthropology" document generated by the Gap Analysis Committee of the Scientific Working Group for Forensic Anthropology (SWGANTH) which calls for "collaborative research with a biomechanist doing controlled experimental trauma studies, preferably on human remains" (SWGANTH 2011). The results of this study lead to the conclusion that exclusive reliance on complete fractures would limit an observer's ability to assess loading direction, as complete fracture types varied even under these laboratory controlled conditions. If practitioners consider only the presence and orientation of complete butterfly fractures, they may be unable to accurately interpret impact direction in all trauma cases.

The understanding of fracture propagation presented here allowed for the reconstruction of impact direction in this experimental set of bending impacts using incomplete fractures and fracture surface characteristics. In this set, incomplete tension wedge butterfly fractures and fracture surface features occurred in consistent locations corresponding to where the bone was likely initially in tension or compression. The results of this study therefore suggest that these features may be more useful for reconstructing loading direction than simply the generation of complete butterfly fractures alone.

REFERENCES

REFERENCES

Berryman, H.E. 2014. "Postmortem Breakage as a Taphonomic Tool for Determining Burial Position." In *Kennewick Man: The Scientific Investigation of an Ancient American Skeleton*, edited by D.O. Owsley and R.L. Jantz, 393–416. College Station, TX: Texas A&M University Press.

Berryman, H.E., N.R. Shirley, and A.K. Lanfear. 2013. "Low-Velocity Trauma." In *Forensic Anthropology: An Introduction,* edited by M.A. Tersigni-Tarrant and N.R. Shirley, 271–90. Boca Raton, FL: CRC Press.

Berryman, H.E., S.A. Symes, O.C. Smith, and S.J. Moore. 1991. "Bone Fracture II: Gross Examination of Fractures." In *Proceedings of the 43rd Annual Meeting of the American Academy of Forensic Sciences*; Anaheim, CA.

DeLand, T.S. 2013. "Studies on the Development and Fracture Mechanics of Cortical Bone." Thesis. Michigan State University.

Emanovsky, P. 2015. "Low-Velocity Impact Trauma: An Ilustrative Selection of Cases from the Joint POW/MIA Accounting Command - Central Identification Laboratory." In *Skeletal Trauma: Case Studies in Context,* edited by N.V. Passalacqua and C.W. Rainwater, 156–66. Chichester, West Sussex, UK: John Wiley & Sons Ltd.

Fenton, T.W., W.H. Birkby, and J. Cornelison. 2003. "A Fast and Safe Non-Bleaching Method for Forensic Skeletal Preparation." *Journal of Forensic Sciences* 48 (1): 1–3.

Fenton, T.W., A.E. Kendell, T.S. DeLand, and R.C. Haut. 2012. "Determination of Impact Direction Based on Fracture Patterns in Long Bones." In *Proceedings of the 64th Annual Meeting of the American Academy of Forensic Sciences*; Atlanta, GA.

Galloway, A. 1999. "Principles for Interpretation of Blunt Force Trauma." In *Broken Bones: Anthropological Analysis of Blunt Force Trauma*, edited by A. Galloway, 1st ed., 35–62. Springfield, IL: Charles C. Thomas.

Gozna, E.R., I.J. Harrington, and D.C. Evans. 1982. *Biomechanics of Musculoskeletal Injury*. Baltimore, MD: Williams & Wilkins.

Khalil, A., D. Raymond, and E.A. Miller. 2015. "An Analysis of Butterfly Fracture Propagation." In *Proceedings of the 67th Annual Meeting of the American Academy of Forensic Sciences;* Orlando, FL.

Kimmerle, E.H., and J.P. Baraybar. 2008. "Differential Diagnosis of Skeletal Injuries." In *Skeletal Trauma: Identification of Injuries Resulting from Human Rights Abuse and Armed Conflict,* edited by E.H. Kimmerle and J.P. Baraybar, 21–94. Boca Raton, FL: CRC Press.

Kress, T.A. 1996. “Impact Biomechanics of the Human Body.” Dissertation. University of Tennessee, Knoxville, TN.

Kroman, A.M., and S.A. Symes. 2013. “Investigation of Skeletal Trauma.” In *Research Methods in Human Skeletal Biology*, edited by E.A. DiGangi and M.K. Moore, 219–40. Oxford, UK: Elsevier.

L’Abbé, E.N., S.A. Symes, E. Chapan, J.E.S. Pinheiro, K.E. Stull, and D. Raymond. 2014. “The Rorschach Butterfly: The Use of Nomenclature in Lieu of Understanding the Effects and Components of Kinetic Energy in Bone Trauma Interpretations.” In *Proceedings of the 66th Annual Meeting of the American Academy of Forensic Sciences*; Seattle, WA.

Martens, M., R. van Audekercke, P. de Meester, and J.C. Mulier. 1986. “Mechanical Behaviour of Femoral Bones in Bending Loading.” *Journal of Biomechanics* 19 (6): 443–54.

Martin, R.B., D.B. Burr, N.A. Sharkey, and D.P. Fyhrie. 2015. “Mechanical Properties of Bone.” In *Skeletal Tissue Mechanics*, edited by R.B. Martin, D.B. Burr, N.A. Sharkey, and D.P. Fyhrie, 355–422. New York: Springer.

Nordin, M., and V.H. Frankel. 2012. *Basic Biomechanics of the Musculoskeletal System*. 4th ed. Baltimore, MD: Lippincott Williams & Wilkins.

Passalacqua, N.V., and T.W. Fenton. 2012. “Developments in Skeletal Trauma: Blunt-Force Trauma.” In *A Companion to Forensic Anthropology*, edited by Dennis C Dirkmaat, 400–411. Chichester, West Sussex, UK: Blackwell Publishing, Ltd.

Reber, S.L., and T. Simmons. 2015. “Interpreting Injury Mechanisms of Blunt Force Trauma from Butterfly Fracture Formation.” *Journal of Forensic Sciences* 60 (6): 1401–11.

Rockhold, L.A., and N.P. Hermann. 1999. “A Case Study of a Vehicular Hit-and-Run Fatality: Direction of Force.” In *Broken Bones: Anthropological Analysis of Blunt Force Trauma*, edited by Alison Galloway, 287–90. Springfield, IL: Charles C. Thomas.

Smith, O.C., E.E. Pope, and S.A. Symes. 2003. “Look until You See: Identification of Trauma in Skeletal Material.” In *Hard Evidence: Case Studies in Forensic Anthropology*, edited by D.W. Steadman, 138–54. Old Tappan, NJ: Pearson Education.

Scientific Working Group for Forensic Anthropology. 2011. "Trauma Analysis." nist.gov/system/files/documents/2018/03/13/swganth_trauma.pdf

Symes, S.A., E.N. L’Abbé, E.N. Chapman, I. Wolff, and D.C. Dirkmaat. 2012. “Interpreting Traumatic Injury to Bone in Medicolegal Investigations.” In *A Companion to Forensic Anthropology*, edited by D.C. Dirkmaat, 340–89. Malden, MA: Wiley-Blackwell.

Symes, S.A., O.C. Smith, H.E. Berryman, C.E. Peters, L.A. Rockhold, S.J. Haun, et al. 1996. “Bones: Bullets, Burns, Bludgeons, Blunderers, and Why.” Workshop conducted at the 48th

Annual Meeting of the American Academy of Forensic Sciences; Nashville, TN.

Teresinski, G., and R. Madro. 1999. “The Evidential Value of Wedge-Shaped Tibial and Femoral Fractures in Cases of Car-to-Pedestrian Collisions.” *Z Zagadnien Nauk Sadowych* 40: 72–85.

Thomas, T.S., and T. Simmons. 2011. “The Relationship between Directionality of Force and the Formation of Butterfly Fractures.” In *Proceedings of the 63rd Annual Meeting of the American Academy of Forensic Sciences*; Chicago, IL.

Ubelaker, D.H., and B.J. Adams. 1995. “Differentiation of Perimortem and Postmortem Trauma Using Taphonomic Indicators.” *Journal of Forensic Sciences* 40 (3): 509-12.

Wheatley, B.P. 2008. “Perimortem or Postmortem Bone Fractures? An Experimental Study of Fracture Occurrences in Deer Femora.” *Journal of Forensic Sciences* 53 (1): 69–72.

Wieberg, D.A.M., and D.J. Wescott. 2008. “Estimating the Timing of Long Bone Fractures: Correlation between the Post-Mortem Interval, Bone Moisture Content, and Blunt Force Trauma Characteristics.” *Journal of Forensic Sciences* 53 (5): 1028–34.

PAPER 5: FRACTURE CHARACTERISTICS IN CONCENTRATED 4-POINT BENDING OF HUMAN FEMORA

Abstract

This paper reports the results of concentrated 4-point bending experiments on nine human femora. Martens and colleagues' (Martens et al. 1986) experimental method was replicated with the goals of producing similar complex fracture patterns and evaluating them using three analytical strategies: fracture morphology, failure mode analysis, and fractography. Fracture morphologies included oblique (3/9) and comminuted (6/9) fractures. Both compression and tension wedge fragments were produced, demonstrating the interpretive limitations of butterfly/wedge morphology. Failure mode analysis could be used to identify compression, tension, and shear features and interpret loading direction in 7/9 experiments. At least one fractographic feature was identified in all femora, but sufficient features to interpret crack propagation were present in only 7/9 experiments. In these cases, interpretations matched actual crack propagation. The results suggest failure mode analysis and fractography can help resolve cases involving extensive fragmentation. However, relevant features must be present to interpret fractures using these strategies.

Introduction

Anthropologists have traditionally used a comparative morphological approach to describe and interpret long bone fractures (L'Abbé et al. 2019). Using this strategy, analysts classify fracture patterns using shape-based (e.g. butterfly, transverse, oblique, spiral) categories or clinical eponyms (e.g., Colles, Messerer, Monteggia). These patterns are often associated with particular types of loading (e.g., bending, torsion) or injury scenarios (e.g., a fall onto an outstretched hand). This terminology can be useful for providing concise, universally understood descriptions of the degree and pattern of trauma (Galloway, Zephro, and Wedel 2014). However, research has shown that morphology is only reliable for describing fractures and not necessarily for interpreting their cause (L'Abbé et al. 2019; Isa et al. 2018; Agnew et al. 2020).

Butterfly fractures present an example of the interpretive limitations of the morphological approach. Butterfly fractures are associated with blunt force impacts causing a bone to bend (Sharir, Barak, and Shahar 2008; Martin et al. 2015; Galloway, Zephro, and Wedel 2014; Gozna, Harrington, and Evans 1982; Smith, Pope, and Symes 2003; Kimmerle and Baraybar 2008a; Levine 1986). Because cortical bone exhibits lower material strength in tension than compression, fracture is expected to initiate at the point of greatest tensile stress opposite the applied load. As the crack progresses, shear stresses exceed the bone's shear strength, causing the crack to branch in the direction of maximal shear before total fracture on the compression side (Sharir, Barak, and Shahar 2008; Martin et al. 2015). The expected result of long bone bending is a triangular fragment with its apex on the tension side. This pattern is sometimes called a "tension wedge" because initial failure occurs on the tension side (Kress et al. 1995), but is more often described as a butterfly fracture due to its winged shape (Rockhold and Hermann 1999; L'Abbé et al. 2019; Ubelaker and Adams 1995; Galloway, Zephro, and Wedel 2014).

Based on this understanding, the presence and orientation of butterfly fractures are often used to infer loading direction (e.g. Rockhold and Hermann 1999; Love and Christensen 2018).

In reality, however, recognition of butterfly morphology is insufficient to interpret this pattern of trauma (L'Abbé et al. 2019). Fractures produced in bending may not exhibit classic butterfly morphology (Kress et al. 1995; Martens et al. 1986; Reber and Simmons 2015; Khalil, Raymond, and Miller 2015; Teresinski and Madro 1999; Agnew et al. 2020; L'Abbé et al. 2019; Isa et al. 2018). Several authors even report butterfly fractures in a reverse orientation (Kress et al. 1995; Martens et al. 1986; Teresinski and Madro 1999). These have been described as "compression wedges" because the apex occurs on the compression side (Kress et al. 1995). These fracture patterns deviate from expectations for long bone bending and cannot be interpreted using traditional comparative morphology. While small percentages have been reported in 3-point bending (Kress et al. 1995), Martens et al. (Martens et al. 1986) report a high frequency of compression wedges in concentrated 4-point bending. This raises two questions: how do these fractures form, and what analytical strategies be applied to interpret them?

A limitation of the morphological approach is that it makes simplistic associations between broad fracture pattern categories and specific injury scenarios. Modern approaches to the analysis of blunt force trauma instead use smaller units of analysis to reconstruct how a bone failed. One strategy involves failure mode analysis, wherein analysts identify fracture characteristics associated with tension, compression, and shear failure. While there is currently a lack of standardized terminology for these features, various authors have discussed similar fracture characteristics (Symes et al. 2012; L'Abbé et al. 2019; Berryman 2014; Rockhold and Hermann 1999; Emanovsky 2015; Isa et al. 2018). In a recent publication L'Abbé et al. (L'Abbé et al. 2019) describe fracture characteristics associated with failure in tension as "[…] straight (in

2-dimensions) with a mottled bone surface in cross-section where perpendicular edges of pulled apart bone are noticeable"; compression characteristics as "zipper-like tears in bone (2-dimensional) with distinct ridges and valleys in cross-section"; and shear characteristics as "curved, diagonal lines across a long bone" (L'Abbé et al. 2019, 190). Using these features, anthropologists were able to determine the direction the bone was bent and, along with soft tissue evidence, determine the impact site in a case study involving a pedestrian-vehicle accident.

Isa et al. (Isa et al. 2018) describe similar fracture characteristics in a sample of femora broken in 3-point bending experiments. Fracture characteristics associated with the path of fracture propagation included a transverse crack at initiation in tension, incomplete fractures branching from the main crack along principal shear planes, failure angle shifts as fracture branches curve to run parallel to the bone's long axis, and breakaway spurs at the point of total fracture in compression. Fracture surfaces were mottled and billowy with relatively flat topography toward the side of the bone under tension, and jagged with steep topography toward the side under compression. Using these features, loading direction could be accurately interpreted for all cases in the experimental sample (Isa et al. 2018).

A recent advance in the analysis of blunt force trauma is the formal application of fractography (Christensen et al. 2018; Love and Christensen 2018; Christensen and Hatch 2019). Fractography is the study of fracture surface features and the relationship of these features to crack propagation (Hull 1999). Fractographic methods have been applied to a variety of industrial materials including metal, glass, and ceramics to interpret the causes of failure. While failure mode analysis could be considered a form of fractography, Christensen et al. (Christensen et al. 2018) recently proposed a method for applying formal, standardized terminology and visualization techniques from the field of fractography to describe and interpret features

observed on fractured bone surfaces. They report the presence of fractographic features in the same 3-point bending sample assessed by Isa et al. (Isa et al. 2018), including bone mirror, bone hackle, wake features, arrest ridges, and cantilever curl, and obtain low inter- and intra-observer error using these features to determine crack propagation direction. As expected, crack propagation opposed loading direction in all cases.

Recent studies suggest the promise of failure mode analysis and fractography for interpreting skeletal trauma in forensic cases. However, continued research on the applications of these methods is useful to clarify their strengths and limitations. In the 3-point bending sample investigated by Isa et al. (Isa et al. 2018) and Christensen et al. (Christensen et al. 2018), experiments generally produced one primary fracture. This meant that assessment included one of two complementary fracture surfaces (proximal and distal), and crack propagation was evaluated in one direction (e.g., posterior to anterior). It is of interest to evaluate whether these methods can be applied to resolve more complex cases, like the compression wedge fractures produced using Martens and colleagues' loading configuration (Martens et al. 1986).

In order to investigate the phenomenon of compression wedge fractures, the current study replicated the experimental methods of Martens et al. (Martens et al. 1986) with the goal of generating similar fracture patterns in human femora. Subsequently, three analytical strategies (comparative morphology, failure mode analysis and forensic fractography of bone) were applied to interpret the resulting fractures. The specific goals of this study were 1) to perform Martens-style concentrated 4-point bending experiments on human femora; 2) to document fracture formation in these experiments using high-speed video; 3) to apply each analytical strategy to describe and interpret fractures; and 4) to compare interpretations to documented fracture propagation and loading direction.

Materials and Methods

Specimens

The experimental sample included nine whole, biomechanically fresh human femora obtained from adult male donor cadavers. These included five unpaired femora and two pairs of femora from seven individuals. The procurement organizations obtained consent for research on donor remains in accordance with the Uniform Anatomical Gift Act. Femora were stored at -20 °C and thawed completely at room temperature before testing. Storage at this temperature has been shown to have a negligible effect on the mechanical properties of bone (Cowin 2001; Kaye et al. 2012; van Haaren et al. 2008). Prior to experimentation, each femur was dissected and carefully cleaned of soft tissue. This enabled proper anatomical orientation of specimens within the experimental fixture and allowed for visualization of fracture propagation during testing.

Concentrated 4-point bending experiments

Bending is the most common method used to test the mechanical performance of whole bones (Sharir, Barak, and Shahar 2008). Testing is typically performed using one of two methods: 3-point and 4-point bending. In 3-point bending the bone is positioned on two supports. A one-pronged loading device is applied to the opposite surface at a point halfway between the two outer supports. In this type of test, the maximum load occurs at the point of load application. In 4-point bending, however, a two-pronged loading device is applied to the opposing surface equidistant from the two outer supports. This testing method subjects the entire section of bone between the two loading prongs to a uniform moment (Sharir, Barak, and Shahar 2008).

In the current study, experiments were performed with a custom-built fixture (Figure 5.1) installed onto a servo-hydraulic machine (Instron; Norwood, MA). This fixture was used to apply concentrated 4-point bending loading according to the specifications reported by Martens

et al. (Martens et al. 1986). Each femur was placed onto adjustable outer supports positioned at a distance equivalent to 60% of the maximum length. Two inner loading probes were placed at the midshaft at a distance equivalent to 10% of the maximum length. This paper refers to the current experiments and those of Martens et al. as "concentrated" 4-point bending because the loading points are more closely positioned than in typical 4-point bending tests.

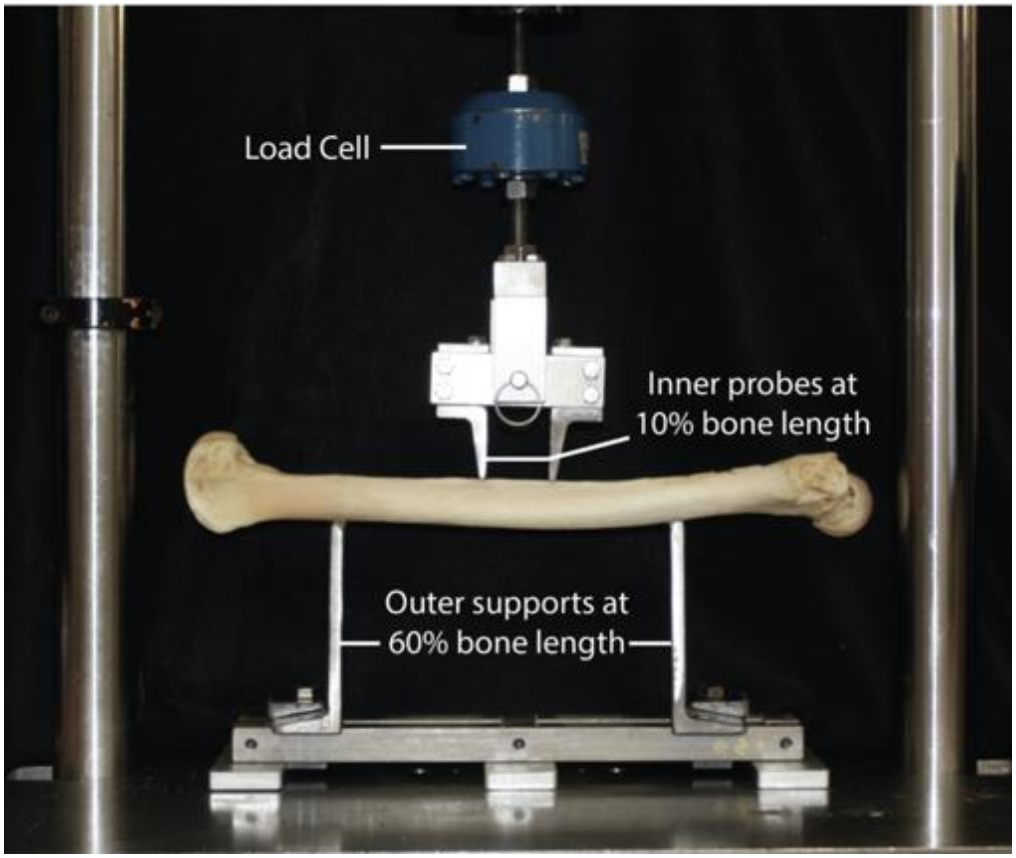

Figure 5.1: Concentrated 4-point bending fixture following the specifications described by Martens et al. (1986). Image depicts posterior loading.

The five unpaired femora were placed in the impact fixture such that the anterior diaphysis rested on the outer supports and the loading probes were applied to the posterior diaphysis. For the two sets of paired experiments, the left femur was loaded on the posterior surface and the right femur was loaded on the anterior surface.

Failure was induced via position-controlled displacement of the loading probes at a rate of 2 Hz over 20 mm. Force and displacement data were recorded by an actuator-mounted load transducer (3210AF-5K, 5000 lb capacity, Interface; Scottsdale, AZ) and a linear variable differential transformer (LMT-711P35, ±3.5" stroke, G.L. Collins Corporation; Long Beach, CA). Energy to failure was calculated as the area under the load-displacement curve up to the peak load.

All experiments were filmed with a high-speed camera (Fastcam Mini AX 200, Photron Ltd; Tokyo, Japan) at 40,000 frames per second. All images were oriented such that the distal end of the femur was at image left and the impact surface was up. Photron software was used to generate still frames of fracture propagation throughout each experiment. These images were used to assess fracture initiation and termination relative to the loading sites for each experiment.

Fracture assessment

Following experimentation, femora were cleaned of remaining soft tissue using hot water maceration. Relevant features of the fractures and their surfaces were subsequently documented and assessed. Complete fracture morphology was assessed to allow for comparison of results with other long bone bending studies. Fractures were classified as "transverse" (approximately perpendicular to the bone's long axis), "oblique" (diagonal to the bone's long axis), or "comminuted" (dividing the bone into more than two pieces) (Galloway, Zephro, and Wedel 2014). Comminuted fractures were further assessed for the presence of wedge fragments. Following Kress et al. (Kress et al. 1995), these were classified "tension wedge" if the apex was positioned toward the tension side (opposing the applied load) and "compression wedge" if the apex was positioned toward the compression (loading) side.

Femora were also assessed for the presence of fracture characteristics associated with tension, compression, and shear failure modes (Table 5.1). While there is currently no standard terminology for these fracture characteristics, descriptions are based on those provided by L'Abbé et al. (L'Abbé et al. 2019) and Isa et al. (Isa et al. 2018) as discussed above**.**

Failure mode	Fracture characteristics
Tension	Straight fracture margin (viewed in 2 dimensions) with perpendicular edges and a mottled, billowy fracture surface
Shear	Fractures angle and/or branch from the main crack at initial angles of 30-45 degrees and may eventually curve along the long axis of the bone
Compression	Saw-toothed or zipper-like fracture margin (viewed in 2 dimensions) with triangular ridges and valleys in cross-section

Table 5.1: Failure mode fracture characteristics. Adapted from L'Abbé et al. (L'Abbé et al. 2019) and Isa et al. (Isa et al. 2018).

Fracture surfaces were examined for the presence of fractographic features described by Christensen et al. (Christensen et al. 2018) and Love and Christensen (Love and Christensen 2018) (Table 5.2). Prior to examination, the fracture surfaces of each bone fragment were coated with dual-contrast fingerprint powder in order to enhance visualization of the features of interest. These surfaces were then examined macroscopically using oblique lighting.

Feature	Definition
Bone mirror	A relatively featureless region of a fractured bone surface near the fracture initiation site
Bone hackle	Angular or rounded ridges aligned in the direction of propagation resulting from increasing crack speed and instability
Arrest ridges	Large raised ridges or peaks perpendicular to the direction of crack propagation resulting from drastic changes in crack propagation velocity
Cantilever curl	A curved lip that occurs just before total fracture of a bone loaded in bending.

Table 5.2: Fractographic features. Definitions follow Love and Christensen (Love and Christensen 2018).

Interpretation

Failure mode analysis was applied to interpret failure in tension, compression, and shear. The orientation of these fracture characteristics was used to interpret the direction the bone bent

prior to failure. Given prior knowledge of unidirectional bending, loading direction was inferred from bending direction. Fractography was applied to interpret fracture propagation including the location of crack initiation and termination sites. Given prior knowledge of unidirectional bending, loading direction was interpreted opposite the direction of initial crack propagation. Finally, interpretations were compared to the actual loading direction and fracture propagation sequences captured in experiment videos.

Results

All 4-point bending experiments produced fracture. Maximum failure loads ranged from 5039.4 to 9040.8 N (mean=7195.7±1408.6 N). Maximum displacement prior to failure ranged from 6.4 to 10.9 mm (mean =8.4±1.7 mm). The energy absorbed prior to failure ranged from 17.9 to 57.2 J (mean=35.9±15.4 J). Results for each experiment are shown in Table 5.3.

Specimen	Side	Load	Max Load (N)	Max Displacement (mm)	Energy Absorbed (J)
16-2048	L	PA	5039.4	6.55	17.9
16-2031	L	PA	5864.4	6.43	20.4
16-2021	L	PA	6405.1	7.66	26.9
17-0006	R	AP	6812.2	6.50	22.7
16-2047	R	PA	6959.5	8.46	33.2
16-0044	R	AP	7056.1	8.46	28.3
16-2073	R	PA	8565.0	10.85	57.2
17-0006	L	PA	9019.1	10.28	53.1
16-0044	L	PA	9040.8	9.95	50.0

Table 5.3: Mechanical results.

Fracture initiated from a single location in all nine experiments. While propagation sequence differed in each experiment, two general patterns were observed. In 7/9 experiments initial failure occurred within the midshaft loading region, opposite one of the loading probes or between probes. In 2/9 experiments (16-2031 and 16-2048) fractures initiated in the distal shaft and terminated on the loading surface near the distal probe. Crack propagation for each experiment is shown in the Appendix of this chapter.

Fracture morphology

Complete fracture types included oblique and comminuted fractures (Figures 5.2 and 5.3). Among the seven posterior loading experiments, two produced oblique fractures of the distal shaft and five produced comminuted midshaft fractures, three of which exhibited wedge fragments. Two experiments (16-2073 and16-2021) produced compression wedge fragments while the third (17-0006 L) produced a tension wedge fragment. One anterior loading experiment (17-0006 R) produced comminuted midshaft fractures without wedge fragments. The other anterior loading experiment (16-0044 R) produced an oblique midshaft fracture.

Failure mode analysis

Fracture characteristics indicative of tension, compression, and shear were present in 7/9 experiments. These were identified in cases involving midshaft failure but not in the two experiments involving failure in the distal shaft (16-2031 and 16-2048). In each of the seven cases in which they were present, tension characteristics (straight margins, mottled fracture surface) were identified at one location corresponding to the site of fracture initiation. In contrast, compression characteristics (zipper-like margins, ridges and valleys) were often identified at multiple locations. These occurred only where fractures terminated on the loading surface; they were not observed where fractures terminated on the opposing surface.

Fracture angulation and curvature indicative of shear failure occurred between the areas of tension and compression. Incomplete fracture branches were always concentrated near the tensile initiation site. Incomplete fracture branches terminated as they approached the longitudinal axis. However, complete fracture branches often continued to curve, terminating on the surface opposite the applied load.

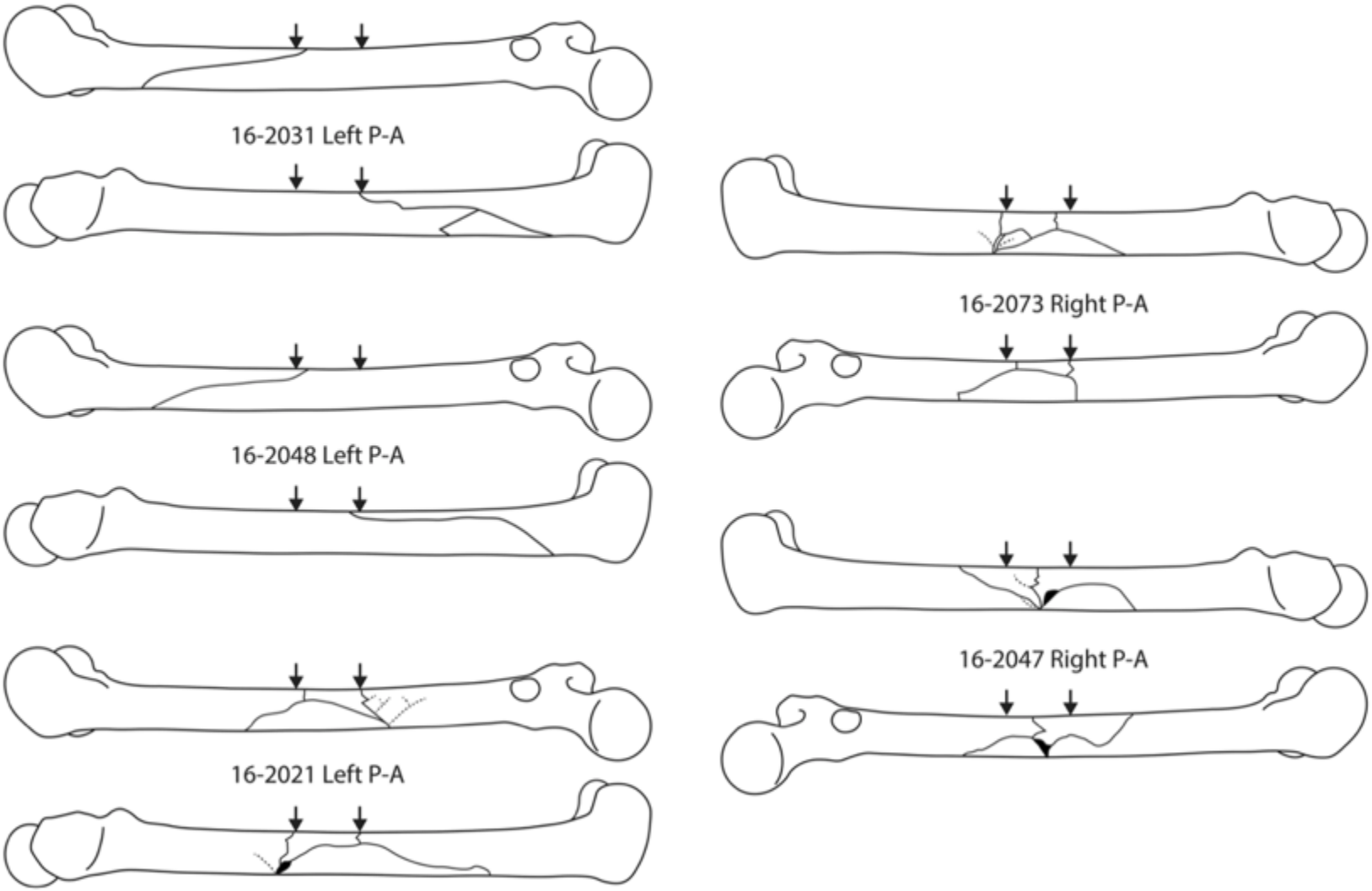

Figure 5.2: Unpaired experiments. Loading was applied posterior to anterior at the location indicated by the arrows. The solid lines indicate complete fractures while the dashed lines indicate incomplete fractures.

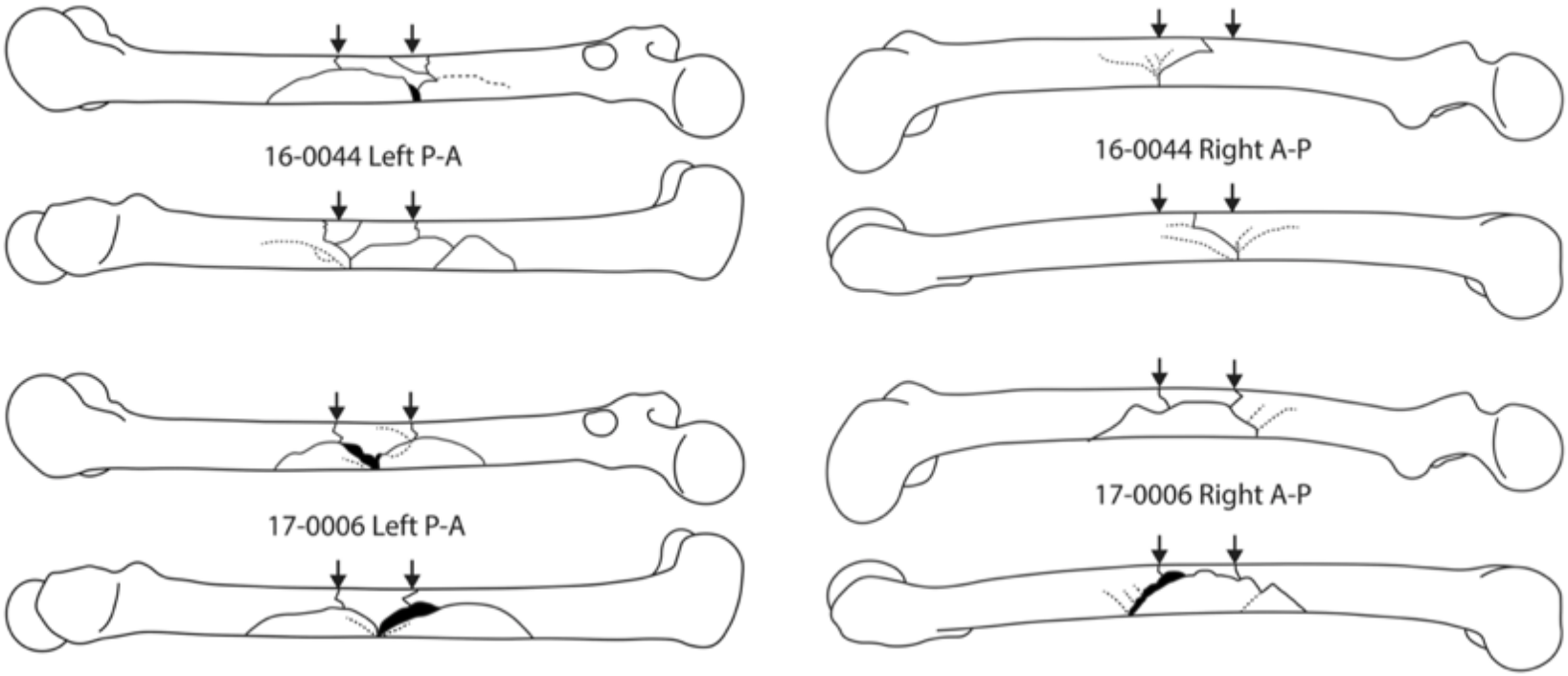

Figure 5.3: Paired experiments. Loading was applied to left femora posterior to anterior and to right femora anterior to posterior at the locations indicated by the arrows. The solid lines indicate complete fractures while the dashed lines indicate incomplete fractures.

Fractography

Nine bending experiments produced 35 bone fragments examined for fractographic features. Table 5.4 summarizes the presence of these features on each fragment. The number of features observed in a single fragment ranged from 0 to 4 (m=2.5±1.1).

Bone mirror was the least frequently observed fractographic feature in the sample. It was present in at least one fragment in 7/9 femora and in 10/35 total fragments examined (Table 5.4; Figure 5.4). Mirror occurred only in the area corresponding to initial failure. Because fracture initiated from exactly one location in each experiment, only fracture surfaces at that location exhibited bone mirror. Articulating fracture surfaces did not always display mirror. It is possible that this is due to the loss of small fragments of bone at the initiation site (see Appendix).

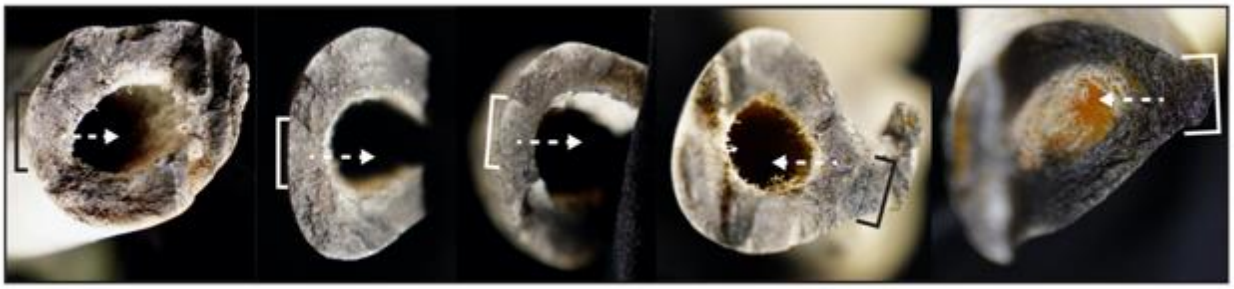

Figure 5.4: Examples of bone mirror in the the 4-point bending sample. Anterior is image left. Brackets denote bone mirror and dashed lines denote direction of crack propagation. Fragments pictured: 16-2021 D; 17-0006 L D; 16-2073 C; 17-0006 R A; 16-2047 A.

Bone hackle was the most frequently observed fractographic feature. It was present in at least one fragment in all nine femora and in 32/35 total fragments examined (Table 5.4; Figure 5.5). Because fractures propagated in multiple directions after initiation, hackle was often observed in multiple planes within a single specimen.

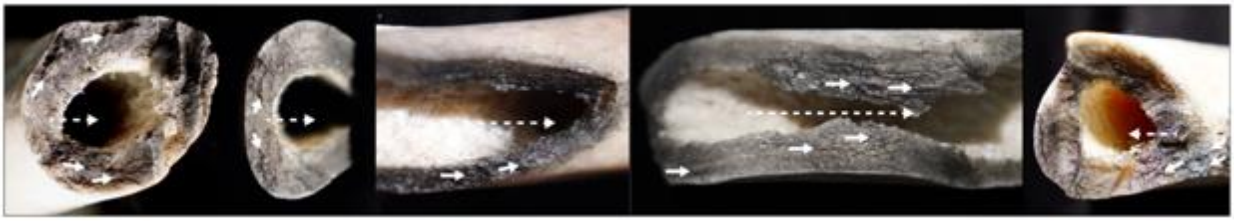

Figure 5.5: Examples of bone hackle in the the 4-point bending sample. Anterior is image left. Solid lines denote bone hackle and dashed lines denote direction of crack propagation. Fragments pictured: 16-2021 D; 17-0006 L D; 16-2021 A; 16-2021 B; 17-0006 R A.

Arrest ridges were present in at least one fragment in 7/9 femora and in 23/35 total fragments examined (Table 5.4; Figure 5.6). This feature occurred in areas approaching total fracture. Because there were often multiple sites of fracture termination in a single femur, arrest ridges were present on multiple fragments and in multiple locations.

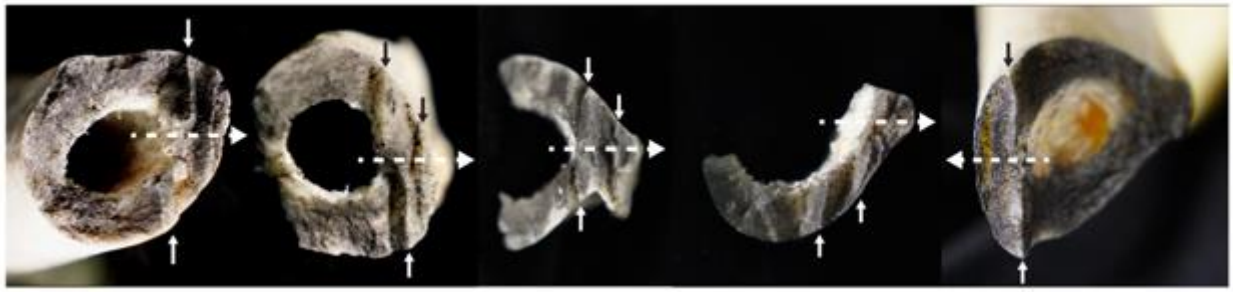

Figure 5.6: Examples of arrest ridges in the the 4-point bending sample. Anterior is image left. Solid arrows denote arrest ridges and dashed lines denote direction of crack propagation. Fragments pictured: 16-2021 D; 17-0006 R D; 17-0006 L C; 17-0006 R A; 16-2047 A.

Cantilever curl was present in at least one fragment in 7/9 femora and in 21/35 total fragments examined (Table 5.4; Figure 5.7). Like arrest ridges, cantilever curl was often present on multiple fragments in a single femur due to the production of multiple termination sites.

Interpretations

Table 5.5 summarizes the interpretations made using failure mode analysis and fractography for the 4-point bending sample. Loading direction was accurately interpreted using failure mode analysis in 7/9 experiments. Figure 5.8 provides examples of interpretations made using failure mode analysis.

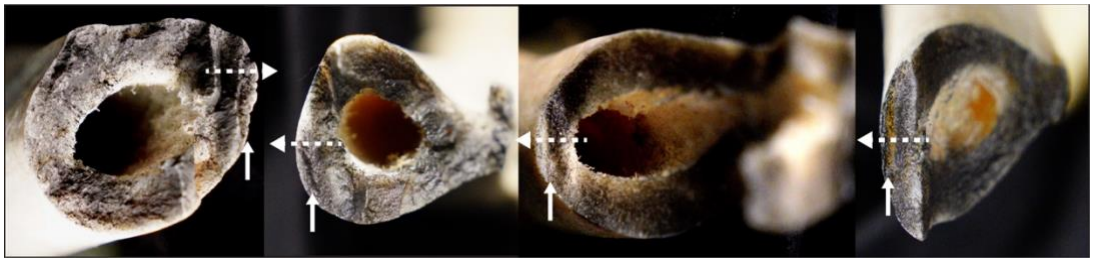

Figure 5.7: Examples of cantilever curl in the 4-point bending sample. Anterior is image left. Solid arrows denote cantilever curl and dashed lines denote direction of crack propagation. Fragments pictured: 16-2021 D; 17-0006 R A; 16-2047 D; 16-2047 A.

Crack propagation was accurately interpreted using fractography in 7/9 experiments. In each of these cases, interpreted initiation sites matched initiation sites observed in experiment video. Many femora exhibited multiple termination sites. When fractographic features were present at these locations, termination sites were accurately interpreted. However, some termination sites could not be interpreted due to the absence of relevant fractographic features. For the seven aforementioned experiments loading direction was accurately interpreted based on the direction of initial crack propagation. Figure 5.9 provides an example of interpretations made using fractography. Due to the absence of relevant features in experiments 16-2031 and 16-2048, loading direction could not be interpreted using either failure mode analysis or fractography.

Specimen	Side	Load	Fragments	Type	Fragment	BM	BH	AR	CC
16-2031	**L**	PA	3	Oblique distal	A	0	0	0	0
					B	0	1	0	0
					C	0	1	0	0
16-2048	**L**	PA	2	Oblique distal	A	0	0	0	0
					B	0	1	0	0
16-2021	**L**	PA	4	Comminuted	A	0	1	1	1
					B	1	1	0	0
					C	0	1	1	1
					D	1	1	1	1
16-2073	**R**	PA	5	Comminuted	A	0	1	1	0
					B	0	1	1	1
					C	0	1	0	0
					D	1	1	0	0
					E	0	1	1	1
16-2047	**R**	PA	4	Comminuted	A	0	1	0	0
					B	0	1	1	1
					C	1	1	1	1
					D	0	1	1	1
16-0044	**L**	PA	6	Comminuted	A	0	1	1	1
					B	1	1	1	1
					C	0	1	1	1
					D	0	0	1	1
					E	0	1	1	1
					F	1	1	0	0
	R	AP	2	Oblique midshaft	A	1	1	1	1
					B	1	1	0	1
17-0006	**L**	PA	5	Comminuted	A	0	1	1	1
					B	0	1	1	0
					C	0	1	1	1
					D	1	1	1	0
					E	0	1	1	1
	R	AP	4	Comminuted	A	0	1	1	1
					B	0	1	0	0
					C	0	1	1	1
					D	1	1	1	1

Table 5.4: Presence of fractographic features in the 4-point bending sample. Bone mirror=BM, bone hackle=BH, arrest ridges=AR, cantilever curl=CC; present=1, absent=0). Fragments are labeled in figures in the Appendix.

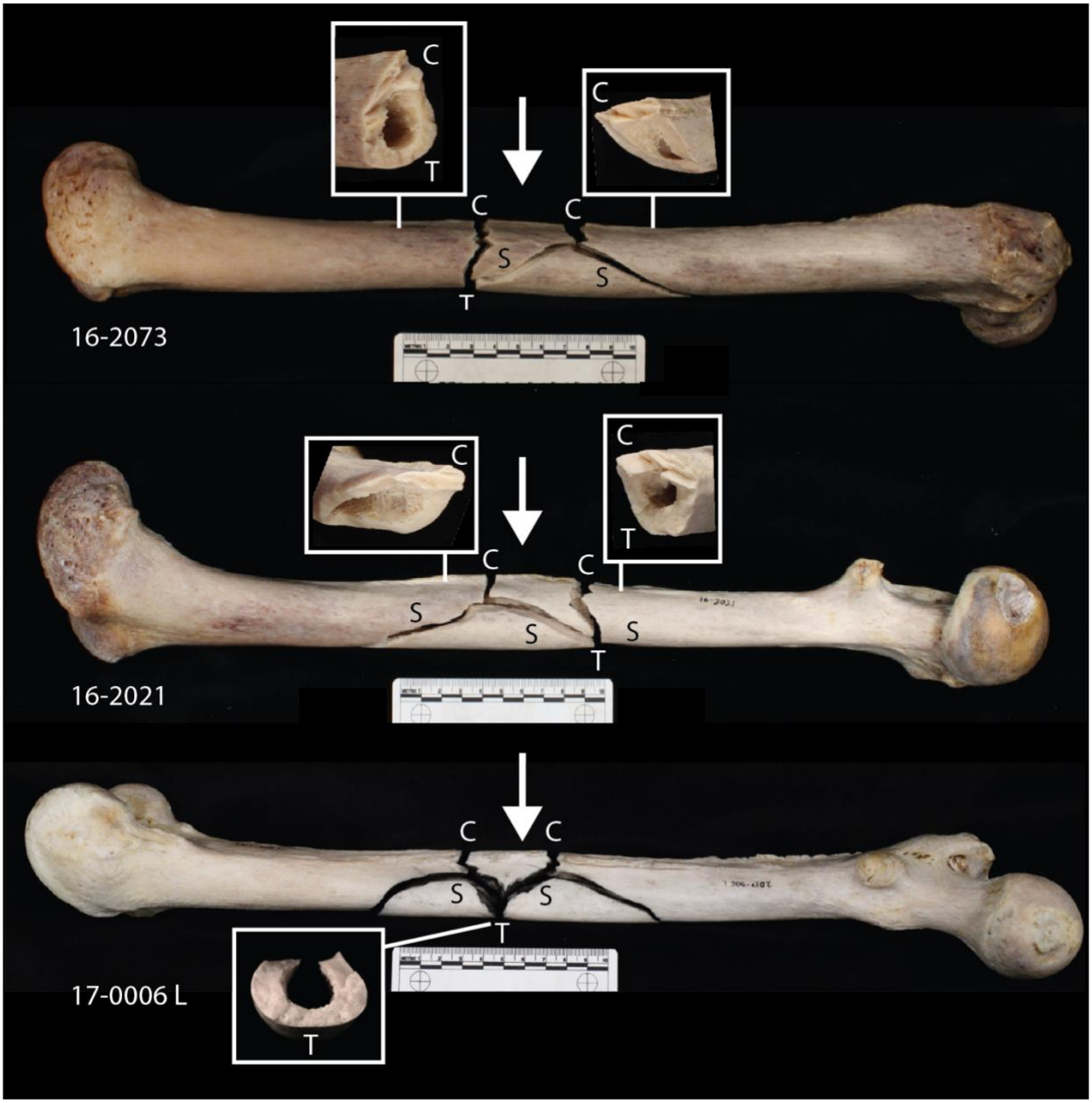

Figure 5.8: Examples of failure mode analysis in three specimens (16-2073, 16-2021, 17-0006 L). Fracture characteristics of tension (T), shear (S), and compression (C) are indicated. Large arrow represents interpreted loading direction for the experiment.

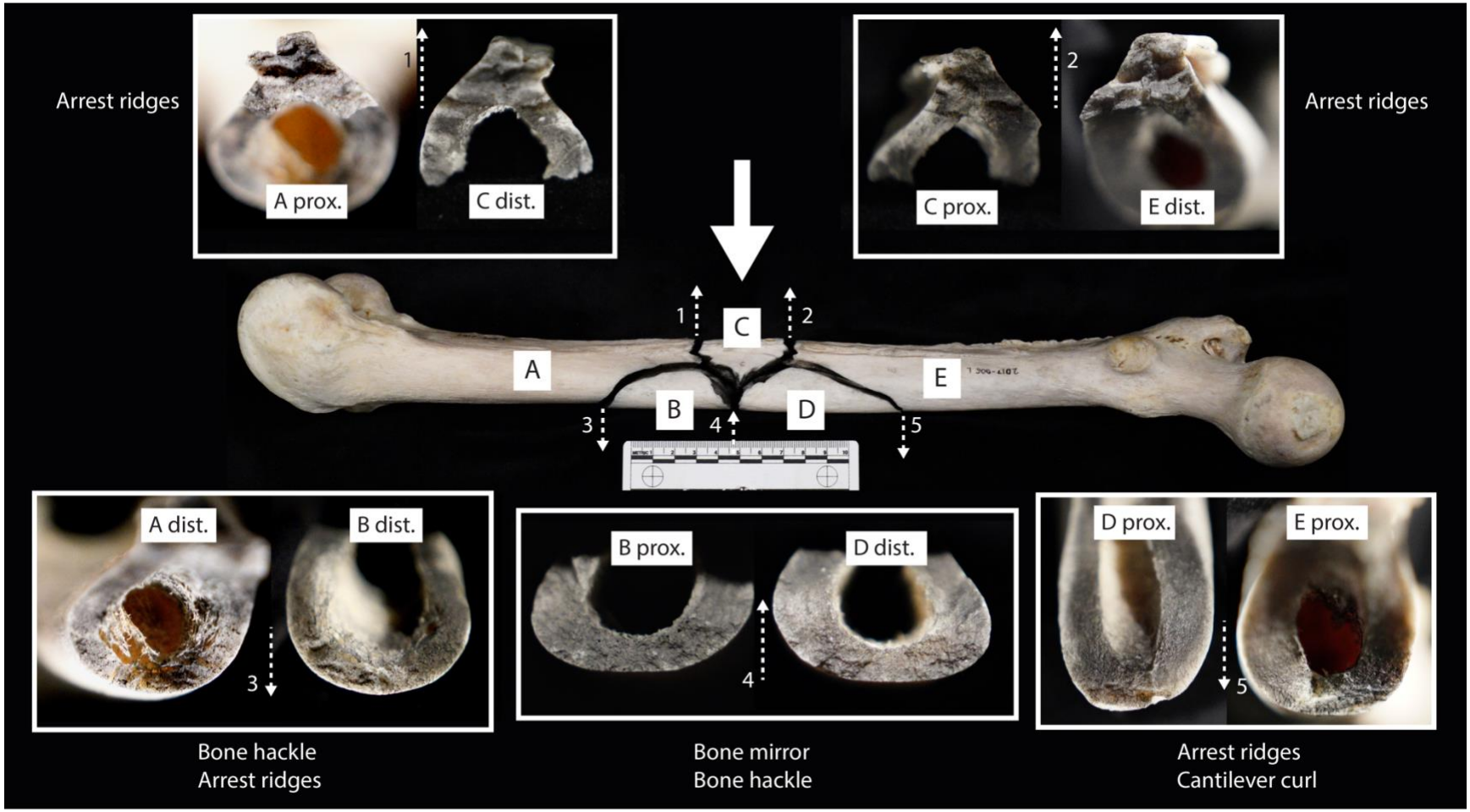

Figure 5.9: Detailed example of fractographic interpretation in specimen 17-0006 L. Dashed lines indicate interpreted crack propagation direction. Large solid arrow indicates interpreted loading direction for the experiment. Fractographic assessment revealed bone mirror on the anterior distal surface of D, indicating the site of fracture initiation. Arrest ridges were observed at multiple locations, indicating two fracture termination sites in the posterior midshaft (fragments A proximal/C distal; fragments C proximal/E distal), one in the anterior distal shaft (fragments A and B distal) and one in the anterior proximal shaft (fragments D and E proximal). Based on the anterior initiation site, loading direction is interpreted as posterior to anterior.

			Failure Mode Analysis			Fractography	
Specimen	**Side**	**Load**	**Tension**	**Compression**	**Load**	**Initiation**	**Termination**
16-2031	L	PA	-	-	-	-	-
16-2048	L	PA	-	-	-	-	-
16-2021	L	PA	Ant. Prox.	Post.	PA	Ant. Prox.	Post. (2)
16-2073	R	PA	Ant. Dist.	Post.	PA	Ant. Dist.	Post. (2)
16-2047	R	PA	Ant. Dist.	Post.	PA	Ant. Dist.	Post. (2)
16-0044	L	PA	Ant. Prox.	Post.	PA	Ant. Prox.	Ant. Prox. Post. (3)
	R	AP	Post.	Ant.	AP	Post.	Ant. Dist. Ant.
17-0006	L	PA	Ant. Mid.	Post.	PA	Ant. Mid.	Post. (2)
	R	AP	Post. Prox.	Ant.	AP	Post. Prox.	Ant. Prox. Ant. Dist. Ant. (2) Post. Dist.

Table 5.5: Interpretations made using failure mode analysis and fractography. Interpretations could not be made using either method for two specimens (16-2031 and 16-2048) due to the absence of relevant features.

Discussion

The first goal of the current study was to perform concentrated 4-point bending experiments according to the methods reported by Martens et al. (Martens et al. 1986) with the aim of producing similar fracture patterns and documenting their formation. The majority of the current experiments (7/9) produced fractures in the midshaft loading region, while two experiments produced oblique fractures of the distal shaft. These results are consistent with those of Martens and colleagues (Martens et al. 1986). They report midshaft bending fractures in most experiments (28/33) and oblique distal shaft fractures in a smaller number of cases (5/33).

However, the current results contrast with Martens and colleagues' findings on fracture patterns. Martens et al. report midshaft fractures occurred in a "Y-shaped" pattern resulting in the

separation of a triangular wedge of bone. These fractures were always oriented with the wedge apex toward the posterior surface, regardless of whether loading was applied posteriorly or anteriorly. Subsequently, they hypothesize that the "Y" or wedge orientation is determined by the structural geometry of the posterior femoral shaft (particularly the linea aspera) rather than the loading direction (Martens et al. 1986). In the current study only 3/7 posterior loading experiments produced wedge fractures. In two cases, the apex was oriented posteriorly (consistent with Martens et al.) while in the third the apex was oriented anteriorly (not consistent with Martens et al.). Neither of the two anterior bending experiments produced wedge fractures. Therefore, the results are inconclusive as to the relationship between loading direction and wedge orientation. However, the results indicate that structural geometry is not the only determinant, as posterior loading experiments produced fractures with apices oriented both anteriorly and posteriorly.

Another goal of the current study was to evaluate the fracture patterns produced in these experiments using three analytical frameworks (comparative morphology, failure mode analysis, and fractography). The current concentrated 4-point bending experiments produced fracture patterns more complex than those reported in 3-point bending of human femora (Fenton et al. 2012; Christensen et al. 2018; Isa et al. 2018). Additionally, most of the current 4-point bending experiments produced multiple fragments, making this sample a unique test case for evaluating various methods of interpreting long bone fractures.

The findings of this study demonstrate several limitations of the comparative morphology approach to trauma analysis. First, the use of categories based on complete fracture morphology provides little information about the events causing fracture. Four-point bending experiments produced a variety of complete fracture patterns including oblique and comminuted fractures

with and without wedge fragments. This result is consistent with other experimental studies that have demonstrated variation in fracture patterns produced under the same loading conditions (Fenton et al. 2012; Martens et al. 1986; Kress et al. 1995; Reber and Simmons 2015; Khalil, Raymond, and Miller 2015; Agnew et al. 2020; Isa et al. 2018). Second, the results indicate that loading direction cannot be interpreted based on complete fracture morphology. Two experiments produced butterfly fractures with the wedge apex on the compression (loading) side rather than the expected tension side. Finally, the designations "compression wedge" and "tension wedge" are purely descriptive and are unrelated to the manner in which these fractures form. Experiment videos demonstrate that regardless of wedge orientation, fractures always initiated on the side of the bone under tensile stress. These results are consistent with those of Reber and Simmons (Reber and Simmons 2015). In experiments on sheep femora, they report fracture initiation always occurred in tension regardless of the location of wedge fragments.

In contrast, the results of the study suggest that analysis of failure modes (i.e., tension, compression, and shear) can be applied to describe and interpret fracture characteristics in cases involving complex fractures produced in bending. Fracture characteristics indicative of tension, shear, and compression were identified in 7/9 of the current experiments. Given prior knowledge of unidirectional bending, loading direction could be accurately interpreted in each of these cases. Loading direction could only be interpreted in experiments where failure occurred at the midshaft between the inner loading probes, the region theoretically experiencing the maximum bending moment. In contrast, experiments producing failure of the distal shaft produced limited features used in failure mode analysis or fractography. Martens et al. (Martens et al. 1986) hypothesize that failure occurs in the distal femur when shear force in this region is critical, causing fracture at a location with a lower bending moment.

While similar, failure mode analysis and fractography involve different analytical strategies. Failure mode analysis is used to identify fracture characteristics indicative of failure in tension, shear, and compression and subsequently interpret how a bone was bent prior to failure (i.e., areas of convexity and concavity). In contrast, the forensic fractography of bone method (Christensen et al. 2018) is applied to determine the location of crack nucleation and direction of crack propagation. While it has yet to be specifically tested outside the context of bending, this method is hypothetically applicable in other types of failure besides bending.

The results of the current study provide evidence fractography can be applied to assess crack propagation in cases involving complex fracture patterns produced in bending. At least one fractographic feature was present in all nine femora and in 32/35 fragments examined in the sample. Using these features, it was possible to interpret crack propagation in the seven experiments involving midshaft failure. Fractographic interpretations matched video of crack initiation and propagation in all cases. However, with the exception of bone hackle, fractographic features were mostly absent in the two femora exhibiting distal oblique fractures. In the absence of additional evidence of crack nucleation or termination crack propagation could not be interpreted. One possible explanation for the absence of these features is fracture surface area. Cortical bone was particularly thin in both femora. Love and Christensen (Love and Christensen 2018) report fewer fractographic features when fracture surface area is small.

This work represents a focused investigation of fractures produced under concentrated 4-point bending, a specific set of experimental loading conditions. Advantages of experimental trauma studies are that they make possible direct observation of fracture formation as well as direct comparison between interpretations and known loading. However, there are several limitations associated with this and other experimental studies.

First, the conditions tested in these experiments are simplistic compared to those involved in real-world forensic cases. This study applied Martens and colleagues' (Love and Christensen 2018) experimental methods with the goal of replicating their fracture results, specifically the production of compression wedge fractures. These experiments involved quasistatic loading rather than dynamic impacts, as would be expected in forensic cases. Furthermore, forensic cases likely involve the application of multiple types and directions of forces. In contrast, the current study applied only a unidirectional bending load. The methods investigated in this study should also be explored cases involving different types of loading conditions and in different areas of the skeleton. Finally, while the methods presented here describe the interpretation of fracture on individual bones, trauma analysis in forensic cases must also consider the total bone trauma pattern and contextual information available (L'Abbé et al. 2019).

Conclusions

This paper contributes new data on the utility of various analytical frameworks for describing and interpreting long bone fractures in a sample of experimentally generated blunt force trauma. The implications of this research for practice are as follows.

First, while shape-based morphological categories can be useful for concisely describing complete fracture patterns, the results of this study demonstrate limitations of using these categories to interpret fractures. The orientation of wedge fragments could not be used to interpret loading direction. Experiments produced fragments in both "compression wedge" and "tension wedge" orientations relative to the loading surface. However, even the categories of "compression wedge" and "tension wedge" should be understood as descriptive rather than interpretive terms. Experiment video showed that regardless of complete fracture morphology all fractures initiated in tension, consistent with expectations based on mechanical theory.

Second, this study attempts to systematically investigate fracture characteristics various authors have associated with tension, compression, and shear failure in a sample of experimentally generated trauma. The results demonstrate these characteristics can be identified in cases involving complex long bone fractures produced in bending. In the current sample, this process led to correct interpretation of loading direction in all cases for which these features were present.

Finally, this study contributes data to the growing body of research on the application of fractography to skeletal trauma analysis. One contribution of this study is that it demonstrates fractography can be used to reconstruct multidirectional crack propagation paths generating multiple bone fragments. Even small and irregularly shaped fragments contained features useful for reconstructing crack propagation. Another contribution of this study to fractography is the use of video confirmation of results. Fractographic interpretations matched direct observations of crack propagation in all cases.

APPENDIX

APPENDIX

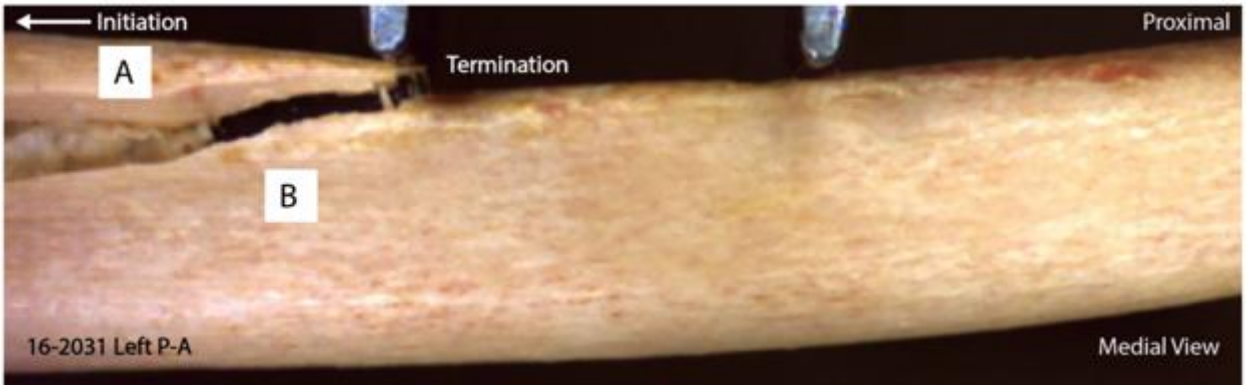

Figure A.1: Video still showing fracture propagation in 16-2031. Loading direction is posterior to anterior. Crack propagation is from anterior distal to posterior proximal.

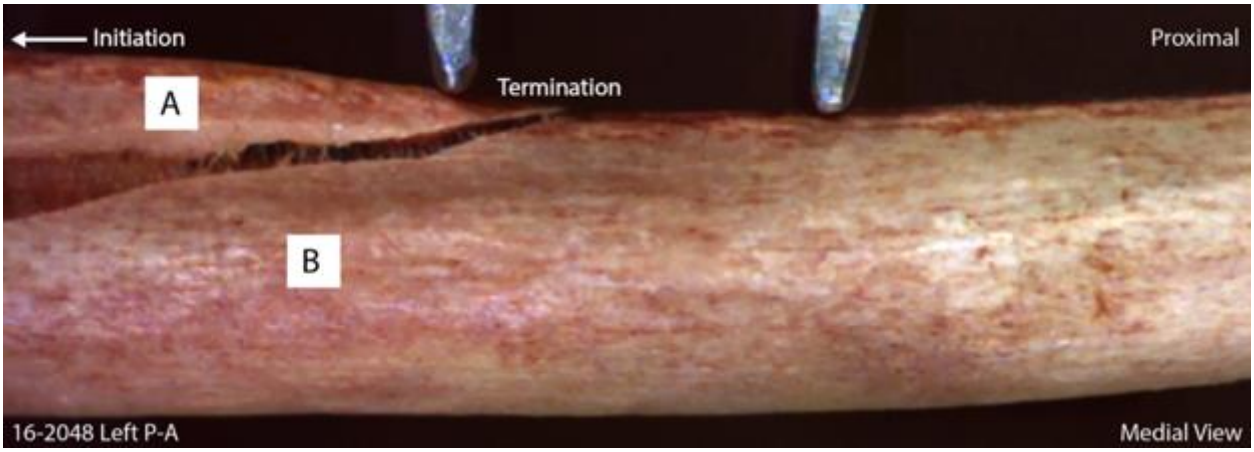

Figure A.2: Video still showing fracture propagation in 16-2048. Loading direction is posterior to anterior. Crack propagation is from anterior distal to posterior proximal.

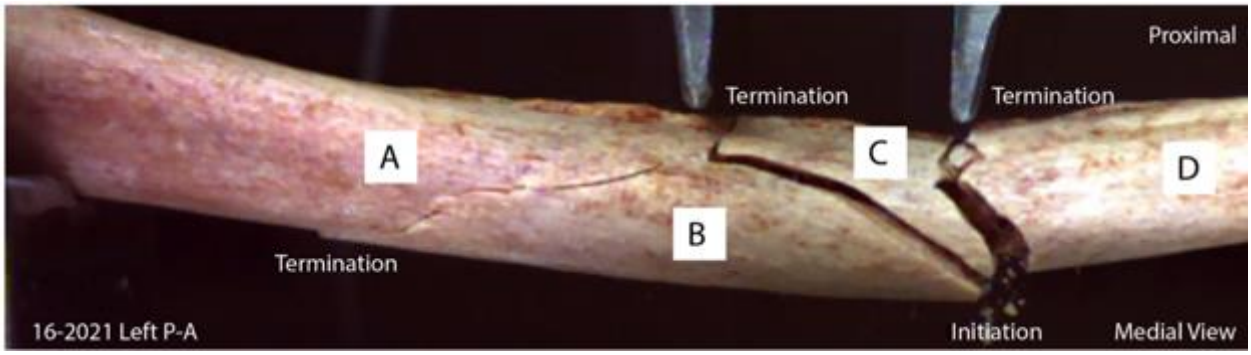

Figure A.3: Video still showing fracture propagation in 16-2021. Loading direction is posterior to anterior. Crack initiation is anterior proximal. Crack terminations are posterior (2) and anterior distal.

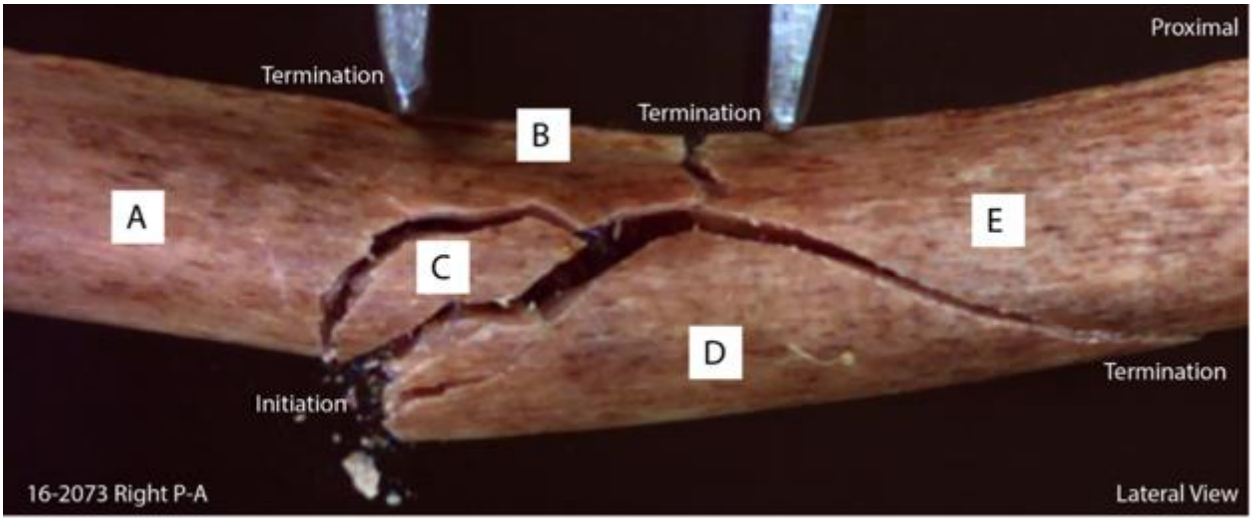

Figure A.4: Video still showing fracture propagation in 16-2073. Loading direction is posterior to anterior. Crack initiation is anterior distal and crack terminations are posterior (2) and anterior proximal.

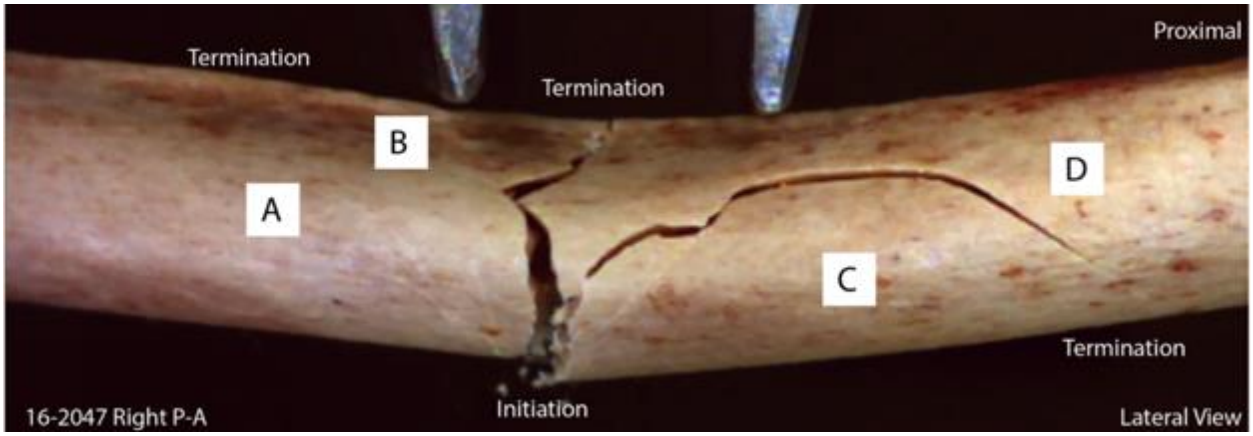

Figure A.5: Video still showing fracture propagation in 16-2047. Loading direction is posterior to anterior. Crack initiation is anterior distal and crack terminations are posterior (2) and anterior proximal.

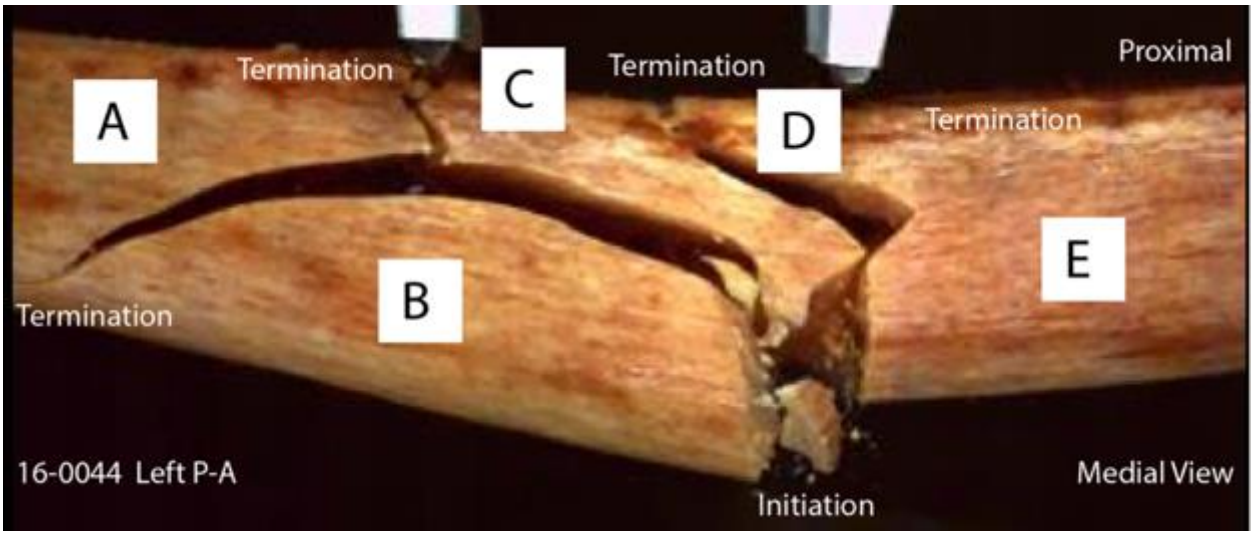

Figure A.6: Video still showing fracture propagation in 16-0044 L. Loading direction is posterior to anterior. Crack initiation is anterior proximal and crack terminations are posterior (3) and anterior distal.

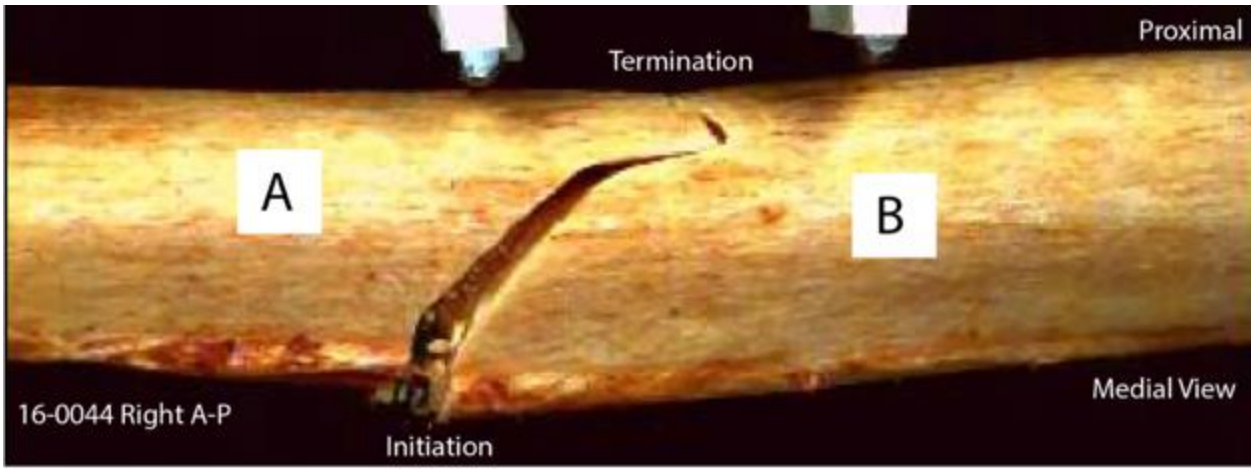

Figure A.7: Video still showing fracture propagation in 16-0044 R. Loading direction is anterior to posterior. Crack propagation is from posterior to anterior.

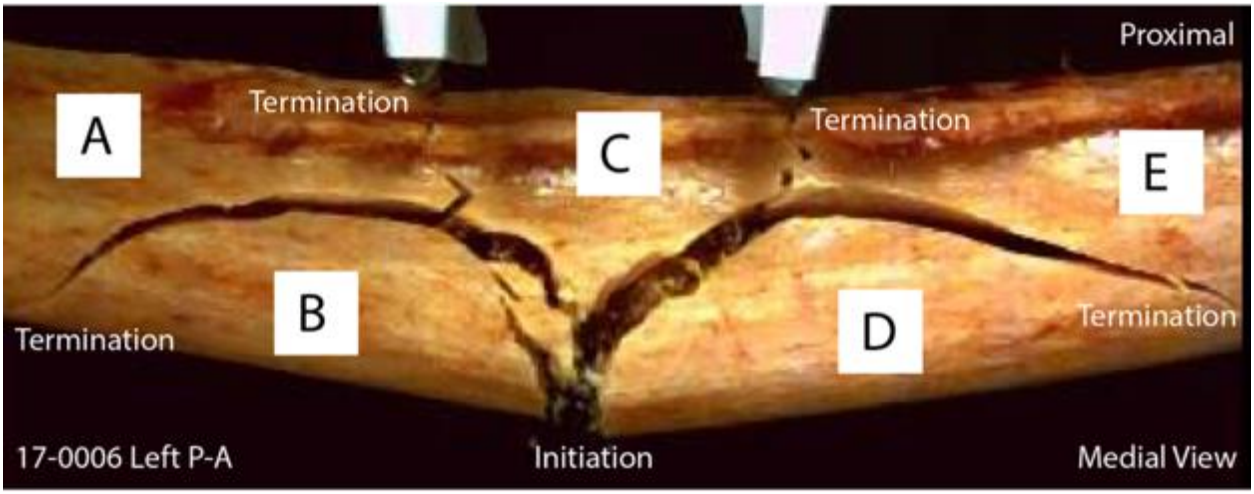

Figure A.8: Video still showing fracture propagation in 17-0006 L. Loading direction is posterior to anterior. Crack initiation is anterior midshaft and crack terminations are posterior (2), anterior distal, and anterior proximal.

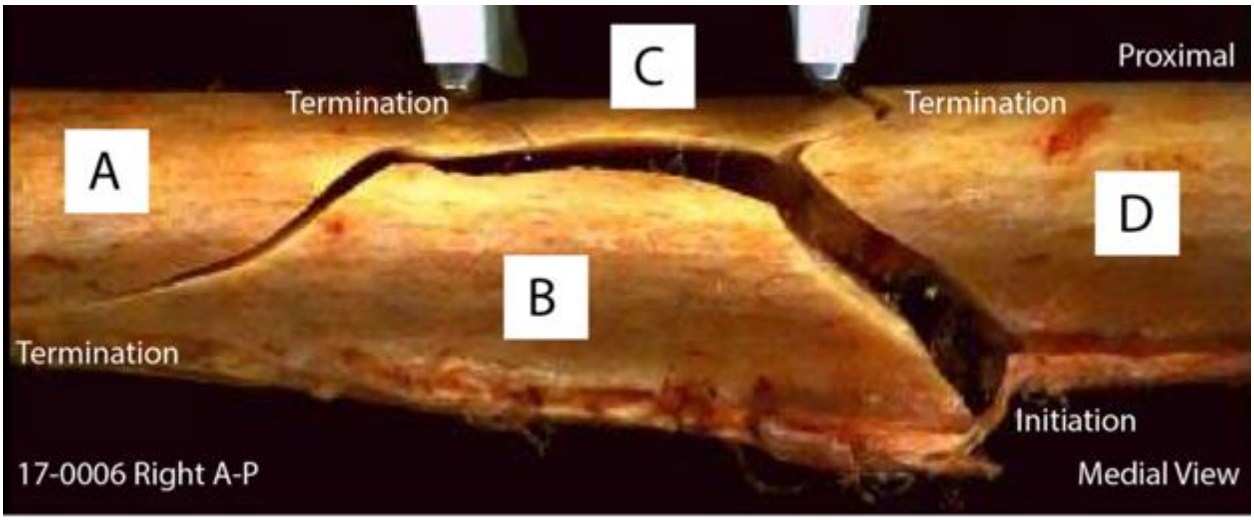

Figure A.9: Video still showing fracture propagation in 17-0006 R. Loading direction is anterior to posterior. Crack initiation is posterior proximal and crack terminations are anterior (2) and posterior distal.

REFERENCES

REFERENCES

Agnew, A.M., A.L. Harden, S. Akshara, J.H. Bolte IV, and Y. Kang. 2020. "Rib Fractures: An Experimental Approach to Identifying Intrinsic Sources of Variability." In *Proceedings of the 72nd American Academy of Forensic Sciences Annual Scientific Meeting*. Anaheim, CA.

Berryman, H.E. 2014. "Postmortem Breakage as a Taphonomic Tool for Determining Burial Position." In *Kennewick Man: The Scientific Investigation of an Ancient American Skeleton*, edited by D.O. Owsley and R.L. Jantz, 393–416. College Station, TX: Texas A&M University Press.

Christensen, A.M., and G.M. Hatch. 2019. "Forensic Fractography of Bone Using Computed Tomography (CT) Scans." *Journal of Forensic Radiology and Imaging* 18 (December 2018): 37–39.

Christensen, A.M., J.T. Hefner, M. Smith, J. Webb, M. Bottrell, and T.W. Fenton. 2018. "Forensic Fractography of Bone." *Forensic Anthropology* 1 (1): 32–51.

Cowin, S.C. 2001. *Bone Biomechanics Handbook*. Boca Raton, FL: CRC Press.

Emanovsky, P. 2015. "Low-Velocity Impact Trauma: An Ilustrative Selection of Cases from the Joint POW/MIA Accounting Command - Central Identification Laboratory." In *Skeletal Trauma: Case Studies in Context*, edited by N.V. Passalacqua and C.W. Rainwater, 156–66. Chichester, West Sussex, UK: John Wiley & Sons Ltd.

Fenton, T.W., A.E. Kendell, T.S. DeLand, and R.C. Haut. 2012. "Determination of Impact Direction Based on Fracture Patterns in Long Bones." In *Proceedings of the 64th Annual Meeting of the American Academy of Forensic Sciences*. Atlanta, GA.

Galloway, A., L. Zephro, and V.L. Wedel. 2014. "Classification of Fractures." In *Broken Bones*, edited by V.L. Wedel and A. Galloway, 2nd ed., 59–72. Springfield, IL: Charles C. Thomas.

Gozna, E.R., I.J. Harrington, and D.C. Evans. 1982. *Biomechanics of Skeletal Injury*. Edited by E.R. Gozna, I.J. Harrington, and D.C. Evans. *Biomechanics of Musculoskeletal Injury*. Baltimore: Williams & Wilkins.

Huelke, D.F., L.J. Buege, and J.H. Harger. 1967. "Bone Fractures Produced by High Velocity Impacts." *American Journal of Anatomy* 120 (1): 123–31.

Hull, D. 1999. *Fractography: Observing, Measuring and Interpreting Fracture Surface Topography*. Cambridge, MA: Cambridge University Press.

Isa, M.I., T.W. Fenton, T. Deland, and R.C. Haut. 2018. "Assessing Impact Direction in 3-Point

Bending of Human Femora: Incomplete Butterfly Fractures and Fracture Surfaces." *Journal of Forensic Sciences* 63 (1): 38–46.

Kaye, B., C. Randall, D. Walsh, and P. Hansma. 2012. "The Effects of Freezing on the Mechanical Properties of Bone." *Open Bone Journal* 4 (1): 14–19.

Khalil, A., D. Raymond, and E.A. Miller. 2015. "An Analysis of Butterfly Fracture Propagation." In *Proceedings of the 67th Annual Meeting of the American Academy of Forensic Sciences*. Orlando, FL.

Kimmerle, E.H., and J.P. Baraybar. 2008a. "Differential Diagnosis of Skeletal Injuries." In *Skeletal Trauma: Identification of Injuries Resulting from Human Rights Abuse and Armed Conflict*, edited by E.H. Kimmerle and J.P. Baraybar, 21–94. Boca Raton, FL: CRC Press.

Kimmerle, E.H., and J.P. Baraybar. 2008b. "Variation in Gunfire Wounds by Skeletal Region." In *Skeletal Trauma: Identification of Injuries Resulting from Human Rights Abuse and Armed Conflict*, edited by E.H. Kimmerle and J.P. Baraybar, 401–48. Boca Raton, FL: CRC Press.

Kress, T.A., D.J. Porta, J.N. Snider, P.M. Fuller, J.P. Psihogios, W.L. Heck, S.J. Frick, and J.F. Wasserman. 1995. "Fracture Patterns of Human Cadaver Long Bones." In *Proceedings of the International Research Council on the Biomechanics of Impact (IRCOBI)*, 155–69.

L'Abbé, E.N., S.A. Symes, D.E. Raymond, and D.H. Ubelaker. 2019. "The Rorschach Butterfly, Understanding Bone Biomechanics Prior to Using Nomenclature in Bone Trauma Interpretations." *Forensic Science International* 299: 187–94.

Levine, R.S. 1986. "An Introduction to Lower Limb Injuries." *SAE Technical Papers*.

Love, J.C., and A.M. Christensen. 2018. "Application of Bone Fractography to a Medical Examiner Sample: A Case Series." *Forensic Anthropology* 1 (4): 221–27.

Martens, M., R. van Audekercke, P. de Meester, and J.C. Mulier. 1986. "Mechanical Behaviour of Femoral Bones in Bending Loading." *Journal of Biomechanics* 19 (6): 443–54.

Martin, R.B., D.B. Burr, N.A. Sharkey, and D.P. Fyhrie. 2015. "Mechanical Properties of Bone." In *Skeletal Tissue Mechanics*, edited by R.B. Martin, D.B. Burr, N.A. Sharkey, and D.P. Fyhrie, 355–422. New York: Springer.

Reber, S.L., and T. Simmons. 2015. "Interpreting Injury Mechanisms of Blunt Force Trauma from Butterfly Fracture Formation." *Journal of Forensic Sciences* 60 (6): 1401–11.

Rockhold, L.A., and N.P. Hermann. 1999. "A Case Study of a Vehicular Hit-and-Run Fatality: Direction of Force." In *Broken Bones: Anthropological Analysis of Blunt Force Trauma*, edited by Alison Galloway, 287–90. Springfield, IL: Charles C. Thomas.

Ryan, J.R., R.T. Hensel, G.G. Salciccioli, and H.E. Pedersen. 1981. “Fractures of the Femur Secondary to Low-Velocity Gunshot Wounds.” *Journal of Trauma - Injury, Infection and Critical Care*.

Sharir, A., M.M. Barak, and R. Shahar. 2008. “Whole Bone Mechanics and Mechanical Testing.” *Veterinary Journal* 177 (1): 8–17.

Smith, O.C., E.E. Pope, and S.A. Symes. 2003. “Look until You See: Identification of Trauma in Skeletal Material.” In *Hard Evidence: Case Studies in Forensic Anthropology*, edited by D.W. Steadman, 138–54. Old Tappan, NJ: Pearson Education.

Symes, S.A., E.N. L’Abbé, E.N. Chapman, I. Wolff, and D.C. Dirkmaat. 2012. “Interpreting Traumatic Injury to Bone in Medicolegal Investigations.” In *A Companion to Forensic Anthropology*, edited by D.C. Dirkmaat, 340–89. Malden, MA: Wiley-Blackwell.

Teresinski, G., and R. Madro. 1999. “The Evidential Value of Wedge-Shaped Tibial and Femoral Fractures in Cases of Car-to-Pedestrian Collisions.” *Z Zagadnien Nauk Sadowych* 40: 72–85.

Ubelaker, D.H., and B.J. Adams. 1995. “Differentiation of Perimortem and Postmortem Trauma Using Taphonomic Indicators.” *Journal of Forensic Sciences* 40 (3): 509–12.

van Haaren, E.H., B.C. van der Zwaard, A.J. van der Veen, I.C. Heyligers, P.I.J.M. Wuisman, and T.H. Smit. 2008. “Effect of Long-Term Preservation on the Mechanical Properties of Cortical Bone in Goats.” *Acta Orthopaedica* 79 (5): 708–16.

CONCLUSIONS

Anthropologists can potentially contribute a great deal to the assessment of trauma in the human skeleton. They can differentiate between normal human variation and traumatic defects and provide valuable information regarding timing and mechanism of injury. However, there is currently a lack of standard guidelines or validated methods for making higher resolution interpretations based on blunt force fracture patterns. This is due in part to the complexity of blunt force trauma, as many variables affect fracture behavior. Trauma research is needed to evaluate which of these are most relevant and to what degree they can be reconstructed from fracture patterns.

Contributions to Theory and Practice

This dissertation represents a body of work documenting the formation of fracture in human crania and femora in response to several extrinsic variables relevant to blunt force trauma. This research addresses the need for experimental trauma studies identified by the National Institute of Standards and Technology (NIST) Organization of Scientific Area Committees for Forensic Sciences (OSAC 2016). One contribution is the production of detailed documentation of the impact conditions used to perform testing, forces generated during testing, fracture behavior following impact, and fracture patterns described in a manner relevant to anthropologists. These results contribute to a "database" that can be used to recognize and interpret patterns of trauma in future cases (Boyd and Boyd 2018). This research contributes to interpretive theory by linking the explored variables with resultant fracture patterns, and by refining hypotheses that may help direct future studies. Contributions are also made to methodological theories. These papers compare various fracture features and assess their utility

for reconstructing variables of interest. Ultimately, this dissertation adds to the iterative model of trauma research wherein increasingly focused hypotheses are tested, refined, and retested.

Papers 1, 2, and 3 contribute findings on cranial fracture behavior. Paper 1 investigated hypotheses regarding how cranial fractures form relative to the impact site. The results demonstrate that this process is more complex than typically depicted and that fractures can form both at and peripheral to the impact site. The study suggests potential impact surface effects on the location of fracture initiation: broader surfaces more frequently produced peripheral initiation than more focal ones. Comparison of the current results with those obtained in other studies (Kroman, Kress, and Porta 2011; Gurdjian, Webster, and Lissner 1950) suggest that, given similar impact surfaces, the anatomical location of impact may be an important determinant of fracture initiation. Specifically, low-parietal impacts near the sutures of the temporal region may be more likely to produce peripheral failure than impacts to the superior vault. Finally, the results contribute to methodological theory regarding impact site identification. Linear fractures can occur peripherally without damage at the POI, indicating they are poor units of analysis for identifying impact site. At the time of submission of this dissertation, this paper has been published in *Forensic Science International* (Isa et al. 2019).

Paper 2 investigated largely methodological hypotheses related to the identification of impact sites and determination of impact sequence. Specifically, this paper addressed the hypotheses that certain fracture types can be used to identify cranial impact sites, and that multiple cranial impacts to the same region can be sequenced using Puppe's rule. The results support these hypotheses and contribute to methodological theory regarding the identification of impact sites. Specifically, the results provided evidence that circumferential and depressed fractures occur predictably at impact sites, and that newer fracture lines do not cross preexisting

ones. In contrast, linear fractures occurred peripheral to the impact site and tended to complicate preexisting fracture patterns, making them poor indicators of impact site and sequence. The results also suggest potential refinement of these hypotheses. First, impact surface may affect the success of impact site identification and sequence: a focal surface produced more circumferential and depressed defects, meanwhile broader surfaces produced more linear fractures and complicate preexisting fractures. Second, the type and severity of fracture produced in an initial impact may affect the fracture type produced in subsequent impacts. Specifically, the formation of depressed fractures was more frequent after the production of an initial depressed fracture.

Meanwhile, paper 3 investigated the hypotheses that impact surface and input energy affect the type and location of cranial fractures produced. The results supported this hypothesis, but indicated these two variables have interactive effects. A more focal impact surface produced smaller defect sizes and a smaller range of variation in fracture types than broader impact surfaces. Increased input energy produced more damage to the cranial vault in experiments with a small, focal surface and a broad, curved surface. However, impacts with a broad, flat surface produced similar fracture patterns at both levels of input energy. These results further refine hypotheses regarding impact surface and energy effects. Specifically, with broader impact surfaces that impart broader distributions of stresses, fracture may be strongly influenced by stress concentrations developed at local irregularities. Individual variation may play a more important role in fracture outcomes with broad impact surfaces than with focal impact surfaces.

Finally, papers 4 and 5 investigated loading direction in human femora. Various units of analysis were assessed. The hypotheses were that features of interest would be both present and oriented in a predictable manner relative to the direction of impact. Paper 4 investigated complete fracture type, incomplete fracture features proposed by Fenton et al. (Fenton et al.

2012), and tension and compression features of fracture surfaces produced in 3-point bending with axial compression. Paper 5 investigated complete fracture type, a larger suite of tension and compression features, and the newly proposed method of fractography. The sample in paper 5 included multi-fragmentary complex fractures produced in concentrated 4-point bending. The results demonstrate that complete fractures provide little information related to loading direction. However, features associated with tension and compression occur in predictable locations relative to loading direction. Furthermore, fractographic features occur in predictable locations relative to the locations of fracture initiation and termination. These results will contribute to methodological theories by directing analysts toward more predictable units of analysis. At the time of submission of this dissertation, Paper 4 (3-point bending) has been published in the *Journal of Forensic Sciences* (Isa et al. 2018).

While this research has clear forensic relevance, it also contributes tools for bioarchaeological and paleoanthropological research that apply forensic methods to analyze and interpret skeletal trauma. Experimental research aimed at documenting fracture formation in response to known variables and critically evaluating methodological strategies is needed to improve, inform, and provide new tools for the analysis of the proximate, or mechanical cause of trauma. Improved analyses of proximate cause along with careful contextualization with archaeological, taphonomic, and material evidence solidify the foundations for interpretations of ultimate cause, including the physical and sociocultural context of the injuries.

Future Directions

This research focused on several extrinsic factors (the point, number, and direction of impact, impact surface, and kinetic energy) and their role in influencing fracture patterns. However, future research is needed to document the effects of other independent variables such

as impact velocity, and to document impact surfaces with greater resolution. Additionally, there is a need to examine these same extrinsic variables in different parts of the skeleton. There is reason to assume that the occipital, which exhibits different structural properties than the parietal, responds differently to similar impacts. Additionally, it is important to evaluate whether features investigated in the femur are similarly useful in assessing trauma to other bones with smaller cortical areas.

Moving forward, a productive area of anthropological research will focus on the human factors in skeletal trauma analysis. One area of research involves the systematic investigation of intrinsic variables thought to be relevant to fracture production. The project design of this dissertation was heavily focused on two sides of Berryman and colleagues' (Berryman, Berryman, and Saul 2018) fracture assessment triad: extrinsic factors and fracture behavior. The results of these studies clearly demonstrate that intrinsic factors related to individual variation plays an important role in fracture production. The current research considers effects of intrinsic factors, particularly to explain and further hypothesize differences obtained in similar impacts to different individuals. However, the project design provided limited ability to systematically investigate the effects of specific intrinsic factors such as density, cortical thickness, degree of cranial suture closure, and whole bone geometry (e.g. size, area, and moment of inertia). This type of research will require large sample sizes of PMHS and significant planning in order to acquire samples across an appropriate range of intrinsic variation. The ongoing work of Agnew, Harden, and colleagues on rib fractures (Agnew et al. 2020; Harden et al. 2019) represents a promising methodology in this regard.

In addition to evaluating which extrinsic and intrinsic variables are relevant and to what extent they affect fracture outcomes, it is also necessary to contemplate how this improved

understanding will affect methodological theories: how will these factors be documented and incorporated into interpretations of skeletal fractures? The current research investigated some current methodological theories for data collection. However, the ability of analysts to identify and correctly interpret these features needs validation in order to meet *Daubert* standards (Daubert v. Merrill Dow Pharmaceuticals, Inc. 1993). According to *Daubert*, scientific evidence is considered valid if it is empirically tested, subjected to peer-review, has acceptable error rates, and is accepted in scientific community. A recent review by Dempsey and Blau (Dempsey and Blau 2020) concludes that there is yet no method for analyzing blunt force trauma which meets the standard for admissibility for scientific evidence, largely due to lack of error rates.

Biomechanics-based research is important to establish baseline data and improve interpretive theory regarding how certain intrinsic and extrinsic variables affect fracture patterns. It is through this type of research that it becomes clear which aspects of fracture behavior show promise for use in interpretive methods. Methodological research is also necessary for establishing scientific validity in trauma analysis. As has been done with age, sex, and other components of the biological profile, it is also important to evaluate the success of particular methods for interpreting trauma in known cases. Future research is needed to investigate the success of particular methodologies when applied to independent, known samples of trauma.

REFERENCES

REFERENCES

Agnew, A.M., A.L. Harden, S. Akshara, J.H. Bolte IV, and Y. Kang. 2020. "Rib Fractures: An Experimental Approach to Identifying Intrinsic Sources of Variability." In *Proceedings of the 72nd American Academy of Forensic Sciences Annual Scientific Meeting*, 165. Anaheim, CA: American Academy of Forensic Sciences.

Berryman, H.E., J.F. Berryman, and T.B. Saul. 2018. "Bone Trauma Analysis in a Forensic Setting: Theoretical Basis and a Practical Approach for Evaluation." In *Forensic Anthropology: Theoretical Framework and Scientific Basis*, edited by C.C. Boyd and D.C. Boyd, 213–34. Chichester, West Sussex, UK: John Wiley & Sons Ltd.

Boyd, C.C., and D.C. Boyd. 2018. "The Theoretical and Scientific Foundations of Forensic Anthropology." In *Forensic Anthropology: Theoretical Framework and Scientific Basis2*, edited by C.C. Boyd and D.C. Boyd, 1–18. Chichester, West Sussex, UK: John Wiley & Sons, Inc.

Daubert v. Merrill Dow Pharmaceuticals, Inc. 1993, 509 U.S.57.

Dempsey, Nicholas, and Soren Blau. 2020. "Evaluating the Evidentiary Value of the Analysis of Skeletal Trauma in Forensic Research: A Review of Research and Practice." *Forensic Science International* 307: 110140.

Fenton, T.W., A.E. Kendell, T.S. DeLand, and R.C. Haut. 2012. "Determination of Impact Direction Based on Fracture Patterns in Long Bones." In *Proceedings of the 64th Annual Meeting of the American Academy of Forensic Sciences*. Atlanta, GA.

Gurdjian, E.S., J.E. Webster, and H.R. Lissner. 1950. "The Mechanism of Skull Fracture." *Journal of Neurosurgery* 7 (2): 106–14.

Harden, A.L., Y. Kang, K. Moorhouse, J. Stammen, and A. Agnew. 2019. "Human Rib Fracture Characteristics and Relationships with Structural Properties." In *International Research Council on Biomechanics of Injury (IRCOBI)*, 465–74. Florence, Italy.

Isa, M.I., T.W. Fenton, T. Deland, and R.C. Haut. 2018. "Assessing Impact Direction in 3-Point Bending of Human Femora: Incomplete Butterfly Fractures and Fracture Surfaces ,,." *Journal of Forensic Sciences* 63 (1): 38–46.

Isa, M.I., T.W. Fenton, A.C. Goots, E.O. Watson, P.E. Vaughan, and F. Wei. 2019. "Experimental Investigation of Cranial Fracture Initiation in Blunt Human Head Impacts." *Forensic Science International* 300: 51–62.

Kroman, A.M., T.A. Kress, and D. Porta. 2011. "Fracture Propagation in the Human Cranium: A Re-Testing of Popular Theories." *Clinical Anatomy* 24 (3): 309–18.

National Institute of Standards and Technology Organization of Scientific Area Committees for Forensic Sciences. 2016. “Research Needs Assessment: Controlled Experimental Bone Trauma Studies.” https://www.nist.gov/topics/organization-scientific-area-committees-forensic-science/osacresearch-and-development-needs.